Function and Regulation of Kinesin-1, -2 and -3

A thesis submitted to The University of Manchester for the degree of Doctor of Philosophy in the Faculty of Life Sciences

2010

Kim Diane Brownhill

Table of Contents

Final word count – 65,390

List of Figures

List of Tables

Abstract

The University of Manchester
Kim Diane Brownhill
Doctor of Philosophy
Function and Regulation of Kinesin-1, -2 and -3
27th July 2010

In this work the functions of the microtubule motors kinesin-1, -2 and -3 have been analysed in various settings. The reconstitution of microtubule-dependent motor activity *in vitro* has been primarily used to dissect the contributions of individual motors to cargo motility in two specific scenarios.

Initially the regulation of kinesin-1 in a cell cycle-dependent manner has been examined by studying the ability of rat liver endoplasmic reticulum (ER) tubules to move in cytosols prepared from *Xenopus laevis* egg extracts arrested in interphase, meiosis or mitosis. It was found that kinesin-1-driven ER motility is significantly disrupted during metaphase *in vitro*. This is likely due to the recruitment or loss of binding partners which has a concomitant influence upon kinesin-1 activity. This work presents the first evidence that kinesin-1-driven ER movement, and not simply network morphology, varies during cell division. Furthermore, it is postulated that the replication of such regulation of kinesin-1 activity *in vivo* may contribute to the well documented changes in organelle positioning and cargo transit through membrane trafficking pathways which occur during cell division.

The fungal metabolite brefeldin A (BFA) induces tubulation of several compartments located within the secretory and endocytic pathways in a microtubule-dependent fashion. The identity of the motor(s) responsible for this motility remains unconfirmed and controversial since several reports with conflicting data have been published. The contributions of kinesin-1, -2 and -3 to these processes have been investigated using *in vitro* motility assays in which rat liver Golgi membranes were combined with *Xenopus laevis* egg extract cytosol in the presence of BFA. Function blocking antibodies and dominant negative proteins were used to perturb the activities of various kinesin motors. This data indicates a particular isoform of kinesin-3, KIF1C, is solely responsible for the movement of BFA-induced tubules *in vitro*. This work was complemented by *in vivo* immunofluorescence studies using the HeLaM cultured cell line. Transient transfections of dominant negative proteins, or siRNA-mediated depletion, were used to disrupt the activities of various kinesin motors, either in isolation or in combination with each other. This approach revealed a contribution of KIF1C and kinesin-1 to the movement of early endosomal BFA-induced tubules *in vivo*.

Declaration

No portion of the work referred to in this thesis has been submitted in support of an application for another degree or qualification at this or any other university or institute of learning.

Copyright statement

I. The author of this thesis (including any appendices and/or schedules to this thesis) owns any copyright in it (the “Copyright”) and she has given The University of Manchester the right to use such Copyright for any administrative, promotional, educational and/or teaching purposes.

II. Copies of this thesis, either in full or in extracts, may be made **only** in accordance with the regulations of the John Rylands University Library of Manchester. Details of these regulations may be obtained from the Librarian. This page must form part of any such copies made.

III. The ownership of any patents, designs, trade marks and any and all other intellectual property rights except for the Copyright (the “Intellectual Property Rights”) and any reproductions of copyright works, for example graphs and tables (“Reproductions”), which may be described in this thesis, may not be owned by the author and may be owned by third parties. Such Intellectual Property Rights and Reproductions cannot and must not be made available for use without the prior written permission of the owner(s) of the relevant Intellectual Property Rights and/or Reproductions.

IV. Further information on the conditions under which disclosure, publication and exploitation of this thesis, the Copyright and any Intellectual Property Rights and/or Reproductions described in it may take place is available from the Dean of the Faculty of Life Sciences.

Acknowledgments

Firstly, I would like to thank Viki for her help, guidance and encouragement throughout my studies. I shall always be grateful to have been given the opportunity to study in such a friendly and enthusiastic laboratory. I have learnt more in four years than I thought possible and have enjoyed my time here immensely.

I have made many friends including Becky, Cécile, Jo, Marcin, Neftali and Yen Ching who have each helped and supported me. Without these people my PhD would have been a lot harder to complete. In particular Becky has been a brilliant teacher and mentor and someone I could always talk to when things weren't going as planned. Cécile has grown to be a very good friend as we experienced the highs and lows of studying for a PhD together and I feel sure we will remain close in the future.

Finally, I would like to thank my Mum and Dad who have always supported and encouraged me, despite still not having the slightest idea what I have spent the last few years studying!

List of abbreviations

+TIP	Plus end tracking protein
A/S	Acetate sucrose
AAA	ATPase associated with diverse cellular activities
AMPA	α-amino-3-hydroxy-5-methylisoxazole-4-propionate
ANOVA	Analysis of variance
AP	Adaptor protein
APC	Adenomatous polyposis coli
ApoER2	Apolipoprotein E Receptor 2
APS	Ammonium persulphate
ATP	Adenosine-5'-triphosphate
BCCP	Biotin carboxyl carrier protein
BFA	Brefeldin A
BicD	Bicaudal D
BRB80	Brinkley reassembly buffer
CDK1	Cyclin-dependent kinase-1
C-kin	Kinesin with motor domain located at the C-terminus
CLIMP-63	Cytoskeleton-linking membrane protein of 63 kDa
COPI	Coat protein complex I
COPII	Coat protein complex II
CSF	Cytostatic factor
DABCO	1,4-Diazabicyclo(2,2,2)octane
DAPI	4',6-Diamidino-2-phenylindole
DHC	Cytoplasmic dynein-1 heavy chain
DIC	Cytoplasmic dynein-1 intermediate chain
DLIC	Cytoplasmic dynein-1 light intermediate chain
DMSO	Dimethyl sulfoxide
DTT	Dithiothreitol
EB	End binding protein
EDTA	Ethylenediaminetetraacetic acid
EGTA	Ethyleneglycoltetraacetic acid
E-MAP-115	Epethial microtubule-associated protein of 115 kDa
ER	Endoplasmic reticulum
ERES	ER exit sites
ERGIC	ER-to-Golgi intermediate compartment
FEZ1	Fasciculation and elongation protein ζ1
Gadkin	γ1-Adaptin and kinesin interactor
GFP	Green flourescent protein
GRIF1	γ-Aminobutyric $acid_A$ receptor-interacting factor 1
GRIP1	Glutamate receptor-interacting protein 1
GSK3	Glycogen synthase kinase 3
GST	Glutathione S-transferase
GTP	Guanosine-5'-triphosphate
HCG	Human chorionic gonadotropin
HEPES	4-(2-hydroxyethyl)-1-piperazineethanesulfonic acid
HRP	Horseradish peroxidase
HSC70	Heat shock cognate protein of 70 kDa
IB	Immunoblot
IF	Immunofluorescence
IgG	Immunoglobulin G
Io	Interphase *Xenopus laevis* egg extract membrane
IP	Immunoprecipitation
IPTG	Isopropyl β-D-1-thiogalactopyranoside
Is	Interphase *Xenopus laevis* egg extract cytosol

JIP	c-Jun N-terminal kinase–interacting protein
KAP3	Kinesin-associated protein 3
KBP	KIF1-binding protein
KCA-1	Kinesin cargo adaptor protein-1
KHC	Kinesin-1 heavy chain
KIF	Kinesin family
KLC	Kinesin-1 light chain
KRP(85/95)	Kinesin related protein (85/95)
LC7	Light chain 7
LC8	Light chain 8
M6PR	Mannose-6-phosphate receptor
MAP	Microtubule-associated protein
M-kin	Kinesin with motor domain located in the centre of the protein
MMR	Marc's modified ringer's buffer
Mo	Metaphase *Xenopus laevis* egg extract membrane
MPF	Maturation-promoting factor
Ms	Metaphase *Xenopus laevis* egg extract cytosol
MTOC	Microtubule organising centre
ND	No difference
N-kin	Kinesin with motor domain located at the N-terminus
NSD	No significant difference
OIP106	O-linked N-acetylglucosamine transferase interacting protein 106
PBS	Phosphate-buffered saline
PCR	Polymerase chain reaction
PFA	Paraformaldehyde
PIPES	1,4-Piperazinediethanesulfonic acid
PMSF	Phenylmethanesulfonyl fluoride
PMSG	Pregnant mare serum gonadotropin
SDS	Sodium dodecyl sulfate
SDS-PAGE	Sodium dodecyl sulphate polyacrylamide gel electrophoresis
siRNA	Small interfering RNA
SNX	Sorting nexin
STB	Shiga toxin-B
SUK	Sea urchin kinesin
TAC	Tip attachment complex
TBS	Tris-buffered saline
TCTEX-1	T-complex testis-specific protein-1
TEMED	N,N,N',N'-Tetramethylethylenediamine
TGN	Trans-Golgi network
TNF	Tumour necrosis factor
TPR	Tetratricopeptide repeat
uKHC	Ubiquitously expressed kinesin-1 heavy chain
VE-DIC	Video-enhanced differential interference contrast microscopy
VSV-G	Vesicular stomatitis virus glycoprotein
VTC	Vesicular-tubular transport carriers
XB	Extract buffer
XTC	*Xenopus laevis* tissue culture
γ-TuRCs	γ-tubulin ring complexes

1. Introduction

Organelles display a characteristic position within eukaryotic cells which is often essential to their function. For example, whilst the endoplasmic reticulum (ER) is distributed throughout the cell, the Golgi apparatus is normally restricted to a location very close to the nucleus. Moreover, many of these organelles are not static but are subject to a constant flux of material which is transiting the secretory or endocytic pathways. This transfer of cargo between compartments requires dynamic structures which can detect and respond to changes in their microenvironment as and when required. In certain situations a more radical change in organelle position is necessary, such as during cell division when the Golgi apparatus becomes scattered throughout the cell to aid correct segregation between daughter cells (see section 1.5.3). This movement and positioning of organelles, as well as the transit of numerous cargoes throughout the cell is dependent upon the cytoskeleton and its associated molecular motors. Given the wide-ranging and crucial tasks performed by motor proteins it is perhaps not surprising that their activities are often regulated, both temporally and spatially.

1.1 Cytoskeleton

The eukaryotic cytoskeleton is composed of three major filament types, microtubules, actin and intermediate filaments. These dynamic networks are essential for determining the spatial organisation of the cell and driving intracellular transport.

1.1.1 Actin and intermediate filaments

Actin is a polarised filament, with a rapidly polymerising ‘barbed’ end and a slower growing ‘pointed’ end. Filaments usually adopt a specific orientation within the cell, with the barbed end facing the plasma membrane or organelle and the pointed end directed towards the cytoplasm. The subunits which constitute the actin filament are globular polypeptides which are able to bind and hydrolyse adenosine-5'-triphosphate (ATP). Three different types of actin are expressed in vertebrates, termed α, β and γ, however α-actin expression is restricted to muscle cells. The actin polymer consists of two extended filaments wrapped around each other to form a helix, and these can be bundled together in the cell to form an extremely strong structure. These fibres can be organised in multiple ways to give rise to microvilli, lamellipodia, filopodia and stress fibres. Aside from these specialised structures, further populations of actin filaments exist within the cell, especially in close proximity to the plasma membrane, which play prominent roles in driving cell movement and changes to cell shape [1].

Myosin motors move along actin filaments and in doing so transport a wide range of cargoes throughout the cell (reviewed in [2]). The myosin motor family is divided into eighteen classes on the basis of sequence homology, termed myosin I-XVIII. Humans have 40 myosin genes encoding motors from twelve of these classes. With the exception of myosin VI and myosin IX, all motors travel towards the barbed end of the actin filament. Each myosin has a highly conserved motor domain at the N-terminus, which interacts with actin and binds and hydrolyses ATP which is required to drive motor activity. The neck domain is located adjacent to the motor and often contains IQ domains which enable recruitment of light chains such as the calcium-binding protein, calmodulin (reviewed in [2]). At the C-terminus of the protein is located a tail

domain which exhibits the most diversity between myosin motors where a variety of functional motifs are often located [1].

In contrast to actin, intermediate filaments, whose major function is to provide mechanical strength and rigidity to cells, are not expressed in all eukaryotes, or even within all cell types. These structures are noted for their strength, conferring resistance to bending and stretching, whilst retaining flexibility. Intermediate filaments do not bind or hydrolyse a nucleoside triphosphate and motor proteins do not travel along these tracks. The monomers which constitute intermediate filaments are elongated polypeptides which oligomerise to form a staggered tetramer, the building block of the filament. These oligomers associate with each other in eight parallel protofilaments to form the final structure. Heterogeneity within these subunits gives rise to different types of intermediate filaments which are organised into six classes on the basis of sequence and structural homology, including nuclear lamins, neurofilaments and keratins, which often display a cell type-specific distribution [1]. In comparison to other cytoskeletal networks it is less well understood how intermediate filaments are polymerised and depolymerised, or how these events are regulated. The microtubule cytoskeleton, and associated molecular motors cytoplasmic dynein-1 and kinesin-1, have been implicated in influencing the organisation of intermediate filaments (see section 1.3.5) [3-5].

1.1.2 Microtubules

Microtubules are polar, linear structures composed of α- and β-tubulin heterodimers arranged into a series of protofilaments. They are extremely dynamic filaments due to the presence of so-called ‘plus’ ends which polymerise and depolymerise tubulin at a faster rate than the opposing ‘minus’ end. The polymerisation and depolymerisation of tubulin is regulated by hydrolysis of guanosine-5'-triphosphate (GTP) (reviewed in [6]). To be integrated into a growing microtubule the β-subunit of the tubulin dimer must be GTP-bound and once incorporated, is slowly hydrolysed to GDP. The balance between GTP- and GDP-bound tubulin at the plus tip is responsible for controlling microtubule dynamics. With a GDP-bound tubulin cap the microtubule is more prone to shrink in a process known as catastrophe, whereas a GTP-bound tubulin tip promotes microtubule growth, also known as rescue (Figure 1.1). A further level of regulation of microtubule dynamics is provided by post-translational modifications such as acetylation which promotes stabilisation and reduces the probability of depolymerisation (see section 1.3.5) [7]. This ability to tightly regulate microtubule dynamics becomes extremely important during certain processes such as cell division, where microtubules are dramatically reorganised to form the mitotic spindle necessary to separate sister chromatids (see section 1.5.1) (reviewed in [8]).

Microtubules are organised typically in non-polarised interphase cells with most minus ends located at a site close to the nucleus called the microtubule organising centre (MTOC), the major site of microtubule nucleation, whereas the plus tips radiate out towards the cell periphery (Figure 1.2). In polar cells this organisation can be markedly different, for example in epithelial cells the majority of microtubules are organised so that plus ends are located at the basal surface and minus ends point towards the apical surface (reviewed in [9]). Newly polymerising

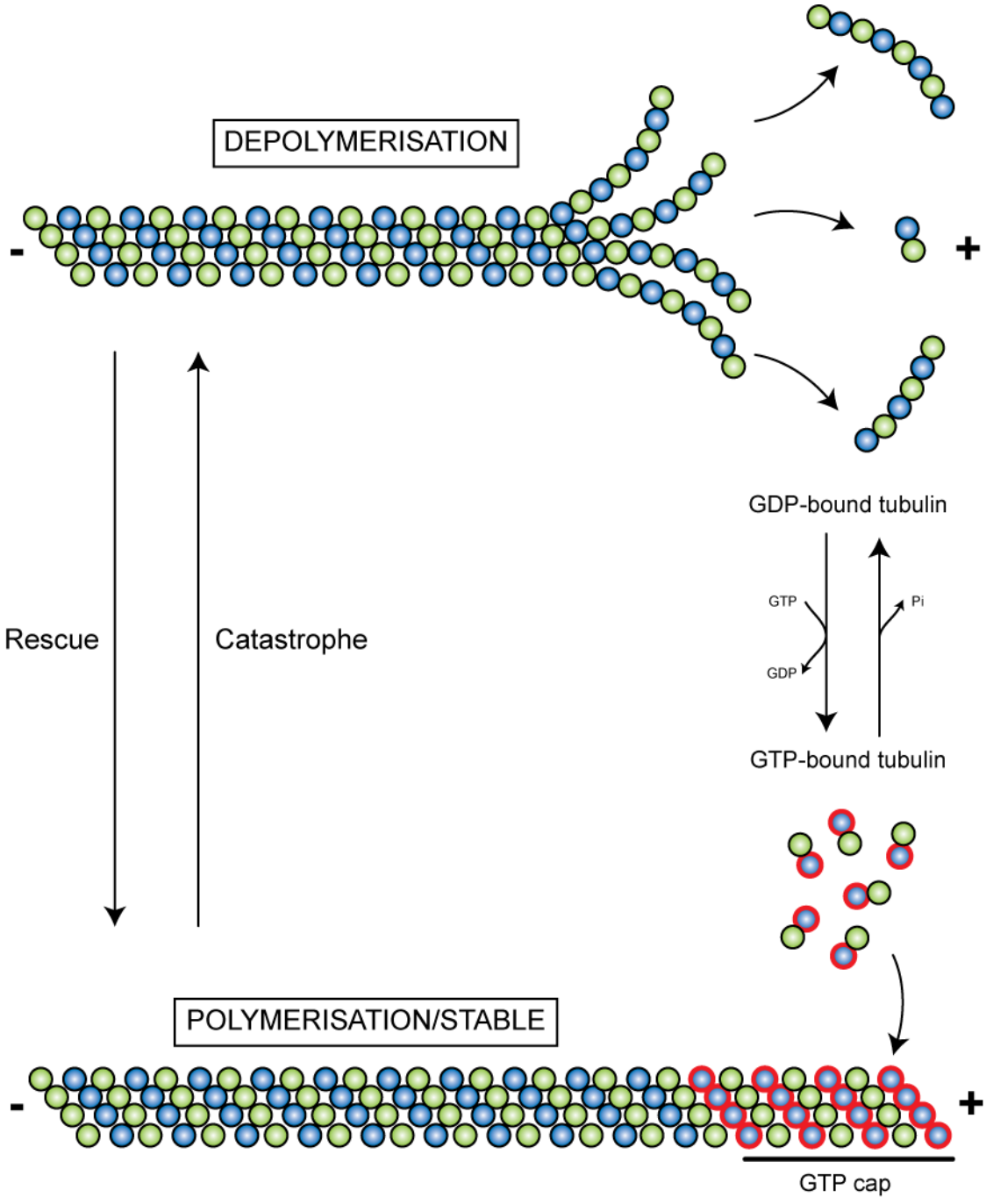

Figure 1.1 - Mechanism of microtubule dynamics and stability

The roles of GTP- and GDP-bound β-tubulin at the microtubule plus tip in controlling microtubule dynamics and stability are outlined. α-tubulin is shown in green, β-tubulin is shown in blue. GTP-bound β-tubulin is denoted by a red outline. During polymerisation GTP-bound β -tubulin-containing tubulin dimers bind at the plus tip to generate a so-called 'GTP cap'. During depolymerisation GDP-bound β-tubulin-containing tubulin is released from the microtubule.

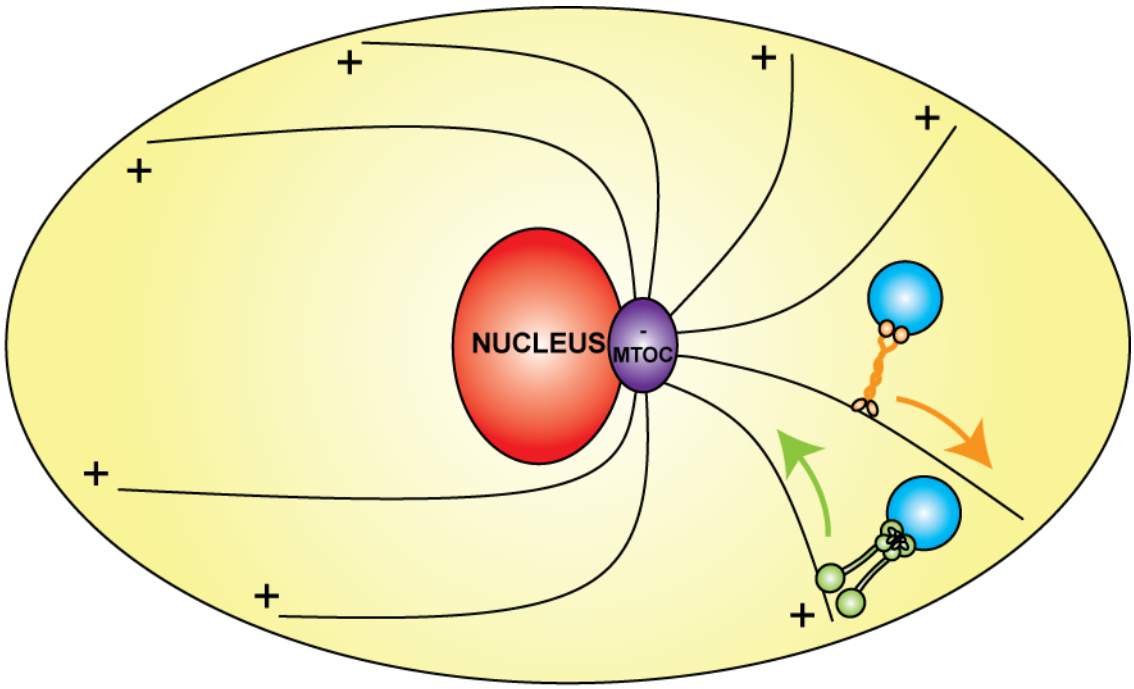

Figure 1.2 - Microtubule organisation in interphase non-polar cells

The arrangement of microtubules in interphase, non-polar cells is shown with minus ends located close to the nucleus at the MTOC and plus tips radiating out towards the cell periphery. Plus end-directed motors (such as kinesin-1) are shown in orange, minus end-directed motors (such as cytoplasmic dynein-1) are shown in green carrying cargo (blue) in specific directions along the microtubule.

microtubules emanate from nucleation sites containing γ-tubulin ring complexes (γ-TuRCs), often located close to centrosomes [10]. Interestingly, the Golgi apparatus has also been reported to nucleate microtubules, since γ-TuRCs interact with centrosomal matrix A kinase anchoring protein, which binds Golgi matrix protein of 130 kDa [11]. Plus end tracking proteins (+TIPs), which associate specifically with the growing end of microtubules, either directly or via binding to a linker protein, serve to stabilise microtubule dynamics and often link the microtubule to particular cellular structures such as kinetochores or the cell cortex. This group of +TIPs consists of particular microtubule motor proteins including cytoplasmic dynein-1, as well as non-motor proteins such as end binding (EB) proteins (reviewed in [12]).

1.2 Microtubule motors

Movement of cargo along the microtubule cytoskeleton is driven by microtubule motors which hydrolyse ATP to ADP and in doing so convert chemical energy into mechanical movement. These motors can be subdivided into two broad superfamilies, the dyneins and the kinesins. Dynein motors travel towards the minus end (cell centre) whereas the majority of kinesins move towards the plus tip (cell periphery) (Figure 1.2), although there are exceptions to this rule.

Kinesin family (KIF) members, play an integral role in driving intracellular cargo transport. To date, 45 mammalian KIF genes have been identified, but the total number of KIF proteins expressed is uncertain since it is believed multiple isoforms can be generated by alternative mRNA splicing [13]. Kinesins are broadly separated into fifteen families based upon phylogenetic analyses, termed kinesin-1 to kinesin-14B (reviewed in [14]). Kinesin motors are also crudely subdivided based upon the location of their motor domain either C-terminal (C-kin), N-terminal (N-kin), or somewhere in the middle of the protein (M-kin). To date all N-kins, which constitute kinesin-1 to kinesin-12 families, move towards the plus end of the microtubule whereas all C-kins, belonging to kinesin-14A and kinesin-14B families, move towards the minus end. Only the kinesin-13 family contains M-kins, and when bound to microtubules these motors promote depolymerisation (reviewed in [15]). Members of the kinesin-1, kinesin-2 and kinesin-3 families together with cytoplasmic dynein-1 are primarily responsible for interphase membrane movement and so will be discussed in further detail. The tissue-specific distributions, cell cycle-specific functions and known splice variants of these kinesin motors in human, rat and *Xenopus* are summarised in Table 1.1.

1.2.1 Kinesin-1

Kinesin-1 is the founding member of the kinesin superfamily, being first characterised in 1985 by Vale and co-workers as a protein capable of inducing microtubule movement on glass coverslips [16]. Metazoan kinesin-1 has been reported to transport a wide range of membranous cargoes such as mitochondria, lysosomes and ER (reviewed in [14]), as well as non-membranous cargoes including mRNAs [17] and intermediate filaments [4]. The motor also has well-documented roles in the secretory and endocytic pathways (see section 1.4). Not surprisingly, given its wide-ranging functions, perturbation of kinesin-1 expression is embryonic lethal in mice [18].

The motor conventionally has a heterotetrameric structure composed of two heavy chains (KHC) and two light chains (KLC) which perform distinct functions. The heavy chains are linked together by coiled coil interactions and to each heavy chain a single light chain is bound (Figure 1.3 A). The N-terminal globular head domain of KHC engages with the microtubule and is the site of ATP binding and hydrolysis and is therefore often referred to as the motor domain. The motor moves in a so-called 'hand-over-hand' mechanism, such that with every discrete 8 nm step taken along the microtubule the two head domains of the tetramer exchange leading and trailing roles [19]. A short neck linker region connects the head to the stalk of KHC, which has a coiled coil structure. The stalk is intersected by two hinge domains which allow kinesin-1 to flex and fold (see section 1.3.3). At the C-terminus of KHC is located a globular domain referred to as the tail. Each KLC engages with KHC via a region known as the heptad repeat [20]. Both KHC and KLC are capable of interacting with cargoes (see Tables 1.1 and 1.2) and it has been suggested that in some circumstances binding to both subunits is necessary to activate kinesin-1 activity (see section 1.3.3). It should be noted however that there are numerous examples, especially in neuronal transport, in which the KLC subunit is not required for kinesin-1 function and where adaptor or scaffold proteins operate instead (see section 1.3.4) (reviewed in [15]). Furthermore, in lower organisms, such as the filamentous fungus *Neurospora crassa*, KLCs are not expressed [21].

Duplication of the KHC gene, *kif5,* has led to the expression of three different KHC proteins in mammals, termed KIF5A, KIF5B and KIF5C. Whilst KIF5B is ubiquitously expressed, KIF5A and KIF5C expression have been reported to be limited to neurons [22, 23]. However, this finding has recently been questioned since both KIF5A and KIF5C mRNA has been detected in the human lung epithelial cell lines A549 and NHBE [24], raising the possibility that the three KHC isoforms are co-expressed, at least in some cell types. Similarly, there are four *klc* genes in mammals leading to expression of four KLC isoforms termed KLC1-4 [25-27]. KLC2 is ubiquitously expressed, whereas KLC1 has been reported to be enriched in neuronal tissue and KLC3 expression is restricted to spermatids [26, 27]. However, there may be multiple variants of each isoform due to alternative mRNA splicing. Indeed, there have been reported to be at least nineteen human KLC1 splicing isoforms, termed KLC1A-S, which differ only at the extreme C-terminus, a property thought to be important in conferring the specificity of cargo binding [28]. Indeed, KLC1B has been found to localise to the ER and mitochondria [29, 30] whereas KLC1D is enriched at the Golgi apparatus [31]. Furthermore, KLC1B is required for rat liver ER tubule motility *in vitro*, whereas KLC1D is necessary to support the portion of rat liver Golgi vesicle motility driven by kinesin-1 *in vitro* [30]. However, the majority of interactions between KLC and cargo mapped to date are via the tetratricopeptide repeat (TPR) domain of KLC (see Table 1.3), which does not differ between splicing isoforms. The mechanism by which KLC1 isoforms may determine the specificity of kinesin-1 cargo binding therefore remains undetermined.

1.2.2 Kinesin-2

Kinesin-2 was originally identified in sea urchin eggs biochemically [32] and the purified protein was subsequently shown to support microtubule plus end-directed transport *in vitro* [33]. The motor has a heterotrimeric structure composed of two motor subunits termed KIF3A and KIF3B

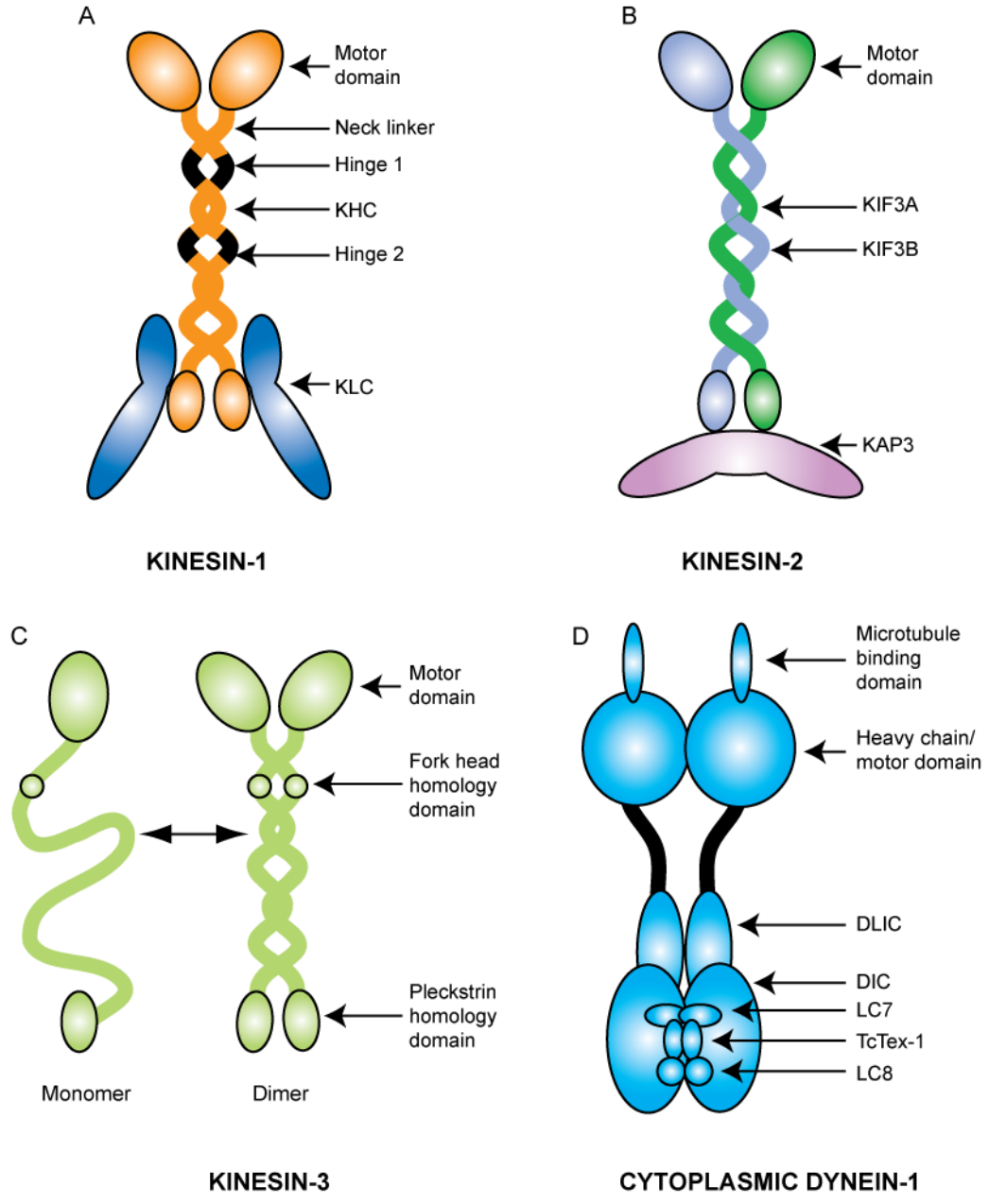

Figure 1.3 - Structure of kinesin-1, kinesin-2, kinesin-3 and cytoplasmic dynein-1

The structure and major subunits of kinesin-1 (A), kinesin-2 (B), kinesin-3 (C) and cytoplasmic dynein-1 (D) are shown. The reported dimerisation of some kinesin-3 family members is illustrated. Adapted from [34].

and a non-motor, cargo-binding subunit called kinesin-associated protein 3 (KAP3) (also known as KIFAP3) (Figure 1.3 B). Another KIF3 protein has been detected in human neurons termed KIF3C, which associates only with KIF3A. This kinesin-2 heterodimer has been reported to drive the dendritic transport of a subset of RNA granules [35]. However the precise functions of the KIF3A/C motor remains uncertain since KIF3C knockout mice have no obvious neuronal or developmental defects [36]. These are the only documented examples of motor subunit heterodimerisation within the kinesin superfamily, and the advantages that this may confer remain undetermined.

Both KIF3A and KIF3B have a structure similar to that of KHC with an N-terminal globular head domain which interacts with microtubules and binds and hydrolyses ATP, a coiled coil stalk which mediates dimerisation, and a C-terminal globular tail domain which interacts with KAP3. The majority of reported interactions between kinesin-2 and cargoes are via KAP3 and these include the non-muscle spectrin fodrin [37], p150*glued* of the dynactin complex [38], and the tumour suppressor adenomatous polyposis coli protein (APC) [39]. Two isoforms of KAP3 are generated by alternative mRNA splicing within the C-terminus termed KAP3A and KAP3B [40]. The specific functions of these isoforms are unknown, although it has been suggested that they may each bind a specific subset of cargoes. Interestingly, metazoans have another kinesin-2 family member gene, *kif17*, which is believed to form a homodimer and not recruit an associated subunit such as KAP3 [41]. KIF17 appears to be specifically expressed in neurons and its most well documented role is in dendritic trafficking of the neurotransmitter receptor N-methyl-aspartate receptor subunit 2B, a process which may contribute to higher brain function in vertebrates linked to memory and learning [42, 43]. The KIF17 motor was not studied in this work and all subsequent referrals to kinesin-2 will denote the KIF3A/KIF3B/KAP3 complex.

Kinesin-2 is known to function in a wide range of processes and perturbation of KIF3 motor activity often results in severe developmental faults. Indeed, both *kif3a* and *kif3b* knockout mice die during mid-gestation displaying severe defects in neurogenesis, mesoderm patterning, and left-right body asymmetry [44, 45]. A role for kinesin-2 as a tumour suppressor has also been recognised due to its interaction with APC and observations that the conditional *kap3* knockout mouse displays brain tumours [46]. The acute defects observed following perturbation of kinesin-2 function may be linked to the well-documented roles of this motor within the secretory and endocytic pathways (see section 1.4). Kinesin-2 family members also function in the formation of sensory cilia and intraflagellar transport, the movement of cargoes within cilia and flagella (reviewed in [15]). For example, kinesin-2 is implicated in the transport of the G-protein-coupled receptor, opsin, within the mammalian photoreceptor cilium [47].

1.2.3 Kinesin-3

KIF1 forms the kinesin-3 family together with KIF13, KIF14 and KIF16. KIF1A and its *Caenorhabditis elegans* homologue Unc104 were the first kinesin-3 motors discovered by virtue of their homology to KHC [23, 48]. In mammals, in addition to KIF1A, two other KIF1 isoforms are expressed called KIF1B and KIF1C. Similar to kinesin-1 and kinesin-2, these motors have a

globular N-terminal motor, a coiled coil stalk, and a globular C-terminal tail domain (Figure 1.3 C).

Alternative mRNA splicing of the *kif1b* gene gives rise to two isoforms, with murine KIF1Bα lacking the C-terminal 620 amino acids in comparison to KIF1Bβ, resulting in completely different tail domains [49]. Differences within the tail have been proposed to direct particular KIF1 isoforms to specific subsets of cargoes. KIF1Bα is specifically targeted to mitochondria and supports mitochondrial transport *in vitro* [50] and positioning *in vivo*, a function which may be dependent upon an interaction with KIF1 binding protein (KBP) [51]. Indeed, when a deletion mutant of KBP which can no longer interact with KIF1Bα was overexpressed in the mouse fibroblast cell line NIH-3T3, mitochondrial aggregation was observed [51]. KBP does not mediate the interaction of KIF1Bα with mitochondria but appears to improve the motility of the motor by increasing its processivity along the microtubule. Although the precise function of KBP remains unclear, the protein has been shown to be required for axonal growth in zebrafish and mutations within the KBP gene give rise to the neurological disorder Goldberg-Shprintzen syndrome [52]. KIF1Bβ is targeted to synaptic vesicle precursors [53], as well as lysosomes in non-neuronal cells [54]. Expression of KIF1A is limited to neurons where this motor plays an important role in the axonal trafficking of presynaptic vesicle precursors [55, 56]. The major reported role of KIF1C is in trafficking of Golgi contents from the cis-Golgi to the ER in response to the fungal metabolite brefeldin A (BFA), although this has been contested (see section 1.4.2.2). Both KIF1A and KIF1Bβ also contain a pleckstrin homology domain at the C-terminus which is proposed to be important for binding phospholipids [57], and may therefore facilitate membrane attachment [58].

KIF1 motors are predominantly monomeric but it is has been suggested that in certain situations they are able to homodimerise via coiled coil interactions and thereby become capable of processive movement. Indeed, KIF1A was observed to dimerise *in vitro* and translocated along microtubules at a velocity similar to that observed for fluorescently labelled Unc104 in *Caenorhabditis elegans* [59, 60]. It is suggested that the oligomerisation of KIF1 motors may occur specifically on cargoes *in vivo*, perhaps in a concentration-dependent manner, meaning KIF1 motor function is activated specifically when membrane-bound [59]. In this scenario the binding of KIF1A to phosphatidylinositol-4,5-bisphosphate on cargoes would induce clustering of the motor, triggering dimerisation and motor activation [58, 59]. However, this model has recently been disputed by Hammond and co-workers who observed that both exogenously-expressed and endogenous rat KIF1A exists in a dimeric, inactive state in COS cells [61]. Interestingly, a study by Okada and Hirokawa revealed monomeric KIF1A is capable of diffusive movement along microtubules mediated by weak electrostatic interactions between positively charged residues of the motor domain and negatively charged residues of tubulin, which keeps KIF1A in close proximity to the microtubule as it travels from one binding site to the next [62]. The advantages that monomeric KIF1 transport may convey compared to dimeric processive motility *in vivo* are unknown.

The other members of the kinesin-3 family are KIF13, KIF14 and KIF16. Two isoforms of KIF13 and KIF16 are expressed in mice termed A and B (reviewed in [15]). KIF13A is implicated in driving movement of lysosomal hydrolases from the trans-Golgi network (TGN) to the endocytic system (see section 1.4.3). KIF13B, also known as guanylate kinase-associated kinesin, is involved in the transport of phosphatidylinositol-3,4,5-trisphosphate-containing vesicles to axon tips, which is proposed to be important for determining neuronal polarity [63]. KIF14 is suggested to perform essential functions during cell division, being implicated in both chromosome segregation [64] and cytokinesis [65]. While the function of KIF16A remains poorly understood, KIF16B is involved in driving plus end-directed movement of early endosomes, dependent upon binding of the motor to the phospholipid phosphatidylinositol 3-phosphate (see sections 1.3.4 and 1.4.4) [66].

1.2.4 Cytoplasmic dynein-1

In contrast to plus end-directed motility, cytoplasmic movement towards the microtubule minus end is almost entirely performed by a single motor, cytoplasmic dynein-1. The backbone of this motor is cytoplasmic dynein-1 heavy chain (DHC), which contains a C-terminal ring of six ATPase associated with diverse cellular activities (AAA) domains. The first and third AAA domains are the major sites of ATP binding and hydrolysis which underlie motor function [67, 68]. A small globular structure emerges from this motor domain which allows binding to microtubules [69]. The tail domain, located at the N-terminus of the subunit, mediates homodimerisation of DHC and also provides a scaffold allowing recruitment of several non-catalytic dimeric subunits. Cytoplasmic dynein-1 intermediate chain (DIC) and light intermediate chain (DLIC) bind directly to DHC. The remaining subunits, light chain 8 (LC8), light chain 7 (LC7) (also known as roadblock) and T-complex testis-specific protein 1 (TCTEX-1) are recruited via DIC (Figure 1.3 D) (reviewed in [1, 70, 71]). The extremely diverse array of cargoes transported by cytoplasmic dynein-1 necessitates the precise spatial and temporal regulation of motor activity and cargo binding. This is believed to be mediated, at least in part, by the association of the motor with a wide range of adaptor proteins such as dynactin, Lissencephaly 1, Bicaudal D (BicD), NudE-like, Zeste White-10, nuclear distribution protein E and Spindly (reviewed in [72]).

Dynactin is the most studied cytoplasmic dynein-1-interacting partner. First identified using *in vitro* motility assays [73], this adaptor protein has now been shown to be essential for almost all cellular functions of cytoplasmic dynein-1. Indeed, perturbation of dynactin function produces a phenotype similar to complete loss of cytoplasmic dynein-1 [74]. A specific region of the p150*glued* subunit of dynactin, coiled coil-1, has been shown to directly bind DIC [75]. Dynactin has been reported to support motor function in several ways including linking the motor to cargoes [76] and improving motor processivity [77, 78]. However, these functions are contested and the exact mechanism by which dynactin supports cytoplasmic dynein-1 function remains uncertain [79, 80]. Interestingly, the p150*glued* subunit of dynactin has also been shown to interact with kinesin-1 [81], kinesin-2 [38] and the kinesin-5 family member Eg5 [82], raising the possibility that dynactin may also contribute to the regulation of bidirectional motility.

Additionally, DIC has also been observed to interact with KLC1 and KLC2 directly in rat brain cytosol [83].

1.3 Motor regulation

Given the varied and important tasks performed by microtubule motor proteins it is not surprising that their activities can be regulated. There are several common mechanisms which are observed recurrently to control cargo transport and these are discussed briefly below, with an emphasis on kinesin-1.

1.3.1 Motor phosphorylation

The first indication that kinesin-1 function may be influenced by its phosphorylation status was provided by Lee and Hollenbeck who showed that kinesin-1 isolated from chick brain existed in several different isoelectric isoforms [84]. Furthermore, the level of kinesin-1 phosphorylation was found to correlate to the cargo binding of kinesin-1, with the membrane-associated motor predominantly highly phosphorylated with soluble kinesin-1 less so. Several subsequent studies have observed changes in the phosphorylation status of both KHC and KLC *in vivo* which are proposed to regulate kinesin-1 function as described below.

The unloading of cargoes once the motor complex has reached the required destination is likely to be a tightly regulated event. The heat shock cognate protein of 70 kDa (HSC70) has been shown to induce release of kinesin-1 from membranes [85] and this behaviour is suggested to be mediated by the phosphorylation of KLCs by glycogen synthase kinase 3 (GSK3). Morfini and co-workers have showed that KLCs are a substrate for GSK3 *in vivo* and propose a model in which GSK3 phosphorylation increases the accessibility of KLCs to HSC70 and leads to dissociation of kinesin-1 from cargoes [86]. Since GSK3 is often enriched at sites of membrane delivery such a mechanism could contribute to the correct deposition of cargoes at specific sub-cellular destinations [86].

Similarly, phosphorylation of a component of cytoplasmic dynein-1 promotes dissociation of the motor from ER cargo in *Xenopus laevis* eggs. Phosphorylation of DLIC by cyclin-dependent kinase-1 (CDK1) stimulates release of cytoplasmic dynein-1 from ER membranes, leading to cessation of ER motility [87, 88]. Interestingly, this mechanism operates in a cell cycle-dependent context since DLIC phosphorylation occurs specifically in metaphase-arrested *Xenopus laevis* egg extracts and ER network formation is perturbed only in mitotic and meiotic extracts *in vitro* (see section 1.5.2) [89].

KLC phosphorylation has also been shown to be important in mediating an interaction between kinesin-1 and the cell signalling protein, 14-3-3. Following phosphorylation of KLC2 at serine 575 by an as yet unidentified kinase, an interaction between kinesin-1 and 14-3-3 was induced in the rat neuronal cell line, PC12 [90]. The importance of this interaction has still to be elucidated, but it has been proposed that 14-3-3 may act as a scaffold protein linking other cargoes to kinesin-1, or may relay signalling information to the motor.

Modulation of the phosphorylation status of KHC can also induce changes in kinesin-1 activity. Perhaps the best studied example is the role of kinesin-1 in supporting insulin secretion from pancreatic β-cells in response to high blood glucose levels. Donelan and co-workers have shown that under basal conditions KHC present on β-granules is phosphorylated by casein kinase 2 [91]. However, an elevation in blood glucose levels results in an increase in intracellular calcium concentration, triggering dephosphorylation of KHC by protein phosphatase 2Bβ. This is proposed to activate kinesin-1 activity and thereby promote the movement of β-granules from the storage pool to the plasma membrane. This motility is necessary to replenish the readily releasable pool of β-granules and underlies a second wave of insulin secretion [91].

Interestingly, phosphorylation can also regulate kinesin-1 activity whilst the motor remains cargo-bound. Treatment of the mouse fibroblast cell line L929 with the proinflammatory cytokine tumour necrosis factor (TNF) induced a switch in mitochondrial positioning from an evenly spread distribution throughout the cell to a polar perinuclear clustering [92]. This response is due to the activation of kinase pathways by TNF, possibly p38 mitogen-activated kinase-dependent, which results in hyperphosphorylation of both KLC1 and KLC2, which is proposed to lead to kinesin-1 inactivation [93]. Surprisingly, phosphorylation of KLC2 is mediated by a kinesin-1-associated kinase, suggesting that there may be a subset of kinases permanently bound to the motor which are able to influence kinesin-1 function. In this study the ability of kinesin-1 to bind mitochondria is unaffected and it is therefore one of the few examples in which kinesin-1 activity is modulated without disruption of the motor-cargo interaction.

It is likely that the phosphorylation status of cargoes also influences their ability to interact with kinesin-1. For example, the neuronal microtubule-associated protein (MAP) tau binds KLC only following phosphorylation by GSK3 in rat cortical neurons [94]. Treatment with GSK3 inhibitors leads to reduced tau phosphorylation, perturbation of the interaction with kinesin-1 and decreased axonal transport of the protein. The influence that cargo phosphorylation may have upon motor binding, and how motors recognise and respond to changes in cargo phosphorylation status, is a poorly understood topic.

1.3.2 Calcium signalling

Recent work has suggested that localised changes in intracellular calcium concentration are also capable regulating kinesin-1 motor activity. The adaptor protein milton associates with KHC independently of KLC, at least in *Drosophila melanogaster* [95], and this complex is important in moving mitochondria. Positioning of mitochondria is especially important in neurons where the organelle needs to be localised to subcellular regions where energy demand is highest, often requiring transport over long distances and frequent relocation. Under normal circumstances milton mediates an association between KHC and the outer mitochondrial transmembrane GTPase protein Miro. Two EF motifs located within Miro are capable of sensing intracellular calcium levels. Following high calcium influx these two domains are proposed to bind KHC, thereby preventing the interaction of kinesin-1 with microtubules and leading to inhibition of mitochondrial motility [96]. Since elevated levels of calcium influx often occur at areas of high metabolic demand it is thought that this mechanism may mediate the targeting of mitochondria

to regions of the cell where they are most needed [96]. Interestingly, both retrograde and anterograde mitochondrial motility is inhibited in response to calcium influx in a Miro-dependent manner, raising the possibility that this protein is also able to modulate cytoplasmic dynein-1 activity.

However, this model has recently been disputed by MacAskill and co-workers who observed that Miro interacted directly with KIF5A/B/C in cultured rat hippocampal neurons with the interaction disrupted by elevated calcium levels, resulting in cessation of mitochondrial movement [97]. Nevertheless, the rat and human homologues of milton, γ-aminobutyric $acid_A$ receptor-interacting factor 1 (GRIF1) and O-linked N-acetylglucosamine transferase interacting protein 106 (OIP106) respectively, have been shown to bind both mitochondria and KHC and are capable of influencing mitochondrial positioning in cultured neuronal and fibroblastic cell lines [95, 98].

1.3.3 Autoinhibition of kinesin-1

It is proposed that the binding of the KHC tail to the motor domain of kinesin-1 is the basis of an autoinhibitory mechanism, thought to prevent the futile hydrolysis of ATP when the motor is not bound to cargo and accumulation of kinesin-1 at microtubule plus ends. This concept stems from electron microscopy studies which showed that under physiological salt concentrations native bovine kinesin-1 in solution adopts a flexed conformation with KHC head and tail domains in close proximity [99, 100]. Later work by Coy and co-workers using recombinantly expressed *Drosophila melanogaster* KHC revealed that deletion of the tail activated the ATPase activity of the motor in the absence of cargo binding, whilst the addition of exogenous tail restored inhibition [101]. It is now thought two intramolecular interactions underlie the autoinhibition of kinesin-1, and are dependent upon hinge domains located within KHC which allow the molecule to flex. In addition to the interaction between KHC head and tail domains, the TPR motif of KLC pushes the motor domain of each KHC apart and likely perturbs the interaction between kinesin-1 and microtubules [102]. Therefore kinesin-1 adopts a default inactive conformation and its activation is dependent upon unfolding.

This kinesin-1 autoinhibition model necessitates the docking of both KHC and KLC with cargoes to fully unfold kinesin-1 and thereby promote motor activity. Indeed, the transport of c-Jun N-terminal kinase–interacting protein 1 (JIP1) by kinesin-1 requires binding of fasciculation and elongation protein ζ1 (FEZ1) to KHC. Blasius and co-workers showed that the binding of JIP1 to KLC was not sufficient to induce kinesin-1 activity, whereas when both JIP1 and FEZ1 were bound motor activity was activated [103]. Since human FEZ1 protein is a target of protein kinase C *in vitro* [104], it is feasible that phosphorylation regulates the binding of FEZ1 to KHC. FEZ1 may not be a true kinesin-1 cargo but instead may function as an activator of motor function by cooperating with JIP1 to relieve the autoinhibitory conformation. Perhaps there are several proteins whose binding to kinesin-1 is intended only to aid unfolding of the motor and prime it for transport, and thereby operate as activators rather than genuine cargoes of kinesin-1.

1.3.4 Rab GTPases

There are numerous examples in which a kinesin motor does not interact with a particular cargo via an integral membrane protein, but is dependent upon peripherally-associated accessory proteins which are often labelled adaptors. The list of kinesin-1 adaptor proteins is extensive and continues to grow (reviewed in [15]). Where a clear interaction between KHC or KLC and a protein binding partner has been shown these are included in Tables 1.1 and 1.2. In this section the contribution of Rab GTPases as adaptors and potential regulators of motor function will be briefly discussed.

Members of the Rab family of GTPases represent a broad group of proteins which are implicated in controlling the association of motors with particular cargoes, particularly within the secretory and endocytic pathways (reviewed in [105]). Rabs can exist in either GTP- or GDP-bound forms, with various effector molecules being activated or recruited specifically by the GTP-bound Rab. There are several examples in which Rabs have been observed to control microtubule motor activity, either directly or indirectly as described below.

Rabkinesin-6 activity is proposed to be regulated by Rab6 [106], a GTPase implicated in controlling Golgi positioning, Golgi-to-ER trafficking and constitutive exocytosis (see sections 1.4.2.1 and 1.4.3) [107]. Rab6-GTP localises to the Golgi whereas Rab6-GDP does not and the artificial conversion of Rab6 into a GDP-bound form reportedly stimulates dissociation of the Rabkinesin-6 motor from the Golgi [106]. It should be noted, however, that the role of Rabkinesin-6 in Golgi positioning or trafficking remains uncertain since the motor has been primarily reported to play a role in cytokinesis (see section 1.4.2.1) [108, 109].

The kinesin motor KIF16B functions within the endocytic pathway (see section 1.4.4) and its recruitment to early endosomes is proposed to be indirectly controlled by Rab5. KIF16B interacts with cargo by binding the phospholipid phosphatidylinositol 3-phosphate, the formation of which is controlled by Rab5 and its effector Vps34, a phosphatidylinositol-3-OH kinase [66]. In this model GTP-Rab5 modulates the generation of phosphatidylinositol 3-phosphate by its direct interaction with Vps34, thereby mediating the binding of KIF16B to the endosomal membrane [66].

There are several examples in which cytoplasmic dynein-1 function has been shown to be indirectly controlled by Rab GTPases. GTP-Rab7, which is associated with late endosomes and lysosomes, interacts with Rab7-interacting lysosomal protein, which in turn binds the p150*glued* subunit of the dynactin complex leading to recruitment of cytoplasmic dynein-1 to the vesicle [110, 111]. Furthermore, Rab6 indirectly regulates cytoplasmic dynein-1 function via its effector, BicD. GTP-Rab6 has been observed to recruit BicD to the TGN and a subset of cytoplasmic vesicles in HeLa cells, with BicD subsequently recruiting cytoplasmic dynein-1 [112]. This binding has been suggested to be important for cargo transport within the coat protein complex I (COPI)-independent ER-to-Golgi trafficking pathway (see section 1.4.2.1).

1.3.5 Microtubule modifications

Assorted microtubule post-translational modifications as well as the binding of MAPs are known to influence the ability of various motors to bind and move along the microtubule cytoskeleton. It is possible that particular modifications demarcate distinct sub-populations of microtubules and in doing so are able to exert control over motor-dependent trafficking.

Microtubule acetylation, the addition of an acetyl group to the lysine 40 residue of α-tubulin, has been shown to promote the microtubule binding and motility of kinesin-1 *in vitro* [113]. This is proposed to be important for the trafficking of JIP1 to a specific subset of neurites in cultured mouse hippocampal neurons. Following treatment with trichostatin A, a drug with inhibits histone deacetylases and thereby leads to an increase in tubulin acetylation, JIP1 was unusually targeted to all neurite tips. Similarly, kinesin-1 has been shown to specifically interact with detyrosinated tubulin in extracts prepared from bovine brain [114]. Detyrosination, the removal of the C-terminal tyrosine residue from α-tubulin, enhances the binding of kinesin-1 and this may be important in mediated the interaction between vimentin intermediate filaments and the microtubule cytoskeleton. This data is corroborated by the observation that fluorescently labelled KIF5C preferentially moves along detyrosinated microtubules *in vivo* [115].

MAPs are proteins which interact with microtubules and by doing so influence their stability. The binding of a particular isoform of MAP4 to microtubules *in vitro* has been shown to inhibit kinesin-1 microtubule gliding [116]. This is due to the failure of kinesin-1 to translocate efficiently along the microtubule whilst the microtubule-binding capabilities of the motor remain unaffected. The association of the neuronal MAP, tau, with microtubules is suggested to modulate both kinesin-1 and cytoplasmic dynein-1 function. Single molecule assays have indicated that tau induces detachment of kinesin-1 from microtubules and pausing and reversal of cytoplasmic dynein-1 movement [117].

Another MAP implicated in controlling kinesin-1 activity is epithelial-associated protein of 115 kDa (E-MAP-115), also known as ensconsin and MAP7. E-MAP-115 is a stabilising MAP whose binding to microtubules is proposed to be modulated in a cell cycle-dependent manner [118]. During early prophase E-MAP-115 is hyperphosphorylated in HeLa cells leading to its dissociation from microtubules and a concomitant increase in microtubule dynamics, thought to be necessary for mitotic spindle formation. From prometaphase onwards E-MAP-115 is dephosphorylated, leading to its progressive reassociation with microtubules and stabilisation of the cytoskeleton. Recently, the *Drosophila melanogaster* homologue of this protein, ensconsin, has been shown to be required for all studied kinesin-1 functions in the polarised fly oocyte [119]. Ensconsin is proposed to exert this control by promoting the microtubule binding and motility of kinesin-1. It is unknown whether a similar mechanism operates in mammalian cells but this study highlights E-MAP-115 as a potential regulator of kinesin-1 function.

1.4 Transport in the secretory and endocytic pathways

The role of microtubule motors in assisting the transit of cargoes through the secretory and endocytic pathways in metazoan cells will be discussed here with an emphasis on kinesin motors.

1.4.1 ER-to-Golgi traffic

The main compartments within the secretory pathway in higher eukaryotes are the ER, the ER-to-Golgi intermediate compartment (ERGIC), and the Golgi apparatus which lies in close proximity to microtubule minus ends. Secretory and membrane proteins as well as those which function within the exocytic and endocytic pathways are synthesised, correctly folded and oligomerised as necessary within rough ER. These proteins exit the ER at specialised areas known as ER exit sites (ERES) usually in coat protein complex II- (COPII) coated vesicles. Material leaving ERES sheds the COPII coat and undergoes homotypic fusion before being delivered to the ERGIC in vesicular-tubular transport carriers (VTCs) and subsequently to the cis face of the Golgi apparatus in a microtubule- and COPI-dependent fashion [120]. It should be noted that this is not necessarily the route taken by all cargoes since procollagen has been reported to move to the Golgi in carriers lacking ERGIC markers, indicating it bypasses this intermediary compartment [121].

Since these processes involve movement towards the cell centre, a role for the minus end-directed motor cytoplasmic dynein-1 has been proposed. Perturbation of cytoplasmic dynein-1 inhibited ER-to-Golgi trafficking of vesicular stomatitis virus glycoprotein (VSV-G) in COS cells [122]. Furthermore, a transitory direct interaction between the dynactin subunit p150*glued* and the COPII component Sec23 has been observed [123]. However, the importance of this association in delivering material from ER to ERGIC remains uncertain given the COPII coat is thought to be shed soon after budding [120]. The interaction may contribute to the entry of cargo into ERES as well as ERES tethering, perhaps by mediating the association of ERES with microtubules [123, 124]. It is possible that cytoplasmic dynein-1 mediates trafficking of VTCs towards the cell centre via the association of dynactin with other membrane receptors such as spectrin, which is often present on the surface of organelles and has been proposed to anchor dynactin to the Golgi apparatus [76].

An interaction between cytoplasmic dynein-1 and budding COPI vesicles is important in driving cargo transport through the ERGIC compartment as well as Golgi-to-ER trafficking (see section 1.4.2). The recruitment of the motor to COPI vesicles is regulated by the small GTPase Cdc42, a regulator of actin dynamics. The current model proposes that binding of Cdc42 during vesicle budding prevents the recruitment of cytoplasmic dynein-1 to the vesicle. Following coat formation the γ-COP subunit of COPI displaces Cdc42 allowing association of the motor and initiation of vesicle motility [125].

Kinesin-1 has also been localised to ERES and has been implicated in controlling ERES biogenesis and positioning and, surprisingly, ER-to-Golgi trafficking. Sar1-GTP, the small

GTPase which triggers COPII coat formation, has been suggested to influence kinesin-1 recruitment to ERES in a permeabilised cell system [126]. Furthermore, depletion of KIF5B in HeLa cells caused clustering of COPII components close to the nucleus and a delay in ER-to-Golgi trafficking of VSV-G protein potentially as a result of abnormal VTC formation [124].

1.4.2 Golgi-to-ER traffic

Proteins exiting the Golgi are either moved forward through the secretory pathway or are trafficked back to the ER via one of at least two known routes, termed COPI-dependent and -independent (Figure 1.4).

1.4.2.1 COPI-dependent and –independent pathways

Cargoes which are moved back to the ER from the Golgi include escaped ER-resident proteins and Golgi-resident glycosylation enzymes. The COPI-dependent and -independent pathways represent distinct routes via which material is trafficked, with COPI coat formation being necessary in the former, and each requires the activity of a different subset of microtubule motors.

The COPI-dependent pathway stems mainly from the cis-Golgi and requires kinesin-2 activity, at least in HeLa cells where depletion of KAP3 resulted in perturbation of the COPI-dependent retrograde trafficking of KDEL-containing cargoes [127]. Whether the interactions between COPI, Cdc42 and cytoplasmic dynein-1 as described in section 1.4.1 function in this pathway, as well as in forward trafficking of COPI vesicles towards the Golgi, is uncertain. Interestingly, COPI-positive membranes are only rarely observed moving away from the Golgi *in vivo* perhaps indicating that the coat is shed soon after budding in this retrograde pathway [128, 129].

The COPI-independent retrieval pathway originates from the TGN and is used to transport cargoes such as Shiga toxin-B (STB). The motor responsible for this motility remains elusive but it is not kinesin-2 since no abrogation of Shiga-like toxin-1 transport to the ER was observed following KAP3 depletion [127]. Rabkinesin-6 has been implicated in this pathway since motility is known to be dependent upon the activity of the small GTPase Rab6 [130]. However, the major documented role of this motor is in cytokinesis, with protein expression levels shown to be lower during interphase [108, 109]. The contribution of Rabkinesin-6 to cargo motility in this pathway remains uncertain and the involvement of other microtubule motors is undetermined. Rab6-positive fluorescently labelled tubules are often observed to move bidirectionally *in vivo* [112] suggesting cytoplasmic dynein-1 may also contribute to their motility. Indeed, the p150*glued* subunit of dynactin is known to interact with Rab6 directly [131], and indirectly via BicD [132]. Interestingly, kinesin-1 has also been shown to interact with BicD, albeit weakly, making this motor a candidate for moving Rab6-positive tubules towards microtubule plus ends [133]. The purpose of such bidirectional motility is unknown, although it appears to be a common feature within membrane trafficking pathways.

1.4.2.2 BFA

Yet another form of ER-to-Golgi trafficking is observed in cells treated with the fungal metabolite BFA. BFA causes a block in trafficking from the Golgi to the ER [134], as well as the tubulation

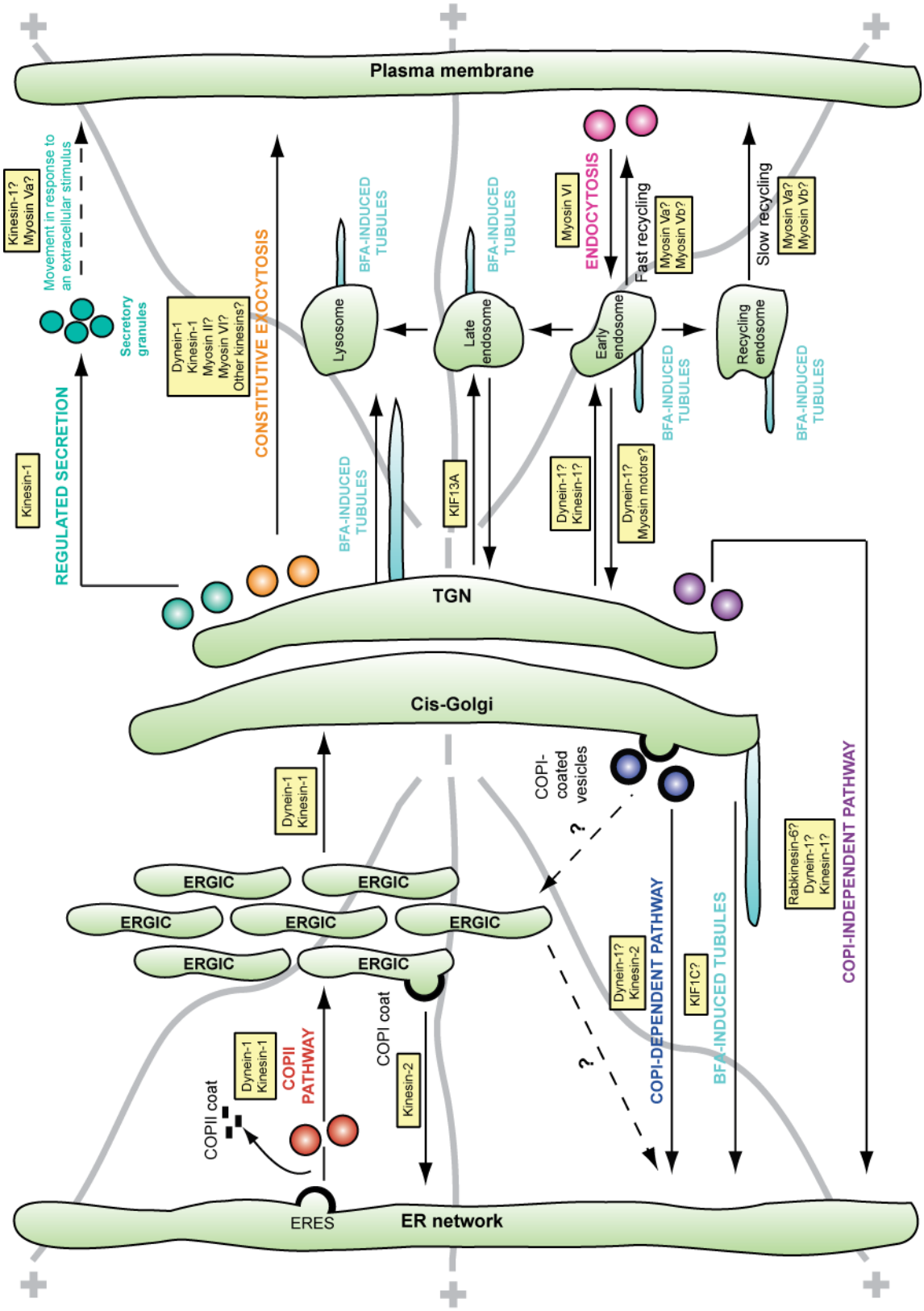

Figure 1.4 - Motor function within the secretory and endocytic pathways

The major transport steps in the secretory and endocytic pathways are outlined together with the associated microtubule and actin motors. Arrows show the direction of cargo transport between the various compartments, with potential pathways denoted by dotted lines. Microtubules are shown in grey. Adapted from [34].

of several compartments located within the secretory and endocytic pathways including the cis-, medial- and trans-Golgi, TGN, early endosomes, recycling endosomes, late endosomes and lysosomes (Figure 1.4) [135-139]. This results in accumulation of material in the ER and loss of the Golgi as a discrete organelle. Tubules positive for cis-, medial- and trans-Golgi markers fuse with the ER [140], whereas tubules emanating from the TGN mix with the early endocytic system [141]. BFA exerts these effects primarily by inhibiting the activities of Sec7-type GTP-exchange factors including GBF1, thereby preventing activation of the small GTPase Arf1 leading to perturbation of COPI coat formation [142]. The BFA target which causes inhibition of ER-to-Golgi transport is undetermined, although it is proposed to interfere with cargo export from the ER.

BFA-induced tubulation of secretory and endocytic organelles is known to be dependent upon the microtubule cytoskeleton and ATP [138], but the motor(s) responsible for this motility is uncertain. Since tubules move away from the Golgi, a plus end-directed motor is implicated in these processes. Indeed, initial studies identified kinesin-1 as being required for the motility of BFA-induced cis-Golgi tubules since an anti-KHC antibody, H1, blocked cis- and medial-Golgi tubule formation [143]. BFA-induced tubulation can be reconstituted *in vitro* by mixing a fraction enriched in Golgi membranes isolated from rat liver with cytosol prepared from *Xenopus laevis* egg extracts in the presence of BFA. In agreement with the *in vivo* data, pre-incubation of Golgi membranes with the H1 antibody caused a profound inhibition of tubule formation [144]. However, when kinesin-1 function was perturbed using the well characterised function-blocking anti-KHC antibody sea urchin kinesin (SUK)4, no inhibition of motility was observed. Subsequently, the H1 antibody was found to recognise two polypeptides by western blotting neither of which are kinesin-1, raising doubts over the specificity of this reagent and the validity of the *in vivo* data. Indeed, Feiguin and co-workers observed that suppression of KHC expression in cultured rat hippocampal neurons had no effect upon the BFA-induced redistribution of the cis/medial Golgi marker mannosidase II or the trans-Golgi marker NBD-ceramide back to the ER [145]. Instead, this study reported that tubules positive for the TGN-localised mannose-6-phosphate receptor (M6PR) did not form in the absence of KHC, indicating that different motors may be responsible for the motility of specific subsets of BFA-induced tubules.

Another motor implicated in driving the motility of BFA-induced tubules is the kinesin-3 family member, KIF1C. Overexpression of a dominant negative form of KIF1C, KIF1C305-9, which lacks the ability to bind ATP while retaining the ability to bind cargoes, prevented the retrograde flow of cis-Golgi contents to the ER in response to BFA in the NIH-3T3 cultured embryonic mouse fibroblastic cell line [146]. However, this data was refuted by studies on the KIF1C knockout mouse which displayed a normal response to BFA [147]. It is possible that other motors are able to compensate for the absence of KIF1C in the knockout mouse which is not possible when dominant negative proteins are used. A link between the kinesin-4 family member KIF21A and tubule motility has been recently made since this motor binds another target of BFA, BFA-inhibited guanine nucleotide-exchange protein [148]. However, the

importance of this interaction remains to be determined since KIF21A is reported not to associate with membranes, at least in neurons [149].

The identity of the motor(s) responsible for moving BFA-induced tubules remains a contentious and poorly understood area. The motility of endosomal and lysosomal tubules has been studied very little and it is unknown whether a single motor is responsible for all tubule motility or a cohort of motors function, perhaps co-ordinately, to drive these large scale changes in membrane organisation. The situation is further complicated by the observation that perturbation of myosin II function caused a delay in BFA-induced fusion of the cis-Golgi with ER [150], implying actin motors may also play important roles in these transport processes. It is undetermined whether the transfer of material between ER, Golgi and the endocytic system observed following BFA treatment represents an enhanced version of trafficking pathways which operate normally in untreated cells or whether this motility is specifically induced by the drug. Interestingly, tubules positive for the KDEL receptor have been observed to extend away from the Golgi in untreated cells in a microtubule-dependent fashion with similar dynamics to those induced by BFA treatment, before retracting back towards the Golgi or breaking away and travelling towards the cell periphery [151].

1.4.3 Post-Golgi trafficking

Proteins delivered to the Golgi from the ER which do not undergo retrograde trafficking back to the ER are either moved forward through the secretory pathway or are sorted to the endocytic system (Figure 1.4).

Certain cargoes are delivered from the TGN to the endocytic pathway, either directly or via the plasma membrane, in a process dependent upon clathrin and its associated adaptor protein (AP) complexes. Lysosomal hydrolases are transported to the late endosome from the TGN in complex with M6PR. The kinesin-3 family member KIF13A is implicated in this process since it has been observed to interact directly with the β1-adaptin subunit of AP1 and its overexpression resulted in the mislocalisation of AP1 and M6PR [152]. Following deposition of lysosomal hydrolases at the late endosome M6PR is trafficked back to the Golgi, although the motor responsible for this movement remains unidentified. Kinesin-1 has also been linked to trafficking between the Golgi and endocytic system via its interaction with γ1-adaptin and kinesin interactor (Gadkin), an accessory factor of AP1 [153]. A model is proposed in which Gadkin mediates the motility of a subset of TGN-derived vesicles positive for the recycling endosomal marker, transferrin receptor, dependent upon its direct interactions with KLC2 and AP1.

Cargoes destined for the secretory pathway traverse the Golgi stack undergoing any necessary modifications before reaching the TGN where they are sorted and packaged into a variety of transport carriers. During constitutive exocytosis, which all cell types perform, following release from the TGN carriers move to and fuse with the plasma membrane in a microtubule-dependent manner (reviewed in [71]). A function for myosin II in carrier budding from the TGN in vertebrate cells has been proposed although this remains controversial [154, 155]. Myosin VI and Rab8, together with the effector protein optineurin, are implicated in the initial movement of cargoes

away from the Golgi [156]. Indeed, fibroblast cells isolated from the Snell's Waltzer myosin VI knockout mouse exhibited a defect in alkaline phosphatase secretion [157]. Transport of carriers towards the plasma membrane is dependent upon the activity of kinesin-1, another unidentified plus end-directed microtubule motor, and unexpectedly cytoplasmic dynein-1 [133]. Furthermore, when Rab6 expression was depleted carrier motility became disorganised, suggesting this GTPase may coordinate the activities of multiple motors which function within this transport step [133]. The latter stages of transport through the actin rich cell cortex, enabling docking and fusion of carriers with the plasma membrane, is likely to require the activities of myosin motors. Interestingly, Rab6 is also suggested to control docking of exocytic vesicles to the plasma membrane by interacting with the cortical protein ELKS [133]. During regulated secretion, which is performed only by certain cell types, cargoes are still sorted and packaged into vesicles at the TGN and move away using kinesin-1 [158], but they are then stored within the cell and only dock and fuse with the plasma membrane in response to a specific extracellular stimulus. Roles for myosin Va [159] and kinesin-1 [91] in this final transport step have been suggested.

The situation is considerably more complex in polarised cells where cargoes must be directed to specific regions of plasma membrane and will only be discussed briefly here (reviewed in [160]). In neurons, TGN-derived carriers can be either targeted to the axon or the dendrite. The Reelin receptor, Apolipoprotein E Receptor 2 (ApoER2), which interacts indirectly with KLC1 via JIP1 and JIP2, is directed specifically to axons [161]. Other cargoes such as the α-amino-3-hydroxy-5-methylisoxazole-4-propionate (AMPA) receptor, which interacts indirectly with KHC via glutamate receptor-interacting protein 1 (GRIP1), are directed to dendrites [162]. The mechanism underlying the ability of kinesin-1 to recognise and target these cargoes to different regions of the plasma membrane is poorly understood, but it is hypothesised that scaffold molecules may convey information to the motor regarding the appropriate destination of the cargo. In epithelial cells, where microtubules are organised longitudinally, carriers can be directed to the apical or basolateral membranes. Minus end-directed motors including cytoplasmic dynein-1 [163] and the kinesin-14B family member KIFC3 [164], as well as kinesin-1 [24], have been implicated in the targeting of cargoes to the apical membrane.

1.4.4 Endocytosis

Endocytosis involves the uptake of material, such as nutrients and signalling molecules, from outside the cell. During clathrin-mediated endocytosis the binding of proteins to cell surface receptors initiates a cascade of events which trigger the invagination of the plasma membrane into clathrin-coated vesicles. These vesicles initially deliver their contents to the early endosome where material is then sorted (Figure 1.4). This initial inward movement of cargoes through the actin rich cell cortex has been proposed to driven by propulsion generated by actin polymerisation [165] and myosin VI activity [166]. The positioning and rapid motility of early endosomes is controlled by cytoplasmic dynein-1 [167] and the kinesin-3 family member KIF16B [66], enabling both inward and outward movement [167].

Cargoes which are to be returned to the plasma membrane, such as transferrin and its receptor, undergo fast or slow recycling where they are trafficked directly to the cell surface or indirectly via the recycling endosome, respectively. The myosin Va and Vb motors appear integral to recycling endosome positioning and motility and the transport of transferrin receptor to the cell surface was delayed when the function of these two motors was perturbed [168]. Kinesin-1 has also been implicated in this transport step since perturbation of kinesin-1 function was observed to slow cycling of transferrin to the plasma membrane in Chinese hamster ovary cells [169]. Meanwhile, those cargoes which are to be degraded remain within early endosomes, which subsequently mature into late endosomes and fuse with lysosomes. Alternatively, a specific subset of proteins, including STB, are delivered directly from early endosomes to the TGN in a process linked to the activities of cytoplasmic dynein-1 and Cdc42 [170, 171]. Interestingly, it appears trafficking from the endocytic system to the Golgi is not always dependent upon microtubules since the cargo receptor TGN38 has been shown to move from early endosomes to the TGN following treatment with the microtubule depolymerising agent nocodazole [172], perhaps pointing to myosin function in this pathway.

Members of the sorting nexin (SNX) protein family also perform important functions during endocytosis and endosomal sorting, implicated in driving membrane curvature and providing a link to microtubule motors. SNX proteins each contain a Phox-homology domain, a phosphoinositide-binding motif, which mediates binding to membranes enriched in particular phosphoinositides (reviewed in [173]). Perhaps the best characterised function of SNX proteins is in the retrieval of cargoes from the endocytic system to the TGN. This is dependent upon a protein complex called retromer, which in mammals consists of several SNX proteins including SNX1, SNX2, SNX5 and SNX6 (reviewed in [174]). This complex is proposed to link cargoes to cytoplasmic dynein-1 since both SNX5 and SNX6 have been shown to interact with the p150*glued* subunit of dynactin [175]. Additionally, SNX4, a protein involved in transport between the early and recycling endosome has been observed to associate with cytoplasmic dynein-1 [176, 177]. Other members of the SNX family are implicated in cargo recycling from the endocytic system to the plasma membrane and in clathrin-mediated endocytosis (reviewed in [174]).

Both late endosomes and lysosomes are highly motile and move bidirectionally [178] with inward movement dependent upon cytoplasmic dynein-1 [179]. Perturbation of kinesin-2 function resulted in the clustering of late endosomes around the MTOC [180], suggesting the motor contributes to the outward movement of this organelle. A variety of plus end-directed motors have been linked to driving lysosome motility including kinesin-1 [181], kinesin-2 [180], and KIF1Bβ3 [54]. The contribution of actin motors to late endosome and lysosome motility and positioning has not been investigated in detail, although myosin VIIa has been found associated with lysosomes [182].

1.5 Organelle dynamics in mitosis

1.5.1 Cell cycle

The vertebrate cell cycle is comprised of a series of sequential and tightly regulated events which are separated into four discrete stages termed G1, S, G2 and M phases. G1, G2 and S phases are collectively referred to as interphase during which cell growth and DNA replication occur to prepare the cell for division. During mitotic M phase the cell divides to generate two diploid daughter cells, whereas meiotic M phase comprises two rounds of division resulting in four haploid daughter cells [1].

M phase can be further subdivided into five distinct phases called prophase, prometaphase, metaphase, anaphase and telophase. During prophase chromatin condenses and each centrosome, which is duplicated during S phase, moves to opposite poles of the cell. In higher eukaryotes, the nuclear envelope disassembles during prometaphase allowing highly dynamic microtubules to contact a specialised region of each chromosome known as the kinetochore. This is in contrast to yeast where the nuclear envelope remains intact throughout cell division. This connection underlies the alignment of chromosomes during metaphase at the metaphase plate, located equidistant between each centrosome. Sister chromatids are separated during anaphase and pulled towards opposite poles of the cell and the nuclear envelope reforms and chromatids unfold during telophase. Cytokinesis is necessary to separate the cytoplasm and plasma membrane and once completed marks the end of M phase [1].

The serine/threonine cyclin-dependent protein kinases (CDKs), and their cyclin binding partners have essential regulatory roles in these processes, with different CDKs operating at various points of the cell cycle (reviewed in [183]). When in complex with their relevant cyclin binding partner, CDKs each phosphorylate a specific set of substrate proteins, triggering cell cycle progression. CDK1, the master regulator of cell division, associates with cyclin B during mitosis leading to phosphorylation of multiple target proteins (reviewed in [1, 183]). The complex of CDK1 and cyclin B is required for the transition from G2 to M phase, whereas exit from M phase requires inactivation of CDK1 (reviewed in [184]). The association with cyclins is partly responsible for regulating CDK1 function, with binding required for CDK1 activity, and as such is tightly regulated. This is achieved by strict control of cyclin synthesis and degradation leading to fluctuation in cyclin levels during the cell cycle. Cyclins are targeted for proteasome-mediated degradation by the addition of poly-ubiquitin tags [185]. There are two mammalian B-type cyclins, termed B1 and B2, which both bind CDK1 specifically during M-phase [186]. Cyclin B1 is more highly expressed then cyclin B2, and is essential for survival [187].

During the transformation from interphase to mitosis several fundamental changes in membrane organisation and organelle dynamics occur, which are closely linked to changes in microtubule motor function (reviewed in [188]), some of which are discussed below.

1.5.2 ER motility and inheritance

The ER typically adopts an extended tubular-lamellar network characterised by the formation of three-way junctions between neighbouring tubules. Continuous with the nuclear envelope, the ER network is concentrated around the nucleus but extends to the periphery of the cell lying in close proximity to the plasma membrane. Rough and smooth ER is differentiated by the presence or absence of ribosomes on the membrane surface respectively. In recent years it has become apparent that the ER is not a static organelle, but is constantly moving and remodelling. In plant cells this motility is largely dependent upon the actin cytoskeleton and its associated myosin motors (reviewed in [189]). Contrastingly, in animal cells microtubule-dependent transport and anchoring plays a much larger role with a smaller contribution from actin filaments. Several complementary studies, comprising a wide range of cultured epithelial cell lines, have observed that when the microtubule cytoskeleton is depolymerised the ER network slowly retracts towards the cell centre [190-193], highlighting the close relationship between these two networks. There are a variety of means by which the ER network is linked to the microtubule cytoskeleton. Some of these are stable long-lived connections believed to be necessary to maintain the ER structure and morphology, whereas others are much more dynamic and underlie movement of ER tubules.

Early studies observing fluorescently labelled ER in living cultured epithelial cells indicated that the majority of ER motility is in an outward direction from the cell centre towards the cell periphery, thus implicating a plus end-directed microtubule motor [193, 194]. The major plus end-directed motor studied in relation to ER motility is kinesin-1 and several studies have linked this motor to the outward movement of ER tubules. A role for kinesin-1 in driving ER movement was first proposed in 1988 by Dabora and Sheetz following the observation that the *in vitro* motility of ER membranes isolated from chick embryo fibroblasts was dependent upon microtubules and ATP, although no evidence specifically linking kinesin-1 to ER motility was provided [195]. This hypothesis was supported by data showing that suppression of KHC expression in cultured rat hippocampus neurons promoted retraction of the ER towards the nucleus [145], and a reduction in ER motility [196]. Recently, inhibition of kinesin-1 function using the dominant negative kinesin-1 protein KHCct was shown to potently inhibit ER motility *in vitro* [30], and a portion of outward-directed ER tubule movements in the monkey kidney epithelial cell line, VERO [197].

The binding of kinesin-1 to ER cargo is dependent upon at least two ER-associated proteins, kinectin and p180. Kinectin is an integral ER membrane protein initially identified by Toyoshima and co-workers as interacting with the KHC tail [198]. When the interaction between kinectin and kinesin-1 was disrupted in HeLa cells, either via small interfering RNA (siRNA)-mediated depletion of kinectin or overexpression of the binding regions necessary for the interaction, collapse of the ER towards the cell centre was observed [199]. Interestingly, kinectin does not simply anchor kinesin-1 to the ER but is also capable of promoting the ATPase activity of the motor, indicating it may aid unfolding of the kinesin-1 molecule (see section 1.3.3) [200]. Another integral ER membrane protein, p180, has also been reported to bind KHC [201]. p180

is specifically located on rough ER since it associates with ribosomes and its interaction with kinesin-1 remains tenuous since all data to date is *in vitro* and no *in vivo* association between the two proteins has been observed. The influence this association has upon ER morphology remains to be investigated, and the ability of p180 to bind both kinesin-1 and ribosomes simultaneously may indicate the interaction is more important in controlling mRNA localisation rather than ER positioning. Recent data showing that the exogenous addition of a particular isoform of KLC, KLC1B, inhibited ER motility *in vitro* [30], indicates KLC also binds ER and that engagement of KLC with an ER localised receptor is required for motility. However, the identities of any KLC binding partners on the ER remain elusive.

Several observations suggest kinesin-1 activity is not solely responsible for driving ER motility. Instead, it is believed several distinct mechanisms operate, perhaps co-ordinately, to move and anchor the ER to the microtubule cytoskeleton, making the situation decidedly more complex. Indeed, fixed cell analysis of fibroblasts isolated from the *kif5b* knockout mouse embryo revealed no apparent defects in ER morphology [18], and *kinectin* knockout mice displayed normal ER positioning [202]. Furthermore, inhibition of kinesin-1 function in VERO cells had only a subtle effect on ER distribution, resulting in a slight decrease in ER intensity at the cell periphery and a switch towards a more lamellar morphology, while a subset of outward tubule movements persisted even when kinesin-1 function has been perturbed [197]. Other motors, including cytoplasmic dynein-1 [89, 197] and myosin V [203], have been reported to contribute to ER motility in certain situations. Furthermore, the microtubule +TIP EB1 interacts directly with the ER transmembrane protein stromal interaction molecule 1 to form a tip attachment complex (TAC) [204]. This allows ER tubules to elongate together with the EB1-positive plus end of a growing microtubule. In this situation ER tubules link selectively to the growing plus tips of microtubules and ER tubule extension is driven by microtubule polymerisation and is independent of motor activity.

The integral rough ER membrane protein, cytoskeleton-linking membrane protein of 63 kDa (CLIMP-63), binds microtubules directly and provides a stable connection between the two networks [205]. This interaction is important to the correct positioning of the ER network since overexpression of CLIMP-63 in cultured cells results in ER collapse towards the cell centre. There are several other proteins which have been reported to bind both microtubules and ER and may thereby contributed to ER positioning and morphology, including the calcium-binding protein p22 [206].

Changes are known to occur to ER positioning and morphology during cell division, although a high degree of variability between cell types and organisms is apparent. Whilst it is known that the CLIMP-63-mediated interaction between ER and microtubules is regulated in a cell cycle-dependent manner, with the protein becoming hyperphosphorylated at three serine residues causing dissociation from microtubules and perturbation of ER positioning [207], how ER motility is modulated during cell division is poorly understood. The major reported changes that

occur to ER positioning and morphology during mitosis in mammalian cells and budding yeast will be briefly outlined.

The main structural change to occur to the ER during cell division in mammalian cells is the breakdown of the nuclear envelope during prometaphase, dependent upon the activity of cytoplasmic dynein-1, leading to spreading of nuclear envelope components throughout the ER [208]. The rest of the network remains continuous during cell division and does not breakdown into vesicles or fragments but is reported to be excluded from the region occupied by the mitotic spindle with stochastic partitioning between daughter cells thought to occur during anaphase [209-211] (Figure 1.5). Normally, ER membrane fusion events are mediated partially by the activities of the AAA ATPase p97 and its cofactor p47 [212]. Semi-intact cell assays indicated that p47 is a substrate of CDK1 leading to perturbation of p97 function and the mitotic inhibition of ER tubule fusion [211]. Additional changes in the organisation of the ER during mitosis have also been observed in a range of cultured cell lines and developing *Caenorhabditis elegans* embryos. There appears to be a switch from the reticular interphase ER structure consisting of relatively short tubules which are highly branched, to a more cisternal, sheet-like morphology during mitosis, with very few tubules remaining [213, 214]. This change is proposed to be driven by the dramatic reorganisation of the microtubule cytoskeleton during cell division.

By contrast, in budding yeast nuclear envelope breakdown does not occur and the mitotic spindle forms inside the nucleus, meaning the nuclear envelope and perinuclear ER are separated together with DNA in a microtubule-dependent fashion. The rest of the ER network which lies just beneath the plasma membrane extends into the growing bud where it becomes anchored at the tip by a multiprotein tethering complex called the exocyst, before spreading throughout the cortex (reviewed in [215]). The inheritance of cortical ER is dependent upon the myosin V family member, Myo4, and its adaptor protein, She3, which travel along actin filaments positioned along the mother-bud axis [216].

Since cells round up considerably during division, the imaging of ER tubule motility during mitosis is a difficult procedure. However, progress has been made in studying changes to ER motility during the cell cycle by reconstituting motility *in vitro* using *Xenopus laevis* egg extracts. When membrane and cytosol fractions from interphase extracts are mixed together an extensive ER network is able to form which is solely dependent upon the activity of cytoplasmic dynein-1. However, if an identical assay is performed using cytosol prepared from metaphase-arrested extracts, the network fails to form [217]. This inhibition of motility is due to the metaphase-specific phosphorylation of DLIC by CDK1, which triggers dissociation of the motor from ER membranes and thereby inhibits movement [89].

This dependence of ER motility in *Xenopus laevis* eggs upon cytoplasmic dynein-1 may appear at odds with the previously described data indicating kinesin-1 plays a prominent role in ER movement. In fact kinesin-1 is present on ER in *Xenopus laevis* eggs but is inactive and evidence suggests that kinesin-1-driven ER motility is activated during development. When

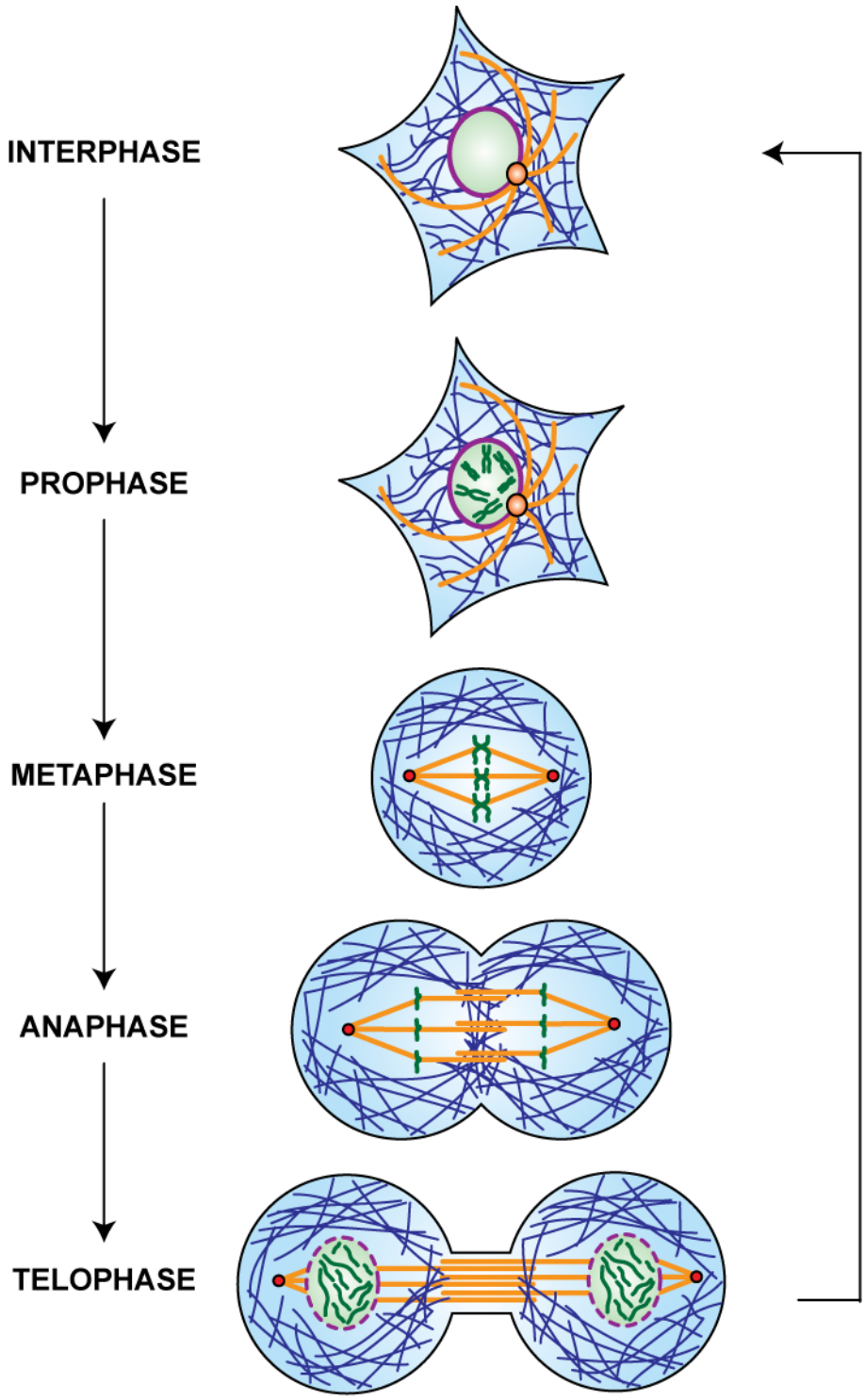

Figure 1.5 - ER inheritance in mammalian cells

ER inheritance in mammalian, non-polar cells during mitosis is outlined. Microtubules are shown in orange, ER in blue, nuclear envelope in purple, centrosomes in red and chromosomes in green. Adapted from [213].

membranes isolated from *Xenopus laevis* eggs were mixed with cytosol prepared from somatic *Xenopus laevis* tissue culture (XTC) cells a portion of ER motility was supported by kinesin-1 [218]. This was reliant upon the activation of membrane-bound kinesin-1 and was not simply due to recruitment of the motor from the cytosol to the ER cargo. It is probable that the relative contributions of cytoplasmic dynein-1 and kinesin-1 to ER movement are precisely controlled and under certain situations one motor may take prominence thus allowing the tight temporal and spatial regulation of ER network remodelling. The movement of *Xenopus laevis* egg ER exclusively by a single motor likely represents an extreme situation where the opposing motor has been completely inactivated, but is still responsive to particular stimuli and can be activated under certain situations.

Despite these advances, how the ER is correctly segregated between daughter cells and whether ER motility changes during cell division remains a contentious and poorly understood area, especially in mammalian cells.

1.5.3 Golgi inheritance and trafficking processes

Unlike the ER network, the Golgi apparatus undergoes major structural changes in its organisation during cell division. In mammalian cells the lateral connections between adjacent Golgi stacks are lost during prophase allowing conversion of the compact interphase Golgi structure into small vesicles as well as larger vesicular and tubular structures during metaphase [219]. Two models exist to explain the fate of these fragments whereby they are either stochastically partitioned between daughter cells during anaphase [220], or subsequently fuse with the ER and are inherited together with this organelle [221] (reviewed in [215]). Fusion of Golgi fragments occurs during telophase leading to reformation of the interphase perinuclear Golgi ribbon. In budding yeast the Golgi is organised into numerous units dispersed throughout the cytoplasm during interphase. A *de novo* model of Golgi inheritance is proposed in which complete intact Golgi structures are produced anew, emanating from ERES (reviewed in [215]).

Given the drastic alterations in morphology and positioning of organelles within the secretory pathway during mitosis it is perhaps not surprising that the flux of material through trafficking pathways is subject to alteration during cell division. Protein synthesis, secretion, pinocytosis, and clathrin-mediated endocytosis are all downregulated during cell division. Warren and co-workers showed that the transport of newly synthesised VSV-G protein to the plasma membrane is blocked during mitosis and resumes during telophase [222], and subsequent work revealed cargo transit is inhibited early in the secretory pathway with the protein being retained in the ER [223]. Indeed, ERES have been observed to disassemble during mitosis resulting in a block in ER-to-Golgi transport [224]. Reconstitution of this process in semi-intact cell assays has indicated that this inhibition is dependent upon the phosphorylation of p47 by CDK1. Both fluid endocytosis, phagocytosis and clathrin-mediated endocytosis are completely suppressed throughout mitosis in a range of cultured cell lines [225, 226], while the *in vitro* formation of BFA-induced tubules is blocked in the presence of metaphase *Xenopus laevis* egg extract cytosol [144].

Due to the integral role kinesin-1 plays in these processes it is possible that regulation of the activity of this motor may contribute to the large scale changes in cargo trafficking and organelle motility which occur during cell division. Unlike cytoplasmic dynein-1, kinesin-1 has no documented roles specifically in mitosis. The motor is reported to contribute to the translocation and orientation of the female meiotic spindle in *Caenorhabditis elegans* and this is dependent upon the interaction of KLC1 and KLC2 with kinesin cargo adaptor protein-1 (KCA-1) [227]. However, no KCA-1 homologues exist outside of nematodes and actin-dependent transport appears to play a much more prominent role in mammalian cells [228]. Therefore, if kinesin-1 is controlled in a cell cycle-dependent manner it is likely that rather than switching from interphase- to mitotic-specific functions, the activity of the motor may be downregulated or even inhibited specifically during cell division.

1.5.4 *Xenopus laevis* egg extracts

Membrane motility can be reconstituted using cytoplasmic extracts prepared from *Xenopus laevis* eggs in cell-free motility assays. These extracts have several distinct advantages over other *in vitro* assays or *in vivo* studies, especially when investigating microtubule motor regulation (reviewed in [229]). The cytosol is diluted very little during preparation meaning extracts with a high concentration of motors are generated, capable of supporting a high level of microtubule-dependent motility at room temperature which is easily visualised using video-enhanced differential interference contrast (VE-DIC) microscopy. Furthermore, several protein modifications such as phosphorylation are supported, meaning membrane motility can be correlated to post-translational modifications under virtually identical assay conditions. The activity of a single microtubule motor can often be studied in isolation, allowing the contribution that a motor makes to a complex process to be investigated without the effects of other motors distorting results. This is an increasingly useful attribute as it becomes apparent that often motors do not work in isolation *in vivo* but cooperate and coordinate with each other, with bidirectional motility a common feature [230, 231]. This often makes *in vivo* studies a difficult means of trying to identify how a particular motor may be regulated. Interestingly, the ability to reconstitute membrane motility in these assays is not limited to *Xenopus laevis* since rough ER- and Golgi-enriched fractions isolated from rat liver are both motile when mixed with cytosol prepared from interphase *Xenopus laevis* egg extracts [89, 232].

Importantly, the natural conversion of *Xenopus laevis* eggs between cell cycle states can be utilised to generate extracts arrested in meiosis, mitosis and interphase. *Xenopus laevis* eggs are naturally arrested in metaphase II of meiosis when laid. This is due to the high level of cytostatic factor (CSF) which maintains a high level of maturation-promoting factor (MPF) [233]. MPF is a complex of cyclin B and CDK1 [234, 235]. Fertilisation triggers a high level of calcium influx into the egg and calcium release from intracellular stores, which subsequently inactivates CSF, triggering cyclin B degradation and thereby inactivation of MPF. These events lead to release from the meiotic arrest and entry into interphase, allowing embryonic development to progress [236].

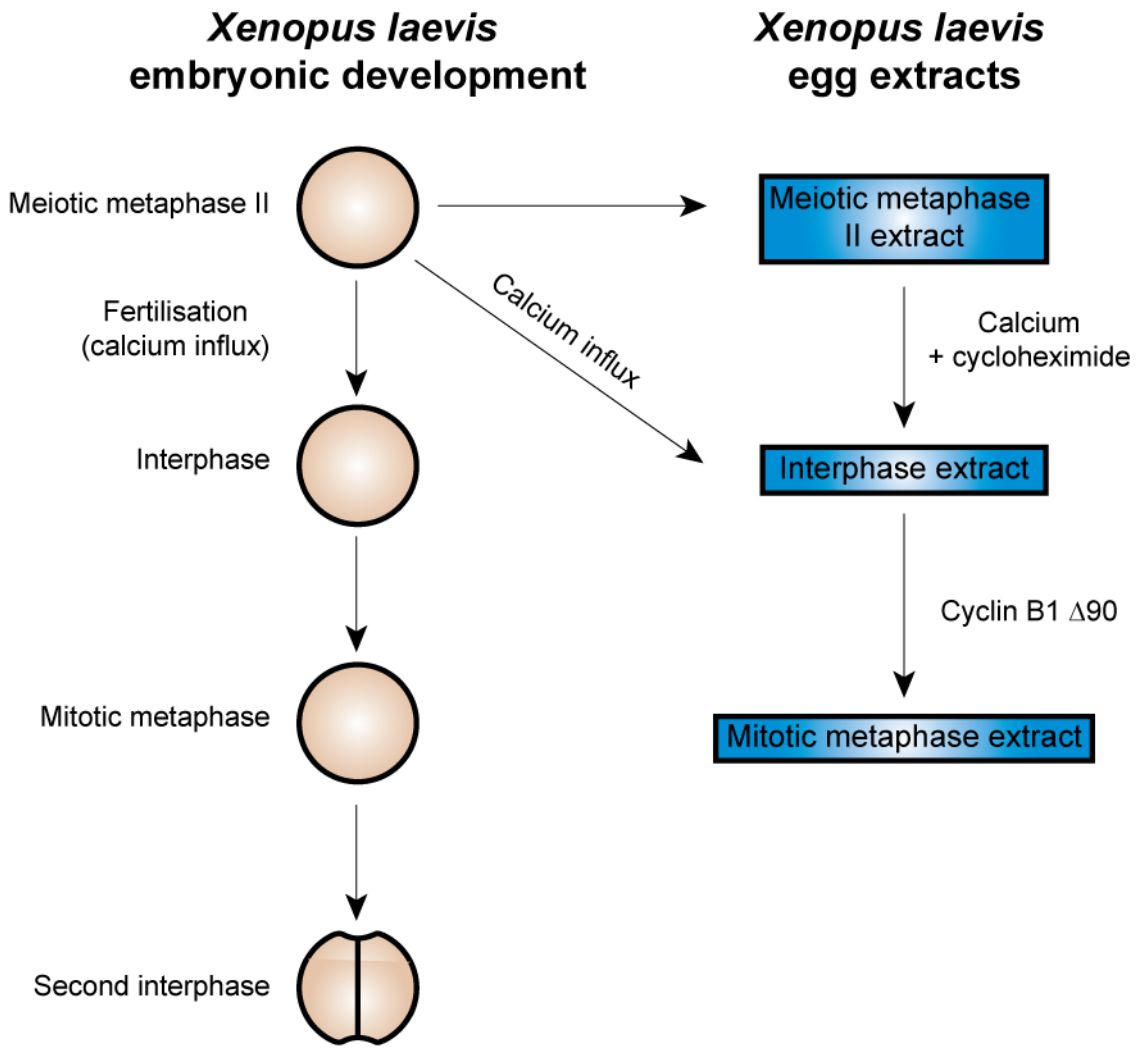

Figure 1.6 - Generation and conversion of *Xenopus laevis* egg extracts

The initial cell division events following fertilisation of *Xenopus laevis* eggs are outlined. These events can be manipulated to generate *Xenopus laevis* egg extracts arrested in meiotic metaphase II, mitotic metaphase or interphase. Treatment of a meiotic metaphase II extract with calcium and cycloheximide stimulates conversion to interphase. Treatment of an interphase extract with cyclin B1 Δ90 protein promotes conversion to mitotic metaphase.

Extracts prepared from *Xenopus laevis* eggs can be arrested in different cell cycle states by artificially manipulating the events which control the transition between interphase and metaphase (Figure 1.6). By injecting *Xenopus laevis* frogs with hormones which induce the laying of eggs, a high number of unfertilised eggs arrested in metaphase II of meiosis are obtained. If extract preparation is performed in the presence of calcium chelators, to eliminate any free calcium capable of triggering conversion to interphase, meiotic metaphase II-arrested extracts can be generated [237]. Due to the high level of MPF and CSF present in these samples which underlie the meiotic arrest, they are often referred to as CSF extracts. Treatment of CSF extracts with exogenous calcium simulates the events which occur following fertilisation and thereby prompts conversion into interphase. If cycloheximide is included during the activation step the extract will be arrested in interphase due to an inability to regenerate metaphase cyclins [237].

Alternatively, extracts arrested in interphase can be made directly from meiotic eggs. The simplest method is to perform the preparation in the absence of calcium chelators, meaning any calcium present in buffers or released from eggs following crushing will stimulate conversion into interphase. Extracts prepared in this manner are termed Newmeyer in reference to Donald Newmeyer who initially documented this protocol [238]. Interphase Newmeyer extracts can be converted to a mitotic metaphase arrest by treatment with a mutant form of the cyclin B1 protein, termed cyclin B1 Δ90 [236]. Cyclin B1 regulates the activity of the key mitotic kinase CDK1, with binding of the cyclin required for CDK1 function (see section 1.5.1) [233, 236]. Normally the level of cyclin B1 is tightly regulated and to inactivate CDK1, the cyclin is targeted for degradation by the proteasome by the addition of ubiquitin tags [185]. Cyclin B1 Δ90 is a truncated version of the wild-type protein lacking 90 amino acids from the N-terminus, rendering the protein unable to be ubiquitinated whilst retaining the ability to interact CDK1 [236]. Therefore the mutant cyclin B1 is non-degradable rendering CDK1 constitutively active, meaning the extract is arrested in mitotic metaphase.

1.6 Aims of the studies

This study was comprised of two major sections, both examining the function and regulation of kinesin motors. Firstly, the regulation of kinesin-1 in a cell cycle-dependent manner will be investigated, and secondly the identity of the motor(s) responsible for moving BFA-induced tubules will be probed.

1.6.1 Cell cycle regulation of kinesin-1

The initial aim of this project is to determine if, similar to cytoplasmic dynein-1 [89], kinesin-1-driven ER motility is regulated in a cell cycle dependent manner *in vitro*. To answer this question rough ER isolated from rat liver will be combined with cytosol prepared from interphase, meiotic metaphase or mitotic metaphase *Xenopus laevis* egg extracts. It is known that rat liver rough ER is motile in interphase cytosol *in vitro,* where it forms an extensive network characterised by the formation of three-way junctions between neighbouring tubules [232]. Importantly, this motility is known to be exclusively dependent upon kinesin-1 [30], meaning any perturbation of movement in metaphase cytosols can be attributed to modulation of kinesin-1 activity.

If ER motility is affected following incubation with metaphase cytosols, it is aimed to identify the mechanism underlying this modulation. There are a number of potential scenarios by which this may occur and these are outlined in Figure 1.7. These include modulation of the interaction between kinesin-1 and ER cargo, or between the motor and the microtubule, specifically in metaphase cytosol. Phosphorylation of kinesin-1 may occur specifically in the interphase or metaphase assay, which has a corresponding effect upon motor function. Alternatively, the ability of kinesin-1 to bind or hydrolyse ATP may be regulated in a cell cycle-dependent manner. The interaction between KHC and KLC subunits of kinesin-1 following incubation with interphase or metaphase cytosol will also be investigated. Finally, it is possible that binding partners interact with kinesin-1 specifically following incubation with interphase or metaphase cytosol which are capable of modulating motor activity. Each of these possibilities will be investigated in turn to identify which, if any, is responsible for controlling kinesin-1 activity in a cell cycle-dependent manner *in vitro*.

1.6.2 Motility of BFA-induced tubules

The aim of the project is to identify the motor(s) responsible for the motility of BFA-induced tubules. Initially, *in vitro* motility assays will be performed using Golgi membranes isolated from rat liver to reconstitute the motility of BFA-induced tubules which has been used successfully in similar previous studies [144]. The activities of kinesin-1, kinesin-2 and KIF1C, which play prominent roles in driving membrane motility in interphase metazoan cells (see sections 1.2.1, 1.2.2 and 1.2.3), will be perturbed *in vitro* using dominant negative proteins and function-blocking antibodies. The contribution of KIF1C to this process will be investigated in detail due to the controversy surrounding the role of this motor in driving retrograde trafficking from the Golgi to the ER in response to BFA (see section 1.4.2.2) [146, 147].

This *in vitro* approach will be complemented by *in vivo* studies using the human epithelial cell line, HeLaM. The activities of kinesin-1, kinesin-2 and KIF1C will be disrupted using transient transfection of dominant negative constructs and siRNA-mediated depletion. The ability of cis-Golgi, TGN, endosomal and lysosomal tubules to form will be assessed using immunofluorescence studies incorporating antibodies raised against markers for each of these compartments.

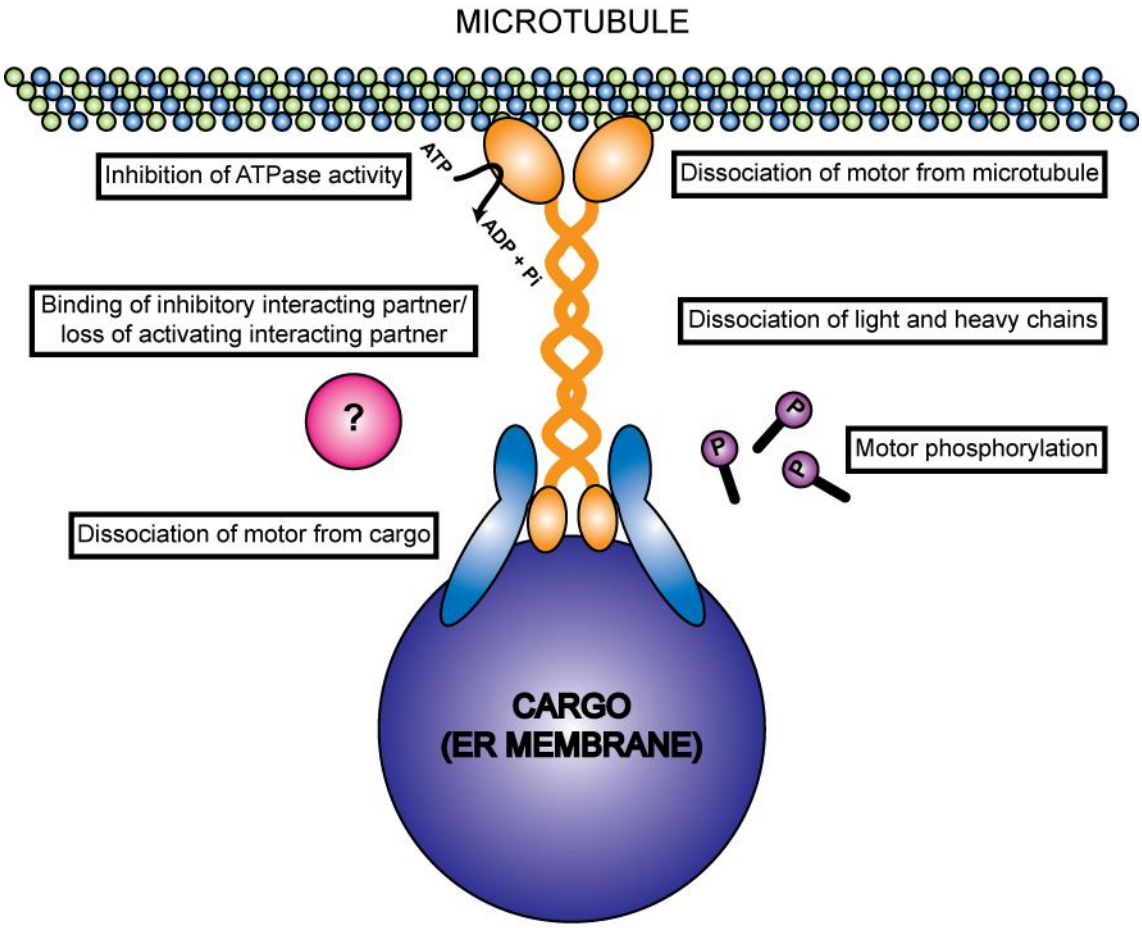

Figure 1.7 - Potential mechanisms of kinesin-1 regulation

Schematic of the kinesin-1 motor with KHC (orange) and KLC (blue) bound to cargo and microtubules. Outlined are potential mechanisms by which kinesin-1 activity may be regulated.

Table 1.1 – Expression of kinesin-1, -2 and -3 motors in various species

Kinesin family	Motor/ subunit	Isoform	Splice variants	Tissue-specific expression	Cell cycle-specific function(s)	Human accession number	Rat accession number	Xenopus accession number/reference
Kinesin-1	KIF5	KIF5A		Neuronal [23]*	None known	NM004984	NM212523.1	NM001102745.1
		KIF5B		Ubiquitous	The *Caenorhabditis elegans* homologue of KIF5B, UNC-116, has been reported to be involved in the translocation of the female meiotic spindle to the egg cortex [227]	NM004521.2	NM057202.1	NM001128654.1
		KIF5C		Neuronal [22]*	None known	NM004522.1	NM001107730.1	Unknown
	KLC	KLC1	KLC1A	Unknown	The *Caenorhabditis elegans* homologue of KLC1 has been reported to be involved in the translocation of the female meiotic spindle to the egg cortex [227]	BK000678	NM001081972.1	NM001087151.1
			KLC1B	Unknown		BK001166	NM001081973.1	Unknown
			KLC1C	Unknown		AY180164	NM001081974.1	Unknown
			KLC1D	Unknown		BK001163	Unknown	Unknown
			KLC1E	Unknown		BK001164	Unknown	Unknown
			KLC1F	Unknown		BK000680	Unknown	Unknown
			KLC1G	Unknown		BK001170	Unknown	Unknown
			KLC1H	Unknown		BK000682	Unknown	Unknown
			KLC1I	Unknown		BK000681	Unknown	Unknown
			KLC1J	Unknown		BK001172	Unknown	Unknown
			KLC1K	Unknown		BK001167	Unknown	Unknown
			KLC1L	Absent from human liver tissue [28]		ENST00000303439	Unknown	Unknown
			KLC1M	Unknown		BK000683	Unknown	Unknown
			KLC1N	Unknown		BK001168	Unknown	Unknown
			KLC1O	Unknown		BK000679	Unknown	Unknown
			KLC1P	Unknown		BK001169	Unknown	Unknown
			KLC1Q	Unknown		BK000684	Unknown	Unknown
			KLC1R	Unknown		BK001171	Unknown	Unknown
			KLC1S	Unknown		BK001165	Unknown	Unknown
		KLC2	KLC2A	Ubiquitous	The *Caenorhabditis elegans* homologue of KLC2 has been reported to be involved in the translocation of the female meiotic spindle to the egg cortex [227]	NM022822.2	BC166555.1	Unknown
			KLC2B			NM001134774.1	Unknown	Unknown
			KLC2C			NM001134775.1	Unknown	Unknown
			KLC2D			NM001134776.1	Unknown	Unknown
		KLC3		Enriched in mouse spermatids [26]	None known	NM177417.2	NM138520.1	[239]
		KLC4	KLC4A	Unknown	None known	NM201521.1	NM001009601.1	Unknown
			KLC4B	Unknown	None known	NM201522.1	Unknown	Unknown
			KLC4C	Unknown	None known	NM201523.1	Unknown	Unknown
			KLC4D	Unknown	None known	NM138343.2	Unknown	Unknown
Kinesin-2	KIF3A			Ubiquitous	Localised to the mitotic spindle and centrosomes in mitotic HeLa cells [240]	NM007054	NM053486.1	NM001090799.1
	KIF3B			Ubiquitous		NM004798	NM001106529.1	XM002939655.1
	KIF3C			Neuronal [241]*		NM002254	NM053486.1	XM002942110.1

	KAP3			Ubiquitous	Overexpression of mutant KIF3B in NIH-3T3 cells results in aberrant mitosis [240]	NM014970.2	NM001105964.1	NM001092562
	KIF17	KIF17A		Neuronal [42]*	None known	NM020816.2	Unknown	Unknown
		KIF17B			None known	NM001122819.1	Unknown	Unknown
Kinesin-3	KIF1	KIF1A		Neuronal [55]*	None known	NM004321	XM343630.4	XM002933334.1
		KIF1B	KIF1Bα	Unknown	None known	NM183416.3	NM057200.1	XM002939557.1
			KIF1Bβ	Enriched in mouse motor neurons [242]*	None known	NM015074.3	Unknown	Unknown
		KIF1C		Enriched in human brain and skeletal muscle [146]	None known	NM006612.5	NM145877.1	XM002942910.1
	KIF13	KIF13A	KIF13Aa	Enriched in mouse brain, lung, heart, kidney, and testes [243]	None known	NM022113.4	NM001107462.1	Unknown
			KIF13Ab		None known	NM001105566.1	Unknown	Unknown
			KIF13Ac		None known	NM001105567.1	Unknown	Unknown
			KIF13Ad		None known	NM001105568.1	Unknown	Unknown
		KIF13B		Ubiquitous	None known	AF279865	NM213626.1	Unknown
	KIF14			Enriched in mouse brain and kidney [243]	Implicated in cytokinesis and chromosome segregation [64, 65]	NM014875.2	Unknown	Unknown
	KIF16	KIF16A		Enriched in mouse lung, heart, kidney and testes [243]	None known	AK122666	Unknown	Unknown
		KIF16B		Enriched in mouse lung [243] and testes [13]	None known	NM024704.3	NM001107783.2	Unknown

* It should be noted that the tissue-specific distribution of several kinesin motors, especially those which are reported to be specifically expressed in neurons, is controversial and the mRNA of several of these motors has recently been detected in human epithelial cell lines [24].

Table 1.2 – KHC interacting partners

Cargo	KHC isoform and/or binding region	Species	Reference	Notes
Disrupted-In-Schizophrenia-1	KIF5A Within amino acids 706-829	Rat	[244]	The interaction is responsible for linking kinesin-1 to a complex of NudE-like/Lissencephaly 1/14-3-3. This is important for axonal localisation of the complex.
Enabled	Within amino acids 714-975	*Drosophila*	[245]	Enabled is an actin polymerisation factor. The interaction is proposed to negatively regulate kinesin-1 activity.
FEZ1	KIF5B Within amino acids 750-955	Rat	[103]	FEZ1 binding to KHC is required for JIP1 transport. See section 1.3.3.
GRIF1	KIF5B and KIF5C	Rat	[98]	GRIF1 is the rat homologue of the *Drosophila melanogaster* protein milton. It is proposed to be important in mitochondrial positioning. See section 1.3.2.
GRIP1	KIF5A, KIF5B and KIF5C Within amino acids 807-934	Mouse	[162]	The interaction may be important for the dendritic targeting of AMPA receptors. See section 1.4.3.
Kinectin	KIF5A, KIF5B and KIF5C Within amino acids 828-900	Human	[198, 200]	Kinectin is an integral ER membrane protein. Binding of kinectin to KHC increases the ATPase activity of the motor. See section 1.5.2.
Milton	Within amino acids 810-891	*Drosophila*	[95, 246]	Milton links KHC to mitochondria independently of KLC. It is homologous to OIP106 and GRIF1. See section 1.3.2.
Myosin Va	KIF5B Within amino acids 763-856	Mouse	[247]	The interaction may be important in coordinating actin and microtubule transport. It is proposed that both motors may bind a subset of the same cargoes.
OIP106	KIF5B and KIF5C	Human	[98]	OIP106 is the human homologue of the *Drosophila melanogaster* protein milton. It is proposed to be important in mitochondrial positioning. See section 1.3.2.
p120 catenin	KIF5B and KIF5C	Mouse	[248, 249]	p120 catenin is a component of adherens junctions. The interaction is proposed to be important for the cell surface trafficking of cadherins.
p180	KIF5B Within amino acids 867-907	Human	[201]	p180 is an integral ER membrane protein with the ability to bind ribosomes. The interaction is proposed to be important for the correct localisation of mRNA. See section 1.5.2.
Ran-binding protein 2	KIF5B and KIF5C Within amino acids 640-964	Mouse	[250]	The interaction is observed in retina and brain tissue. It is proposed that kinesin-1 may be delivering unknown cargoes to Ran-binding protein 2. No interaction seen with KIF5A.
Synaptosome-associated protein of 23 kDa and 25 kDa	KIF5B Within amino acids 814-907	Human	[251]	Synaptosome-associated protein of 25 kDa is specifically neuronally expressed.
Syntabulin	Within amino acids 814-963	Rat	[252]	It is proposed that syntabulin may link kinesin-1 to syntaxin and thereby mediate its axonal transport.
UNC-76	Within amino acids 675-975	*Drosophila*	[253]	UNC-76 is the *Drosophila melanogaster* homologue of FEZ1. UNC-76 may regulate kinesin-1 activity to facilitate axonal transport.
α-Dystrobrevin β-Dystrobrevin	KIF5A and KIF5B Within amino acids 804-934	Mouse	[254]	The interaction may be important for transport of the dystrophin-associated protein complex in neurons.

Table 1.3 – KLC interacting partners

Cargo	KLC isoform and/or binding region	Organism	Reference	Notes
Amyloid precursor protein	KLC1 and KLC2 Within amino acids 167-541	Mouse	[255]	Amyloid precursor protein plays a key role in Alzheimer's disease. The interaction with KLC is proposed to be important in the axonal transport of the protein.
Calsyntenin-1	KLC1	Mouse	[256]	Calsyntenin-1 is a neuronal transmembrane protein belonging to the cadherin superfamily. The interaction may link other cargoes to kinesin-1.
Collapsin response mediator protein-2	KLC2 Within amino acids 168-542	Mouse	[257]	This interaction links tubulin to kinesin-1 and may be important in driving the transport of soluble tubulin into the axon.
DIC	KLC1 and KLC2	Rat	[83]	The interaction is proposed to be important for localising cytoplasmic dynein-1 to particular sites of function.
Frat	KLC1	Mouse	[239]	Frat is homologous to the *Xenopus* protein GBP and is a GSK3-binding protein. The interaction is proposed to be important for transport of Wnt signalling complexes.
Gadkin	KLC2	Rat	[153]	Gadkin associates with kinesin-1 and AP1 and may be important in mediating trafficking between the TGN and endocytic system. See section 1.4.3.
GBP	XKLC4 Within amino acids 1-44	*Xenopus*	[239]	GBP is homologous to the vertebrate protein Frat. Kinesin-1 may compete with GSK3 to bind GBP. The interaction may be important for targeting of GBP to the dorsal side of the embryo and cortical rotation.
GLUT4	KLC1	Rat	[258]	GLUT4 is a glucose transporter protein. The interaction is proposed to be important for the translocation of intracellular vesicles to the plasma membrane in response to insulin.
HSC70	KLC1	Mouse	[85]	The phosphorylation of KLC by GSK3 promotes binding of HSC70 which aids cargo removal from kinesin-1. See section 1.3.1.
JIP1	KLC1 Within amino acids 1-176	Mouse	[161]	The concentration of JIP1 protein at the nerve terminal is dependent upon the interaction with kinesin-1. It is involved in the axonal targeting of ApoER2 (see sections 1.3.3 and 1.4.3) and amyloid precursor protein.
JIP2	KLC1 Within amino acids 1-176	Mouse	[161]	Involved in the axonal targeting of ApoER2. See section 1.4.3.
JIP3	KLC1 Within amino acids 1-176	Mouse	[161]	JIP3 can form oligomeric complexes with itself and JIP2.
JIP4	KLC1 Within amino acids 192-422	Mouse	[259]	The interaction between KLC and JIP4 is decreased when cells are serum starved.
Kinase D-interacting substrate of 220 kDa/ankyrin repeat-rich membrane spanning	KLC1 Within amino acids 83-296	Rat	[260]	The cargo is a conserved transmembrane protein mainly expressed in brain and neuroendocrine cells. The interaction is proposed to mediate the recruitment of other cargoes to kinesin-1.

KCA-1	KLC1 and KLC2	*Caenorhabditis elegans*	[227]	The interaction is proposed to be important for orientation of the female meiotic spindle. See section 1.5.3.
Outer dense fibre-1	KLC3	Rat	[261]	The interaction is proposed to be important during spermatogenesis.
Sunday driver	KLC1 and KLC2 Within amino acids 4-163	*Drosophila*	[262]	It is proposed that sunday driver acts as an adaptor protein linking kinesin-1 with a subset of neuronal vesicles. Homologous to JIP3.
Tau	KLC1 and KLC2	Rat	[263]	Kinesin-1 is important for the axonal transport of tau, a protein implicated in Alzheimer's disease.
TorsinA	KLC1 Within amino acids 251-332	Rat	[264]	Mutation of torsinA gives rise to early torsion dystonia, which may be linked to the intracellular trafficking of the protein.
UNC-14	KLC2	*Caenorhabditis elegans*	[265]	The protein is involved in neurite outgrowth.
UNC-16	KLC2 Within amino acids 1-174	*Caenorhabditis elegans*	[265]	UNC-16 is the *Caenorhabditis elegans* homologue of JIP3. The axonal localisation of UNC-16 is dependent upon its interaction with kinesin-1.
14-3-3 protein	KLC2 Within amino acids 354-599	Rat	[90]	14-3-3 proteins constitute a diverse family implicated in several signal transduction pathways. The interaction is dependent upon phosphorylation of KLC. See section 1.3.1.

2. Materials and Methods

2.1 Solutions/reagents

The following reagents were purchased from Sigma-Aldrich, Gillingham, UK: 1,4-Diazabicyclo(2,2,2)octane (DABCO), 1,4-piperazinediethanesulfonic acid (PIPES), 4',6-diamidino-2-phenylindole (DAPI), ammonium persulphate (APS), ampicillin, aprotinin, ATP, bromophenol blue, casein, chymostatin, colloidal Coomassie, Coomassie brilliant blue, creatine phosphate, creatine phosphokinase, cycloheximide, cysteine, D-biotin, dimethyl sulfoxide (DMSO), dithiothreitol (DTT), ethidium bromide, ethyleneglycoltetraacetic acid (EGTA), fish skin gelatine, glass wool, GTP, histone H1, isopropyl β-D-1-thiogalactopyranoside (IPTG), kanamycin, Kodak BioMax MR Film, leupeptin, N,N,N',N'-Tetramethylethylenediamine (TEMED), Na-β-glycerophosphate, nocodazole, paraformaldehyde (PFA), pepstatin, phenylmethanesulfonyl fluoride (PMSF), Ponceau S, reduced L-glutathione, sodium borohydride, sodium azide, sterile phosphate-buffered saline (PBS), sterile trypsin containing ethylenediaminetetraacetic acid (EDTA), taxol, Triton X-100, Tween-20, β-mercaptoethanol.

The following reagents were purchased from Fisher Scientific, Leicestershire, UK: 4-(2-hydroxyethyl)-1-piperazineethanesulfonic acid (HEPES), acetic acid, $CaCl_2$, EDTA, ethanol, glutaraldehyde, glycerol, glycine, HCl, K-acetate, KCl, KH_2PO_4, methanol, $MgCl_2$, $MgSO_4$, Na_2HPO_4, Na-acetate, NaCl, sodium dodecyl sulfate (SDS), sucrose, trichloroacetic acid, Tris-HCl.

The following reagents were purchased from VWR International, West Sussex, UK: Chloroform, KOH, Mg-acetate, Na-acetate, NaOH, Na-pyrophosphate, phenol.

Acetate buffer

100 mM K-acetate, 3 mM Mg-acetate, 5 mM EGTA, 10 mM HEPES, pH 7.4 with KOH

Acetate sucrose buffer (A/S)

100 mM K-acetate, 3 mM Mg-acetate, 5 mM EGTA, 10 mM HEPES, pH 7.4 with KOH, 150 mM sucrose

Activation mix

100 mM KCl, 1 mM $MgCl_2$, 4 mM $CaCl_2$

ATP

100 mM stock made with 100 mM $MgCl_2$, pH 7.0 with NaOH

Bacterial lysis buffer

1 mM PMSF, 1 % (v/v) Triton X-100, 0.2 % (v/v) Tween-20 in PBS

Brinkley reassembly buffer (BRB80)

80 mM PIPES, 1 mM $MgCl_2$, 1 mM EGTA, pH 6.8 with KOH

BFA

10 mg/ml stock in methanol (Enzo Life Sciences, Exeter, UK)

Complete media

Dulbecco's Modified Eagle Medium (Biowhittaker, Lonza, Berkshire, UK), 1 % (v/v) L-Glutamine (200 mM in 0.85 % (w/v) NaCl solution) (Biowhittaker), 10 % (v/v) HyClone Foetal Calf Serum (Perbio, Northumberland, UK)

Coomassie stain

50 % (v/v) ethanol, 7.5 % (v/v) acetic acid, 0.2 % (w/v) Coomassie brilliant blue

Coomassie destain

40 % (v/v) methanol, 10 % (v/v) acetic acid

Cycloheximide

10 mg/ml stock in DMSO

Energy mix (20x)

150 mM creatine phosphate, 20 mM ATP, 20 mM $MgCl_2$, 2 mM EGTA, pH 7.7

Extraction buffer

80 mM Na-β-glycerophosphate, 15 mM $MgCl_2$, 20 mM EGTA, pH 7.3 with NaOH. The following additions were made just before use: 1 mM DTT, 1 µg/ml protease inhibitors

Human chorionic gonadotropin (HCG)

1500 U/ml in phosphate-buffered water (Intervet, Cambridgeshire, UK)

Histone H1

20 mg/ml stock in water (type III-S from calf thymus)

Histone kinase cocktail

2 mg/ml histone H1, 0.1 mM ^{32}P-γ-ATP (PerkinElmer, Cambridgeshire, UK) in extraction buffer

Immunoprecipitation (IP) buffer

10 mM Tris-HCl, 80 mM Na-β-glycerophosphate, 10 mM Na-pyrophosphate, pH 7.7, 1 % (v/v) Triton X-100. Just before use 10 µg/ml protease inhibitors was added

Laemmli sample buffer (3x)

180 mM Tris-HCl, 20 % (v/v) glycerol, 6 % (w/v) SDS, 15 % (v/v) β-mercaptoethanol, 0.01 % (w/v) bromophenol blue

LB medium

25 g of granulated LB (Melford Laboratories, Suffolk, UK) per litre of distilled water

Marc's modified ringer's (MMR) buffer (1x)

0.1 M NaCl, 2 mM KCl, 1 mM $MgCl_2$, 2 mM $CaCl_2$, 5 mM HEPES, 0.1 mM EGTA, pH 7.8 with NaOH

Mock activation mix

100 mM KCl, 1 mM $MgCl_2$

Motility buffer

20 mM PIPES, 10 mM K-acetate, 4 mM $MgSO_4$, pH 6.7 with KOH. The following additions were made just before use: 10 µM taxol, 1 mg/ml casein, 4 mM ATP, 7.5 mM creatine phosphate, 4 U/ml creatine phosphokinase, 0.5 % (v/v) β-mercaptoethanol

Mowiol mounting solution

25 % (v/v) glycerol, 0.1 g/ml Mowiol 4-88 (Calbiochem, Nottingham, UK), 0.1 M Tris-HCl, pH 8.5, 2.5 % (w/v) DABCO

NET buffer

150 mM NaCl, 5 mM EGTA, 50 mM Tris-HCl, 0.05 % (v/v) Triton X-100, pH 8.0

NET-G buffer

150 mM NaCl, 5 mM EGTA, 50 mM Tris-HCl, 0.05 % (v/v) Triton X-100, 0.25 % (v/v) fish skin gelatine, pH 8.0

Nocodazole

10 mM stock in DMSO

PBS

137 mM NaCl, 2.7 mM KCl, 4.3 mM Na_2HPO_4, 1.47 mM KH_2PO_4, pH 7.4

Phosphocellulose column buffer

0.1 M PIPES, 1 mM KOH, 1 mM $MgSO_4$, 1 mM EGTA, pH 6.9 with KOH. The following additions were made just before use: 0.1 mM GTP, 1 mM DTT

Pregnant mare serum gonadotropin (PMSG)

200 U/ml in phosphate-buffered water (Intervet, Buckinghamshire, UK)

Ponceau S stain

0.2 % (w/v) Ponceau S, 3 % (w/v) trichloroacetic acid

Protease inhibitors

10 mg/ml leupeptin, 10 mg/ml chymostatin, 10 mg/ml pepstatin, 10 mg/ml aprotinin in DMSO

Sodium dodecyl sulphate polyacrylamide gel electrophoresis (SDS-PAGE) resolving buffer

1.5 M Tris-HCl, pH 8.8, 10 % (w/v) SDS

SDS-PAGE stacking buffer

0.5 M Tris-HCl, pH 6.8, 10 % (w/v) SDS

SDS-PAGE running buffer

25 mM Tris-HCl, 25 mM glycine, 0.1 % (w/v) SDS, pH 8.3

TE buffer

10 mM Tris-HCl, pH 7.5, 1 mM EDTA

T-Tris-buffered saline (T-TBS)

20 mM Tris-HCl, 150 mM NaCl, pH 7.7 with HCl, 0.1 % (v/v) Tween-20

Transfer buffer

25 mM Tris-HCl, 0.2 M glycine, 20 % (v/v) methanol, 0.02 % (w/v) SDS, pH 8.3

Tubulin purification buffer A

0.1 M PIPES, pH 6.9 with KOH, 25 % (v/v) glycerol. The following additions were made just before use: 0.1 % (v/v) β-mercaptoethanol, 0.1 mM GTP

Tubulin purification buffer B

0.1 M PIPES, pH 6.9 with KOH. The following additions were made just before use: 0.1 % (v/v) β-mercaptoethanol, 0.2 mM GTP, 0.1 mM PMSF

Tubulin purification buffer C

0.5 M PIPES, 1 mM EGTA, 1 mM $MgSO_4$, pH 6.9 with KOH. The following additions were made just before use: 10 mM β-mercaptoethanol, 0.1 mM GTP

Extract buffer (XB)

100 mM KCl, 1 mM $MgCl_2$, 0.1 mM $CaCl_2$, 10 mM HEPES, 50 mM sucrose, pH 7.7 with KOH

2.2 Cell-based assays

2.2.1 Cell culture

HeLaM cells were obtained from Graham Warren, EMBL, Heidelberg, Germany and are a subclone of the human cervical cancer cell line, HeLa. HeLaM cells were cultured in complete

media in 8 % CO_2 and passaged in T75 flasks (Corning, Flintshire, UK) using PBS and 0.5 mg/ml trypsin and 0.2 mg/ml EDTA.

2.2.2 Transient transfection

HeLaM cells were plated at a density of 70,000 cells per well in a 12-well plate (Corning) on 13 mm coverslips (no. 1.5 thickness) to give a confluency of approximately 70 % the following day. Transfection was performed using the cationic transfection reagent JetPEI (QBiogene, Cambridgeshire, UK) in accordance with manufacturer's 'Quick protocol', where 2 µg of DNA and 4 µl of JetPEI are used per well of a 12-well plate. However, when transfecting mApple-Golgi DNA, it was necessary to titrate the amount of DNA used, since perturbation of Golgi structure was observed when the protein was highly expressed (data not shown). To this end, 20 ng of mApple-Golgi DNA was used per well of a 12-well plate along with 1.98 µg of the other construct being transfected. mApple is a monomeric fluorophore with a maximal excitation and emission spectra of 568 nm and 592 nm, respectively [266]. It was generated by the mutation of 18 amino acids of the mOrange fluorophore and is listed under the accession number DQ336160. The Golgi targeting tag is the N-terminal 81 amino acids of the human beta 1,4-galactosyltransferase protein, a Golgi-resident glycosylation enzyme, which is linked to mApple at the C-terminus. A similar fragment of the bovine form of the enzyme has previously been shown to be sufficient for retention of the protein within the Golgi [267].

2.2.3 KIF1C siRNA

An ON-TARGETplus siRNA SMARTpool containing four duplexes directed against human KIF1C RNA (catalogue number L-010354, accession number NM006612) and a siGENOME non-targeting siRNA control (catalogue number D-001210) were purchased with target sequences listed below (Dharmacon, Thermo Fisher Scientific, Northumberland, UK). To analyse whether KIF1C protein levels were efficiently reduced following siRNA treatment, HeLaM cells were plated in 10 cm dishes (Corning) at a density of 800,000 cells per dish to give a confluency of approximately 60 % the following day. Transfection of SMARTpool KIF1C siRNA at a final concentration of 0.5 nM, 1 nM, 5 nM, 10 nM and 20 nM was performed using INTERFERin (Autogen Bioclear, Wiltshire, UK) in accordance with the manufacturer's instructions and OptiMEM (Invitrogen, Paisley, UK) was used as a source of reduced serum media. All four duplexes were present in each transfection at an equal concentration. After 72 hours, cells were placed on ice and washed twice with ice cold PBS. To lyse the cells 500 µl of BRB80 containing 0.5 % (v/v) Triton X-100 and 10 µg/ml protease inhibitors was added and left on ice for 10 minutes with gentle agitation. The cells were scraped into the buffer using a cell scraper (Greiner Bio One, Gloucestershire, UK) and transferred to a 1.5 ml microfuge tube. Samples were centrifuged at 14,000 rpm (22,800 g_{av}) at 4 °C for 10 minutes in a microcentrifuge to remove cell nuclei and debris, and the supernatant was recovered. The protein concentration was determined using a bicinchoninic acid assay (Pierce, Thermo Fisher Scientific, Northumberland, UK) in accordance with manufacturer's instructions and samples were stored at -80 °C. To perform western blotting 25 µg of each sample was run on an 8 % SDS-PAGE gel as described in section 2.4.1 and immunoblotted with anti-KIF1C and anti-TAT1 antibodies as described in sections 2.3 and 2.4.4.

For all subsequent experiments treatment with KIF1C-specific and non-targeting siRNA at a final concentration of 0.5 nM was performed, with 13 mm coverslips (no. 1.5 thickness) added to the dishes as appropriate. All four duplexes of the SMARTpool were included in each experiment at an equal concentration (i.e. 0.125 nM to give a final siRNA concentration of 0.5 nM). This concentration of siRNA was chosen because it was determined to be the lowest concentration which maximally reduced KIF1C protein levels in HeLaM cells. If necessary, after 48 hours coverslips were transferred to a 12-well plate and transfection with dominant negative kinesin constructs was performed as described in section 2.2.2.

KIF1C-specific siRNA	Target Sequence
Duplex 1	GCAGCAAGGCAUCGACAUA
Duplex 2	GGAGCUGUGUCGCACCUAU
Duplex 3	CGAAUGAGACGGCAGCGUU
Duplex 4	GAACCAGAGUGCUCAGCUA
Non-targeting siRNA	**Duplex sequence**
Duplex 1	UAGCGACUAAACACAUCAA

2.2.4 BFA treatment

For labelling with anti-transferrin receptor, anti-EEA1, anti-TGN46 antibodies, or when co-transfected with mApple-Golgi, HeLaM cells were treated with 2 µg/ml BFA for 10 minutes, 8 minutes, 12 minutes, or 10 minutes respectively, since these time points were judged to give the maximum number of cells displaying tubules positive for these markers in untransfected cells (data not shown). Cells were fixed and immunolabelled as appropriate (see sections 2.2.5 and 2.3).

To determine whether microtubule dynamics play a role in moving cis-Golgi tubules, low doses of nocodazole were used to inhibit microtubule dynamics without depolymerising microtubules. Cells were treated with 100 nM nocodazole for 5 minutes and then with 100 nM nocodazole and 2 µg/ml BFA for 10 minutes, fixed in methanol as described in section 2.2.5.1 and immunolabelled as necessary. The concentration of nocodazole required to inhibit microtubule dynamics was optimised using live cell imaging of HeLaM cells transfected with tomato-EB3 (see section 2.5.1), a microtubule plus end tracking protein, and green fluorescent protein (GFP)-tubulin (data not shown).

To quantify the effects of motor inhibition upon the tubulation of the various compartments investigated, the absence or presence of tubules in 100 cells per condition was counted. Each experiment was repeated two additional times to obtain three average values per condition. These values were then used for statistical analysis. SPSS 15.0 (SPSS, Surrey, UK) was used to perform a one-way analysis of variance (ANOVA) test followed by a two-sided Dunnett's post-hoc test, allowing the comparison of multiple test groups to a single control group simultaneously. This was used in preference to multiple student t-tests since analysis is faster

and the probability of performing a type I error i.e. rejecting the null hypothesis when it is actually true is reduced.

2.2.5 Immunofluorescence

2.2.5.1 Methanol fixation

Coverslips were washed in PBS and excess liquid was removed using filter paper (Whatman, Kent, UK) before placing in -20 °C methanol for 5 minutes. Coverslips were washed once in PBS for 5 minutes and then immunolabelled as necessary.

2.2.5.2 PFA fixation

Coverslips were washed in PBS and dried on filter paper and transferred to 3 % (w/v) PFA in PBS and incubated at room temperature for 30 minutes. Coverslips were washed 3 x 5 minutes in PBS with the first wash containing 0.1 M glycine to block reactive groups. Cells were permeabilised to allow subsequent entry of the antibody by incubating in 0.1 % (v/v) Triton X-100 in PBS for 5 minutes. Coverslips were washed 3 x 5 minutes with PBS and then immunolabelled as necessary.

2.2.5.3 PFA/Glutaraldehyde fixation

Coverslips were processed as described in section 2.2.5.2 except 0.25 % (w/v) glutaraldehyde was included in the incubation with 3 % (w/v) PFA. To block reactive groups, coverslips were washed 3 x 5 minutes with a freshly made 1 mg/ml sodium borohydride solution in PBS.

2.2.5.4 Antibody labelling

Antibodies were diluted to the appropriate concentration as described in section 2.3.1 in 25 µl PBS. The solution was placed on a sheet of parafilm and the coverslip was dried on filter paper and placed cells facing down onto the drop of antibody for 30 minutes in the dark. Excess primary antibody was removed with 3 x 5 minutes washes in PBS in a 12-well plate. Coverslips were placed cells facing down onto a drop of appropriately diluted secondary antibody in PBS as described in section 2.3.2 and left for 30 minutes in the dark. Again, coverslips were washed 3 x 5 minutes in PBS in a 12-well plate to remove excess secondary antibody, with the first wash containing 100 µl of a 1 µg/ml DAPI solution to stain cell nuclei. After the final wash coverslips were dipped in distilled water to prevent the formation of salt crystals on the surface of the coverslip, dried thoroughly on filter paper, and mounted with cells facing down on 6 µl of Mowiol mounting solution on a microscope slide. Coverslips were left in the dark overnight at room temperature to allow the mounting solution to set.

The Alexa594-conjugated phalloidin dye (Invitrogen) was used to stain actin at a dilution of 1 in 40 in PBS. Cells were fixed in PFA as described in section 2.2.5.2 and coverslips were processed identically as described above except no incubation with secondary antibody was necessary.

2.2.5.5 Imaging

Images were taken using a BX60 microscope (Olympus, Watford, UK) fitted with a 60x 1.40 N.A. PlanApo objective and a Roper Scientific CoolSnap ES camera (Photometrix, Arizona, USA). The camera was controlled using MetaVue software (Molecular Devices, California,

USA). Images were captured in 16-bit greyscale and subsequent figure preparation was performed using PhotoShop CS2 (Adobe, California, USA) and Adobe Illustrator CS2 (Adobe).

2.3 Antibodies

2.3.1 Primary antibodies

Antibody	Antigen	Host species	Usage	Fixation	Blocking buffer	Source
Calreticulin	Calreticulin	Rabbit	1:100 (IF)	PFA/ Glutaraldehyde	N/A	Affinity Bioreagents, Thermo Fisher Scientific, Northumberland, UK
DLIC	DLIC	Sheep	1:1000 (IB)	N/A	5 % milk	Laboratory generated
EEA1	Early endosome antigen 1	Mouse	1:500 (IF)	PFA	N/A	BD Transduction Laboratories
ERGIC53	ERGIC protein of 53 kDa	Mouse	1:500 (IF)	PFA	N/A	Axxora UK, Nottingham, UK
Hsp70	Heat shock protein of 70 kDa	Mouse	1:250 (IF)	PFA	N/A	Affinity Bioreagents, Thermo Fisher Scientific
IC74	DIC	Mouse	1:1000 (IB)	N/A	5 % milk	Chemicon, Millipore,
k2.4	KIF3A subunit of kinesin-2	Mouse	1:500 (IB)	N/A	5 % milk	Hybridoma Bank, University of Iowa, Iowa, USA
KIF1C	KIF1C	Rabbit	1:1000 (IB)	N/A	NET-G	Abcam, Cambridge, UK
KIF1C serum	KIF1C	Rabbit	1:300 (IF)	PFA or methanol	N/A	Dr. Marcin Wozniak, The Bristol Institute of Transfusion Sciences, Bristol UK
L1	KLC	Mouse	IP	N/A	N/A	Chemicon, Millipore
L2	KLC	Mouse	IP	N/A	N/A	Chemicon, Millipore
LAMP1	Lysosomal-associated membrane protein 1	Mouse	1:300 (IF)	Methanol	N/A	Hybridoma Bank, University of Iowa
Myc	Myc	Rabbit	1:150 (IF)	PFA or methanol	N/A	Chemicon, Millipore
p150*glued*	p150*glued*	Mouse	1:2000 (IB)	N/A	NET-G	BD Transduction Laboratories
SUK4	KHC	Mouse	IP	N/A	N/A	Hybridoma Bank, University of Iowa
TAT1	α-tubulin	Mouse	1:1000 (IB)	N/A	NET-G	Prof. Keith Gull, University of Oxford, Oxford, UK
			1:100 (IF)	Methanol	N/A	
TGN46	TGN46	Sheep	1:500 (IF)	Methanol	N/A	Dr. Martin Lowe, University of Manchester, Manchester, UK
Transferrin receptor	Transferrin receptor	Mouse	1:100 (IF)	Methanol	N/A	Zymed, Invitrogen
Ubiquitously expressed KHC (uKHC)	KHC	Rabbit	1:2000 (IB)	N/A	NET-G	Prof. Ron Vale, UCSF, San Francisco, USA

The abbreviations used to denote antibody usage are immunoblot (IB), immunofluorescence (IF) and immunoprecipitation (IP).

2.3.2 Secondary antibodies

Conjugated tag	Anti-species	Host species	Usage	Source
Alexa594	Mouse	Donkey	1:800	Molecular Probes, Invitrogen
	Rabbit	Donkey	1:800	
Alexa488	Mouse	Donkey	1:400	Molecular Probes, Invitrogen
	Rabbit	Donkey	1:400	
Cy3	Mouse	Donkey	1:800	Jackson ImmunoResearch, Stratech, Suffolk, UK
	Rabbit	Donkey	1:800	
	Sheep	Donkey	1:800	
Cy5	Mouse	Donkey	1:800	Jackson ImmunoResearch
	Rabbit	Donkey	1:800	
Horseradish peroxidise (HRP)	Mouse	Donkey	1:3000	DakoCytomation, Cambridgeshire, UK
	Rabbit	Donkey	1:3000	
	Sheep	Donkey	1:3000	

2.4 Protein analysis

2.4.1 SDS-PAGE

Mini protean III hand cast 1 mm thick resolving gels were made using SDS-PAGE resolving buffer, polyacrylamide (ProtoGel, National Diagnostics, Atlanta, USA), distilled water, TEMED and 10 % (w/v) APS and overlaid with 100 % ethanol. Once the resolving gel had set, the ethanol was poured away and any excess was removed with filter paper. Stacking gels were made with SDS-PAGE stacking buffer, polyacrylamide, distilled water, TEMED and 10 % (w/v) APS and poured on top of the resolving gel and a 15-well comb was inserted. Once the stacking gel was set the comb was removed and samples loaded, including 5 µl of protein marker (Benchmark 10 kDa protein ladder – Invitrogen). Samples were heated at 95 °C for 5 minutes prior to loading, except if stated otherwise. Gels were run at 100 Volts until the dye front had reached the bottom of the gel and then stained with Coomassie (see section 2.4.2), colloidal Coomassie (see section 2.4.3) or transferred to nitrocellulose membrane for western blotting (see section 2.4.4).

2.4.2 Coomassie stain

Following SDS-PAGE, the stacking gel was discarded and the resolving gel was transferred to Coomassie stain and left for 1 hour with gentle rocking. The gel was washed with Coomassie destain solution until all background staining was removed.

2.4.3 Colloidal Coomassie stain

Following SDS-PAGE, the stacking gel was discarded and the resolving gel was fixed in 40 % (v/v) methanol and 7 % (v/v) acetic acid for 1 hour with gentle rocking. Four parts colloidal Coomassie was combined with 1 part methanol, shaken vigorously to mix, and added to the gel to stain for 2 hours with gentle rocking. The gel was then de-stained in 25 % (v/v) methanol and 10 % (v/v) acetic acid for 30 seconds and then in 25 % (v/v) methanol with gentle rocking until background staining had been fully removed.

2.4.4 Western blot

Following SDS-PAGE, gels were transferred onto Protran nitrocellulose membrane (Whatman) in transfer buffer using a Mini Trans-Blot Electrophoretic Transfer Cell (Bio-Rad Laboratories, Hertfordshire, UK) for 90 minutes at 100 Volts. The nitrocellulose was stained with Ponceau S solution to visualise proteins, excess stain was removed with distilled water, and protein markers were marked using ink. The membrane was incubated with NET-G solution or 5 % (w/v) non-fat milk (Marvel) in T-TBS for 1 hour with gentle rocking to block any non-specific antibody binding. The membrane was then incubated with the primary antibody (made up in NET-G solution or 5 % (w/v) non-fat milk in T-TBS as appropriate) and left for 1 hour with gentle rocking. The membrane was washed 3 x 5 minutes with NET buffer or T-TBS and then the HRP-conjugated secondary antibody (made up in the same solution as the primary antibody) was added for a further hour with gentle rocking. The membrane was washed 3 x 5 minutes with NET buffer or T-TBS and then briefly with equal volumes of the two chemiluminescence reagents (Super Signal West Pico Stable peroxide solution, Pierce, Thermo Fisher Scientific). Finally, the membrane was wrapped in cling film, exposed to single emulsion photographic film (Kodak BioMax MR Film) and processed.

2.4.5 IP

A volume of 20 µl of protein G dynabeads (Invitrogen) were transferred to 1.5 ml microfuge tube and washed once with 500 µl IP buffer, using a magnet (Invitrogen) to re-isolate the beads. The beads were incubated with 5 µg of antibody for 1 hour at 4 °C with rotation. The antibody was then removed and the beads were washed once with 500 µl of IP buffer to remove any unbound antibody. The lysate was made up to 500 µl with IP buffer, incubated on ice for 10 minutes, and then centrifuged at 14,000 rpm (22,800 g_{av}) at 4 °C for 10 minutes in a microcentrifuge to remove any debris. After incubation of beads with lysate for 3 hours at 4 °C with rotation, unbound material was removed and the beads were washed four times with 500 µl of IP buffer. The bound material was eluted from the beads with 10 µl of 2x sample buffer, and samples were heated at 100 °C for 5 minutes and subject to SDS-PAGE electrophoresis and western blotting as described in sections 2.4.1 and 2.4.4.

2.5 Molecular biology

2.5.1 Constructs

Name	Source
K430-BCCP	Prof. Rob Cross, University of Warwick, Coventry, UK
Cyclin B1 Δ90	Prof. Tim Hunt, CRUK, London Research Institute, London, UK
EB3-tomato	Dr. Anne Straube, University of Warwick, Coventry, UK
GFP	Clontech, California, USA
GFP-KBPΔ250-81	Mr. Yen Ching Yang, University of Manchester, Manchester, UK
GFP-KHCct	Mr. Yen Ching Yang
GFP-tubulin	Prof. Roger Tsien, University of California, San Diego, USA
Glutathione S-transferase (GST)	GE Healthcare, Buckinghamshire, UK
GST-E-MAP-115	See section 2.5.9.2
GST-KAP3Bct	Dr. Marcin Wozniak
GST-KBPΔ250-81	See section 2.5.9.1

GST-KHCct	Dr. Marcin Wozniak
KAP3B-Myc	Dr. Marcin Wozniak
KIF1CΔ305-9	Dr. Reiner Lammers, University of Tübingen, Tübingen, Germany
mApple-Golgi	Dr. Michael Davidson, University of Florida, Florida, USA

2.5.2 Primers

Name	Sequence
GST-KBPΔ250-281 Forward	ATCATGGGAATTCTGGCGAACGTTCCGTGG
GST-KBPΔ250-281 Reverse	ATCATGCTCGAGTTAAGTCAGGGCCATC
GST-E-MAP-115 Forward	ATCATGGGAATTCTGGCGGAGCTAGGAG
GST-E-MAP-115 Reverse	ATCATGCTCGAGTCATATAACTTCTGCAGT
E-MAP-115 Sequencing 1	CAGGAACGAATGTGTGGGC
E-MAP-115 Sequencing 2	CAGCGTTGTTAACAGACTCC
E-MAP-115 Sequencing 3	ACATCCGCCCTGTCAAGAG
E-MAP-115 Sequencing 4	TGAAGAGAGGACGACTCG
pGex-3 (sequencing)	CCGGGAGCTGCATGTGTCAGAGG
pGex-5 (sequencing)	GGGCTGGCAAGCCACGTTTGGTG

2.5.3 Polymerase chain reaction (PCR)

Each PCR reaction contained 0.1 µg of template DNA, forward and reverse primers at 300 nM final concentration, 1 µl of 0.5 M β-mercaptoethanol (10 mM final concentration), 5 µl of 10x Pfu buffer (Stratagene, Agilent Technologies, Cheshire, UK), 0.4 µl dNTPs (200 µM of each) (Bioline, London, UK), 1 µl (2.5 U) Pfu turbo DNA polymerase (Stratagene), and was made up to 50 µl with autoclaved distilled water. The reactions were then subject to the following cycle in a PCR machine:

95 °C for 5 minutes
And 35 cycles of:
95 °C for 1 minute
? °C (5 °C below the lowest primer melting temperature) for 1 minute
72 °C for 1 minute per kb of the desired product
Followed by:
72 °C for 5 minutes
4 °C hold

A volume of 5 µl of the product was run on a 1 % (w/v) agarose gel (Lonza, Berkshire, UK), along with 5 µl of 1 kb DNA ladder (GeneRuler, Fermentas, York, UK) and stained in 1 % (v/v) ethidium bromide solution to determine whether the PCR had been successful.

2.5.4 DNA digestion

The PCR product was purified using a PCR purification kit (QIAGEN, Crawley, UK) in accordance with the manufacturer's instructions and eluted in 20 µl of elution buffer. The PCR product was incubated with the appropriate restriction enzymes for 2 hours at 37 °C. The vector was incubated with restriction enzymes for 90 minutes at 37 °C, after which 1 µl alkaline

phosphatase (Roche, Hertfordshire, UK) was added to minimise the vector re-annealing, and the incubation was continued for a further 30 minutes.

2.5.5 DNA gel extraction

The restriction digests were run on a 1 % (w/v) agarose gel, stained in ethidium bromide solution as described in section 2.5.3 and the correct bands were excised under low-intensity ultraviolet light. To purify DNA, the agarose slice was placed into a 500 µl microfuge tube with the base pierced and containing a small amount of glass wool. The tube was snap frozen in liquid nitrogen and placed inside a 1.5 ml microfuge tube. The DNA was centrifuged through the glass wool at 11,000 rpm (12,800 g_{av}) at 4 °C for 15 minutes in a microcentrifuge, after which the collection tube was replaced and the centrifugation was repeated. The eluted DNA was made up to 300 µl with TE buffer and half of this was added to 150 µl of phenol, vortexed briefly and centrifuged at 11,000 rpm (12,800 g_{av}) for 1 minute in a microcentrifuge. The upper phase was taken and added to 150 µl chloroform, vortexed and centrifuged as before. The upper phase was again taken and added to 30 µl 3 M Na-acetate. This protocol was repeated with the other 150 µl of eluted DNA using the same tubes of phenol, chloroform and Na-acetate. Finally 900 µl of 100 % ethanol was added to the Na-acetate and DNA mixture, vortexed briefly and centrifuged at 14,000 rpm (22,800 g_{av}) at 4 °C for 15 minutes in a microcentrifuge. The pellet was washed with 70 % (v/v) ethanol and centrifuged at 14,000 rpm (22,800 g_{av}) at 4 °C for 10 minutes in a microcentrifuge, air-dried for 5 minutes and resuspended in 10 µl of autoclaved distilled water.

2.5.6 Ligation

Purified vector and insert were combined at a 3:1 molar ratio, along with 1 µl T4 DNA ligase (Roche) and 1 µl 10x ligation buffer (Roche), and made up to 10 µl with autoclaved distilled water. The ligation mixture was incubated at 4 °C for 48 hours.

2.5.7 Transformation of ligation

A 5 µl measure of the ligation mixture was added to 100 µl of TOP10 competent cells (Invitrogen), left on ice for 30 minutes and heat shocked at 42 °C for 90 seconds. The cells were placed back on ice for 2 minutes, after which 400 µl of LB was added and then incubated at 37 °C for 1 hour. The mixture was plated on LB agar plates containing the appropriate selection antibiotic (either 100 µg/ml ampicillin or kanamycin) and incubated at 37 °C overnight. Colonies from the plates were picked and cultured in 5 ml LB containing 100 µg/ml of the relevant selection antibiotic at 37 °C with agitation overnight. The cells were centrifuged at 5,100 rpm (5,525 g_{av}) at 4 °C for 10 minutes in a benchtop centrifuge to pellet and plasmid DNA was isolated using a QIAprep spin miniprep kit (QIAGEN) in accordance with manufacturer's instructions.

2.5.8 DNA Sequencing

Each sequencing reaction contained 400 ng template, 4 picomoles sequencing primer, 2 µl BigDye v1.1 (Applied Biosystems, Warrington, UK), 4 µl 5x BigDye reaction buffer (Applied Biosystems), and was made up to 20 µl with autoclaved distilled water. The reactions were then subject to the following cycle in a PCR machine:

98 °C for 2 minutes
And 30 cycles of:
98 °C for 30 seconds
50 °C for 15 seconds
60 °C for 4 minutes
4 °C hold

To precipitate the DNA 1 µl of glycogen carrier (Roche), 10 µl of 3 M Na-acetate, 250 µl of 100 % ethanol and 80 µl of distilled water were added to the reaction which was then vortexed and placed on ice for 30 minutes. To pellet the DNA the mixture was centrifuged at 14,000 rpm (22,800 g_{av}) at 4 °C for 30 minutes in a microcentrifuge. The supernatant was removed and the pellet was washed with 750 µl of 70 % (v/v) ethanol and centrifuged for a further 2 minutes as before. The pellet was air-dried for 5 minutes and sent for analysis at the University of Manchester Sequencing Facility, Stopford Building.

2.5.9 Constructs generated

2.5.9.1 pGex-KG-KBPΔ250-81

KBPΔ250-81 is a deletion mutant of human KBP, lacking residues 250-81 resulting in an inability to interact with KIF1B and KIF1C and consequently having an inhibitory effect upon these motors [51]. The KBP sequence is listed under the accession number KIAA1279. The KBPΔ250-81 clone was kindly provided by Dr. Marcin Woźniak, and engineered to encode EcoR1 and XhoI sites at the 5' and 3' ends, respectively, using primers as described in section 2.5.2 and inserted into the pGex-KG vector, which was kindly provided by Dr. Sabine Hilfiker, Rockefeller University, New York, USA. This vector was initially described by Guan and Dixon [268] and differs from commercially available pGex vectors by having a glycine linker sequence between the tag and the multiple cloning site, which is thought to aid correct folding of the recombinant protein and allow more efficient cleaving of the GST tag. DNA sequencing with primers pGex-5 and pGex-3 was performed as described in section 2.5.8 to ensure the insert was in the correct reading frame.

2.5.9.2 pGex-KG-E-MAP-115

RNA was isolated from HeLaM cells using an RNA purification kit (Stratagene) and transcribed to form a cDNA library using a First Strand cDNA Synthesis Kit for RT-PCR (Roche) in accordance with manufacturer's instructions. Primers to amplify human E-MAP-115 from the library were designed based upon the sequence detailed by Masson and Kreis [269] (accession number X73882). PCR was performed using the HeLaM cDNA library as a template and GST-E-MAP-115 forward and reverse primers as described in section 2.5.2, meaning EcoR1 and XhoI sites were engineered at the 5' and 3' ends, respectively. The product was initially inserted into the PCR blunt vector (Invitrogen) and then into the pGex-KG vector. The entire E-MAP-115 DNA was sequenced as described in section 2.5.8 using four sequencing primers as listed in section 2.5.2 to ensure no errors had occurred during PCR amplification.

2.6 Recombinant protein expression

2.6.1 Protein expression and purification

GST, GST-KHCct, GST-KAP3Bct and GST-E-MAP-115 proteins were expressed as follows. A measure of 50 ng of vector was transformed into BL21-CodonPlus competent cells (Invitrogen) and plated onto ampicillin-containing LB-agar plates as described in section 2.5.7. A single colony was picked and transferred to 10 ml ampicillin-containing LB and grown overnight at 37 °C with agitation. This starter culture was added to 1 litre of ampicillin-containing LB and grown at 37 °C with agitation until OD600 was reached between 0.5 and 0.6, after which 0.1 mM IPTG was added and bacteria were grown for a further 3 hours at 37 °C. Bacteria were pelleted by centrifuging at 5,100 rpm (5,525 g_{av}) at 4 °C for 10 minutes in a benchtop centrifuge and the pellets were stored at -20 °C. On the day of the purification the pellets were thawed and resuspended in 25 ml of bacterial lysis buffer and then passed three times through a French press (Thermo Fisher Scientific, Northumberland, UK) to lyse bacterial membranes. The lysate was centrifuged in an F21 rotor (Sorvall, Thermo Fisher Scientific) at 18,000 rpm (38,500 g_{av}) at 4 °C for 30 minutes. The supernatant was incubated for 2 hours at 4 °C with gentle agitation with 1 ml of Fast Flow glutathione sepharose beads (GE Healthcare, Buckinghamshire, UK), which had been washed three times with bacterial lysis buffer. The beads were pelleted by centrifugation at 1,000 rpm (210 g_{av}) in a benchtop centrifuge, and washed three times with bacterial lysis buffer. Beads were transferred to a 1.5 ml microfuge tube and bound proteins were eluted by the addition of 1 ml of 50 mM reduced L-glutathione, pH 8.0 prepared in bacterial lysis buffer, for 1 hour at 4 °C with gentle agitation. Beads were pelleted by centrifugation at 1,000 rpm (210 g_{av}) at 4 °C for 5 minutes in a benchtop centrifuge and the supernatant was collected. The protein was dialysed into acetate buffer using a Slide-A-Lyzer kit (Pierce, Thermo Fisher Scientific) in accordance with manufacturer's instructions, with three changes of dialysis buffer over 24 hours.

2.6.2 GST-KBPΔ250-81

Protein expression and purification were performed as described in section 2.6.1 except 5 mM β-mercaptoethanol was included in all buffers. The omission of β-mercaptoethanol from the purification process resulted in the failure of GST-KBPΔ250-81 to bind glutathione beads (data not shown). Finally, the protein was dialysed into acetate buffer (without β-mercaptoethanol) as described in section 2.6.1.

2.6.3 K430-BCCP

K430-BCCP encodes the first 430 amino acids of rat KIF5C and is tagged at the C-terminus to the N-terminus of a 127 amino acid fragment of biotin carboxyl carrier protein (BCCP) [270]. Protein expression was induced as described in section 2.6.1 except 50 μM D-biotin was added to the culture together with IPTG to biotinylate the expressed protein. Bacterial lysis was performed as described in section 2.6.1 except following bacterial lysis and the clarifying centrifugation the supernatant was removed and stored in 1 ml aliquots. To assess whether the protein could be purified, 50 μl of soluble bacterial lysate was incubated with 15 μl of streptavidin-coated agarose beads (Ademtech, Novagen, Merck Chemicals, Nottingham, UK), which had been washed once with PBS containing 0.5 % (v/v) Triton X-100, for 15 minutes at

room temperature. The beads were washed four times with PBS containing 0.5 % (v/v) Triton X-100 and 10 µl of 2x sample buffer was added to elute bound proteins.

2.7 *Xenopus laevis* egg extracts

Xenopus laevis laid eggs are stably arrested in metaphase II of meiosis due to the presence of CSF. Following natural fertilisation of *Xenopus laevis* eggs, a transient increase in calcium concentration triggers the degradation of CSF, causing the fertilised egg to enter interphase [233]. This process is mimicked *in vitro* by adding calcium-containing activation mix to CSF-arrested extracts.

2.7.1 Preparation of *Xenopus laevis* egg extracts

2.7.1.1 Meiotic metaphase-arrested *Xenopus laevis* egg extracts

Extracts were prepared from laid eggs as described by Murray [237]. Female *Xenopus laevis* frogs (NASCO, California, USA) were injected subcutaneously into the dorsal lymph sac with 50 units PMSG 3-7 days before extract preparation. The day before extract preparation, frogs were injected with 500 units HCG and transferred to isolated tanks containing 100 mM NaCl in distilled water with no food. Approximately 16 hours later eggs were collected, transferred to glass crystallisation dishes and washed three times with MMR buffer. After the final wash as much MMR buffer as possible was removed and 2 % (w/v) cysteine (made immediately before use, pH 7.8 with NaOH) was added to remove the outer jelly coat. The cysteine solution was repeatedly removed and replaced until the eggs were fully de-jellied, as indicated by eggs becoming very compact. Eggs were washed once more with MMR buffer, and then transferred to fresh glass Petri dishes containing XB and washed four times with XB, and then twice with XB containing 5 mM EGTA and 1 mM $MgCl_2$ extra. Eggs were transferred to SW50 tubes (Beckman Coulter) containing 1 ml XB with 10 µg/ml protease inhibitors and 10 µg/ml cytochalasin D. Once the eggs had settled, as much buffer as possible was removed and 1 ml Versilube F-50 oil (GE Healthcare) was layered on top. Eggs were centrifuged at 1,000 rpm (210 g_{av}) for 1 minute then 2,000 rpm (850 g_{av}) for 1 minute at room temperature in a benchtop centrifuge, using 12 ml round-bottom tubes (BD Transduction Laboratories, Oxfordshire, UK) as adaptors. The buffer and oil were removed and eggs were centrifuged at 10,000 rpm (10,700 g_{av}) at 16 °C for 10 minutes in a HB6 rotor (Sorvall, Thermo Fisher Scientific) to crush, using 12 ml round-bottom tubes as adaptors. Extracts were kept on ice and the cytoplasm was removed by piercing the tube with an 18 gauge needle and collected using a 2 ml syringe. Care was taken not to remove any of the egg lipid which sits just above the cytoplasm layer. Protease inhibitors were added to a final concentration of 10 µg/ml, cytochalasin D to 1 µg/ml, sucrose to 150 mM and energy mix to 1x. Extracts were snap frozen in 100 µl aliquots and stored in liquid nitrogen.

2.7.1.2 Newmeyer *Xenopus laevis* egg extracts

Newmeyer extracts were prepared as initially described by Newmeyer and Wilson with some slight modifications [238]. Briefly, extracts were made as described in section 2.7.1.1 except neither extra EGTA nor 1 mM $MgCl_2$ were added to the final washes with XB and the final centrifugation was performed at 4 °C instead of 16 °C. This generates extracts that are in interphase, since CSF is degraded during the preparation due to the lack of EGTA.

2.7.2 Manipulation of *Xenopus laevis* egg extracts

2.7.2.1 CSF *Xenopus laevis* egg extract activation

CSF extract was thawed quickly in the hands and then placed immediately on ice. Activation mix or mock activation mix was added to 1/20th of the volume of the extract and left for 1 hour at room temperature. When treating extracts with activation mix, 100 µg/ml cycloheximide was added to prevent the synthesis of metaphase cyclins.

2.7.2.2 Conversion of Newmeyer *Xenopus laevis egg* extract to mitotic metaphase

Newmeyer extract was thawed quickly in the hands and sea urchin cyclin B1 Δ90 was added to a final concentration of 0.13 mg/ml and energy mix to 1x and left for 1 hour at room temperature [89]. An identical volume of distilled water was added in a duplicate experiment as a negative control.

2.7.2.3 Cytosol and membrane preparation

A 100 µl aliquot of extract was thawed and split into two, with 50 µl being treated with the activation mix or cyclin B1 Δ90 protein, and the other 50 µl with mock activation mix or distilled water as appropriate. Two volumes of A/S containing 1x energy mix was added to the extract which was then centrifuged in a TLA100 rotor (Beckman-Coulter) at 55,000 rpm (116,700 g_{av}) at 4 °C for 30 minutes. This separated the extract into a supernatant (cytosol) and a very compact pellet, on top of which sits a delicate layer of membranes. The cytosol was collected immediately (approximately 120 µl), avoiding the membrane layer. The membranes were resuspended in 50 µl 2 M A/S and layered onto a sucrose gradient made up as follows: 50 µl 2 M A/S, 50 µl membranes in 2 M A/S, 50 µl 1.4 M A/S, 50 µl 0.25 M A/S. The samples were centrifuged in 200 µl thick-walled polycarbonate tubes in a TLS55 rotor (Beckman Coulter) at 50,000 rpm (166,200 g_{av}) at 4 °C for 30 minutes using TLS55 adaptors (Beckman Coulter). The membranes were collected from the 1.4 M/0.25 M A/S interface in 20 µl A/S. When performing biochemical analyses of these fractions, 0.4 µl of membranes and 2.4 µl of cytosol were loaded per lane on an 8 % SDS-PAGE gel, each being the equivalent of 1 µl of crude extract.

2.7.2.4 DLIC immunoblot assay

Xenopus laevis egg extracts were converted between cell cycle states as outlined in sections 2.7.2.1 and 2.7.2.2 and 5 µl samples were taken at specified time points and added to 45 µl sample buffer. Samples were heated at 55 °C for 10 minutes and 5 µl was run on 8 % SDS-PAGE gels (the equivalent of 0.5 µl crude extract) and subject to western blotting with an anti-DLIC antibody.

2.7.2.5 Histone kinase assay

Xenopus laevis egg extracts were converted between cell cycle states as described in sections 2.7.2.1 and 2.7.2.2 and 2 µl samples were taken at specified time points and added to 38 µl of extraction buffer, mixed well and immediately snap frozen in liquid nitrogen and stored at -80 °C. Following thawing, 5 µl of each sample was added to a 500 µl microfuge tube in duplicate and 5 µl of extraction buffer was used as a blank. A measure of 5 µl of histone kinase cocktail was added to each tube and the mixture was pipetted up and down twice to mix and left at room temperature for 30 minutes. The samples were pipetted onto small squares of phosphocellulose

P81 cation exchange paper (Whatman), left to air-dry for 5 seconds and washed 3 x 15 minutes in 150 mM phosphoric acid (in a beaker, stirring) to remove any unincorporated ^{32}P-γ-ATP. The papers were then placed in acetone for 2 minutes, allowed to air dry and transferred to scintillation vials and counted on the ^{32}P channel of a scintillation counter. The addition of histone kinase cocktail to each tube was staggered to ensure the incubation was exactly 30 minutes in each case.

The average counts per minute was calculated for each extract and the background reading (calculated from the extraction buffer-only controls) was subtracted from this value. The specific activity of the ^{32}P-γ-ATP was calculated by adding 5 µl histone kinase cocktail directly onto P81 paper and measuring the counts per minute without any washes. The histone kinase activity of each extract was then calculated as picomoles of ^{32}P incorporated per µl of extract per minute.

2.7.2.6 Conversion of Newmeyer *Xenopus laevis* egg extract to mitotic metaphase in the presence of ^{32}P-γ-ATP

A measure of 60 µl (approximately 1.8 mg) of Newmeyer extract was treated with cyclin B1 Δ90 or an equal volume of water as described in section 2.7.2.2, except energy mix was omitted. After 30 minutes 200 µCi of ^{32}P-γ-ATP (150 mCi/ml, PerkinElmer) was added and the incubation was continued for a further 30 minutes at room temperature. A measure of 1.5 ml of IP buffer was added to each tube and IP with SUK4 or IC74 antibodies or mouse immunoglobulin G (IgG) was performed as described in section 2.4.5. Samples were run on an 8 % SDS-PAGE gel, which was stained with colloidal Coomassie, dried and exposed to single emulsion photographic film.

2.7.2.7 Incubation of interphase and metaphase *Xenopus laevis* egg extract cytosols with ^{32}P-γ-ATP

Both interphase and metaphase cytosols were prepared from CSF and Newmeyer extracts as described in section 2.7.2.3. A measure of 60 µl (approximately 1.2 mg) of each cytosol was each incubated with 80 µCi of ^{32}P-γ-ATP for 30 minutes at room temperature. A measure of 1 ml of IP buffer was added to each tube and IP with the SUK4 antibody or mouse IgG was performed as described in section 2.4.5. Samples were run on an 8 % SDS-PAGE gel, which was stained with colloidal Coomassie, dried and exposed to single emulsion photographic film.

2.8 Preparation of rat liver membrane fractions

2.8.1 Golgi apparatus

A Golgi apparatus enriched fraction was prepared from rat liver as described by Allan and Vale [217]. Solutions of 0.25 M, 1.1 M, 1.25 M, 1.4 M and 2 M sucrose were prepared in acetate buffer. The livers of four adult female rats were dissected and placed in PBS on ice. Livers were weighed, chopped up using a razor blade and homogenised using a Polytron homogeniser in 1 volume of 0.25 M A/S containing 10 µg/ml protease inhibitors. The homogenate was centrifuged at 1680 rpm (600 g_{av}) at 4 °C for 10 minutes in a benchtop centrifuge. The supernatant was removed and gradients were created in SW28 tubes (Beckman Coulter) as follows: 5 ml 1.4 M A/S, 10 ml membranes, 30 ml 0.25 M A/S. The gradient was centrifuged in a SW28 rotor (Beckman Coulter) at 27,500 rpm (100,000 g_{av}) at 4 °C for 1 hour. Membranes at the interface

were removed and their sucrose molarity measured using a hand-held refractometer (Thermo Fisher Scientific), and adjusted to 1.25 M using 2 M A/S as required. Gradients were created in SW28 tubes as follows: 15 ml extract, 15 ml 1.1 M A/S, 15 ml 0.25 M A/S and centrifuged at 22,000 rpm (65,000 g_{av}) at 4 °C for 90 minutes in a SW28 rotor. Membranes at the 0.25 M/1.1 M A/S interface were collected and the protein concentration measured using a Bradford assay in accordance with manufacturer's instructions (Bio-Rad Laboratories). Golgi membranes were diluted to 10 mg/ml with A/S as required, snap frozen in 100 µl aliquots and stored in liquid nitrogen.

2.8.2 ER

A similar method to that described in section 2.8.1 was used to prepare a membrane fraction enriched in rough ER from rat liver. Following centrifugation of the homogenate at 1,680 rpm (600 g_{av}) at 4 °C for 10 minutes, another centrifugation was performed in an F21 rotor at 9,200 rpm (10,000 g_{av}) at 4 °C for 10 minutes and the supernatant was collected. Gradients were created in SW28 tubes as follows: 10 ml 1.7 M A/S, 10 ml 1.4 M A/S, 6 ml 1.1 M A/S, 6 ml membranes. The gradient was centrifuged in a SW28 rotor at 27,500 rpm (100,000 g_{av}) at 4 °C for 2 hours. Membranes were collected from the 1.7 M/1.4 M A/S interface and their sucrose molarity measured using a hand-held refractometer and adjusted to 0.4 M using acetate buffer as required. Membranes were then centrifuged in a SW28 rotor at 27,500 rpm (100,000 g_{av}) at 4 °C for 1 hour. The pelleted membranes were resuspended in 10 ml of A/S containing 10 µg/ml protease inhibitors, and the protein concentration was measured using a Bradford assay in accordance with manufacturer's instructions. ER membranes were diluted and stored as described in section 2.8.1.

2.9 Incubation of rat liver ER with *Xenopus laevis* egg extract cytosols

2.9.1 Incubation and recovery of rat liver ER with interphase and metaphase *Xenopus laevis* egg extract cytosols

Interphase and metaphase cytosols were prepared from either Newmeyer or CSF extracts as described in section 2.7.2.3 and samples were taken to perform histone kinase assays or to assess DLIC phosphorylation to ensure the cytosols were in the correct cell cycle state. A measure of 10 µl (100 µg) of rat liver ER was added to 90 µl of the appropriate cytosol, and left for 1 hour at room temperature and then centrifuged through a 100 µl cushion of 0.8 M A/S in 200 µl thick-walled polycarbonate tubes in a TLS55 rotor at 50,000 rpm (166,200 g_{av}) at 4 °C for 30 minutes using TLS55 adaptors. The supernatant from above the cushion was removed and 10 µl was added to 40 µl of sample buffer. The cushion itself was then removed and 100 µl A/S was added to the pellet to wash. The pellet was centrifuged in a TLS55 rotor at 50,000 rpm (166,200 g_{av}) at 4 °C for 20 minutes using TLS55 adaptors. The pellet was resuspended in 25 µl A/S and then 25 µl 2x sample buffer was added. A volume of 10 µl (the equivalent of 2 µl crude ER membranes or cytosol) was run per lane on 8 % SDS-PAGE gels and subject to western blotting.

When attempting to determine whether the method of re-isolating ER reduces the level of kinesin-1 immunoprecipitated, 100 µl (1 mg) of rat liver ER was added to 200 µl of interphase

cytosol prepared from Newmeyer *Xenopus laevis* egg extracts as described in section 2.7.2.3. This mixture was centrifuged through a 250 µl cushion of 0.8 M A/S in a TLS55 rotor at 50,000 rpm (166,200 g_{av}) at 4 °C for 30 minutes. The supernatant and cushion were removed and the pelleted membranes were resuspended in 500 µl of IP buffer or in 200 µl of A/S, which was added to 300 µl IP buffer. Alternatively, the membrane and cytosol mixture was added to 300 µl 2 M A/S and layered onto a sucrose gradient made as follows: 300 µl 2 M A/S, 300 µl membranes in 2 M A/S, 300 µl 1.4 M A/S, 300 µl 0.25 M A/S. The samples were centrifuged in a TLS55 rotor at 50,000 rpm (166,200 g_{av}) at 4 °C for 30 minutes. The membranes were collected from the 1.4 M/0.25 M A/S interface and made up to 500 µl with IP buffer. As a control 100 µl (1 mg) of ER membranes were added directly to 500 µl IP buffer. Kinesin-1 was immunoprecipitated with the SUK4 antibody as described in section 2.4.5. Samples were run on an 8 % SDS-PAGE gel and stained with colloidal Coomassie as described in sections 2.4.1 and 2.4.3.

2.9.2 Incubation and recovery of rat liver ER with interphase and metaphase *Xenopus laevis* egg extract cytosols in the presence of ^{32}P-γ-ATP

Interphase and metaphase cytosols were made from Newmeyer extracts as described in section 2.7.2.3, and samples were taken to perform histone kinase assays or to assess DLIC phosphorylation to ensure each cytosol was in the correct cell cycle state. A measure of 120 µl of cytosol was incubated with 40 µl (400 µg) ER membranes and 160 µCi of ^{32}P-γ-ATP for 30 minutes at room temperature. This mixture was then centrifuged through a 100 µl cushion of 0.8 M A/S in a TLS55 rotor at 50,000 rpm (166,200 g_{av}) at 4 °C for 30 minutes using TLS55 adaptors. The supernatant from above the sucrose cushion was removed and made up to 1 ml with IP buffer. The sucrose cushion was removed and the membranes were resuspended in 1 ml of IP buffer, transferred to 1.5 ml microfuge tubes and left for 10 minutes on ice. The lysates were clarified by centrifuging in a microcentrifuge at 14,000 rpm (22,800 g_{av}) at 4 °C for 10 minutes. IP from the ER and cytosol samples was performed as described in section 2.4.5. Samples were run on an 8 % SDS-PAGE gel, stained with colloidal Coomassie, dried and exposed to single emulsion photographic film.

2.10 Motility assays

2.10.1 Purification of pig brain tubulin

2.10.1.1 Phosphocellulose column preparation

A measure of 10.3 g of phosphocellulose powder was dissolved in 250 ml of 0.5 M NaOH and left for 5 minutes. The mixture was filtered through a sintered glass funnel and washed with distilled water until the pH of the liquid flowing through was below pH 10.0, as assessed by pH strips (Whatman). The resin was then scraped into 250 ml of 0.5 M HCl, gently stirred and left for 5 minutes. The mixture was again filtered through a sintered glass funnel and washed with distilled water until the pH of the liquid flowing through was above pH 3.0. The resin was scraped into 50 ml of 0.5 M PIPES, pH 6.9, stirred gently and allowed to drip through the funnel (without any suction). The resin was then scraped into 50 ml 0.1 M $MgSO_4$, stirred gently and allowed to drip through the funnel as before. Finally, the resin was scraped into 50 ml phosphocellulose column buffer and carefully poured into a 25 cm x 10 cm column (GE

Healthcare) and 200 ml of phosphocellulose column buffer containing 10 µg/ml sodium azide was layered on top. After 50 ml of buffer had been allowed to flow through, the tap was sealed and the column was stored at 4 °C.

2.10.1.2 Tubulin purification

Microtubules were isolated from pig brain based on the method detailed by Weisenberg and Cianci with some slight modifications [271]. Six fresh pig brains were obtained from the slaughterhouse (Dalehead Foods, Lancashire, UK) and transported to the laboratory in PBS on ice. The rest of the preparation was performed at 4 °C. The brains were rinsed with PBS, the meninges were removed, and the brain was chopped into small pieces. The material was weighed, homogenised in an equal volume of tubulin purification buffer A using a Waring blender and Polytron homogeniser (Thermo Fisher Scientific) and centrifuged in a JA-14 rotor (Beckman Coulter) at 12,000 rpm (13,900 g_{av}) at 4 °C for 30 minutes. The supernatant was removed and centrifuged in a Ti45 rotor (Beckman Coulter) at 30,000 rpm (70,400 g_{av}) at 4 °C for 1 hour. Again, the supernatant was removed and 2 mM EGTA, 1 mM $MgSO_4$, 0.5 mM GTP and 25 % (v/v) glycerol were added and the preparation was incubated at 37 °C for 30 minutes to polymerise microtubules. The material was centrifuged in a Ti45 rotor at 40,000 rpm (125,200 g_{av}) at 30 °C for 1 hour, after which the supernatant was discarded and the pellet was resuspended in 90 ml of tubulin purification buffer B, left on ice for 30 minutes to depolymerise microtubules and then 30 ml of glycerol was added. At this stage the material was snap frozen and stored at -80 °C. The following day the material was centrifuged in a Ti70 rotor (Beckman Coulter) at 40,000 rpm (117,700 g_{av}) at 4 °C for 20 minutes. The supernatant was removed and 2 mM EGTA, 1 mM $MgSO_4$ and 0.5 mM GTP were added and the preparation was incubated at 37 °C for 30 minutes to allow microtubules to polymerise. The material was centrifuged in a Ti45 rotor at 40,000 rpm (125,200 g_{av}) at 30 °C for 1 hour, after which the supernatant was discarded and the pellet was resuspended in 45 ml of tubulin purification buffer C, left on ice for 30 minutes and 12 ml glycerol was added. The preparation was separated into 15 ml aliquots, snap frozen in liquid nitrogen and stored at -80 °C. When needed, an aliquot was thawed and centrifuged in a Ti70 rotor at 42,300 rpm (131,700 g_{av}) at 4 °C for 1 hour. The supernatant was removed and DMSO was added to 10 % (v/v) and then incubated at 37 °C for 30 minutes. The preparation was centrifuged in a Ti90 rotor (Beckman Coulter) at 47,000 rpm (137,000 g_{av}) at 30 °C for 1 hour. The pellet was resuspended in 2 ml of phosphocellulose column buffer.

Tubulin was further separated from any remaining contaminating proteins, especially MAPs, using a phosphocellulose column. The buffer in the pre-prepared column was drained and another 200 ml of phosphocellulose column buffer was added and allowed to flow through. The flow through should have a pH of 6.9 and this was checked using a pH meter. The column was run until the buffer level was just above the resin and then 2 ml of microtubule protein was added. The protein was allowed to enter the resin and then 150 ml of phosphocellulose column buffer was added. Fractions of 3 ml were collected and the OD280 of each fraction was measured, with the purity of the protein assessed by running samples on a 10 % SDS-PAGE gel and staining with colloidal Coomassie as described in section 2.4.3. Fractions were snap frozen in liquid nitrogen and stored at -80 °C until needed.

2.10.1.3 Microtubule polymerisation from purified tubulin

The purified tubulin prepared as described in 2.10.1.2 was thawed and 1 mM GTP was added. Following centrifugation in a TLS55 rotor at 44,000 rpm (130,000 g_{av}) at 4 °C for 30 minutes, the supernatant was removed and taxol was added to a concentration of 20 µM and then incubated at 37 °C for 15 minutes. The material was then layered over a 10 % (w/v) sucrose cushion prepared in BRB80 containing 20 µM taxol, and centrifuged in a SW60 rotor (Beckman Coulter) at 17,200 rpm (30,000 g_{av}) at 30 °C for 25 minutes. The supernatant and cushion were removed and the pellet was washed with BRB80 containing 1 mM GTP and then centrifuged as before. The supernatant was removed and the pellet was resuspended in 300 µl of phosphocellulose column buffer. A Bradford assay was performed to determine the protein concentration and the microtubules were then diluted to 2 mg/ml with phosphocellulose column buffer, separated into 20 µl aliquots, snap frozen and stored in liquid nitrogen until needed.

2.10.2 Motility of rat liver ER membranes with interphase and metaphase *Xenopus laevis* egg extract cytosols

A flow cell was generated by drawing two strips of Apiezon M grease (M&I materials, Lancashire, UK) down either side of a microscope slide, with selotape used as a spacer, and an 18x18 mm^2 (no. 1.5 thickness) coverslip (Corning) placed on top. Pig brain microtubules were diluted to a final concentration of 0.2 mg/ml in BRB80 containing 5 µM taxol. The solution was added to the flow cell and incubated upside down in a humid chamber for 10 minutes to coat the coverslip with microtubules. Unbound microtubules were flushed away with A/S containing 1x energy mix. Interphase and metaphase cytosols were prepared from CSF and Newmeyer extracts as described in section 2.7.2.3. A measure of 1 µl (10 µg) of rat liver ER membranes was added to 9 µl of cytosol, applied to the flow cell and left in a humid chamber for 1 hour to allow an ER network to form. Flow cells were viewed using an Olympus BX60 microscope fitted with a 60x 1.4 N.A. PlanApo objective, a 1.4 N.A. oil immersion condenser and differential interference contrast optics, as described in [218]. Light from a 100 W mercury vapour lamp was passed through water and glass filters and a 546 nm interference filter then directed to the microscope through a 1 mm optical silica filter. Differential interference contrast images were projected onto a Hamamatsu Newvicon camera. A Hamamatsu Argus 10 image processor was used to perform background subtraction and image contrast enhancement in real time. Sequences for analysis were recorded onto DVD using a Panasonic DVD recorder. For quantification analysis twenty fields were chosen at random and the number of three-way junctions per field was counted. From this the average number of three-way junctions per field was calculated. Each experiment was repeated two additional times to obtain three average values per condition. These data were statistically analysed using SPSS 15.0 to perform independent student t-tests.

2.10.3 Motility of rat liver Golgi membranes in the presence of BFA

The assay was performed in a similar manner to that described by Robertson and Allan [144]. Interphase cytosol was prepared from Newmeyer extracts as described in section 2.7.2.3 and then diluted 5-fold with acetate buffer including 100 µg/ml BFA. This mixture was then added to flow cells and incubated for 10 minutes as described in section 2.10.2 to coat the coverslip with

microtubules that polymerised spontaneously in interphase *Xenopus laevis* egg extract cytosol. The BFA was taken from a 2 mg/ml stock diluted in acetate buffer immediately before use. A volume of 1 µl (10 µg) of rat liver Golgi membranes was incubated with 4 µl (4 µg) of antibody for 45 minutes on ice [144] or 2.9 µl (2 µg) of protein for 20 minutes on ice [30]. Incubation with mouse IgG or GST was used as a negative control. When combining incubations with antibodies and GST-KBPΔ250-81, a volume of 2 µl (20 µg) of rat liver Golgi membranes was incubated with 4 µl (4 µg) of antibody and 2.9 µl (2 µg) of GST-KBPΔ250-81 for 45 minutes on ice. Incubation with mouse IgG and GST was used as a negative control.

Of these mixtures, 1 µl was taken and added to 8.5 µl of interphase cytosol prepared from Newmeyer extract and 0.5 µl of freshly diluted 2 mg/ml BFA (i.e. to a final concentration of 100 µg/ml), applied to the flow cell and left inverted in a humid chamber for 1 hour. Flow cells were imaged as described in section 2.10.2. To analyse motility twenty fields were chosen at random and the total length of tubules per field was measured using a map measuring tool. Each experiment was repeated two additional times to obtain three average values per condition. Data was statistically analysed as described in section 2.2.4.

To assess the effects of GST-KBPΔ250-81 upon Golgi vesicle motility, a volume of 1 µl (10 µg) of rat liver Golgi membranes were incubated with 2.9 µl (2 µg) of GST-KBPΔ250-81, or GST as a negative control, for 20 minutes on ice. Of this mixture, 1 µl was taken and added to 9 µl of interphase cytosol prepared from Newmeyer extract, and added to flow cells which had been coated with microtubules as described above. The flow cells were left inverted for 10 minutes in a humid chamber. Twenty randomly chosen fields were imaged using VE-DIC microscopy and each filmed for 30 minutes. The total number of moving vesicles in these fields (i.e. in 10 minutes) was counted. Each experiment was repeated two additional times to obtain three average values per condition. Data was statistically analysed as described in section 2.10.2.

2.10.4 Motility of interphase *Xenopus laevis* egg extract membranes or rat liver ER following incubation with GST-E-MAP-115

Flow cells were coated with microtubules as described in section 2.10.3, except BFA was omitted. A membrane fraction was prepared from Newmeyer extract as described in section 2.7.2.3, except flotation through a sucrose gradient step was not performed. Once pelleted the membranes were resuspended directly into 20 µl of A/S. A volume of 1 µl of these interphase *Xenopus laevis* egg extract membranes, or rat liver ER membranes, was incubated with 1 µl (0.5 µg) of GST or GST-E-MAP-115 protein which had been dialysed into acetate buffer, for 20 minutes on ice. It was found that incubating both interphase *Xenopus laevis* egg extract membranes and rat liver ER membranes with larger amounts of GST-E-MAP-115 such as those described in section 2.10.3 reduced microtubule polymerisation and increased bundling in the assay. Of this mixture, 1 µl was taken and added to 9 µl of interphase cytosol prepared from Newmeyer extract, applied to the flow cell and left inverted in a humid chamber for 1 hour. The final concentration of GST-E-MAP-115 in the assay was approximately 980 nM. Flow cells were viewed as described in section 2.10.2 and images were captured on DVD. Image preparation was performed using PhotoShop CS2 and Adobe Illustrator CS2.

2.10.5 Kinesin-1 bead assays

2.10.5.1 Motility of beads along microtubules polymerised from interphase or metaphase *Xenopus laevis* egg extract cytosol

Microtubules prepared as described in section 2.10.1.3 were passed through a 23.5 gauge needle to shear, and diluted to 1.25 µg/ml in interphase or metaphase cytosol prepared from Newmeyer extract as described in section 2.7.2.3. The solution was applied to a microscope flow cell and left inverted in a humid chamber for 10 minutes. The exogenously-added brain microtubules acts as nucleation sites for microtubule polymerisation which is necessary in metaphase cytosol which is unable to support *de novo* microtubule polymerisation [217]. Any unbound material was flushed away with 40 µl of motility buffer. A volume of 6 µl of K430-BCCP bacterial lysate was incubated with 2 µl of streptavidin-coated magnetic beads (Ademtech, Pessac, France) which have a diameter of 200 nm, which had been washed once with motility buffer. The beads were incubated for 15 minutes at room temperature and then re-isolated using a magnet, and any unbound material was removed by washing the beads once with 50 µl of motility buffer. The beads were diluted in 40 µl of motility buffer and 10 µl was applied to the flow cell and viewed immediately. As a positive control, flow cells were also pre-coated with microtubules polymerised exclusively from pig brain tubulin as described in section 2.10.2 except unbound material was flushed away with motility buffer. To analyse motility, twenty fields were chosen at random and filmed for 30 seconds each and the number of moving beads per field was counted. Each experiment was repeated two additional times to obtain three average values per condition. Data was statistically analysed as described in section 2.10.2.

2.10.5.2 Motility of beads in the presence of interphase or metaphase *Xenopus laevis* egg extract cytosols

Flow cells were pre-coated with microtubules polymerised from purified pig brain tubulin and magnetic streptavidin-coated beads were coated with K430-BCCP as described in section 2.10.5.1. The beads were then diluted in 40 µl of interphase or metaphase cytosol prepared from Newmeyer extract as described in section 2.7.2.3, or A/S containing 1x energy mix, all including 4 mM ATP, 4 U/ml creatine phosphokinase and 0.5 % (v/v) β-mercaptoethanol. A 10 µl volume of this bead suspension was applied to the flow cell and viewed immediately. Motility was quantitated and analysed as described in section 2.10.5.1.

3. Results – Cell cycle regulation of kinesin-1

The aim of this work was to determine if kinesin-1-dependent motility is regulated in a cell cycle-dependent manner, and if so, to determine the mechanism of this regulation.

3.1 Use of *Xenopus laevis* egg extracts in *in vitro* motility assays

Previous studies have performed *in vitro* motility assays using extracts prepared from *Xenopus laevis* eggs as a means of studying microtubule motor regulation (see section 1.5.4) [89, 188, 218, 272]. These assays, in which motor activity is reconstituted in the absence of cells, have several advantages that often make them more amenable and their results easier to interpret than alternative systems or *in vivo* analyses. *Xenopus laevis* egg extracts polymerise microtubules *de novo* and have a relatively high concentration of motors meaning a high level of motor-dependent motility is supported, with both vesicular and tubular membrane movements generated [272]. It has also been shown that at least some regulatory post-translational modifications, such as phosphorylation and dephosphorylation, are supported by this system [89, 217, 272]. Moreover, the activity of a single motor can often be studied in isolation. For example, ER membranes from *Xenopus laevis* egg extracts are moved solely by cytoplasmic dynein-1 in this system, whereas a rat liver ER fraction is moved exclusively by kinesin-1 [30, 272]. This is especially beneficial as it becomes increasingly obvious that motors often do not work in isolation *in vivo* but cooperate and coordinate with each other, making it difficult to unravel how an individual motor is regulated [34, 231, 273]. Indeed reconstitution of membrane motility in this simplified *in vitro* system has been used to dissect mechanisms behind intricate processes such as nuclear membrane breakdown [274].

Perhaps the most important facet of *Xenopus laevis* egg extracts in terms of this project is their ability to interconvert between different cell cycle stages [233] (Figure 1.6), allowing monitoring of changes to motor-dependent motility during both mitosis and meiosis. It was therefore decided to combine cytosols prepared from *Xenopus laevis* egg extracts with rat liver ER membranes in motility assays to determine if, and how, the kinesin-1 motor is regulated during the cell cycle.

3.1.1 Assessment of *Xenopus laevis* egg extract quality

In order to ensure *Xenopus laevis* egg extracts could be reliably converted between cell cycle states, rigorous tests were employed to assess extract quality. Since the phosphorylation status of DLIC is known to change in *Xenopus laevis* egg extracts between interphase and metaphase [89], the mobility of DLIC on SDS-PAGE gels was used as an indicator of cell cycle status. Indeed, DLIC purified from mitotic metaphase extracts has been shown to run with a slower mobility compared to protein isolated from interphase extracts, and this is due to metaphase-specific hyperphosphorylation of DLIC [89].

A CSF *Xenopus laevis* egg extract was treated with activation mix containing calcium to stimulate conversion from meiotic metaphase II into interphase, or with mock activation mix lacking calcium as a negative control, and left for 1 hour at room temperature. Addition of high levels of exogenous calcium simulates the sharp rise in calcium concentration and inactivation of CSF triggered in the egg following fertilisation (see section 1.5.4 and Figure 1.6) [237].

Samples were taken every 15 minutes of the time course, and then run on SDS-PAGE gels and subjected to western blotting with an anti-DLIC antibody. It was necessary to check the phosphorylation status of DLIC at various time points following calcium activation or mock activation since CSF extracts are notoriously difficult to arrest in metaphase II and often convert to interphase, or an intermediary cell cycle state, spontaneously [229]. When a CSF extract was treated with activation mix, there was a gradual downward shift in DLIC mobility from approximately 67 kDa to 62 kDa (Figure 3.1 A), indicating DLIC was dephosphorylated and the extract converted from meiotic metaphase II into interphase. In contrast, following extract mock activation DLIC continued to migrate at the higher molecular weight of approximately 67 kDa, indicating the extract was able to sustain its meiotic metaphase II arrest for up to 1 hour at room temperature.

In a parallel experiment a Newmeyer *Xenopus laevis* egg extract was incubated with recombinantly expressed cyclin B1 Δ90 protein, a non-degradable form of cyclin B1 which stimulates conversion from interphase to mitotic metaphase, or with water as a negative control and left for 1 hour. Cyclin B1 Δ90, initially described by Murray and co-workers in 1989 [236], is sea urchin cyclin B1 protein lacking the first 90 amino acids from the N-terminus. This renders the protein resistant to ubiquitination necessary for its degradation, but still able to interact with CDK1 leading to phosphorylation of histone H1 [185, 236]. Western blotting of extract samples revealed an upward shift in DLIC mobility from approximately 62 kDa to 67 kDa following cyclin B1 Δ90 treatment (Figure 3.1 A). This indicated DLIC phosphorylation had occurred and the extract had converted from interphase into mitotic metaphase. Conversely, when the extract was treated with water, DLIC mobility was unchanged remaining at approximately 62 kDa suggesting the extract stayed in interphase.

Another method employed to assess extract quality was the histone kinase assay. This assay allows the activity of the key metaphase kinase CDK1 to be measured, by monitoring the phosphorylation of histone H1. Since CDK1 phosphorylates histone H1, a higher level of histone H1 phosphorylation indicates a higher level of CDK1 activity [275]. Again, CSF and Newmeyer *Xenopus laevis* egg extracts were converted to interphase or mitotic metaphase respectively, by treatment with activation mix or cyclin B1 Δ90 protein. Samples were taken every 10 minutes up to 1 hour and analysed for histone kinase activity (see section 2.7.2.5). When the CSF extract was activated there was a decrease in histone kinase activity (Figure 3.1 B), from 4.6 pmol/µl/min at the beginning of the assay to 1.6 pmol/µl/min after 1 hour, suggesting CDK1 activity had fallen and the extract had converted from meiotic metaphase II into interphase. Conversely, when the CSF extract was mock activated, histone kinase activity was sustained at a higher level, ranging from 4.5 pmol/µl/min to 6 pmol/µl/min, indicating CDK1 activity was maintained and a meiotic metaphase II arrest was retained for up to 1 hour at room temperature.

Following treatment of a Newmeyer *Xenopus laevis* egg extract with cyclin B1 Δ90 protein there was a gradual increase in histone kinase activity over time, from 0.3 pmol/µl/min at the

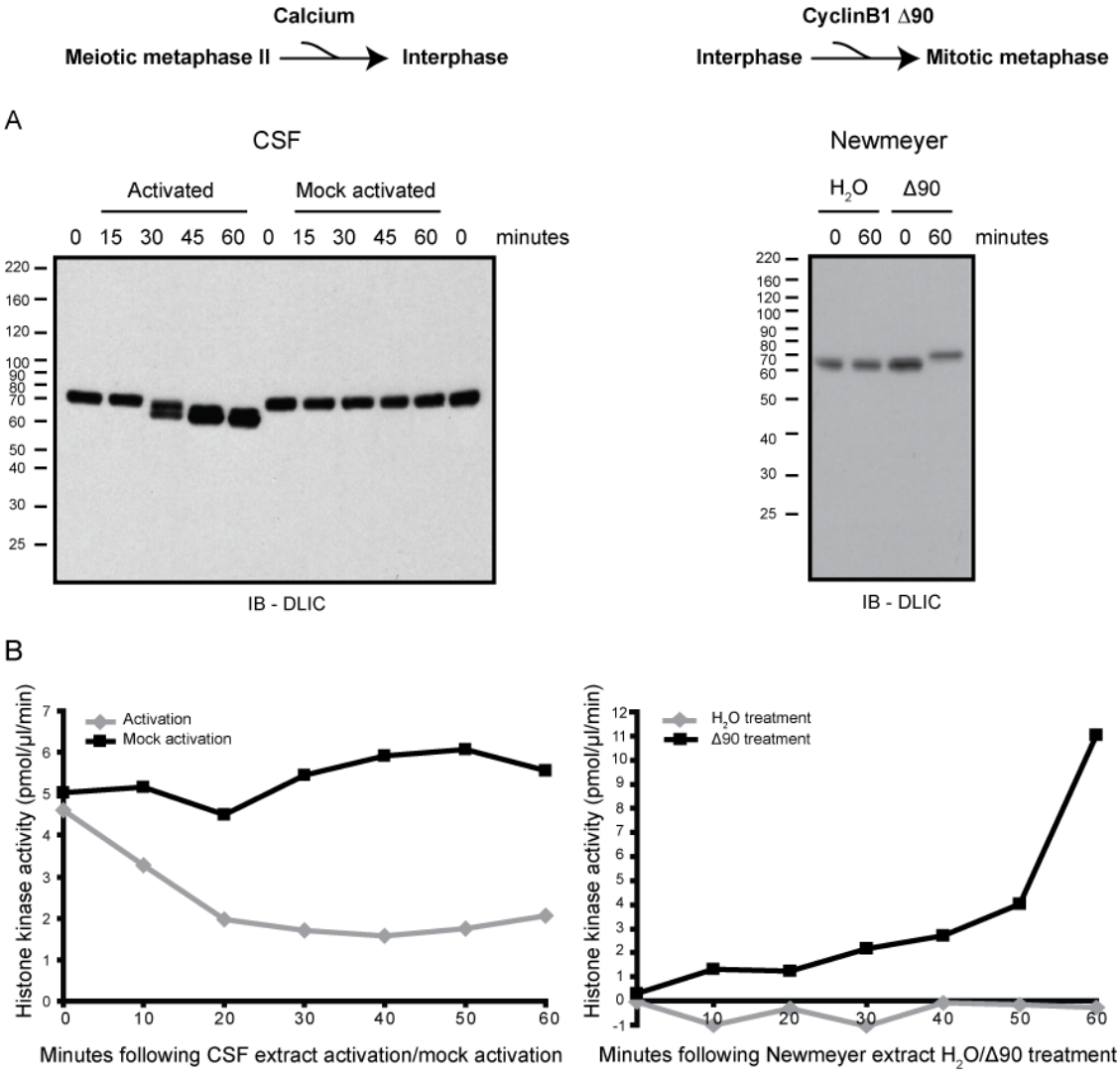

Figure 3.1 - Assessment of *Xenopus laevis* egg extract quality using immunoblotting of DLIC and histone kinase assays

A. A volume of 50 µl of CSF *Xenopus laevis* egg extract was treated with 2.5 µl of activation mix and 100 µg/ml cycloheximide, to stimulate conversion from meiotic metaphase II to interphase, or with an equal volume of mock activation mix lacking calcium. Alternatively, 50 µl of Newmeyer *Xenopus laevis* egg extract was treated with 0.13 mg/ml cyclin B1 Δ90 and 1x energy mix, to stimulate conversion from interphase to mitotic metaphase, or with an identical volume of H_2O. Samples were taken at the specified time points and 0.5 µl of extract was immunoblotted for DLIC.

B. A volume of 50 µl of CSF and Newmeyer *Xenopus laevis* egg extracts was converted to interphase or mitotic metaphase respectively as described in A, with negative controls included. A volume of 2 µl was taken at each specified time point and added to 38 µl of extraction buffer, mixed well and immediately snap frozen in liquid nitrogen. Following thawing 5 µl of each sample was added to 5 µl of histone kinase cocktail and left for 30 minutes at room temperature. Samples were added to phosphocellulose P81 cation exchange paper and the activity of each sample was measured using the ^{32}P channel of a scintillation counter. The background level of activity was deducted from each experimental value. The histone kinase activity of each sample was calculated as picomoles of ^{32}P incorporated per µl of extract per minute. The background reading (calculated from the extraction buffer-only controls) was subtracted from each experimental value, meaning histone kinase activity sometimes drops below zero.

beginning of the assay to 11 pmol/µl/min after 1 hour (Figure 3.1 B), suggesting CDK1 activity had increased and the extract had converted from interphase to meiotic metaphase II. Following treatment with water, histone kinase activity was maintained at a lower level indicating the extract remained in interphase.

3.1.2 Changes in the level of cytoplasmic dynein-1 and dynactin on *Xenopus laevis* egg extract membranes during meiosis and mitosis

Both cytoplasmic dynein-1 and dynactin are known to be released from membranes in *Xenopus laevis* egg extracts upon conversion from interphase into mitotic metaphase [89]. This release is believed to underpin the cell cycle regulation of cytoplasmic dynein-1 in *Xenopus laevis* egg extracts, resulting in profound inhibition of membrane motility during mitosis *in vitro* [89, 217]. Cytoplasmic dynein-1-dependent motility is also known to be inhibited in meiotic metaphase II *Xenopus laevis* egg extracts [217], but the mechanism by which this occurs has not been fully verified. In order to test whether mitotic *Xenopus laevis* egg extracts were behaving as expected, and also to determine whether cytoplasmic dynein-1 and/or dynactin are released from membranes in meiotic metaphase II extracts, it was decided to recapitulate these original experiments.

CSF and Newmeyer *Xenopus laevis* egg extracts were converted to interphase or mitotic metaphase respectively, by treatment with activation mix or cyclin B1 ∆90 protein. Membranes and cytosol were first crudely separated by ultracentrifugation. Membranes were then floated through a sucrose gradient to ensure they were free of any contaminating non-membranous cytoplasmic dynein-1 or dynactin which had co-sedimented during the first pelleting step. Samples of each fraction, equivalent to 1 µl of crude extract, were immunoblotted for DLIC, DIC or p150*glued*. Proportional loading, and not equal protein loading, was used to allow the fairest comparison of cytoplasmic dynein-1 and dynactin levels between fractions. In Newmeyer *Xenopus laevis* egg extracts, a reduced level of both DIC and p150*glued* on membranes was seen in mitotic metaphase with a corresponding increase in the cytosolic fraction (Figure 3.2 A). Immunoblotting for DLIC, whilst displaying the expected changes to DLIC mobility between 62 kDa and 67 kDa, and thus showing the extract was correctly converted between cell cycle states, did not reveal an increased signal in mitotic cytosol. This is probably because the antibody preferentially recognises dephosphorylated DLIC (Addinall and Allan, unpublished data) and therefore gave a reduced signal in the metaphase samples, where the protein is hyperphosphorylated. These results, in agreement with previously published data, reveal cytoplasmic dynein-1 and dynactin are released from membranes into the cytosol upon conversion of *Xenopus laevis* egg extract from interphase into mitotic metaphase [89].

When an identical experiment was performed with CSF *Xenopus laevis* egg extracts, immunoblotting for DLIC revealed the expected band shifts, indicating the extract had converted from meiotic metaphase II into interphase, but no release of either DIC or p150*glued* from meiotic membranes was observed (Figure 3.2 B). The level of both DIC and p150*glued* appeared similar on membranes isolated from interphase and meiotic metaphase II extracts. This data suggests that neither cytoplasmic dynein-1 nor dynactin are released from

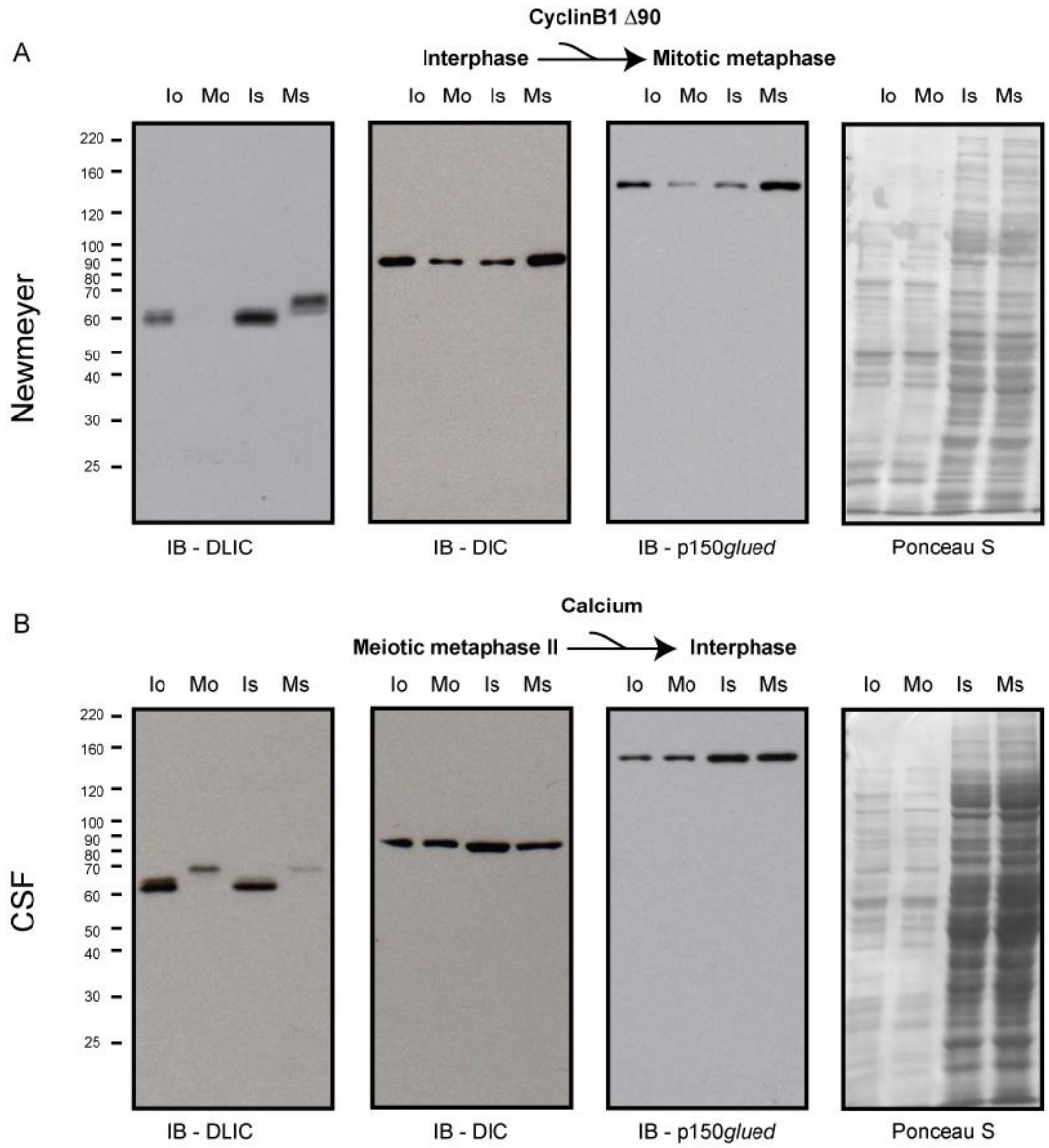

Figure 3.2 - Cytoplasmic dynein-1 and dynactin are released from membranes in mitotic metaphase but not meiotic metaphase II *Xenopus laevis* egg extracts

A. A volume of 50 µl of Newmeyer *Xenopus laevis* egg extract was treated with 0.13 mg/ml cyclin B1 Δ90 and 1x energy mix for 1 hour, to stimulate conversion from interphase to mitotic metaphase, or with an identical volume of H_2O. Two volumes of A/S containing 1x energy mix were added and the extract was then ultracentrifuged to separate into membrane and cytosol fractions. A volume of 120 µl of cytosol was collected and the membranes were resuspended in 50 µl 2 M A/S and layered onto a sucrose gradient consisting of 2 M A/S, membranes in 2 M A/S, 1.4 M A/S and 0.25 M A/S. The gradient was ultracentrifuged to further purify the membrane fraction. The membranes were collected from the 1.4 M/0.25 M A/S interface in 20 µl A/S. A volume of 0.4 µl of interphase (Io) or metaphase (Mo) membranes and 2.4 µl of interphase (Is) or metaphase (Ms) cytosol (the equivalent of 1 µl of crude extract) was immunoblotted for DLIC, DIC or p150*glued*. A Ponceau S stain of the samples is shown.

B. A volume of 50 µl of CSF *Xenopus laevis* egg extract was treated with 2.5 µl of activation mix and 100 µg/ml cycloheximide for 1 hour, to stimulate conversion from meiotic metaphase II to interphase, or with an equal volume of mock activation mix lacking calcium. Membrane and cytosol fractions were generated and immunoblotting was performed as described in A.

membranes in meiotic metaphase II extracts. Therefore membrane release of cytoplasmic dynein-1 and/or dynactin is not responsible for inhibition of membrane motility in meiotic CSF *Xenopus laevis* egg extracts.

3.1.3 Changes to kinesin-1-dependent rat liver ER motility during meiosis and mitosis *in vitro*

To determine whether kinesin-1-dependent motility is regulated in a cell cycle-dependent manner, an ER-enriched membrane fraction isolated from rat liver was mixed with metaphase or interphase *Xenopus laevis* egg extract cytosols. Rat liver ER was used since it has been shown to be motile in interphase *Xenopus laevis* egg extract cytosol [232], where it forms an ER network characterised by three-way junctions between tubules, and importantly, is known to be moved exclusively by kinesin-1 *in vitro* [30]. Therefore any ER motility observed in this assay can be attributed to the activity of kinesin-1. The mixture of ER and cytosol was applied to microscope flow cells which had been pre-coated with microtubules polymerised from purified pig brain tubulin, a commonly used source of microtubules in *in vitro* motility assays [276]. After 1 hour, twenty fields of each flow cell were visualised using VE-DIC microscopy and the level of ER motility was quantified by counting the number of three-way junctions observed per field. This is a widely used method of measuring ER tubule motility *in vitro* and provides a simple and quick means of assessing cargo movement, albeit lacking more detailed quantification of the speed or duration of tubule movement [272]. This analysis parameter was chosen in preference to counting the number of moving tubules per field or the speed of tubule movement since it was found to be much faster and easier to perform, and has been previously reported to provide an accurate estimate of ER motility in this *in vitro* assay [272]. Both meiotic and mitotic metaphase cytosols significantly reduced the mean number of three-way junctions observed per field compared to the interphase cytosol control (Figure 3.3). This data suggests kinesin-1 activity is regulated in a cell cycle-dependent manner, at least *in vitro*.

3.2 Investigating potential mechanisms responsible for the cell cycle regulation of kinesin-1-dependent ER motility

There are a number of potential mechanisms by which kinesin-1 activity may be inhibited in metaphase cytosols (see section 1.6.1 and Figure 1.7) and it was decided to investigate each scenario in turn to determine which, if any, are responsible for the cell cycle regulation of ER motility observed in this assay. It should be noted that the mechanism of regulation was assumed to be the same in both meiotic and mitotic cytosols and consequently some experiments were performed with just one type of metaphase extract.

3.2.1 Interaction of kinesin-1 with the ER membrane

Since regulation of the motor-cargo interaction has been previously shown to underlie cell cycle regulation of cytoplasmic dynein-1 in a similar assay [89], perhaps the most obvious explanation for inhibition of ER motility is that metaphase cytosols stimulate release of kinesin-1 from the rat liver ER. To determine whether this was the case, ER was incubated with interphase, meiotic metaphase II or mitotic metaphase cytosol for 1 hour at room temperature, the same amount of time flow cells are left for when performing the motility assay. ER membranes were then recovered by pelleting through a sucrose cushion, followed by a single wash with A/S to remove

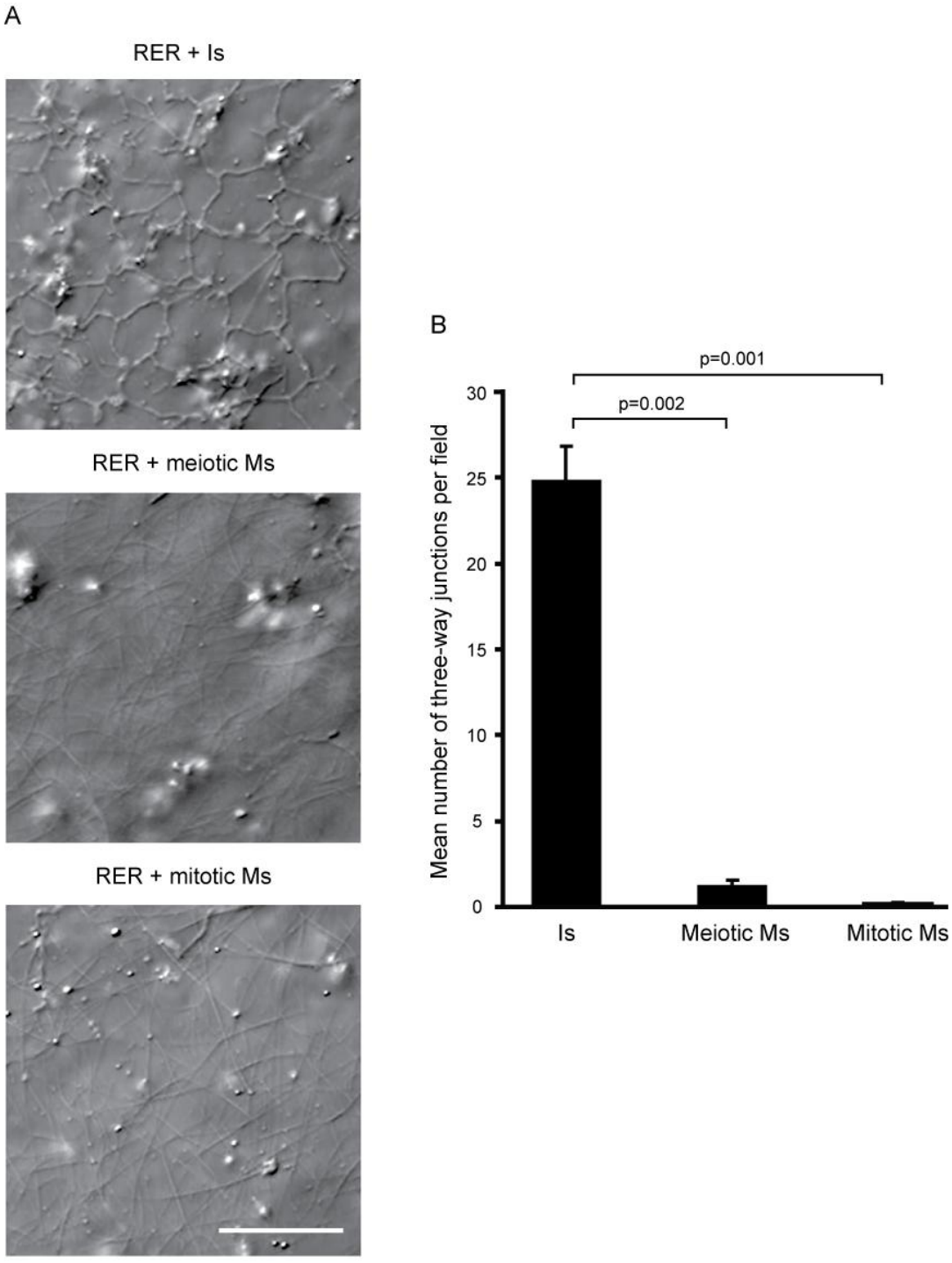

Figure 3.3 - Kinesin-1-driven rat liver ER motility is inhibited by meiotic and mitotic metaphase *Xenopus laevis* egg extract cytosol *in vitro*

A. A volume of 1 µl of rat liver ER membranes were mixed with 9 µl of meiotic or mitotic metaphase *Xenopus laevis* egg extract cytosol, or interphase cytosol prepared from Newmeyer extract as a positive control, and applied to microscope flow cells which had been pre-coated with microtubules polymerised from purified pig brain tubulin for 10 minutes. Flow cells were imaged using VE-DIC microscopy. Scale bar is 10 µm.

B. After 1 hour, twenty randomly chosen fields were observed and from this the mean number of three-way junctions per field was counted. Each experiment was repeated two additional times to obtain three mean values per condition. A mean of these three separate mean values was then calculated and is shown here. Error bars + SEM. P-values were calculated using independent two-sample student t-tests.

any contaminating non-membranous kinesin-1 which may have co-sedimented during pelleting. Samples of this purified ER, along with crude untreated ER, and cytosol fractions were immunoblotted for kinesin-1 using the anti-KHC antibody, uKHC, and with the k2.4 antibody which recognises the KIF3A motor subunit of kinesin-2 [33].

Following treatment with interphase cytosol or meiotic metaphase II cytosol the level of KHC on the re-isolated ER, which runs at approximately 120 kDa, was unchanged compared to the crude ER sample, indicating meiotic metaphase II cytosol does not stimulate release of rat KHC from the membrane (Figure 3.4 A). *Xenopus laevis* KHC ran as a doublet at approximately 120 kDa in both *Xenopus laevis* egg extract cytosol samples. The reason for this is unknown but the upper band does not seem to represent a phosphorylated version of the lower band (Lane and Allan, unpublished data). Importantly, this data suggests that *Xenopus laevis* KHC is not recruited to the rat liver ER membrane since no doublet was observed in the re-isolated ER samples (Figure 3.4 A) [30, 218]. This indicates all ER motility observed in interphase cytosol is driven solely by rat kinesin-1. However, the possibility that the lower running *Xenopus laevis* KHC band is interchanging with the rat liver ER KHC band cannot be excluded. In summary, this data suggests that the inhibition of kinesin-1 driven ER motility is not due to modulation of the interaction between kinesin-1 and ER cargo.

Samples were also blotted for the KIF3A subunit of kinesin-2, a motor which is known to play no role in ER motility in this assay [30]. The amount of KIF3A on the ER, which runs as a doublet, was unchanged following treatment with interphase or meiotic metaphase II cytosol and was similar to that observed in the untreated ER sample. This data indicates kinesin-2 is not lost from, nor recruited to, the ER following treatment with interphase or meiotic metaphase II cytosol.

These experiments were repeated comparing rat liver ER membranes incubated with interphase or mitotic metaphase cytosols prepared from Newmeyer *Xenopus laevis* egg extracts and identical results were obtained (Figure 3.4 B), again supporting the conclusion that disruption of the interaction between kinesin-1 and the ER cargo is not responsible for the metaphase inhibition of motility.

3.2.2 Interaction between rat KHC and KLC

The interaction between the KHC and KLC components of the kinesin-1 motor was next investigated. Metaphase cytosols could potentially prevent interaction between these subunits and thereby render the motor inactive. The most obvious approach to answer this question would be to repeat the experiment described in section 3.2.1, where ER is recovered following incubation with interphase cytosol or metaphase cytosols, and immunoblot with an anti-KLC antibody. If the level of KLC on the ER was reduced following metaphase cytosol treatment, this would indicate that KLC is released from the ER membrane. However, no anti-KLC antibody which works well for immunoblotting was available and moreover this approach would not confirm whether the interaction between KHC and KLC was changed. For example, the interaction between KHC and KLC may be broken but this would not necessarily affect the

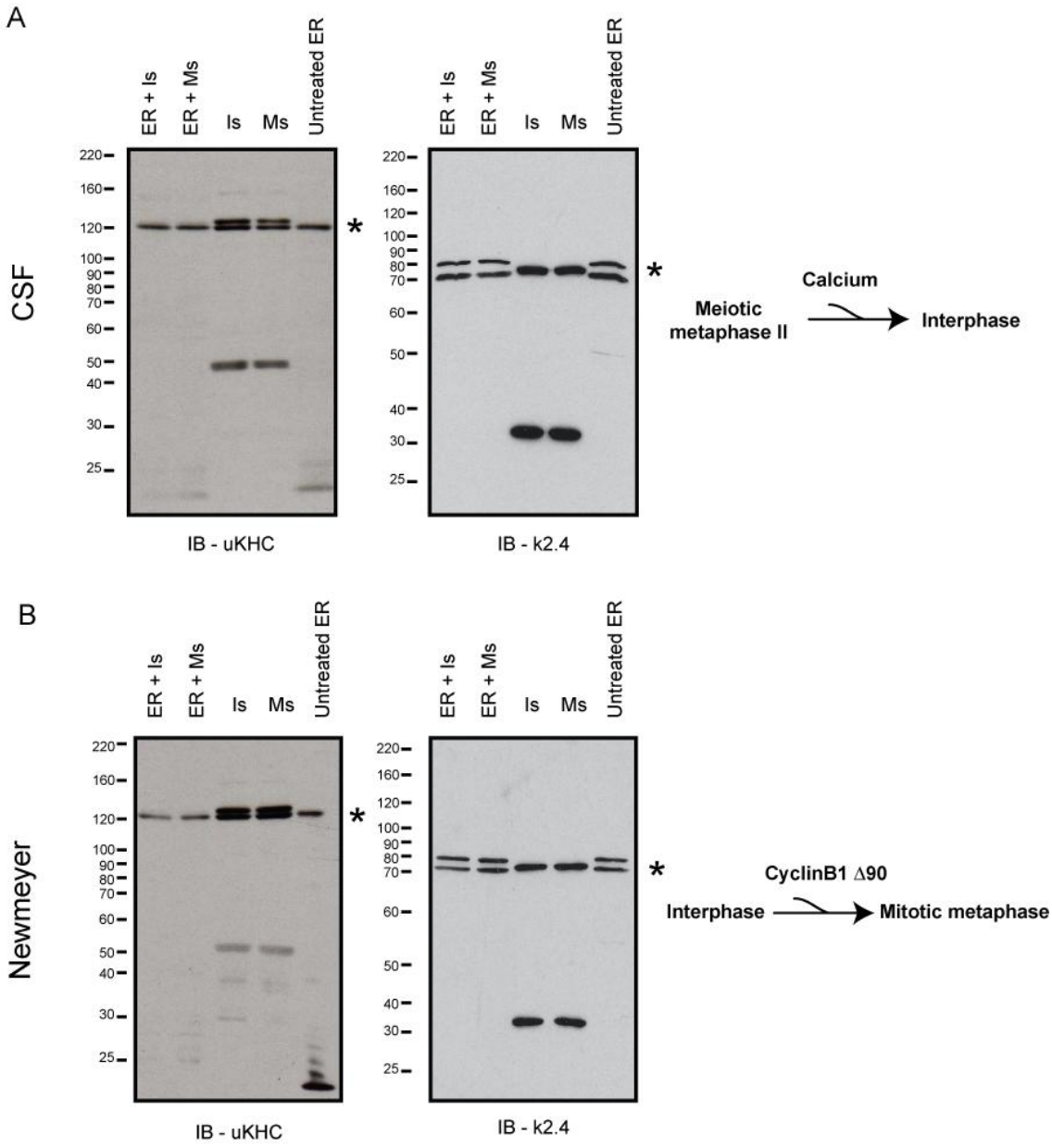

Figure 3.4 - Neither rat KHC nor kinesin-2 is released from rat liver ER membranes following incubation with metaphase cytosols

A. A volume of 10 µl (100 µg) of rat liver ER was incubated with 90 µl interphase cytosol or meiotic metaphase II CSF extract cytosol for 1 hour at room temperature and then ultracentrifuged through a 100 µl cushion of 0.8 M A/S to re-isolate ER membranes. The supernatant from above the cushion was removed and a sample of 10 µl was taken and made up to 50 µl with sample buffer. The cushion itself was then removed and the ER membrane pellet was washed with 100 µl A/S and ultracentrifuged again to re-pellet. The ER membranes were resuspended in 25 µl A/S and made up to 50 µl with sample buffer. A volume of 10 µl (the equivalent of 2 µl of crude ER membranes or cytosol) along with 2 µl of untreated ER, was immunoblotted for KHC or kinesin-2 using the anti-uKHC or k2.4 (anti-KIF3A) antibodies respectively. Asterisks mark the position of KHC and KIF3A.

B. Identical experiments to those described in A were performed but interphase and mitotic metaphase cytosols were prepared from Newmeyer extracts. Asterisks mark the position of KHC and KIF3A.

binding of either subunit to the membrane since both are thought to contain a cargo binding region [30, 198, 201].

It was therefore decided to test the range of available anti-KLC antibodies to determine whether any are capable of specifically immunoprecipitating rat KLC but not *Xenopus laevis* KLC. Immunoprecipitations from rat liver ER or interphase cytosol prepared from Newmeyer *Xenopus laevis* egg extract were performed using the monoclonal anti-KLC antibodies L1 and L2, or with mouse IgG as a negative control. Samples were run on a SDS-PAGE gel and immunoblotted with the anti-KHC antibody, uKHC. KHC was detected in both L1 immunoprecipitates indicating this antibody recognises both rat and *Xenopus laevis* KLC (Figure 3.5 A). However, when the L2 antibody was used, KHC was detected in the rat liver ER sample, but not the interphase *Xenopus laevis* egg extract cytosol sample (Figure 3.5 A). This indicates the L2 antibody is capable of immunoprecipitating rat KLC but not *Xenopus laevis* KLC. Consequently, the KHC-KLC interaction of rat kinesin-1 could be investigated without results being contaminated by *Xenopus laevis* kinesin-1, which is not believed to contribute to rat liver ER motility in this assay (Figure 3.4) [30].

To determine whether the rat liver ER KHC-KLC interaction is disrupted in the metaphase assay, ER was incubated with interphase cytosol or mitotic metaphase cytosol, or A/S for 1 hour at room temperature. A/S was used as a negative control since it is a commonly used buffer in motility assays [217], and is known to have no inhibitory effects upon kinesin-1-dependent ER motility *in vitro* [30]. Rat liver KLC was then specifically immunoprecipitated with the L2 antibody, and mouse IgG was used as a negative control, and samples were immunoblotted for KHC. The level of KHC detected from the rat KLC immunoprecipitate was unchanged following incubation with interphase or mitotic metaphase cytosol compared to the A/S incubation control. This indicates neither interphase nor mitotic metaphase cytosol causes dissociation of the kinesin-1 complex on the rat liver ER membrane (Figure 3.5 B).

3.2.3 Phosphorylation of rat kinesin-1

It is now well established that changes to the phosphorylation status of microtubule motors is a major means of regulating their activity and indeed phosphorylation of DLIC has been shown to correlate with release of cytoplasmic dynein-1 from cargo in mitotic metaphase *Xenopus laevis* egg extracts [89]. Moreover, several studies have revealed that kinesin-1 activity can be regulated by phosphorylation and dephosphorylation of both KHC [91] and KLC [90, 93, 277] (see section 1.3.1). It was therefore feasible that changes to the phosphorylation status of rat kinesin-1 following incubation with either interphase or metaphase cytosol is influencing kinesin-1 activity and thereby responsible for the cell cycle regulation of rat liver ER motility.

It was decided to first determine whether *Xenopus laevis* kinesin-1 phosphate turnover differs between interphase and metaphase cytosols. If no difference was detected then any signal observed when rat liver ER was incubated with *Xenopus laevis* egg extract cytosols could be confidently attributed to changes in rat kinesin-1 phosphorylation status, rather than cytosol contamination. Both interphase and metaphase cytosols were prepared from CSF and

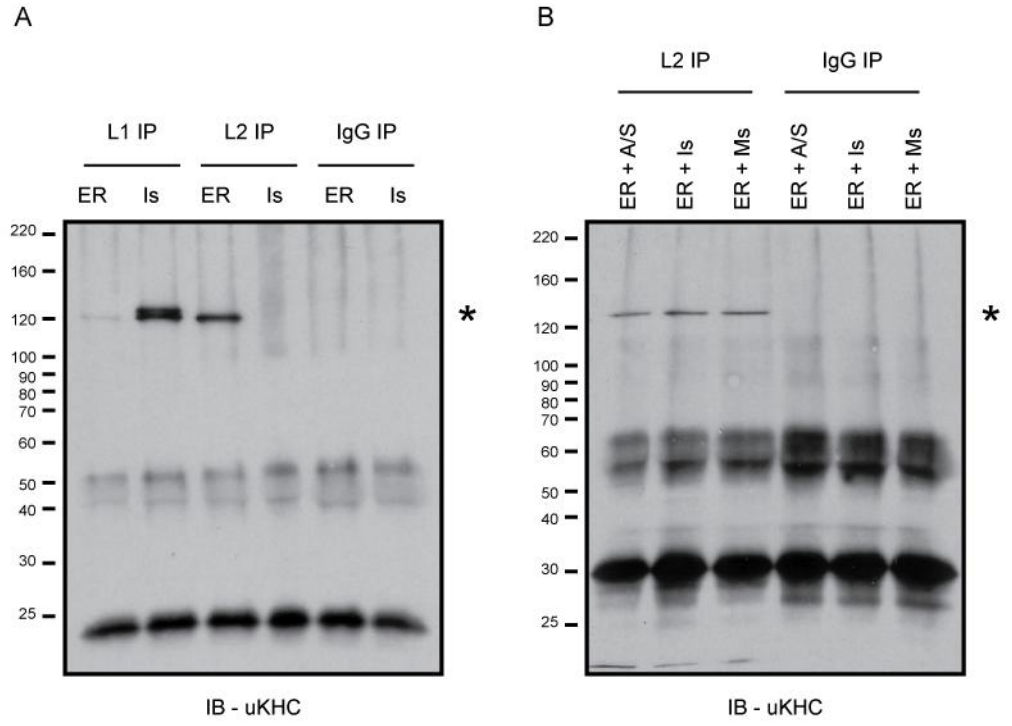

Figure 3.5 - The interaction between rat KHC-KLC on rat liver ER membranes is not disrupted by *Xenopus laevis* egg extract cytosols

A. A volume of 60 µl (600 µg) of rat liver ER or 30 µl (approximately 600 µg) of Newmeyer *Xenopus laevis* egg extract interphase cytosol was immunoprecipitated with the anti-KLC antibodies L1 or L2, or mouse IgG, as described in section 2.4.5. Samples were immunoblotted with the uKHC antibody. The asterisk marks the position of KHC.

B. A volume of 50 µl (500 µg) of rat liver ER membrane was incubated with 200 µl of interphase cytosol or mitotic metaphase cytosol prepared from Newmeyer *Xenopus laevis* egg extract, or with A/S as a positive control, for 30 minutes at room temperature. IP with the anti-KLC antibody L2, or mouse IgG, was performed as described in section 2.4.5. Samples were immunoblotted with the uKHC antibody. The asterisk marks the position of KHC.

Newmeyer *Xenopus laevis* egg extracts which were then incubated with ^{32}P-γ-ATP for 30 minutes at room temperature. Kinesin-1 was immunoprecipitated from these samples with the anti-KHC antibody SUK4 that recognises the motor domain of KHC [278], and IP with mouse IgG was used as a negative control. Importantly, the IP was performed under conditions in which the *Xenopus laevis* KHC-KLC interaction is known not to be disrupted (Figure 3.4 A), meaning KLC will be present in the KHC immunoprecipitate. A doublet band at approximately 120 kDa was observed in each of the SUK4 antibody immunoprecipitates in the colloidal Coomassie stained gel (Figure 3.6 A), corresponding to *Xenopus laevis* KHC. These bands are not observed in the mouse IgG control samples and indicate that kinesin-1 was specifically immunoprecipitated with the SUK4 antibody. Moreover, the intensity of the doublet band appeared comparable in each of the SUK4 immunoprecipitates, indicating that a similar level of kinesin-1 had been immunoprecipitated in each case. No difference in the radiation signal between interphase and metaphase cytosols, or between Newmeyer and CSF extracts was observed (Figure 3.6 B), suggesting that the amount of ^{32}P-γ-ATP kinesin-1 incorporates under each condition is similar and that kinesin-1 phosphate turnover does not change between interphase and metaphase cytosol, or between meiosis and mitosis.

To ensure this negative result was not simply due to failure of the extracts to activate correctly and convert between interphase and metaphase, a sample of each cytosol was immunoblotted for DLIC. In both Newmeyer and CSF *Xenopus laevis* egg extracts DLIC ran at approximately 67 kDa in metaphase cytosols compared to approximately 62 kDa in interphase cytosols (Figure 3.6 C). This suggested DLIC is (hyper)phosphorylated specifically in metaphase samples and that each extract was successfully converted between cell cycle states. Histone kinase assays were also performed with each of the cytosols as another means of confirming the cell cycle status (data not shown). Since *Xenopus laevis* kinesin-1 phosphate turnover does not differ between interphase and metaphase cytosol, any difference in kinesin-1 phosphorylation on rat liver ER could now be attributed more confidently to modification of rat kinesin-1, rather than contamination from extract cytosols.

This data also indicated that the phosphorylation status of *Xenopus laevis* kinesin-1 in egg extracts does not change in a cell cycle-dependent manner. However, it could be argued that since the radiolabel was not present at the actual point of conversion between cell cycle states, the level of steady-state phosphate turnover, as well as the number of phosphorylated sites, could influence the result. For example, if phosphate turnover at a newly phosphorylated site was low it may not be detected in the 30 minutes timeframe used. To more conclusively show *Xenopus laevis* kinesin-1 phosphorylation does not change in a cell cycle-dependent manner, interphase *Xenopus laevis* egg extract was converted to mitotic metaphase by treatment with cyclin B1 Δ90 protein, or alternatively sustained in interphase by treatment with water, in the presence of ^{32}P-γ-ATP for 30 minutes at room temperature. In contrast to the previously described experiment membranes were included in this assay. Kinesin-1 and cytoplasmic dynein-1 were immunoprecipitated using the SUK4 and IC74 (anti-DIC) antibodies respectively, and IP with mouse IgG was used as a negative control. A doublet of similar intensity at

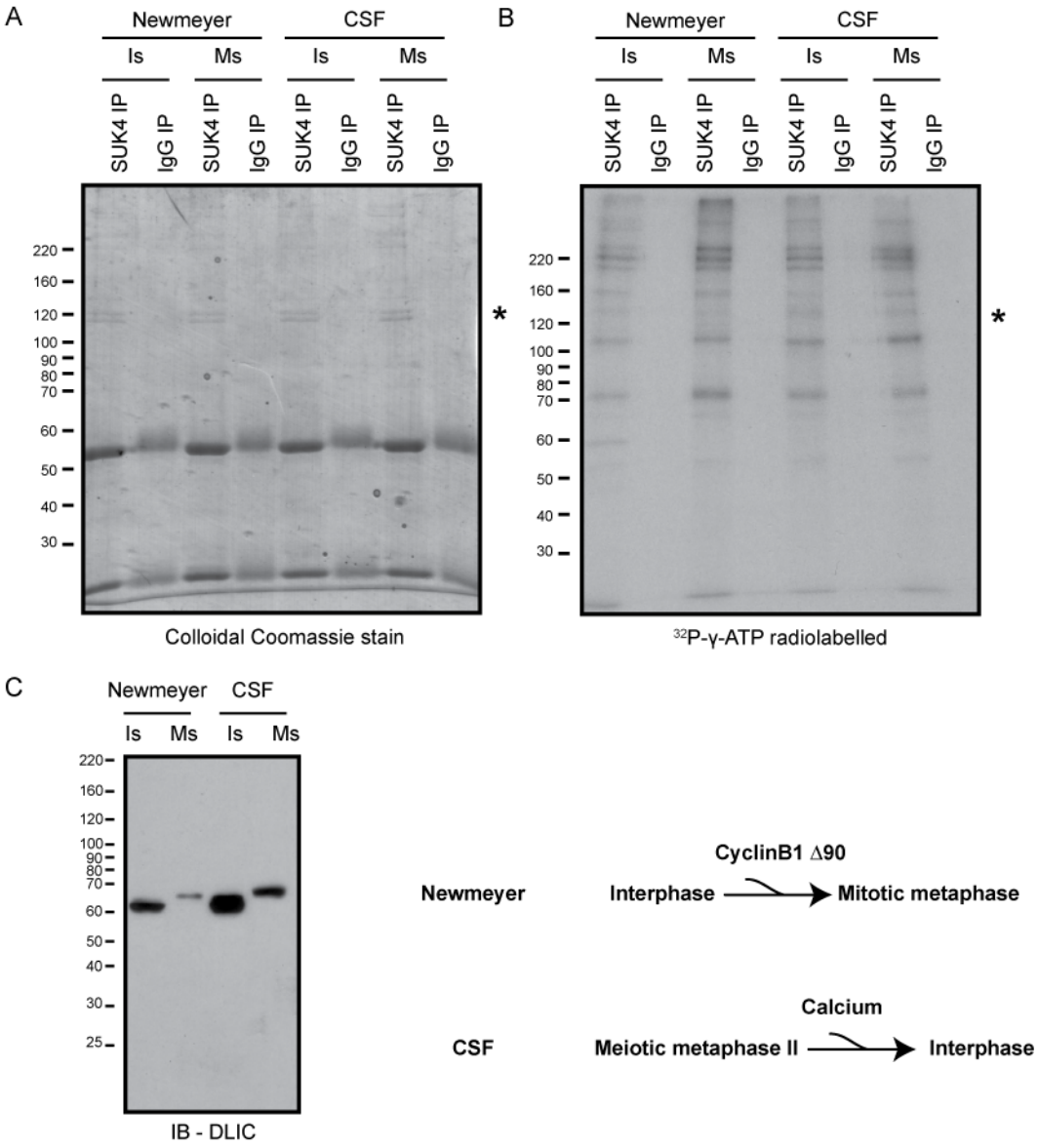

Figure 3.6 - *Xenopus laevis* kinesin-1 phosphate turnover does not differ between interphase and metaphase

A. A volume of 60 µl (approximately 1.2 mg) of interphase, mitotic metaphase, or meiotic metaphase II *Xenopus laevis* egg extract cytosols was incubated with 80 µCi of ^{32}P-γ-ATP for 30 minutes at room temperature after which IP was performed using the anti-KHC antibody SUK4, or mouse IgG, as described in section 2.4.5. Samples were run on an 8 % SDS-PAGE gel, which was stained with colloidal Coomassie, dried and exposed to photographic film. The colloidal Coomassie stained gel is shown. The asterisk indicates the position of KHC.

B. A 24 hour film exposure of the gel in A is shown. The asterisk indicates the position of KHC.

C. A volume of 2 µl of each of the cytosols used in A and B was immunoblotted for DLIC.

approximately 120 kDa was present in each of the SUK4 immunoprecipitate samples, indicating that a comparable amount of kinesin-1 was immunoprecipitated in each case (Figure 3.7 A). A single band at approximately 85 kDa was present in each of the IC74 immunoprecipitates, corresponding to DIC (Figure 3.7 A). An intense band above the 220 kDa marker was also observed, which is thought to be DHC.

Following cyclin B1 Δ90 treatment there was an intense radiation signal in the DIC immunoprecipitate at approximately 67 kDa that was not observed in the water treated sample, which corresponded to the specific metaphase phosphorylation of DLIC (Figure 3.7 B). This indicates the extract was correctly converted from interphase into metaphase and supports the observation of Niclas and co-workers that DLIC is specifically phosphorylated in mitotic metaphase *Xenopus laevis* egg extracts [89]. In contrast, a band at approximately 120 kDa is present in the SUK4 immunoprecipitate following cyclin B1 Δ90 treatment which is not observed in the water treated sample. This may indicate phosphorylation of *Xenopus laevis* KHC is occurring specifically in mitosis. Other bands are also apparent which are more intense in the cyclin B1 Δ90 treatment, including a band above the 220 kDa marker. These may reflect the mitotic phosphorylation of proteins which interact with kinesin-1.

To determine whether the phosphorylation status of kinesin-1 on rat liver ER membrane changes specifically following incubation with interphase or mitotic metaphase cytosol, ER was incubated with each cytosol for 30 minutes at room temperature in the presence of ^{32}P-γ-ATP. ER was then separated from the cytosol by pelleting through a sucrose cushion. The SUK4 antibody was used to immunoprecipitate kinesin-1 from the recovered ER, whereas the IC74 antibody was used to immunoprecipitate cytoplasmic dynein-1 from each of the cytosols to check whether metaphase-specific phosphorylation of DLIC could be observed. A single band at approximately 85 kDa was present in each of the IC74 immunoprecipitates in the colloidal Coomassie stained gel, corresponding to DIC (Figure 3.8 A). An intense band above the 220 kDa marker, believed to be DHC, was also observed. The intensity of these bands was similar in each of the IC74 immunoprecipitates indicating a similar level of cytoplasmic dynein-1 was immunoprecipitated in each case. No bands corresponding to KHC or KLC were observed in the SUK4 immunoprecipitates by colloidal Coomassie staining (Figure 3.8 A). This is likely due to the low level of kinesin-1 on the rat liver ER membrane (see section 3.2.5).

When the gel was exposed to film, there was an intense band at approximately 70 kDa in the DIC immunoprecipitate from mitotic metaphase cytosol which was not observed in the interphase cytosol sample (Figure 3.8). This band corresponded to the metaphase-specific phosphorylation of DLIC and indicated each cytosol is in the correct cell cycle state. This data suggests DLIC in metaphase Newmeyer *Xenopus laevis* egg extracts continues to incorporate phosphate at a relatively high rate following conversion. No differences in the radiation signal in SUK4 immunoprecipitates following incubation with interphase or mitotic metaphase cytosol was observed (Figure 3.8 B), suggesting that kinesin-1 on rat liver ER membranes does not incorporate phosphate under either condition.

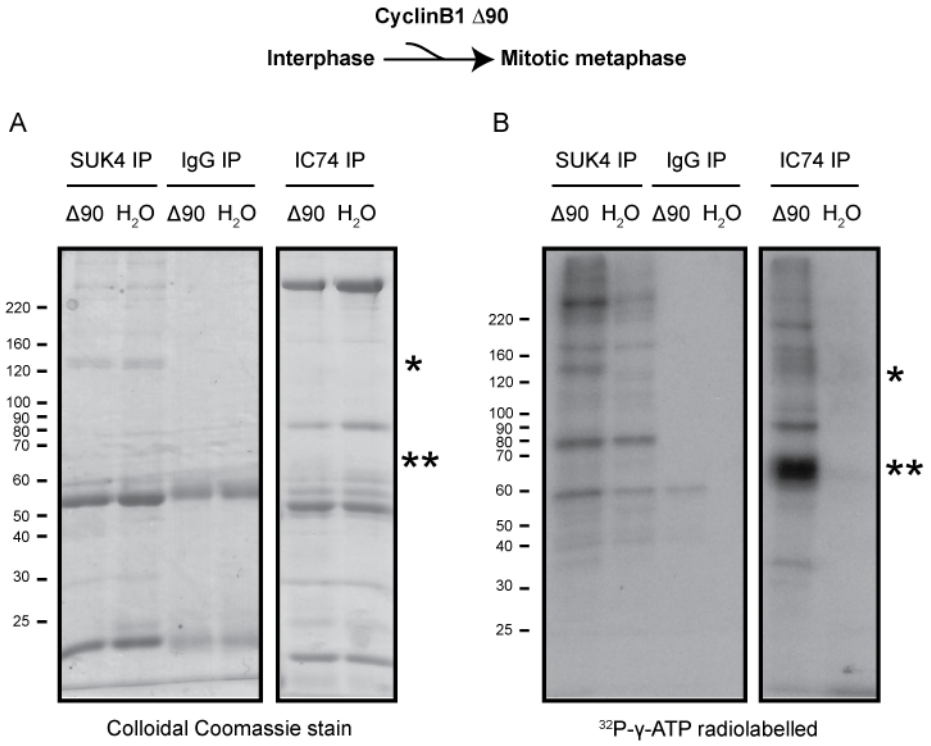

Figure 3.7 - *Xenopus laevis* kinesin-1 is not phosphorylated in a cell cycle-dependent manner

A. A volume of 60 µl (approximately 1.8 mg) of Newmeyer *Xenopus laevis* egg extract was treated with 0.13 mg/ml sea urchin cyclin B1 Δ90 at room temperature to stimulate conversion from interphase to mitotic metaphase, or with an equal volume of H_2O. After 30 minutes, 200 µCi of ^{32}P-γ-ATP was added and the incubation was continued for a further 30 minutes. IP with the anti-KHC antibody, SUK4, or the anti-DIC antibody, IC74, was performed, with mouse IgG as a negative control, as described in section 2.4.5. Samples were run on an 8 % SDS-PAGE gel which was stained with colloidal Coomassie, dried and exposed to photographic film. The colloidal Coomassie stained gel is shown. The asterisk marks the position of KHC, the double asterisk marks the position of DLIC.

B. A 24 hour film exposure of the gel in A is shown. The asterisk indicates the position of KHC, the double asterisk marks the position of DLIC.

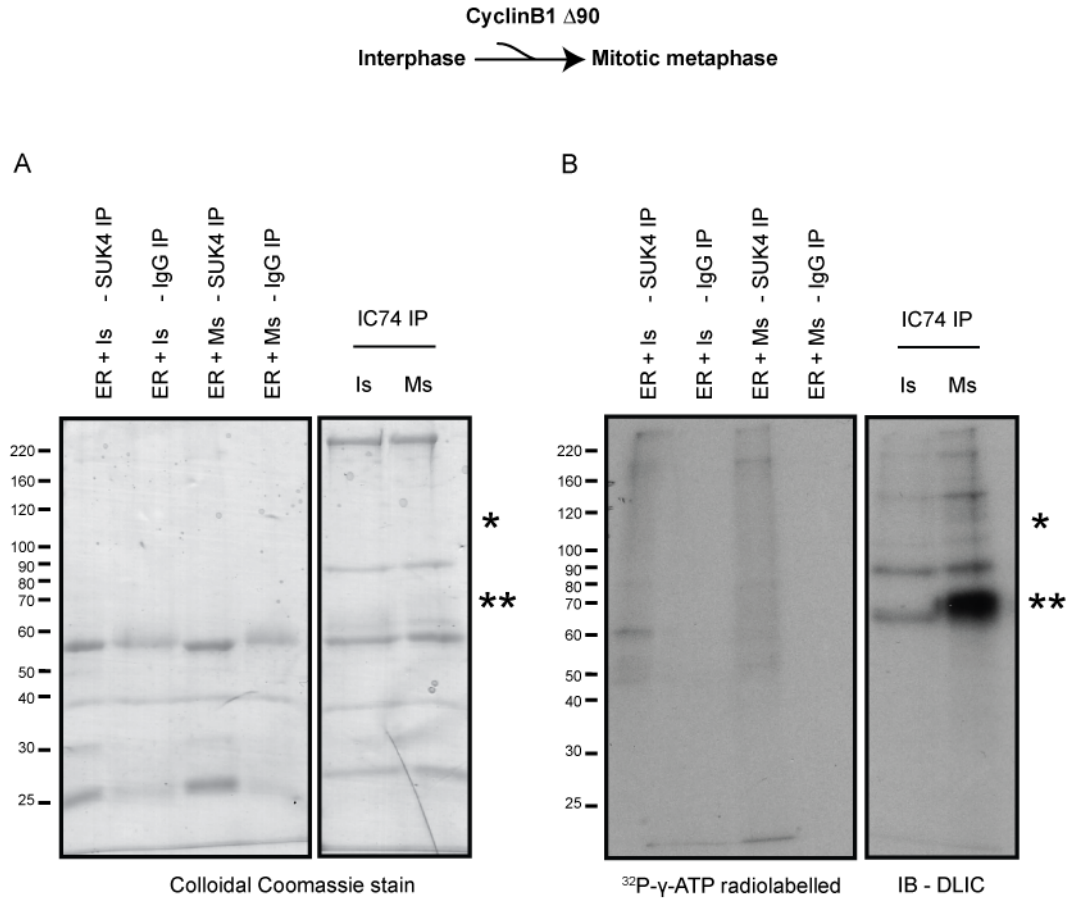

Figure 3.8 - Rat liver kinesin-1 does not become (hyper)phosphorylated following incubation with either interphase cytosol or mitotic metaphase cytosol

A. A volume of 120 µl (approximately 2.4 mg) of interphase or mitotic metaphase Newmeyer *Xenopus laevis* egg extract cytosol was incubated with 40 µl (400 µg) of rat liver ER membranes and 160 µCi of ^{32}P-γ-ATP for 30 minutes at room temperature. The samples were then ultracentrifuged through a 100 µl cushion of 0.8 M A/S to re-isolate membranes. The cytosol fraction from above the cushion was immunoprecipitated with the anti-DIC antibody IC74 while the membrane pellet was immunoprecipitated with the anti-KHC antibody SUK4, or mouse IgG, as described in section 2.4.5. Samples were run on an 8 % SDS-PAGE gel, which was stained with colloidal Coomassie, dried and exposed to photographic film. The colloidal Coomassie stained gel is shown. The asterisk marks the position of KHC, the double asterisk marks the position of DLIC.

B. A 1 week film exposure of the gel in A is shown. The asterisk indicates the position of KHC, the double asterisk marks the position of DLIC.

3.2.4 Use of K430-BCCP protein

Kinesin-1 bead assays were used to investigate whether microtubule modifications, or direct regulation of the KHC head domain, are responsible for the metaphase inhibition of rat liver ER motility. Similar systems have been used successfully in previous studies to determine the directionality of membrane movement [16, 218] as well as calculating motor step sizes and run lengths [279]. Kinesin bead assays allow the direct observation of cargo which is moved exclusively by a single motor. Furthermore, coating beads with recombinant truncated KHC protein allows the study of kinesin-1 motor activity in the absence of autoinhibition by KLC binding (see section 1.3.3) [280].

In this assay, K430-BCCP protein was recombinantly expressed in *Escherichia coli*. This protein encodes amino acids 1 to 430 of rat KIF5C, tagged at the C-terminus to the N-terminus of an 80 amino acid fragment of biotin carboxyl carrier protein (BCCP). Amino acids 1 to 430 of KIF5C encode the motor domain, neck and neck linker, and a small region of stalk 1 of KHC [281-283]. Importantly, this allows the protein to dimerise via coiled coil linkages in the neck domain [284]. However, the absence of the more C-terminal portions of KHC means autoinhibition, via interaction between the KHC tail and motor domains, is prevented [101]. Consequently the motor is constitutively active and unregulated. KIF5C is generally classified as a neuronal KHC isoform of kinesin-1, but a recent study has detected KIF5C mRNA in two human lung epithelial cell lines [24], thus challenging this thinking. Rat KIF5B, the widely considered ubiquitously expressed KIF5 isoform, and KIF5C share 79 % identical amino acid homology within the portion of KHC used in this assay. Furthermore, they share 87 % identical amino acid homology in residues 1 to 350, which are generally considered to encode the motor domain of kinesin-1 [283, 285]. A fragment of the naturally occurring BCCP protein is now widely used as an alternative tag in recombinant protein expression. The advantage of BCCP in comparison to other tags is that it is a smaller protein with a mass of approximately 14 kDa and purification is often found to be more efficient with less contamination [270]. Biotin is added to the culture medium during induction of K430-BCCP expression, leading to biotinylation of the BCCP tag. Streptavidin-coated beads, which bind biotin, can then be used to purify the tagged protein. A schematic of these interactions is shown in Figure 3.9 A.

To determine whether the protein could be expressed and purified, the soluble bacterial lysate was incubated with streptavidin-coated beads. A sample of the total bacterial lysate along with soluble and bead-bound fractions was run on a SDS-PAGE gel and stained with Coomassie. An intense band at approximately 65 kDa, corresponding to K430-BCCP protein, was seen in each fraction and bound specifically to streptavidin-coated beads (Figure 3.9 B). This shows soluble K430-BCCP protein can be produced in *Escherichia coli* and subsequently purified using streptavidin-coated beads. Attempts were also made to express and purify a similar fragment of KIF5B, the ubiquitously expressed isoform of KHC. However, the protein was found to be insoluble despite attempts to optimise expression and purification procedures (data not shown).

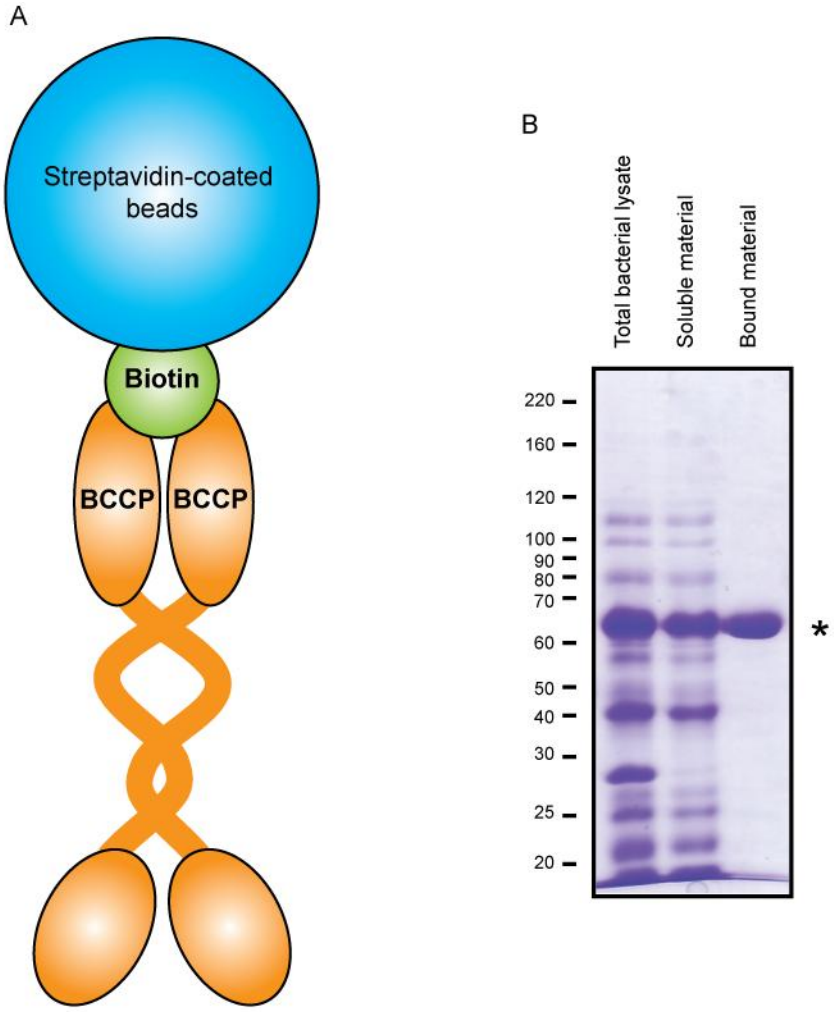

Figure 3.9 - K430-BCCP protein binds streptavidin-coated beads

A. Schematic diagram showing the binding of recombinantly expressed K430-BCCP protein, shown in orange, to biotin which in turn binds streptavidin-coated beads.

B. Expression of K430-BCCP protein was performed as described in section 2.6.3. A volume of 15 µl of streptavidin-coated beads was incubated with 50 µl of soluble bacterial lysate for 15 minutes at room temperature. This sample of bead-bound material, along with 10 µl of the total bacterial lysate and 10 µl of the soluble fraction, were run on an 8 % SDS-PAGE gel and stained with Coomassie. The asterisk marks the position of the K430-BCCP protein.

3.2.4.1 Microtubule post-translational modifications

There are several examples in which modifications of microtubules, such as acetylation [113] and detyrosination [114], can influence the ability of kinesin-1 to both bind and to move along microtubules. It is feasible that such modifications are occurring specifically in the interphase or metaphase assay and underlie the inhibition of kinesin-1-driven ER motility. To investigate this possibility microscope flow cells were coated with microtubules polymerised from purified pig brain tubulin, or from interphase or mitotic metaphase *Xenopus laevis* egg extract cytosols. Pig brain tubulin is a commonly used source of microtubules in motility assays, along which kinesin-1 is known to move [30], and therefore acts as a positive control. Beads were coated with recombinant K430-BCCP protein (Figure 3.9 A) and applied to flow cells in the presence of an energy-regenerating system that converts ADP to ATP, catalysed by the presence of creatine phosphate and the enzyme creatine phosphokinase. Beads were observed moving along microtubules polymerised from each of the three sources and no significant difference in the mean frequency of moving beads per field was detected (Figure 3.10). This data reveals the KIF5C motor domain can bind and move along microtubules polymerised under both interphase and metaphase conditions, indicating modifications to microtubules are not responsible for inhibition of kinesin-1-dependent ER motility by metaphase cytosols. The possibility that the velocity of movement is reduced specifically under one condition cannot be eliminated, although this is not readily obvious by looking at the data by eye. It should also be noted that this data does not exclude the possibility that the interaction between kinesin-1 and microtubules is disrupted in the metaphase assay but this may be dependent upon the presence of KLC and/or more C-terminal portions of KHC, which are absent in this experimental setup.

3.2.4.1 Direct regulation of rat KHC head and neck domains

It was next decided to determine whether direct modulation of the rat KHC head and neck domains, either activation by interphase cytosol or inhibition by metaphase cytosol, is responsible for the cell cycle-dependent regulation of ER motility. To achieve this microscope flow cells were coated with microtubules polymerised from purified pig brain tubulin. Beads were again coated with K430-BCCP protein and diluted into interphase or mitotic metaphase cytosol, or A/S, and applied to flow cells in the presence of an energy-regenerating system. Beads were observed moving along microtubules following incubation with interphase or mitotic metaphase cytosol or A/S, and no significant change in the mean frequency of moving beads per field was detected (Figure 3.11). These results reveal that the KHC motor domain can bind and move along microtubules in the presence of both interphase and mitotic metaphase cytosol, indicating modification of rat KHC head and neck domains, albeit in the absence of KLC, are not responsible for inhibition metaphase inhibition of kinesin-1-driven ER motility.

3.2.5 Binding partners

The last possibility to be investigated was that kinesin-1 binding partners, that have an inhibitory or activating effect upon kinesin-1 activity, bind specifically in metaphase or interphase cytosol, respectively. Initial attempts to identify such proteins involved performing kinesin-1 immunoprecipitations from rat liver ER which had been recovered following incubation with either interphase or metaphase cytosol. It soon became obvious that the level of kinesin-1 on

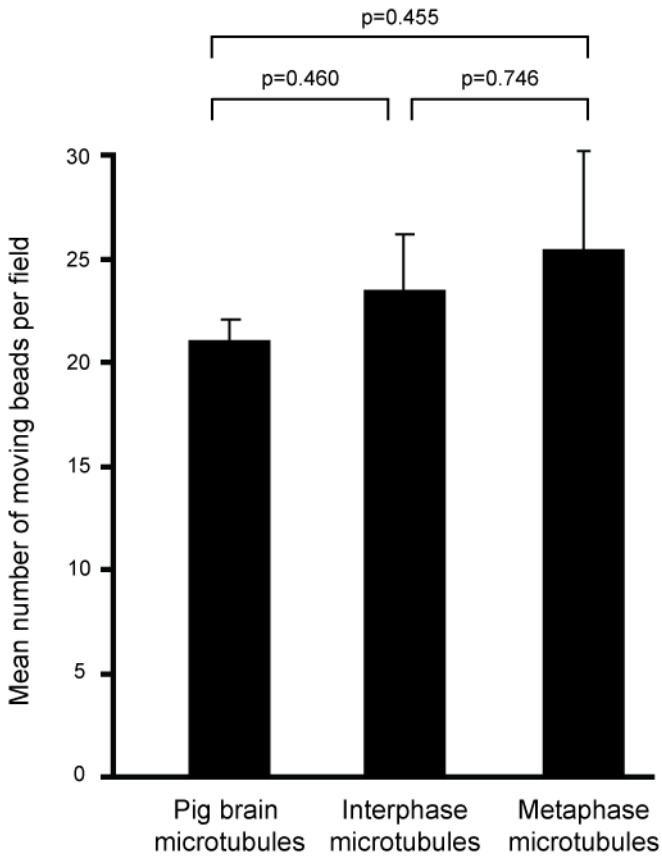

Figure 3.10 - Microtubule modifications are not responsible for inhibition of kinesin-1-dependent motility by mitotic metaphase *Xenopus laevis* egg extract cytosol

Microscope flow cells were coated with microtubules polymerised from purified pig brain tubulin. Alternatively, interphase or mitotic metaphase cytosols were incubated for 10 minutes in microscope flow cells in a humid chamber, during which time microtubules polymerised and adhered to the coverslip. Unbound material was flushed away using motility buffer. A volume of 6 µl of soluble K430-BCCP bacterial lysate was incubated with 2 µl of magnetic streptavidin-coated beads for 15 minutes at room temperature. The beads were diluted in 40 µl of motility buffer and 10 µl was applied to the flow cell. Twenty randomly chosen fields were viewed using VE-DIC microscopy and from this the mean number of moving beads per field was calculated. Each experiment was repeated two additional times to obtain three mean values per condition. A mean of these three separate mean values is shown here. Error bars + SEM. P-values were calculated using independent two-sample student t-tests.

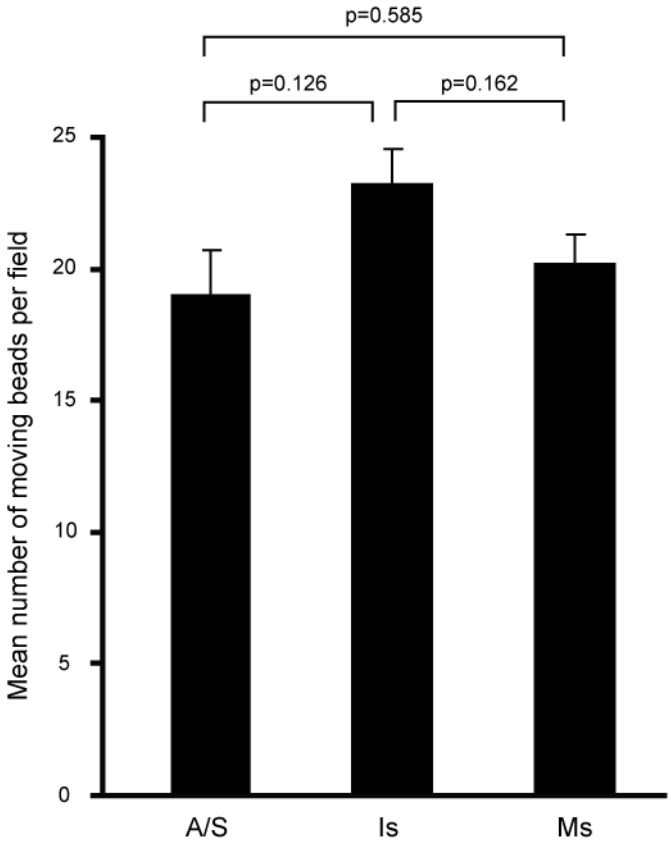

Figure 3.11 - KHC head and neck domains are not inhibited directly by mitotic metaphase *Xenopus laevis* egg extract cytosol

Microscope flow cells were coated with microtubules polymerised from purified pig brain tubulin for 10 minutes in a humid chamber and unbound material was flushed away with motility buffer. A volume of 6 µl of soluble K430-BCCP bacterial lysate was incubated with 2 µl magnetic streptavidin-coated beads for 15 minutes at room temperature. The beads were diluted in 40 µl of interphase cytosol or mitotic metaphase cytosol prepared from Newmeyer *Xenopus laevis* egg extracts, or A/S, in the presence of an energy-regenerating system, and 10 µl was applied to the flow cell. Twenty randomly chosen fields were viewed using VE-DIC microscopy and from this the mean number of moving beads per field was calculated. Each experiment was repeated two additional times to obtain three mean values per condition. A mean of these three separate mean values is shown here. Error bars + SEM. P-values were calculated using independent two-sample student t-tests.

the rat liver ER membrane was much lower than in *Xenopus laevis* egg extracts, which severely hampered progress. Furthermore, the process of re-isolating ER membranes following incubation with interphase or metaphase cytosol was also found to reduce the level of material immunoprecipitated with anti-kinesin-1 antibodies. To illustrate this, kinesin-1 was immunoprecipitated with the SUK4 antibody from rat liver ER which had been re-isolated by pelleting through a sucrose cushion or flotation through a sucrose gradient. The pelleted ER membranes were either resuspended directly in IP buffer or first into A/S, since unpublished data suggested this may also influence the amount of kinesin-1 immunoprecipitated (personal communication, Dr. Marcin Woźniak). Samples were run on SDS-PAGE gels and stained with colloidal Coomassie. The level of material immunoprecipitated from ER membranes following re-isolated either by pelleting or flotation, was reduced compared to when crude untreated ER was used (Figure 3.12 A). This indicates material is either lost through the process of re-isolation, or that the ability of kinesin-1 to bind SUK4 is reduced or inhibited following re-isolation. Additionally, neither the KHC nor the KLC bands, with expected molecular weights of 120 kDa and 70 kDa respectively, were observed even in the SUK4 immunoprecipitate from crude ER (Figure 3.12 A). This suggested attempting to identify kinesin-1 binding partners in the ER fraction may be fraught with technical difficulties owing to the low level of motor in the sample, which is further reduced by re-isolation procedures.

Several attempts were made to overcome these problems by performing scaled-up experiments using a larger starting volume of rat liver ER, or by using different volumes and molarities of sucrose in the cushion or gradient during the re-isolation procedure. Since the ratio of ER to cytosol used in the *in vitro* motility assays was 1:10, it was thought that the volume of cytosol should be at least double the volume of ER membranes in biochemical experiments. Since only approximately 3 ml of extract is produced per batch of eggs, this further limited the amount of ER used. Different antibodies were used to immunoprecipitate kinesin-1 and different batches of ER membranes were also tested. None of these changes were found to greatly affect the outcome (data not shown).

Immunoprecipitations were also performed with the anti-KLC antibody, L2, which has the advantage of specifically recognising rat KLC but not *Xenopus laevis* KLC (Figure 3.5). This avoids the need to re-isolate ER following incubation with *Xenopus laevis* egg extract cytosol. The expected KHC and KLC bands at 120 kDa and 70 kDa respectively were not observed in any of the L2 immunoprecipitates and no obvious differences between incubation with interphase or mitotic metaphase cytosols were apparent (Figure 3.12 B). Bands at approximately 300 kDa and 45 kDa were visible when ER had been incubated with *Xenopus laevis* egg extract cytosol, which were not seen with A/S incubation. However, since both these bands were also found in the control mouse IgG immunoprecipitates it is probable that they represent non-specific binding of *Xenopus laevis* proteins to the beads, likely to be myosin and actin.

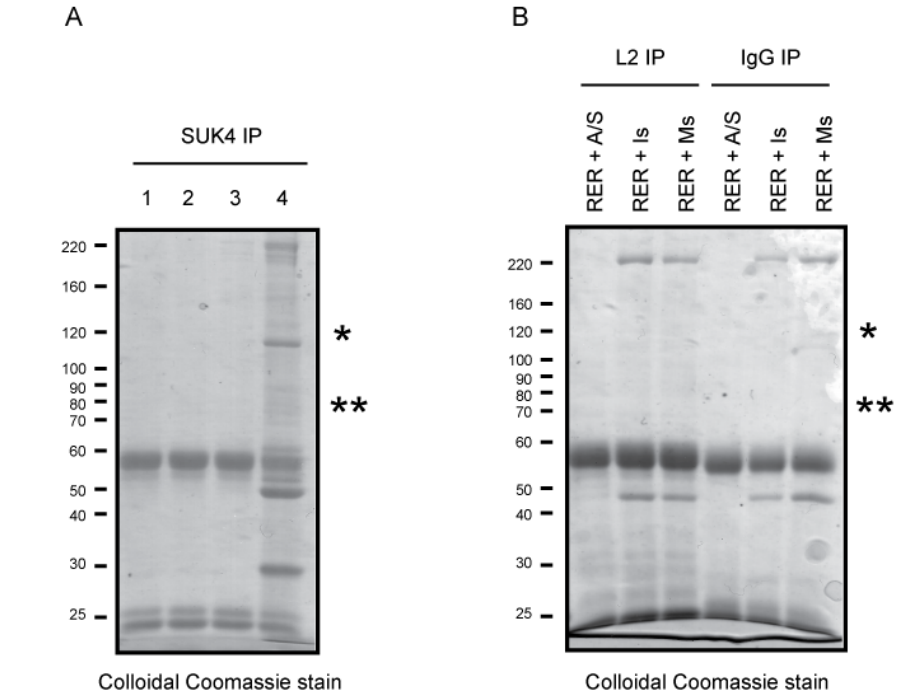

Figure 3.12 - Isolation of rat liver ER membranes by pelleting or flotation reduces the level of material immunoprecipitated with the SUK4 antibody

A. A volume of 100 µl (1 mg) of rat liver ER membranes was added to 200 µl of interphase cytosol prepared from Newmeyer *Xenopus laevis* egg extracts, and this mixture was ultracentrifuged through a 250 µl cushion of 0.8 M A/S. The pelleted membranes were resuspended in 500 µl of IP buffer (lane 1) or in 200 µl of A/S and added to 300 µl of IP buffer (lane 2). Alternatively, the membrane and cytosol mixture was added to 300 µl of 2 M A/S and membranes were re-isolated by flotation through a sucrose gradient (lane 3) and then made up to 500 µl with IP buffer. As a control, 100 µl (1 mg) of rat liver ER membranes were added directly to 400 µl of IP buffer (lane 4). Kinesin-1 was immunoprecipitated with the anti-KHC antibody, SUK4, as described in section 2.4.5. Samples were run on an 8 % SDS-PAGE gel which was stained with colloidal Coomassie. The asterisk marks the position of KHC, the double asterisk marks the position of KLC.

B. A volume of 200 µl (2 mg) of rat liver ER membranes was added to 400 µl of interphase cytosol or mitotic metaphase cytosol prepared from Newmeyer *Xenopus laevis* egg extracts, or with 400 µl of A/S containing 1x energy mix. Samples were incubated for 30 minutes at room temperature and then made up to 1 ml with IP buffer. Kinesin-1 was immunoprecipitated with the anti-KLC antibody L2, or mouse IgG as a negative control, as described in section 2.4.5. Samples were run on an 8 % SDS-PAGE gel which was stained with colloidal Coomassie. The asterisk marks the position of KHC, the double asterisk marks the position of KLC.

Due to the outlined technical difficulties in identifying proteins which interact with kinesin-1 it became unfeasible to continue with this approach. It was therefore decided to switch tack and take a more biased approach to try and identify binding partners which may regulate kinesin-1 in a cell cycle-dependent manner. To this end, proteins which are known to associate with kinesin-1, or modulate motor activity, were screened and those which seemed more likely to operate in a cell cycle context were investigated further. Whilst this is not ideal, since a single protein is investigated at a time making progress very protracted, it was decided worthwhile to explore the most likely candidates further.

3.2.5.1 p150*glued*

p150*glued*, a subunit of the dynactin complex, is known to be mitotically regulated in both HeLa and XTC cell lines where it becomes hyperphosphorylated specifically during M-phase [286]. The association of p150*glued* with mitotic *Xenopus laevis* egg extract membranes is known to be under cell cycle control [89]. Moreover, recent evidence suggests p150*glued* can bind kinesin-1 under certain circumstances and by doing so both positively [81] and negatively regulate kinesin-1 activity (personal communication, Dr. Marcin Woźniak). This evidence pointed towards p150*glued* as a potential regulator of kinesin-1 in a cell cycle-dependent manner.

To determine if an association between p150*glued* and KHC could be replicated, IP experiments were initially performed using *Xenopus laevis* egg extracts since they are known to have a relatively high concentration of motors making any potential interaction easier to observe. KHC was immunoprecipitated with the SUK4 antibody from interphase or meiotic metaphase II membrane fractions prepared by flotation, since the interaction is believed to occur whilst kinesin-1 is bound to cargo [81] (personal communication, Dr. Marcin Woźniak). Immunoprecipitates were immunoblotted for p150*glued* or KHC. A band at approximately 150 kDa corresponding to p150*glued* was detected specifically in the SUK4 immunoprecipitates and not the mouse IgG control of both interphase and metaphase membrane fractions (Figure 3.13 A). This indicates p150*glued* and kinesin-1 interact in both interphase and meiotic metaphase II membrane fractions, although it remains possible that the interaction is mediated through another subunit of the dynactin complex. Since the intensity of the p150*glued* band did not differ when interphase or meiotic metaphase II membrane fractions were used this indicated the interaction does not change in a cell cycle-dependent manner, at least in meiotic *Xenopus laevis* egg extracts. A similar level of KHC was found in both SUK4 immunoprecipitates when immunoblotted with the uKHC antibody, with a double band of similar intensity running at approximately 120 kDa, showing a similar level of KHC was immunoprecipitated in both cases (Figure 3.13 B).

To determine whether a similar interaction is occurring on rat liver ER membranes specifically in the interphase or metaphase assay, kinesin-1 was immunoprecipitated using the anti-KLC antibody L2, following incubation of ER for 30 minutes with interphase or meiotic metaphase II cytosols, or A/S. Immunoprecipitates were immunoblotted for p150*glued* or KHC. The L2 antibody was again used to immunoprecipitate kinesin-1 in order to prevent the need to re-

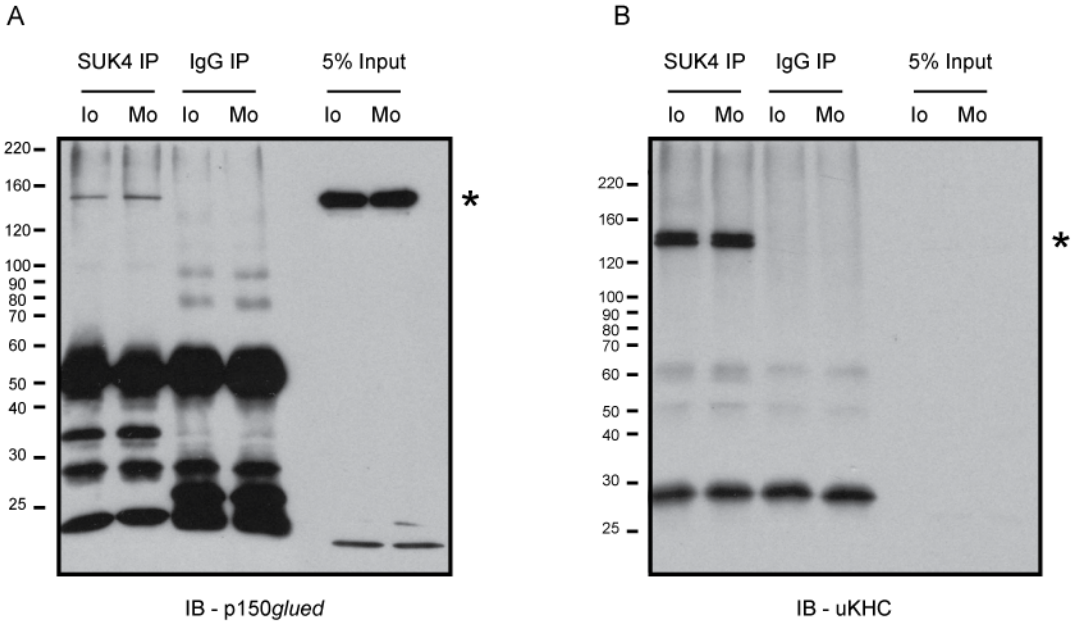

Figure 3.13 - Kinesin-1 and p150*glued* interact equally in membrane fractions isolated from interphase and meiotic metaphase II *Xenopus laevis* egg extracts

A. A volume of 50 µl of CSF *Xenopus laevis* egg extract was treated with 2.5 µl of activation mix and 100 µg/ml cycloheximide for 1 hour, to stimulate conversion from meiotic metaphase II to interphase, or with an equal volume of mock activation mix. Two volumes of A/S containing 1x energy mix were added and the extract was ultracentrifuged to generate a membrane and cytosol fraction. The membranes were resuspended in 50 µl of 2 M A/S and layered onto a sucrose gradient consisting of 2 M A/S, membranes in 2 M A/S, 1.4 M A/S and 0.25 M A/S. Following ultracentrifugation, the membranes were collected from the 1.4 M/0.25 M A/S interface and resuspended in 20 µl of A/S. Each sample was made up to 1 ml with IP buffer, left on ice for 10 minutes and then centrifuged to clarify. Kinesin-1 was immunoprecipitated with the SUK4 antibody as described in section 2.4.5, while mouse IgG was used as a negative control, and samples were immunoblotted with the anti-p150*glued* antibody. The asterisk marks the position of p150*glued*.

B. The same samples as described in A were immunoblotted with the anti-KHC antibody, uKHC. The asterisk marks the position of KHC.

isolate ER membranes following incubation with cytosols. No signal for p150*glued* was detected under any of the conditions tested (Figure 3.14 A). Immunoblotting for KHC revealed a similar level of kinesin-1 has been immunoprecipitated in all cases (Figure 3.14 B). This data may suggest that no interaction between kinesin-1 and p150*glued* exists on untreated rat liver ER membranes and furthermore, no interaction is induced following incubation with interphase or meiotic metaphase II cytosol. Alternatively, it is possible that an interaction does exist but the relatively low level of kinesin-1 on rat liver ER membranes means it cannot be detected. Indeed, the amount of KHC observed in the kinesin-1 IP from rat liver ER was noticeably lower than when interphase or meiotic metaphase II *Xenopus laevis* egg extract membranes were used (Figure 3.13 B).

The next approach taken was to determine whether the total level of p150*glued* on rat liver ER membrane differs following treatment with interphase or metaphase cytosol. ER membranes were incubated with interphase or meiotic metaphase II cytosol, or A/S. The ER was then re-isolated by pelleting membranes through a sucrose cushion, followed by a wash with A/S to remove any contaminating non-membranous dynactin which had co-sedimented during pelleting. Samples of recovered ER along with interphase and meiotic metaphase II cytosols, and untreated rat liver ER membrane, were immunoblotted for p150*glued* and DIC. No p150*glued* was detected on untreated ER membranes indicating dynactin is absent from purified rat liver ER membranes, or is present at a level lower than the threshold of detection for the anti-p150*glued* antibody (Figure 3.15 A). This perhaps explains in part why rat liver ER is moved exclusively by kinesin-1 *in vitro*, whereas *in vivo* data indicates cytoplasmic dynein-1 also contributes to ER motility [197]. Following incubation with both interphase and meiotic metaphase II cytosol, p150*glued* was detected on ER membranes suggesting it was recruited from the cytosol. The intensity of the band, running at approximately 150 kDa, did not differ between interphase and meiotic metaphase II cytosol incubations, indicating the recruitment was similar in both cases. Thus, whilst p150*glued* is recruited from *Xenopus laevis* egg extract cytosols to the ER membrane, this does not differ between cell cycle states and so cannot be responsible for metaphase inhibition of motility.

A small amount of recruitment of DIC to the ER membrane following incubation with interphase and meiotic metaphase II cytosol was also observed, with a band at approximately 85 kDa apparent when using the anti-DIC antibody IC74, although the band intensity was lower than that observed for p150*glued* (Figure 3.15 B). No DIC was detected in untreated ER membranes indicating cytoplasmic dynein-1 is absent from purified rat liver ER membranes, or is present at a level lower than the threshold of detection for the anti-DIC antibody. A Ponceau S stain indicated a similar level of protein was present in each of the membrane samples (Figure 3.15 C).

Since no evidence to support a role for p150*glued* in the metaphase inhibition of kinesin-1 was found it was decided to switch tack and focus on another potential regulator, E-MAP-115.

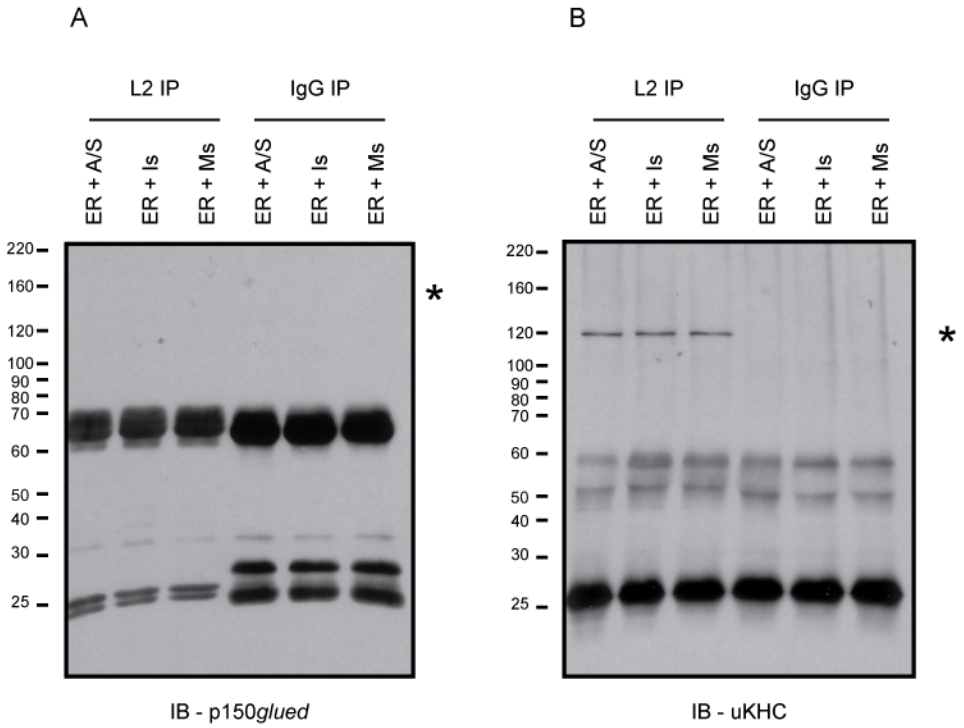

Figure 3.14 - No interaction between kinesin-1 and p150*glued* on rat liver ER membranes is detected following incubation with interphase or meiotic metaphase II *Xenopus laevis* egg extract cytosol

A. A volume of 100 µg (1 mg) or rat liver ER was incubated with 400 µl of interphase or meiotic metaphase II cytosol, or with 400 µl of A/S containing 1x energy mix. After 1 hour at room temperature, each sample was made up to 1 ml with IP buffer, left on ice for 10 minutes and then centrifuged to clarify. Kinesin-1 was immunoprecipitated with the anti-KLC antibody L2, or mouse IgG, as described in section 2.4.5. Samples were immunoblotted with an anti-p150*glued* antibody. The asterisk marks the expected position of p150*glued*.

B. The same samples as described in A were immunoblotted with the anti-KHC antibody uKHC. The asterisk marks the position of KHC.

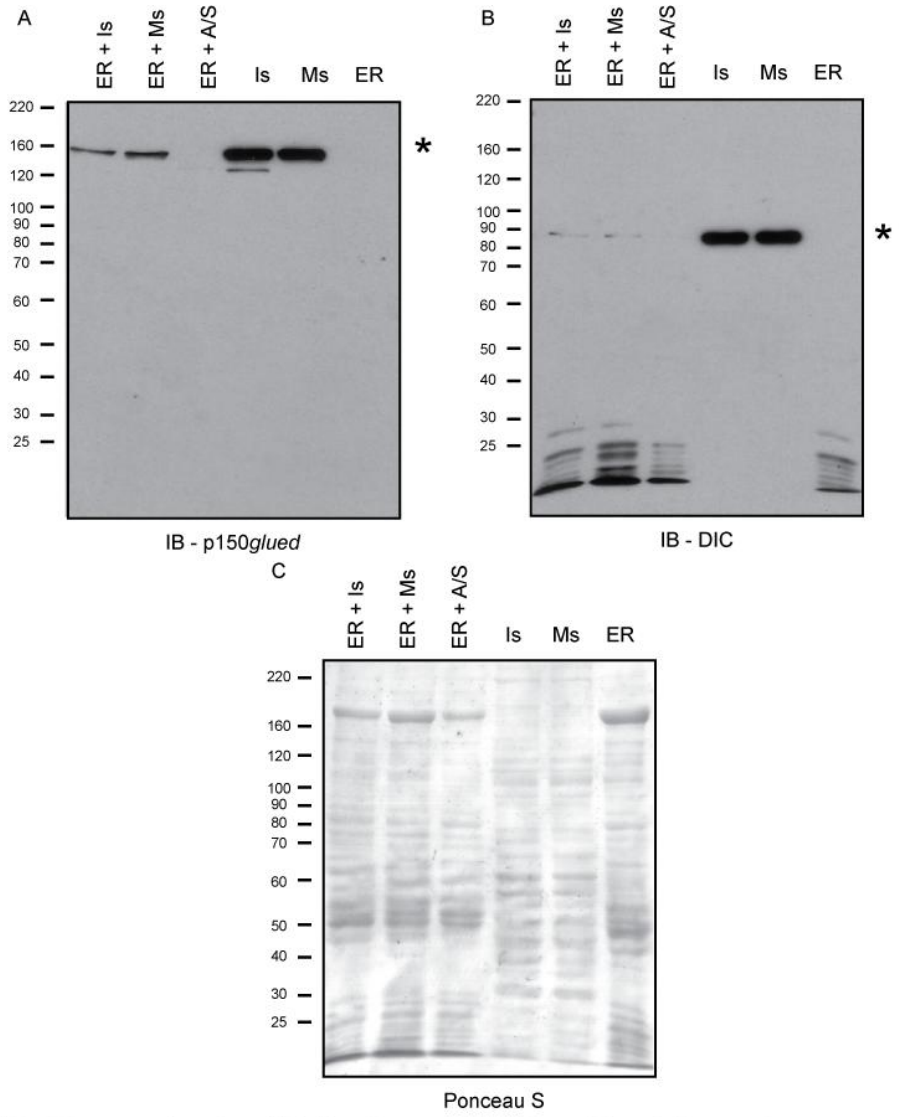

Figure 3.15 - *Xenopus laevis* p150*glued* is recruited to rat liver ER membranes equally following incubation with interphase or meiotic metaphase II cytosol

A. A volume of 10 µl (100 µg) of rat liver ER was incubated with 90 µl of interphase or meiotic metaphase II cytosol, or with 90 µl of A/S containing 1x energy mix. After 1 hour at room temperature, samples were ultracentrifuged through a 100 µl cushion of 0.8 M A/S to re-isolate ER membranes. The supernatant from above the cushion was removed and a sample of 10 µl was taken and made up to 50 µl with sample buffer. The ER membrane pellet was washed with 100 µl of A/S and ultracentrifuged again to pellet. The ER membranes were resuspended in 25 µl A/S and made to 50 µl with sample buffer. A volume of 10 µl (the equivalent of 2 µl of crude ER membranes or cytosol) and 2 µl of untreated ER membranes were immunoblotted with an anti-p150*glued* antibody. The asterisk marks the position of p150*glued*.

B. The same samples as described in A were immunoblotted with an anti-DIC antibody. The asterisk marks the position of DIC.

C. A Ponceau S stain of the samples described in A is shown.

3.2.5.2 E-MAP-115

E-MAP-115, also known as ensconsin and MAP7, is a MAP. First identified in 1993 by Masson and Kreis in HeLa cells [269], the binding of E-MAP-115 to microtubules is thought to influence microtubule dynamics. Binding of the MAP stabilises microtubules and protects them against depolymerisation [269]. For several years it has been known that E-MAP-115 is mitotically regulated, at least in the HeLa cell line, with the protein becoming hyperphosphorylated at the onset of mitosis, an event which coincides with its release from microtubules [118]. This regulation of the interaction between E-MAP-115 and microtubules may be important in driving changes to microtubule dynamics which are necessary to form the mitotic spindle. After prometaphase E-MAP-115 is dephosphorylated and progressively reassociates with microtubules resulting in microtubule stabilisation.

A recent study links E-MAP-115 to kinesin-1 regulation. Ensconsin, the *Drosophila melanogaster* homologue of E-MAP-115, has been shown to be required for all studied kinesin-1 functions in the polarised fly oocyte [119]. Single cell assays indicate ensconsin exerts this control by promoting the recruitment of kinesin-1 to microtubules and its motility. Whilst it is not known whether E-MAP-115 also controls kinesin-1 activity in a similar manner in mammalian systems, these results identified E-MAP-115 as a candidate potentially capable of regulating kinesin-1 activity in a cell cycle-dependent manner.

In ovary extracts prepared from *Drosophila melanogaster,* the microtubule binding and motility of full length KHC was perturbed in ensconsin mutant samples compared to the wild-type extract control but this effect was not observed when a recombinantly expressed truncated version of the motor lacking the C-terminal tail domain was used [119]. This suggests the inhibition of kinesin-1 activity in ensconsin mutant flies is either due to direct targeting of the more C-terminal portion of the motor, or is dependent upon kinesin-1 adopting a folded conformation in which the KHC motor and tail domains interact. These scenarios could explain why no effects upon the motility of KHC motor domain along metaphase microtubules was previously observed (Figure 3.10). It is unknown how ensconsin exerts these effects upon kinesin-1 motility, since no evidence of an interaction between the two proteins was found. Because of this, it seemed unlikely that IP experiments similar to those described for p150*glued* would be of any use. Moreover, an antibody which recognises both rat and *Xenopus laevis* E-MAP-115 by immunoblotting was not available.

Therefore, to investigate whether E-MAP-115 functions as a regulator of kinesin-1, the effects of adding GST-E-MAP-115 protein upon rat liver ER motility *in vitro* were investigated. Human E-MAP-115 DNA was isolated from a HeLaM cell cDNA library and cloned into a GST-tagged bacterial expression vector. Human E-MAP-115 was used since the initial cell cycle studies were based upon this protein [118]. ER was incubated with 0.5 µg of GST-E-MAP-115, or GST, for 20 minutes on ice. The final concentration of GST-E-MAP-115 protein in the assay was approximately 980 nM. Since the endogenous concentration of E-MAP-115 in *Xenopus laevis* egg extracts is unknown it was not possible to determine accurately how many orders of

magnitude more the exogenous protein was present at, in comparison to the native protein. This may be important since overexpression of MAPs has been associated with perturbation of microtubule structure and dynamics [287, 288], and could thereby perhaps have indirect effects upon motor activity. However, the concentration of another MAP, XMAP310, has been reported to be approximately 200 nM in *Xenopus laevis* egg extract [289]. It was therefore assumed that the amount of GST-E-MAP-115 added was approximately 5-10 times the level of endogenous protein. These treated membranes were added to interphase cytosol prepared from Newmeyer *Xenopus laevis* egg extracts, applied to flow cells which had been pre-coated with microtubules polymerised from interphase cytosol and the level of ER motility was monitored using VE-DIC microscopy. If E-MAP-115 positively regulates kinesin-1, the addition of further E-MAP-115 protein may be expected to increase the level of ER motility. In fact, the opposite result was observed. Whereas incubation with GST had no apparent effects upon ER motility, GST-E-MAP-115 almost completely inhibited network formation (Figure 3.16 A). No noticeable differences in microtubules were seen when GST-E-MAP-115 was used at this concentration, although when higher levels of the protein were tested, microtubules looked abnormal with more bundling and less polymerisation observed (data not shown).

To determine whether this inhibitory effect of GST-E-MAP-115 was limited to kinesin-1-driven motility, assays were repeated using membranes isolated by pelleting from interphase Newmeyer *Xenopus laevis* egg extracts, which are known to be moved exclusively by cytoplasmic dynein-1 [89]. Again, incubation of membranes with GST-E-MAP-115 inhibited motility compared to the GST control (Figure 3.16 B). This suggested the effects of GST-E-MAP-115 upon membrane motility are non-specific, perhaps due to extensive coating of microtubules by the MAP, and confident conclusions cannot be drawn from the data.

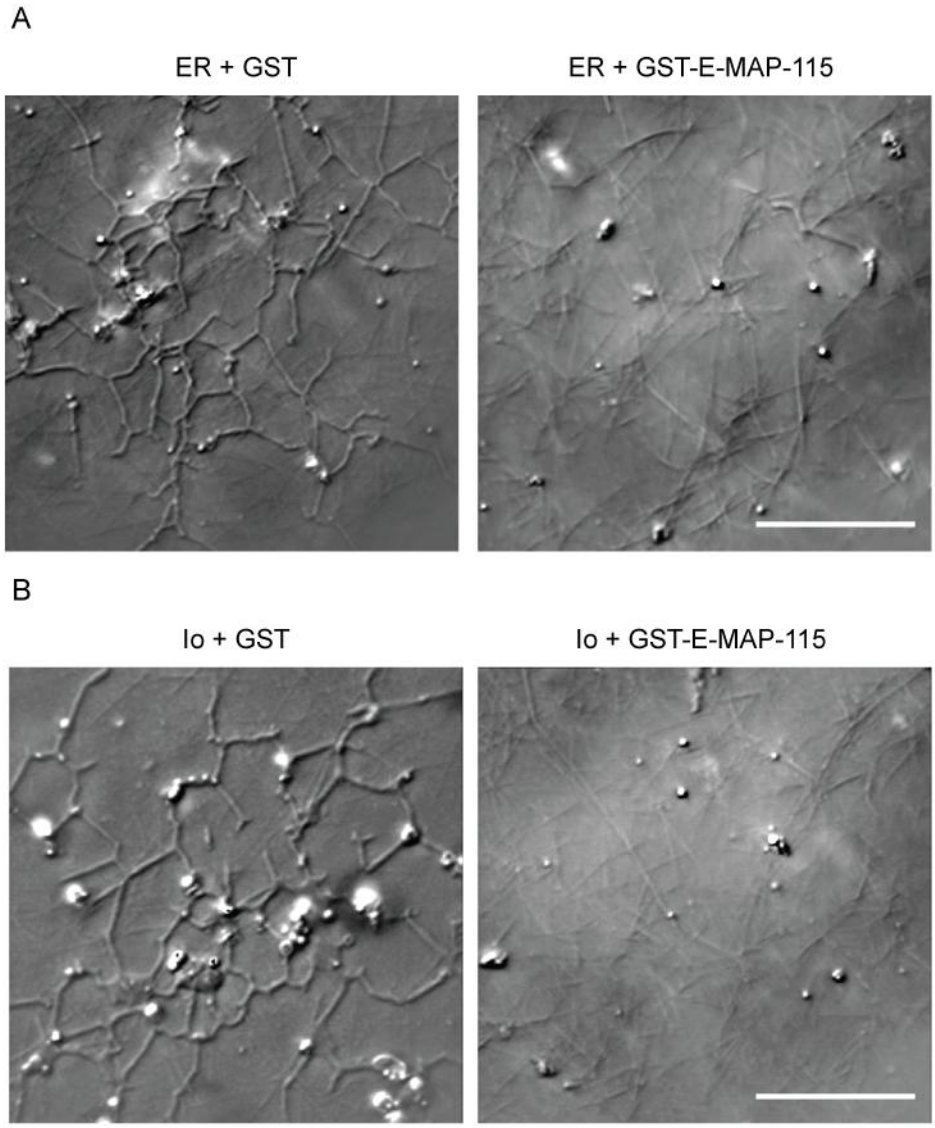

Figure 3.16 - GST-E-MAP-115 inhibits the *in vitro* motility of rat liver ER membranes and interphase *Xenopus laevis* egg extract membranes

A. Interphase cytosol prepared from Newmeyer *Xenopus laevis* egg extracts was diluted 5-fold in acetate buffer and applied to microscope flow cells and microtubules were allowed to polymerise for 10 minutes in a humid chamber. A volume of 1 µl (10 µg) of rat liver ER membranes was incubated with 1 µl (0.5 µg) of GST or GST-E-MAP-115 protein, which had been dialysed into acetate buffer, for 20 minutes on ice. Of this mixture, 1 µl was taken and added to 9 µl of interphase cytosol prepared from Newmeyer *Xenopus laevis* egg extracts, applied to the flow cell and incubated in a humid chamber for 1 hour. Flow cells were imaged using VE-DIC microscopy. Scale bar is 10 µm.

B. A volume of 50 µl of Newmeyer *Xenopus laevis* egg extract was added to 2 volumes of A/S and 1x energy mix and ultracentrifuged to generate a membrane pellet (Io). The pellet was resuspended in 20 µl of A/S and of this 1 µl was used in motility assays with 9 µl of interphase cytosol as described in A. Scale bar is 10 µm.

4. Discussion – Cell cycle regulation of kinesin-1

Kinesin-1 is involved in controlling the positioning and morphology of a wide range of organelles and plays integral roles in trafficking through the secretory and endocytic pathways. It was hypothesised that modulation of the activity of this motor may contribute to the large scale changes in cargo transport and organelle localisation observed during cell division. Therefore the aim of this work was to determine if and how kinesin-1 activity is regulated in a cell cycle-dependent manner. This study was considered worthwhile and viable given the potentially highly significant implications of kinesin-1 regulation during cell division and the relative ease with which the question could be probed using established *in vitro* motility assays.

4.1 Reconstitution of kinesin-1-driven cargo motility *in vitro*

Previous studies have employed motility assays using cytosol and membrane fractions prepared from *Xenopus laevis* egg extracts to reveal that ER motility is inhibited during mitosis due to inhibition of cytoplasmic dynein-1 function [89]. Similar assays were used in this study by combining rat liver ER membranes with *Xenopus laevis* egg extract cytosol to investigate whether kinesin-1 activity is also regulated in a cell cycle-dependent manner. This approach was chosen for several reasons. It is known that rat liver ER membranes are motile in interphase *Xenopus laevis* egg extract cytosol and form a network characterised by three-way junctions occurring between tubules [232]. This network is simply visualised using VE-DIC microscopy and the level of motility can be easily quantitated by counting the number of three-way junctions per field. Furthermore, it has been shown that all ER motility in this assay is due entirely to the function of kinesin-1 [30], meaning any alteration in cargo movement can be attributed to changes in the activity of this motor. Perhaps most importantly in terms of this project is the ability to convert the assay easily between cell cycle states by using meiotic, mitotic or interphase *Xenopus laevis* egg extract cytosol. It was felt that the cell cycle modulation of kinesin-1 function could be probed more easily using this approach in comparison to *in vivo* studies, where cooperation between motors and rounding up of cells during division are inherent problems. *In vivo* analyses were planned if and when a mechanism for kinesin-1 regulation was identified *in vitro*.

To validate any differences in rat liver ER motility between interphase and metaphase and for all subsequent biochemical analyses it was necessary to employ rigorous controls to ensure *Xenopus laevis* egg extracts were in the correct cell cycle state and could be reliably converted between states. In addition to the conventionally used histone kinase assays to achieve this, a new assay was established in which the phosphorylation status of DLIC was monitored over time. A noticeable shift in DLIC mobility can be detected by western blotting between phosphorylated and dephosphorylated forms. This could then be correlated to changes in cell cycle status since DLIC is known to become hyperphosphorylated specifically during metaphase [89]. Compared to histone kinase assays this was a simpler and faster means of determining extract quality, and found to be technically easier for screening numerous extracts concurrently.

The release of *Xenopus laevis* cytoplasmic dynein-1 from ER membranes triggered by phosphorylation of DLIC has previously been shown to be responsible for the mitotic inhibition of ER motility observed in *Xenopus laevis* egg extracts [89]. While these results were recapitulated here in mitotic extracts, this mechanism did not operate in meiotic extracts. Interestingly, a band shift in DLIC mobility by western blotting was observed in CSF extracts, suggesting that it is specifically phosphorylated during meiosis as well as mitosis. However, it is possible that the sites of phosphorylation differ between extract types, or that the shift is due to another post-translational modification. These observations raise questions regarding the cell cycle regulation of cytoplasmic dynein-1 in *Xenopus laevis* egg extracts. Perhaps completely different mechanisms are driving inhibition of ER motility in meiotic versus mitotic extracts. Alternatively, phosphorylation of DLIC may be sufficient to induce inhibition of ER-bound motor activity, and the release of cytoplasmic dynein-1 observed in mitotic extracts is not directly responsible for the cessation of ER motility. Further studies are warranted to probe the reasons underlying these differing observations.

Experiments using ^{32}P-γ-ATP indicated mitotic-specific phosphorylation of *Xenopus laevis* KHC may occur. In terms of *Xenopus laevis* ER-bound kinesin-1 this is perhaps surprising given the motor remains inactive between interphase and metaphase [218]. However, the movement of other kinesin-1-driven cargoes may be regulated in a cell cycle-dependent manner in the *Xenopus laevis* egg and it is feasible that modulation of the phosphorylation status of kinesin-1 may contribute to this. Little is known regarding the specific isoforms of KHC or KLC which are expressed in *Xenopus laevis,* or whether they display any tissue-specific distribution, which may complicate any future studies investigating how kinesin-1 is regulated during cell division in this organism (see Table 1.1). It would be interesting to determine whether any changes in the phosphorylation status of the motor are induced when egg membranes are incubated with XTC cytosol, which could explain how the contribution of kinesin-1 to *Xenopus laevis* ER motility is activated during development [218].

4.2 Significance of metaphase inhibition of rat liver ER motility

When rat liver ER membranes were combined with metaphase cytosols in motility assays, a significant reduction in three-way junctions per field was observed in both meiotic and mitotic conditions. It could be argued that a defect in ER tubule fusion, which is known to be inhibited during mitosis in semi-intact cell assays [211], could be contributing to this result. However, no tubule motility was observed in metaphase assays indicating that cargo motility, and not simply membrane fusion, was affected. This data presents evidence that kinesin-1 activity is regulated in a cell cycle-dependent manner. Given the pivotal functions of kinesin-1, this finding is exciting and may be highly significant, perhaps having widespread implications in cargo transit and organelle morphology, motility and positioning during the cell cycle.

If this regulation is replicated *in vivo* then it has far-reaching consequences. Studies of mammalian ER inheritance to date have concentrated on the morphology and positioning of the organelle, and little work has examined whether ER motility changes during the cell cycle. A role

for cytoplasmic dynein-1 in moving ER tubules in VERO cells has recently been reported [197]. Whether ER movement driven by this motor is regulated in mammalian somatic cells in a similar manner to that previously described in *Xenopus laevis* eggs is undetermined. It is likely that the contributions of kinesin-1 and cytoplasmic dynein-1 to ER motility in somatic cells are precisely controlled allowing spatial and temporal remodelling of the network and it is feasible that this regulation extends to the cell cycle.

There are known to be several connections between the ER and microtubule cytoskeleton in addition to the motors kinesin-1 and cytoplasmic dynein-1. Whilst the interaction mediated by CLIMP-63 is known to be broken during mitosis [207], the implications of this are uncertain since a range of other connections between the two networks would presumably remain intact. Whether the contributions of TACs or myosin motors to rat liver ER motility are also regulated in a cell cycle-dependent manner remains to be determined. Interestingly, it has been reported that myosin V-driven ER motility in *Xenopus laevis* egg extracts is activated specifically during mitosis [290]. One conundrum is what advantage the downregulation of microtubule-dependent ER motility during cell division may confer. It is conceivable that a reduction in ER movement may aid stochastic partitioning between daughter cells, or that dissociation of ER cargo from microtubules is required for correct formation of the metaphase spindle. Indeed, rough ER membranes have been observed to be excluded from the region occupied by the spindle in mitotic HeLa cells [210]. It is also possible that processes, such as cell migration, which require ER movement in interphase, are inhibited or downregulated during cell division, meaning movement is no longer necessary. Alternatively, decreased ER motility may simply be a symptom of a more general reduction in microtubule-dependent cargo movement during the cell cycle.

If kinesin-1 function is regulated during cell division *in vivo*, it is unlikely that the consequences would be limited to ER motility. This study focused upon the ER simply because it is a cargo whose transport is driven exclusively by kinesin-1 in an *in vitro* assay which could be easily manipulated between cell cycle states. Kinesin-1 is known to contribute to the positioning of a range of organelles and trafficking pathways which are altered during cell division (see section 1.5), and it is possible that regulation of this motor contributes to these changes. Moreover, *in vitro* rat liver Golgi vesicle motility, which is partially driven by kinesin-1 [30], is also potently inhibited by metaphase *Xenopus laevis* egg extract cytosol (Robertson and Allan, unpublished data). This supports the theory that large scale changes to microtubule motor transport occur during cell division which influence a range of cargoes, and that the effects of kinesin-1 inhibition during metaphase *in vitro* are not restricted to ER tubule movement.

4.3 Mechanism of kinesin-1 cell cycle regulation

The mechanism responsible for the cell cycle-dependent regulation of kinesin-1-driven ER motility was next investigated. A number of scenarios could be envisaged which could explain how inhibition of cargo movement may be occurring. It was decided to investigate each of these

possibilities in turn, gathering data which would lead to each one being discounted or pursued further.

Several previous studies have revealed that the interaction between kinesin-1 and cargoes can be tightly modulated [86, 90]. It was therefore hypothesised that the inhibition of rat liver ER motility observed in metaphase cytosols is due to release of kinesin-1 from its cargo. However, when ER membranes were recovered following incubation with meiotic or mitotic cytosol no difference in the level of membrane-bound KHC was detected by western blotting. Furthermore, no recruitment of *Xenopus laevis* kinesin-1 to the ER membrane in interphase cytosol was observed. This assay therefore represents one of the few reported examples in which kinesin-1 activity is modulated whilst remaining attached to cargo [93]. The concept of regulation of membrane-bound motors is becoming increasingly prevalent and is often used to explain how bidirectional cargo motility is achieved. Indeed, motors with differing polarities are often found simultaneously bound to the same cargoes, and it has been proposed that motility is coordinated so that when a given motor is engaged with the microtubule the opposing motor is not [273]. This would necessitate the inactivation of motors whilst bound to cargoes. Perhaps in certain situations both kinesin-1 and cytoplasmic dynein-1 are simultaneously bound to ER cargo and can each be regulated without being released from the membrane, allowing coordination of bidirectional tubule motility and rapid remodelling of the network. It should be noted that it remains possible that the association of either KHC or KLC with their ER receptors is modulated by metaphase cytosol but this is not detected since the KHC-KLC interaction remains intact.

Rat liver kinesin-1 was not found to be phosphorylated following incubation with either interphase or metaphase cytosol. In this experimental setup ^{32}P-γ-ATP was included in the incubation of rat liver ER membranes with the appropriate cytosol and kinesin-1 was then immunoprecipitated. However, this approach cannot exclude the possibility that the motor is specifically dephosphorylated in either situation since a reduced level of phosphate incorporation would not be detected. The inclusion of protein phosphatase inhibitors in the assay to test this hypothesis would have likely influenced the cell cycle status of the cytosols. Ideally, a positive control would have been incorporated in which an ER protein, which is known to be phosphorylated specifically following incubation with interphase or metaphase cytosol, would have been immunoprecipitated to show that such modifications were detectable within the parameters of the experiment. This was not possible since no such protein has been identified, although if a CLIMP-63 antibody had been available it would have been interesting to determine whether the previously reported mitotic phosphorylation of this protein was replicated *in vitro* [207]. Nevertheless, this data indicated that kinesin-1 phosphorylation does not occur in the interphase or metaphase assay, ruling out this as a potential mechanism for the metaphase inhibition of rat liver ER motility.

Another possibility is that the kinesin-1 cargo receptor is specifically phosphorylated in the interphase or metaphase assay, and this triggers an effect upon motor activity. The influence of

cargo phosphorylation upon kinesin-1 activity is poorly understood. However, there are a few cases in which changes in the phosphorylation status of cargoes is documented to affect binding to kinesin-1. For example, kinesin-1-driven axonal transport of tau is regulated by phosphorylation. When tau is phosphorylated by GSK3 this promotes binding of tau to kinesin-1 and increases the rate of cargo transport in rat cortical neurons [94]. It would be useful to investigate whether the phosphorylation states of the kinesin-1 ER receptors change in the presence of interphase or metaphase cytosol. Perhaps such modifications are capable of conferring changes in kinesin-1 activity without triggering dissociation of the motor from its receptor. If the interaction between cargo and motor are relatively weak then any change in receptor phosphorylation could have been overlooked in the phosphorylation assays using KHC immunoprecipitates documented in this study. Alternatively, perhaps receptor phosphorylation is responsible for dissociation of KLC or KHC from the ER cargo. KHC is thought to bind the integral ER membrane proteins kinectin [198] and p180 [201], while the ability of exogenously-added KLC1B to specifically perturb rat liver ER motility *in vitro* suggests that a KLC receptor is also present on rat liver ER membranes [30]. Kinectin exists in several different phosphorylation states *in vivo* with three major isoelectric forms detected in embryonic chick brain samples [84]. Within the KHC binding domain of kinectin there are two potential phosphorylation sites for casein kinase 2 and tyrosine kinase [200]. The identity of the ER KLC receptor remains undetermined.

Beads coated with a truncated version of KHC were used to investigate whether microtubule modifications or direct modulation of the KHC motor domain were responsible for the metaphase inhibition of ER motility. Despite no perturbation in the frequency of bead motility being observed in any of the conditions tested it is possible that the absence of more C-terminal portions of KHC, as well as KLCs, is masking any inhibitory effect. Indeed, soluble kinesin-1 is known to adopt an autoinhibitory conformation dependent upon interactions between the KHC head and tail domains, and between KHC and KLC [101, 102]. Alternatively, perhaps the inhibitory mechanism directly targets these absent regions of kinesin-1. For example, binding of an inhibitory interacting partner to KLC in metaphase cytosol resulting in motor inhibition, or dissociation from microtubules, would not be revealed in this assay. Interestingly, similar observations have been made using single cell assays to investigate the influence of ensconsin, the *Drosophila melanogaster* homologue of E-MAP-115, upon kinesin-1-dependent activity in the polarised fly oocyte. A fragment of KHC encoding amino acids 1 to 401 is able to bind and move along microtubules normally *in vitro* using concentrated ovary extracts prepared from *ensconsin* mutant flies. However, when full length KHC is used a significant defect in the ability of kinesin-1 to bind and translocate along microtubules is exposed when ensconsin function is perturbed [119].

To determine whether the inhibition of rat liver ER motility by metaphase cytosol is dependent upon the presence of more C-terminal regions of KHC, kinesin-1 bead assays could be repeated using full length KHC. Whilst this protein is notoriously difficult to express recombinantly, it is possible to purify the protein from brain tissue using sucrose gradients,

which beads could then be coated with. Such experiments have been used in the past to determine the directionality of membrane motility in similar *in vitro* assays [218]. The drawback to this approach is that KIF5A and KIF5C are supposedly enriched in neuronal tissue making it likely that these isoforms, rather than the ubiquitously expressed KIF5B protein, would be isolated. Optimisation of bead assays using kinesin-1 purified from non-neuronal tissues could be attempted to overcome this difficulty and indeed previous studies have documented the isolation of kinesin-1 from rat liver using comparable methods [291]. Additionally, it may be prudent to investigate more fully whether the speed at which beads are moving changes under a specific condition, since it is possible that the microtubule binding capability of the motor is unaffected whereas its processivity or speed of translocation is perturbed. Such calculations have been made from VE-DIC movies in previous studies using the RETRAC object tracking system [144, 218].

Finally, the association of kinesin-1 with a binding partner specifically in the interphase or metaphase assay, which has a concomitant effect upon motor activity, was investigated. However, several technical obstacles were encountered which hindered progress. The major difficulty in this project has been the relatively low level of kinesin-1 on rat liver ER membranes. Despite attempts to scale up experiments using larger volumes of ER membranes, KHC or KLC bands could not be detected by colloidal Coomassie in KHC or KLC immunoprecipitate samples. Furthermore, during re-isolation procedures necessary to recover ER membranes following incubation with *Xenopus laevis* egg extract cytosols, the level of kinesin-1 immunoprecipitated was reduced further. This made it impractical to identify binding partners of kinesin-1 which could be responsible for the metaphase inhibition of ER motility. Unfortunately, despite optimisation attempts, these problems were not overcome during the course of this work and it remains undetermined whether specific proteins bind kinesin-1 differentially between the interphase and metaphase assays. Perhaps a different tack is required to solve these difficulties. Mitotic extracts can be prepared from mammalian cells in a variety of ways. Cells can be arrested in prometaphase by the addition of low doses of the microtubule depolymerising agent nocodazole or mitotic cells can be isolated by shake-off techniques. If kinesin-1 immunoprecipitations were performed from these samples it is possible that KHC and KLC bands would be visible by colloidal Coomassie. Although this approach would not be directly looking at a cargo which is moved solely by kinesin-1, any differences in binding partners between interphase and mitosis could still prove insightful. Furthermore, if any potential candidates were identified using this approach, their influence upon ER network formation could be relatively easily probed by exogenously adding the protein to the *in vitro* assay or by immunodepleting the protein from *Xenopus laevis* egg extract cytosol and quantifying network formation.

Despite these difficulties two potential regulators of kinesin-1 in a cell cycle context, p150*glued* and E-MAP-115, were investigated further. The p150*glued* subunit of the dynactin complex, which is known to be mitotically regulated [286], was found to associate with the motor in *Xenopus laevis* egg extracts, although it is possible that the interaction is indirect, potentially via

another subunit of the dynactin complex. Interestingly, since dynactin has also been reported to interact with kinesin-1 [81], kinesin-2 [38] and the kinesin-5 family member Eg5 [82], in addition to cytoplasmic dynein-1, it is possible that this adaptor protein plays an important role in regulating bidirectional microtubule-dependent cargo transport. Binding of p150*glued* to kinesin-1 has been proposed to have both positive [81] and negative regulatory effects upon cargo motility (personal communication, Dr. Marcin Woźniak). However, since the interaction between p150*glued* and kinesin-1 was not found to differ between interphase and metaphase its importance was not probed further. No interaction between rat kinesin-1 and p150*glued* was detected, although it is possible that the two proteins do interact but due to the relatively low level of the motor on the membrane the association is not detected. Recruitment of *Xenopus laevis* p150*glued* to rat liver ER membranes from both interphase and metaphase cytosol was observed, although the significance of this is unsure given cytoplasmic dynein-1 does not contribute to cargo motility in this assay. The anti-p150*glued* antibody used in this experiment has been shown to be sensitive to the phosphorylation status of the protein, specifically recognising p150*glued* when dephosphorylated at the serine-19 residue [292]. It could therefore be argued that the detection of p150*glued* on rat liver ER membranes following incubation with *Xenopus laevis* egg extract cytosols is not due to recruitment of *Xenopus laevis* dynactin to the ER membrane, but reflects changes in the phosphorylation status of rat p150*glued*.

A role for E-MAP-115 in the inhibition of kinesin-1 activity by metaphase cytosol was probed due to the reported contributions of this mitotically regulated MAP to kinesin-1 function in the polarised *Drosophila melanogaster* oocyte [118, 119]. The effects of adding recombinantly expressed E-MAP-115 to the *in vitro* motility assay were investigated and the protein was found to inhibit cargo movement driven by both kinesin-1 and cytoplasmic dynein-1. However, since E-MAP-115 is reported to be a positive regulator of kinesin-1 activity in *Drosophila melanogaster* [119], and has no documented link to cytoplasmic dynein-1 function, confident conclusions cannot be drawn from the data. It is possible that the effects observed are an indirect consequence of the protein coating microtubules and thereby interfering with all microtubule-dependent cargo motility. Ideally, the levels of endogenous E-MAP-115 on microtubules would have been probed to determine whether any change occurs between interphase and metaphase. This was not possible since an antibody which recognised both rat and *Xenopus laevis* forms of the protein by western blotting was not available. This also meant biochemical experiments to determine whether native kinesin-1 and E-MAP-115 interact, similar to those described for p150*glued* and kinesin-1, could not be performed. It would also be interesting to determine whether the phosphorylation status of E-MAP-115 changes in a cell cycle-dependent manner in *Xenopus laevis* egg extracts, similar to that observed in the HeLa cell line [118]. Such modifications could potentially induce changes in the activity or localisation of the MAP between the interphase and metaphase assays, and have a concomitant effect upon rat kinesin-1 function. Indeed, E-MAP-115 is known to be a direct target of Par1 kinase in the polarised *Drosophila melanogaster* oocyte, an event which is necessary for the anterior localisation of the protein and its ability to control kinesin-1 activity [119].

The binding or release of a kinesin-1 interacting partner specifically in the interphase or metaphase assay remains the most likely explanation for the cell cycle regulation of ER motility. Such differential binding could potentially induce folding or unfolding of the motor on ER membranes and thereby control tubule motility. Whilst it is known that three isoforms of KHC and at least four variants of KLC are expressed in rat (see Table 1.1), the relative contribution of each of these proteins to ER motility in the *in vitro* assay is uncertain. Given that until recently KIF5A and KIF5C were believed to be specifically expressed in neurons the involvement of these proteins in ER motility in somatic cells has not been investigated. If each of these different isoforms contributes to the movement of rat liver ER tubules *in vitro*, it is possible that the activity of each isoform is being controlled by a distinct mechanism, thus further complicating the situation.

4.4 Further future work

Soluble kinesin-1 is normally prevented from hydrolysing ATP or engaging with microtubules by adopting an autoinhibitory conformation [101, 102]. Since kinesin-1 remains bound to rat liver ER membranes in the metaphase assay, it is interesting to speculate how this motor inhibition is maintained. One possibility is that the motor can fold into an autoinhibitory conformation whilst bound to cargo. If this is true it may have implications in the control of bidirectional cargo motility in which the tight control of opposing motors bound simultaneously to the same cargo is hypothesised to occur [273]. Such behaviour has not been documented in any previous studies, perhaps because it is technically a difficult concept to investigate. Regardless of the conformation of kinesin-1 on cargoes, as soon as membranes are solubilised to perform biochemical analyses the motor will fold [30].

The assays performed in this study were devoid of actin-based motility due to the presence of cytochalasin D, an inhibitor of actin polymerisation. However, the actin cytoskeleton is also thought to contribute to the ER movement, with the myosin V motor reported to move smooth ER vesicles isolated from squid axons *in vitro* [203], and myosin V-driven ER motility in *Xenopus laevis* egg extracts reported to be activated specifically during mitosis [290]. To determine whether myosin motors are capable of moving rat liver ER membranes, motility assays excluding cytochalasin D but including nocodazole could be performed. It would then be interesting to determine whether any actin-based rat liver ER motility is also regulated in a cell cycle-dependent manner *in vitro*.

ER membrane fusion mediated by p97 and its cofactor p47 was specifically inhibited *in vitro* when semi-intact Chinese hamster ovary cells were treated with mitotic HeLa cell cytosol [211]. This is due to the mitotic phosphorylation of p47 by CDK1. It may prove insightful to determine whether this mechanism is replicated when rat liver ER membranes are combined with metaphase *Xenopus laevis* egg extract cytosols. This would lend weight to the theory that ER membrane fusion, in addition to tubule motility, is inhibited during cell division. Similar to the approach taken by Kano and co-workers, the effects of adding a non-phosphorylated form of p47 to the metaphase assay could be observed and protein kinase assays could be performed

to determine whether the endogenous protein is specifically phosphorylated in metaphase cytosol [211].

Movement of ER tubules driven by cytoplasmic dynein-1 and kinesin-1 is tightly regulated during the cell cycle *in vitro*. Whether this phenomenon is replicated *in vivo* is unknown. Confocal live cell imaging of mitotic cells expressing a fluorescent ER marker could be attempted to determine whether changes to ER motility occur *in vivo* during cell division. Previous imaging of ER movement in living cells in this laboratory has revealed that the network is highly dynamic and subject to extensive remodelling [197]. Therefore any large scale changes in motility during cell division should be noticeable. Such an approach could also reveal whether the contribution of TACs or myosin motors to ER movement in somatic cells is influenced by cell division. Furthermore, it should be possible to determine whether inward or outward movement is specifically altered by carefully analysing tubule motility in a specific region of the cell of a set area.

5. Results – Motility of BFA-induced tubules

The aim of this work was to determine which microtubule motor(s) is responsible for the motility of BFA-induced tubules.

5.1 Use of *in vitro* motility assays to investigate BFA-induced tubule motility

Previous studies have used *in vitro* motility assays to investigate the motility of BFA-induced membrane tubules. The addition of BFA to experiments in which rat liver Golgi membranes are combined with interphase *Xenopus laevis* egg extract cytosol results in the formation of intricate membrane networks which are positive for cis-Golgi, TGN and early endosome markers [144]. This tubulation is reliant upon microtubules since treatment with the microtubule-depolymerising agent nocodazole blocks network formation. This assay was used as a starting point to the project since, as previously mentioned, the reconstitution of cargo motility using *Xenopus laevis* egg extracts provides a simplified system in which to study microtubule motor behaviour [272]. *In vivo* analyses would be performed later to complement this *in vitro* work. Since BFA-induced cis-Golgi and TGN tubules move away from the Golgi it is likely that a plus end-directed microtubule motor contributes to this movement [138, 293]. Kinesin-1, kinesin-2 and kinesin-3 family members are believed to be primarily responsible for plus end-directed interphase membrane motility [15, 71], and therefore other kinesin families were not studied in this work. A motor belonging to the kinesin-3 family, KIF1C, was of particular interest since it is localised to the ER and Golgi and has been previously implicated in the motility of BFA-induced cis-Golgi tubules, although this data has been refuted [146, 147]. It was decided to perform *in vitro* motility assays with rat liver Golgi membranes following treatment with proteins and antibodies which have an inhibitory effect upon kinesin-1, kinesin-2 and kinesin-3 to determine which, if any, blocked BFA-induced tubule formation.

5.1.1 Function-blocking kinesin antibody pre-incubation

The inhibitory monoclonal kinesin antibodies used were H1, SUK4 and k2.4. The H1 antibody was raised against kinesin-1 isolated from bovine brain [294], but was later found to recognise at least two polypeptides by western blotting, neither of which are kinesin-1 [144]. Whilst the target of H1 remains unknown, the antibody was used as a positive control since it has been previously shown to inhibit the motility of BFA-induced tubules in this *in vitro* assay [144], as well as *in vivo* [143]. SUK4 is an antibody raised against KHC of sea urchin kinesin-1 and was found to inhibit sea urchin microtubule translocation *in vitro*, perhaps through inhibition of the interaction between motor and microtubule [278]. The epitope of KHC recognised by SUK4 was subsequently mapped to between amino acids 312 and 382 of the KHC motor domain in *Drosophila melanogaster* [295]. SUK4 is now a widely used reagent for inhibiting kinesin-1 function, being included in studies using cultured cells [296], *in vitro* motility assays [218] and sea urchin embryos [297]. The k2.4 antibody was raised against the 85 kDa kinesin related protein (85/95) (KRP(85/95)) subunit of sea urchin kinesin-2 [33], which is homologous to the KIF3A motor subunit of mammalian kinesin-2. This antibody has been used to block kinesin-2 function in a range of studies including those using *in vitro* motility assays [30], *Xenopus laevis* eggs [298] and sea urchin embryos [299].

To determine whether any of these function-blocking antibodies has an inhibitory effect upon BFA-induced tubule motility *in vitro,* rat liver Golgi membranes were incubated with each antibody, or with mouse IgG, for 45 minutes on ice. These membranes were then added to interphase cytosol prepared from Newmeyer *Xenopus laevis* egg extracts containing BFA, and applied to microscope flow cells which had been coated with microtubules polymerised from interphase cytosol in the presence of BFA. After 1 hour, the total length of tubules per field was determined. As expected, pre-incubation with the H1 antibody significantly reduced the mean total tubule length per field compared to the mouse IgG incubation control (Figure 5.1). Pre-incubation with either SUK4 or k2.4 antibodies did not significantly affect the mean total length of tubules formed compared to the mouse IgG control. This indicates that kinesin-1 and kinesin-2 do not contribute to the motility of BFA-induced membrane tubules in this *in vitro* assay.

5.1.2 Dominant negative kinesin protein pre-incubation

The inhibitory proteins used to perturb kinesin function were GST-KHCct, GST-KAP3Bct and GST-KBP∆250-81. KHCct encodes the C-terminal domain of rat KHC from amino acids 771 to 963, which has previously been shown to inhibit kinesin-1 activity *in vitro* [30], *in vivo* [197] and in semi-intact cell assays (personal communication, Dr. Marcin Woźniak). It is believed to cause this effect by binding to the motor domain of KHC thereby mimicking the folded autoinhibitory conformation, which kinesin-1 is thought to adopt when not bound to cargo (see section 1.3.3) [30, 101]. KAP3Bct encodes amino acids 512 to 793 of isoform B of the human KAP3 protein, the cargo-binding subunit of kinesin-2, and exerts its dominant negative effect by binding to kinesin-2 cargoes, thereby preventing binding of the endogenous motor (personal communication, Dr. Marcin Woźniak). Another isoform of KAP3, KAP3A, has also been characterised which is generated by alternative splicing within the C-terminus [40]. The purpose of these different isoforms is unknown, but it has been speculated that they may each bind a different subset of cargoes and thereby perform separate functions [40]. GST-KBP∆250-81 is a deletion mutant of the human KIF1B/C binding protein KBP, lacking amino acids 250 to 281. The mutant is unable to bind the motor and is thereby thought to inhibit the motor's activity [51], although the mechanism by which this occurs is unverified. It is unknown how this mutant affects binding between endogenous KBP and KIF1B/C. It was presumed that since neither KIF1Bα nor KIF1Bβ have been localised to the Golgi, or reported to be involved in cargo transport to or from the Golgi, these proteins would be present at a low level, if at all, in the rat liver Golgi fraction. Unfortunately, this could not be verified because of a lack of antibodies. However, it seemed likely that any effects observed following treatment with GST-KBP∆250-281 could be attributed solely to inhibition of KIF1C function.

To determine whether any of these function-blocking proteins have an inhibitory effect upon BFA-induced tubule motility *in vitro,* rat liver Golgi membranes were incubated with each protein, or GST as a negative control, for 20 minutes on ice and the level of BFA-induced membrane motility was analysed identically to the antibody incubation experiments. Following incubation with GST a mean total tubule length per field of 56.6 µm was observed (Figure 5.2). No significant effect upon network formation was detected following incubation with either GST-KHCct or GST-KAP3Bct. This again supports the conclusion that neither kinesin-1 nor kinesin-2

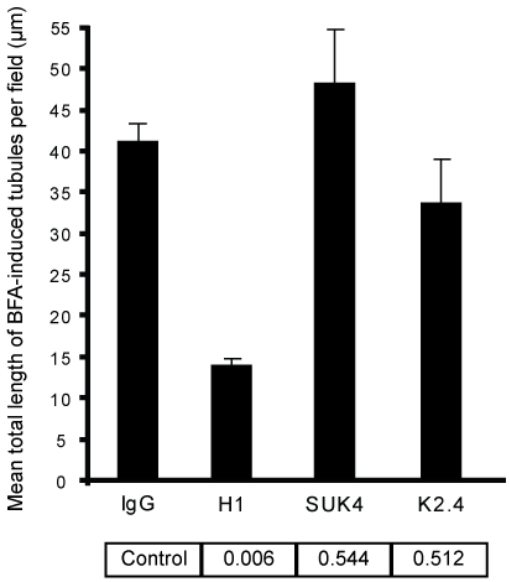

Figure 5.1 - Perturbation of kinesin-1 or kinesin-2 using function-blocking antibodies has no effect upon the ability of BFA-induced tubules to form *in vitro*

Interphase cytosol prepared from Newmeyer *Xenopus laevis* egg extracts was diluted 5-fold in acetate buffer including 100 µg/ml BFA. This mixture was applied to microscope flow cells and microtubules were allowed to polymerise for 10 minutes in a humid chamber. A volume of 1 µl (10 µg) of rat liver Golgi membranes was incubated with 4 µl (4 µg) of the anti-KHC antibody SUK4, the anti-KIF3A antibody k2.4, the H1 antibody as a positive control, or mouse IgG as a negative control, for 45 minutes on ice. Of this mixture, 1 µl was added to 8.5 µl of interphase cytosol and 0.5 µl of 2 mg/ml BFA (i.e. to a final concentration of 100 µg/ml), applied to the flow cell and left for 1 hour in a humid chamber. Twenty randomly chosen fields were imaged using VE-DIC microscopy and the mean total length of tubules per field was measured using a map measuring tool. Each experiment was repeated two additional times to obtain three mean values per condition. A mean of these three separate mean values is shown. Error bars + SEM. P-values (shown in boxes underneath the relevant result) were calculated using a two-sided Dunnett's post-hoc test following a one-way ANOVA using incubation with mouse IgG as the control.

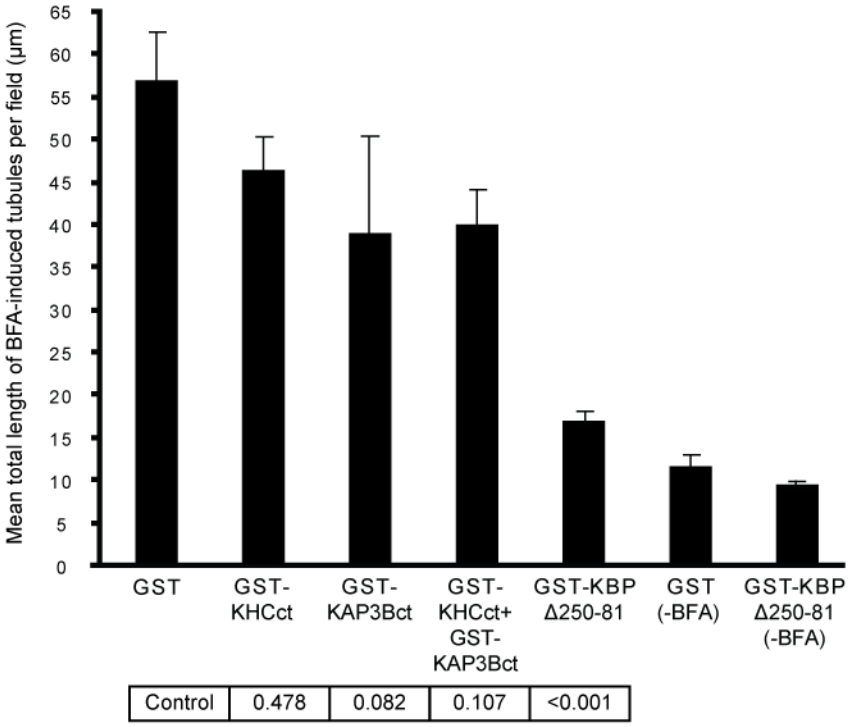

Figure 5.2 - Perturbation of KIF1C using the dominant negative GST-KBP∆250-81 protein inhibits BFA-induced tubule motility *in vitro*

Interphase cytosol prepared from Newmeyer *Xenopus laevis* egg extracts was diluted 5-fold in acetate buffer including 100 µg/ml BFA. This mixture was applied to microscope flow cells and microtubules were allowed to polymerise for 10 minutes in a humid chamber. A volume of 1 µl (10 µg) of rat liver Golgi membranes was incubated with 2 µl (2.7 µg) of the proteins GST-KHCct, GST-KAP3Bct, GST-KBP∆250-81, which have a dominant negative effect upon kinesin-1, kinesin-2 and KIF1C, respectively. Incubations were performed for 20 minutes on ice and GST was used as a control. Of this mixture, 1 µl was added to 8.5 µl of interphase cytosol and 0.5 µl of 2 mg/ml BFA, applied to the flow cell and left for 1 hour in the humid chamber. Alternatively, the assay with GST and GST-KBP∆250-81 was performed in the absence of BFA. Tubule length was determined as described in the legend to Figure 5.1. Error bars + SEM. P-values (shown in boxes underneath the relevant result) were calculated using a two-sided Dunnett's post-hoc test following a one-way ANOVA using incubation with GST as the control.

is necessary for BFA-induced tubule formation in this assay. Furthermore, no inhibition of motility was detected when GST-KHCct and GST-KAP3Bct were combined (Figure 5.2), ruling out the possibility that the motors are working in combination with each other. Pre-incubation with GST-KBP∆250-81 reduced the mean total tubule length per field to 16.8 µm, which corresponds to a p-value of less than 0.001. Experiments in which BFA was omitted were also performed to determine the baseline, uninduced, level of tubule formation in this assay. The mean total tubule length of tubules formed following incubation of rat liver Golgi membranes with GST or GST-KBP∆250-81 in the absence of BFA was 11.5 µm and 9.2 µm, respectively. Therefore the length of tubules formed in response to BFA following incubation with GST-KBP∆250-81 is comparable to the length of tubules formed in the absence of any BFA, and indicates that inhibition of KIF1C reduces tubule motility to the background baseline level. These results suggest KIF1C functions in moving BFA-induced membrane tubules *in vitro* independently of any other motors.

It was next decided to investigate whether treatment of Golgi membranes with GST-KBP∆250-81 in combination with function-blocking antibodies had a greater inhibitory effect upon BFA-induced membrane motility. The thinking behind this was that if no additive inhibitory effects upon tubule length were observed when the activities of multiple motors were blocked simultaneously, this would further verify the hypothesis that KIF1C functions in isolation to move BFA-induced tubules *in vitro*.

To this end, membranes were incubated with GST-KBP∆250-81 together with SUK4, k2.4 or mouse IgG. As expected, the presence of GST-KBP∆250-81 significantly reduced the length of BFA-induced tubules irrespective of the antibody with which it was combined (Figure 5.3). The mean total length of tubules per field observed in the GST with mouse IgG control was 54.7 µm and this decreased to between 12.7 µm and 16.4 µm in the presence of GST-KBP∆250-81 together with various antibodies, correlating to p-values of less than 0.001 in each case. However, when each of these values was compared to GST-KBP∆250-81 combined with mouse IgG as a control, no significant decrease in mean total tubule length per field was detected (Figure 5.3). This suggests no additional inhibitory effect is generated by inhibiting kinesin-1 or kinesin-2 alongside KIF1C, and indicates BFA-induced tubules are moved solely by KIF1C *in vitro*.

5.1.3 Golgi vesicle motility

It could be argued that GST-KBP∆250-81 has an off-target effect, perhaps upon kinesin-1 and/or kinesin-2, which is responsible for the inhibition of BFA-induced tubule formation observed. To determine whether GST-KBP∆250-81 has any effects upon kinesin-1 and/or kinesin-2 function, assays were performed which analysed the effect of this protein upon the vesicle motility of the rat liver Golgi fraction. It has been previously shown that this movement is driven primarily by kinesin-1 and kinesin-2 [30]. Therefore, if GST-KBP∆250-81 affects either of these motors it would be expected to influence vesicle motility in this assay. Rat liver Golgi membranes were incubated with GST-KBP∆250-81, or GST, for 20 minutes on ice and then added to interphase *Xenopus laevis* egg extract cytosol. After 10 minutes, VE-DIC microscopy

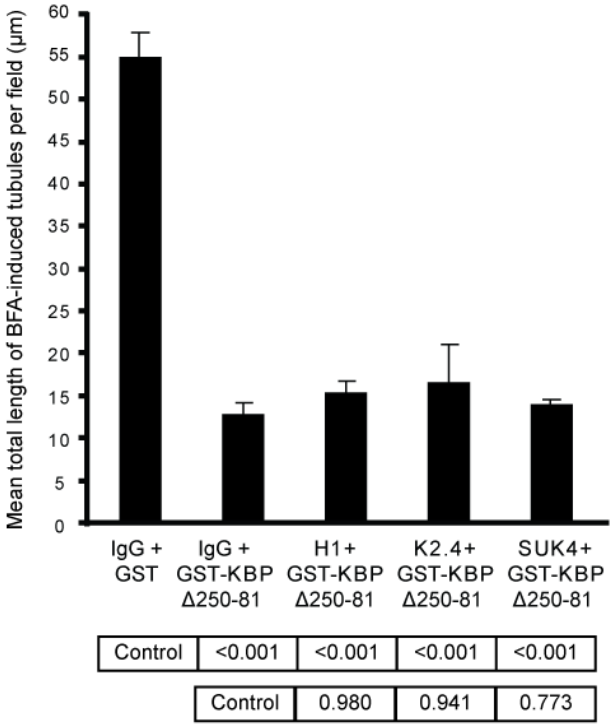

Figure 5.3 - Perturbation of kinesin-1 or kinesin-2 using function-blocking antibodies, in combination with KIF1C inhibition, has no additive inhibitory effect upon BFA-induced tubule motility *in vitro*

Interphase cytosol prepared from Newmeyer *Xenopus laevis* egg extracts was diluted 5-fold in acetate buffer including 100 µg/ml BFA. This mixture was applied to microscope flow cells and microtubules were allowed to polymerise for 10 minutes in a humid chamber. A volume of 2 µl (20 µg) of rat liver Golgi membranes was incubated with 4 µl (4 µg) of the anti-KHC antibody SUK4, the anti-KIF3A antibody k2.4, the H1 antibody, or mouse IgG as a control, along with 2.9 µl (2.9 µg) of GST or GST-KBPΔ250-81, for 45 minutes on ice. Of this mixture, 1 µl was added to 8.5 µl of interphase cytosol and 0.5 µl of 2 mg/ml BFA, applied to the flow cell and left for 1 hour in a humid chamber. Tubule length was determined as described in the legend to Figure 5.1. P-values (shown in boxes underneath the relevant result) were calculated using a two-sided Dunnett's post-hoc test following a one-way ANOVA using incubation with a combination of mouse IgG and GST, or mouse IgG and GST-KBPΔ250-81, as the control.

was used to determine the total number of vesicles moving in 10 minutes. Pre-incubation with GST-KBP∆250-81 had no significant effect on the mean number of moving vesicles compared to the GST control (Figure 5.4). This data indicates that GST-KBP∆250-81 has no effect upon kinesin-1 or kinesin-2 function, at least *in vitro*.

The effects of kinesin motor inhibition upon BFA-induced tubule formation *in vitro* are summarised in Figure 5.13.

5.2 *In vivo* inhibition of BFA-induced tubules

The *in vitro* assay data suggested that KIF1C is responsible for the motility of BFA-induced membrane tubules. Next, a number of approaches were taken to inhibit KIF1C function in HeLaM cells to determine whether this result is replicated *in vivo*.

5.2.1 Transient transfection of dominant negative kinesin constructs

Transient transfection of DNA constructs encoding the dominant negative kinesin proteins used in the *in vitro* motility assay was used in an attempt to determine whether they exerted a similar effect upon the formation of BFA-induced membrane tubules in HeLaM cells. These human cervical cancer cells are a variant of HeLa cells and were chosen since they are amenable to transient transfection and immunofluorescence studies. Furthermore, kinesin motors could be potentially depleted using siRNA if required later in the project.

GFP-KHCct, KAP3B-Myc and GFP-KBP∆250-81 were transiently transfected into HeLaM cells along with the cis-Golgi marker mApple-Golgi to assess tubulation of the cis-Golgi upon BFA treatment, with transfection of GFP being used as a negative control. Additionally, the KIF1C∆305-9 construct was included as another means of inhibiting KIF1C. KIF1C∆305-9 is a substitution mutant of KIF1C with residue 103 within the P-loop converted from lysine to alanine, rendering it incapable of binding ATP whilst retaining the capacity to bind cargo [146]. As such it should compete with and replace the endogenous motor on cargo but be immotile [146]. The cells were left for 24 hours following transfection and then treated with BFA for 10 minutes. This was the length of time determined to give the highest percentage of cells displaying cis-Golgi BFA tubules in untransfected HeLaM cells (data not shown). Cells were then fixed and immunolabelled as necessary. A total of 100 transfected cells on each coverslip were scored to determine the percentage of transfected cells displaying mApple-Golgi-positive BFA tubules. In GFP transfected cells a mean of 81 % of cells displayed mApple-Golgi-positive tubules following BFA treatment (Figure 5.5). No significant change to the percentage of cells displaying mApple-Golgi-positive tubules was detected following transient transfection of any of the dominant negative kinesin constructs compared to the GFP control.

One drawback of using the dominant negative constructs was that no positive controls could be identified *in vivo*. Whilst GFP-KHCct has been shown to inhibit outward ER motility in VERO cells this is only following microinjection of DNA, whilst transient transfection has no effect [197]. Expression of an untagged version of the KBP∆250-81 protein has been shown to cause mitochondrial clustering in NIH-3T3 cells [51], but this could not be replicated in HeLaM cells

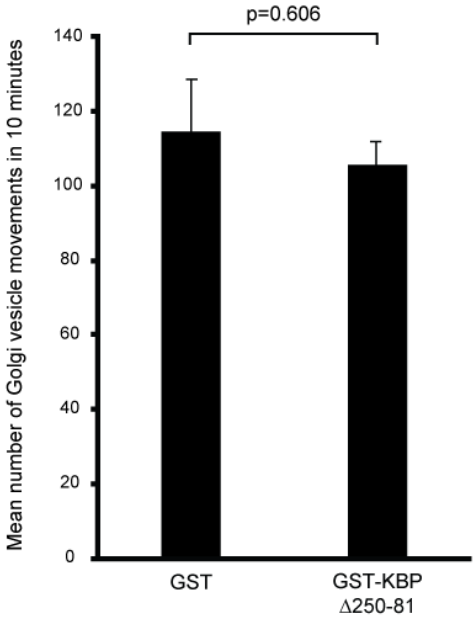

Figure 5.4 - Perturbation of KIF1C using the dominant negative GST-KBPΔ250-81 protein has no effect upon rat liver Golgi vesicle motility *in vitro*

Interphase cytosol prepared from Newmeyer *Xenopus laevis* egg extracts was diluted 5-fold in acetate buffer. This mixture was applied to microscope flow cells and microtubules were allowed to polymerise for 10 minutes in a humid chamber. A volume of 1 µl (10 µg) of rat liver Golgi membranes was incubated with 2 µl (2.9 µl) of GST-KBPΔ250-81 protein, or GST as a negative control, for 20 minutes on ice. Of this mixture, 1 µl was added to 9 µl of interphase cytosol, applied to the flow cell and left for 10 minutes in a humid chamber. Twenty randomly chosen fields were imaged using VE-DIC microscopy and each filmed for 30 seconds. The total number of moving vesicles over twenty fields (i.e. in 10 minutes) was counted. Each experiment was repeated two additional times to obtain three mean values per condition. A mean of these three separate mean values is shown here. Error bars + SEM. The p-value was calculated using an independent student t-test.

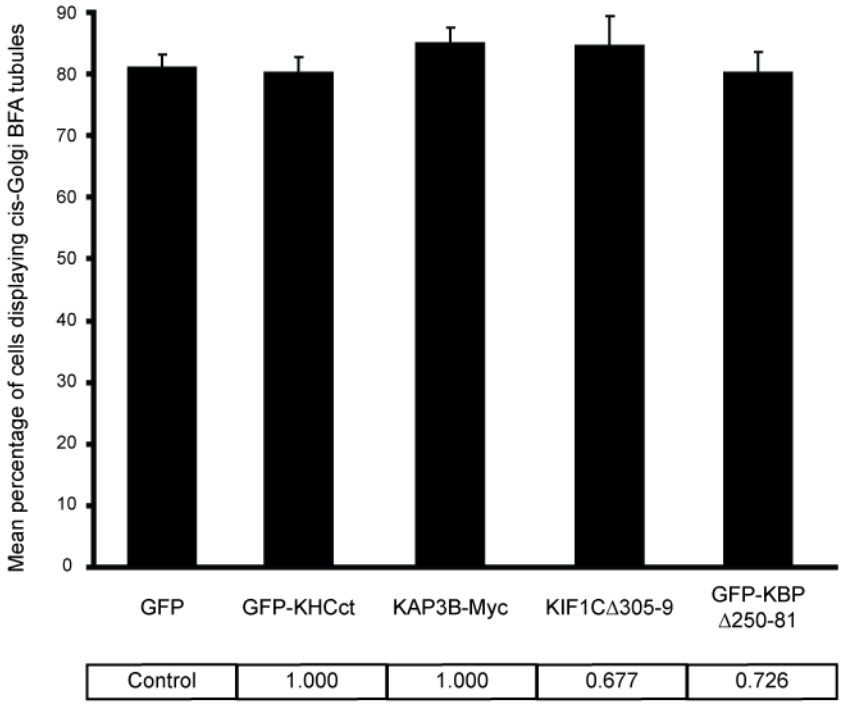

Figure 5.5 - Transfection of constructs which have a dominant negative effect upon kinesin-1, kinesin-2 or KIF1C has no effect upon the ability of cis-Golgi tubules to form in response to BFA in HeLaM cells

HeLaM cells grown on coverslips were transfected with GFP, GFP-KHCct, KAP3B-Myc, KIF1C Δ305-9 or GFP-KBPΔ250-81, along with the cis-Golgi marker mApple-Golgi, for 24 hours using JetPEI. Cells were subsequently treated with 2 µg/ml BFA for 10 minutes, fixed in methanol and immunolabelled as necessary. The ability of tubules to form from the cis-Golgi in response to BFA was measured by counting the percentage of cells which displayed mApple-Golgi tubules, with 100 cells scored per experiment. Each experiment was performed two additional times to obtain three mean values per condition. A mean of these three separate mean values is shown. Error bars + SEM. P-values (shown in boxes underneath the relevant result) were calculated using a two-sided Dunnett's post-hoc test following a one-way ANOVA using GFP transfection as the control.

(data not shown). Moreover, expression of KIF1CΔ305-9 in NIH-3T3 blocked redistribution of the cis-Golgi marker p58 to the ER in response to BFA [146], but this could not be replicated in HeLaM cells when using mApple-Golgi as a cis-Golgi marker (Figure 5.5). There is no verification therefore that any of the dominant negative proteins were exerting their expected inhibitory effects in this experimental setup. Moreover, it was uncertain whether the level or duration of expression of the dominant negative kinesin is also critical to its inhibitory effects. It was therefore decided to change tack and to treat HeLaM cells with KIF1C-specific siRNA to deplete KIF1C.

5.2.2 KIF1C siRNA

This is a notably different approach to that previously used. Dominant negative protein overexpression, in which cargo binding remains viable but motor activity is perturbed, means cargo is bound to the dominant negative protein and excludes the possibility that another motor can compensate for its loss. Contrastingly, depletion of a motor using siRNA could be potentially compensated for by other motors and this should be kept in mind.

5.2.2.1 Optimisation of KIF1C knockdown

A SMARTpool of KIF1C siRNA was used which contains four duplexes targeted against four different regions of human KIF1C. To determine if KIF1C protein levels in HeLaM cells could be effectively and specifically depleted with KIF1C siRNA, cell lysates were prepared following treatment with KIF1C-specific siRNA, or non-targeting siRNA as a negative control, for 72 hours. Samples were immunoblotted for KIF1C or tubulin as a loading control using anti-KIF1C and anti-TAT1 antibodies, respectively. HeLaM cells were treated with KIF1C-specific siRNA at a range of concentrations from 20 nM to 0.5 nM in an attempt to identify the lowest concentration which results in the maximal depletion of KIF1C protein. In non-targeting siRNA-treated, as well as untreated cell samples, a band at approximately 160 kDa corresponding to KIF1C was detected (Figure 5.6 A). This was absent from each of the samples treated with KIF1C-specific siRNA. In contrast the TAT1 signal (Figure 5.6 A) and Ponceau S staining (Figure 5.6 B) remains approximately the same between all samples, indicating an equal amount of protein has been loaded in each lane. The KIF1C antibody also produces a non-specific band at approximately 85 kDa which was found in all lanes. These results indicate that KIF1C can be effectively and specifically depleted in HeLaM cells following treatment with a KIF1C siRNA SMARTpool at a range of concentrations from 0.5 nM to 20 nM. Therefore in all subsequent experiments the KIF1C siRNA SMARTpool was used at a concentration of 0.5 nM.

5.2.2.2 Fixed cell analysis of KIF1C-depleted cells

Initially immunofluorescence experiments were performed on KIF1C-depleted cells using antibodies against a wide range of organelles and filaments to determine if the absence of KIF1C causes any obvious changes to their positioning or morphology. HeLaM cells treated with KIF1C-specific siRNA or non-targeting siRNA for 72 hours were fixed and immunolabelled for ER, microtubules and mitochondria using the anti-calreticulin, anti-TAT1 and anti-Hsp70 antibodies, respectively. Actin was also visualised using Alexa594-conjugated phalloidin dye. No obvious differences between non-targeting siRNA treated and KIF1C-depleted cells in the localisation or morphology of these structures were observed in fixed cells (Figure 5.7).

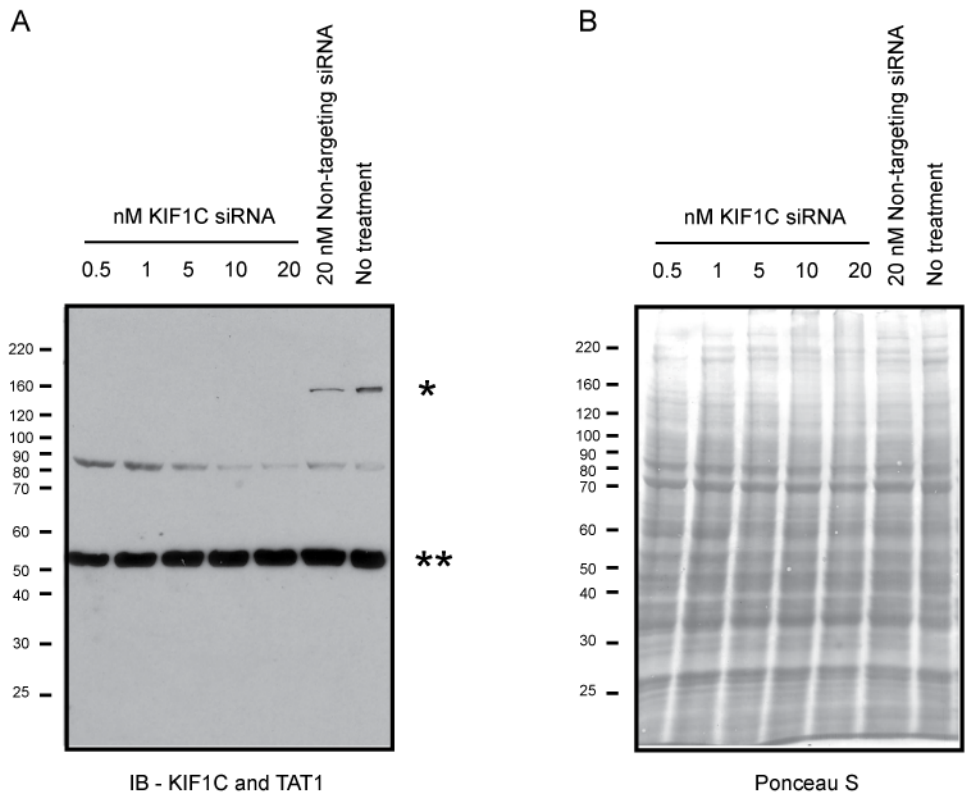

Figure 5.6 - Levels of KIF1C protein in HelaM cells are depleted following treatment with KIF1C siRNA for 72 hours

A. HelaM cells were plated on 10 cm dishes and treated with 20 nM non-targeting siRNA or the specified concentration of a KIF1C siRNA SMARTpool using INTERFERin, or left untreated for 72 hours. Cells were lysed and 25 µg of each sample was run on an 8 % SDS-PAGE gel and immunoblotted with anti-KIF1C and anti-tubulin (TAT1) antibodies. The asterisk marks the position of the KIF1C band, the double asterisk marks the position of the TAT1 band. The KIF1C antibody also shows a non-specific band at approximately 85 kDa.

B. A Ponceau S stain of the samples described in A is shown.

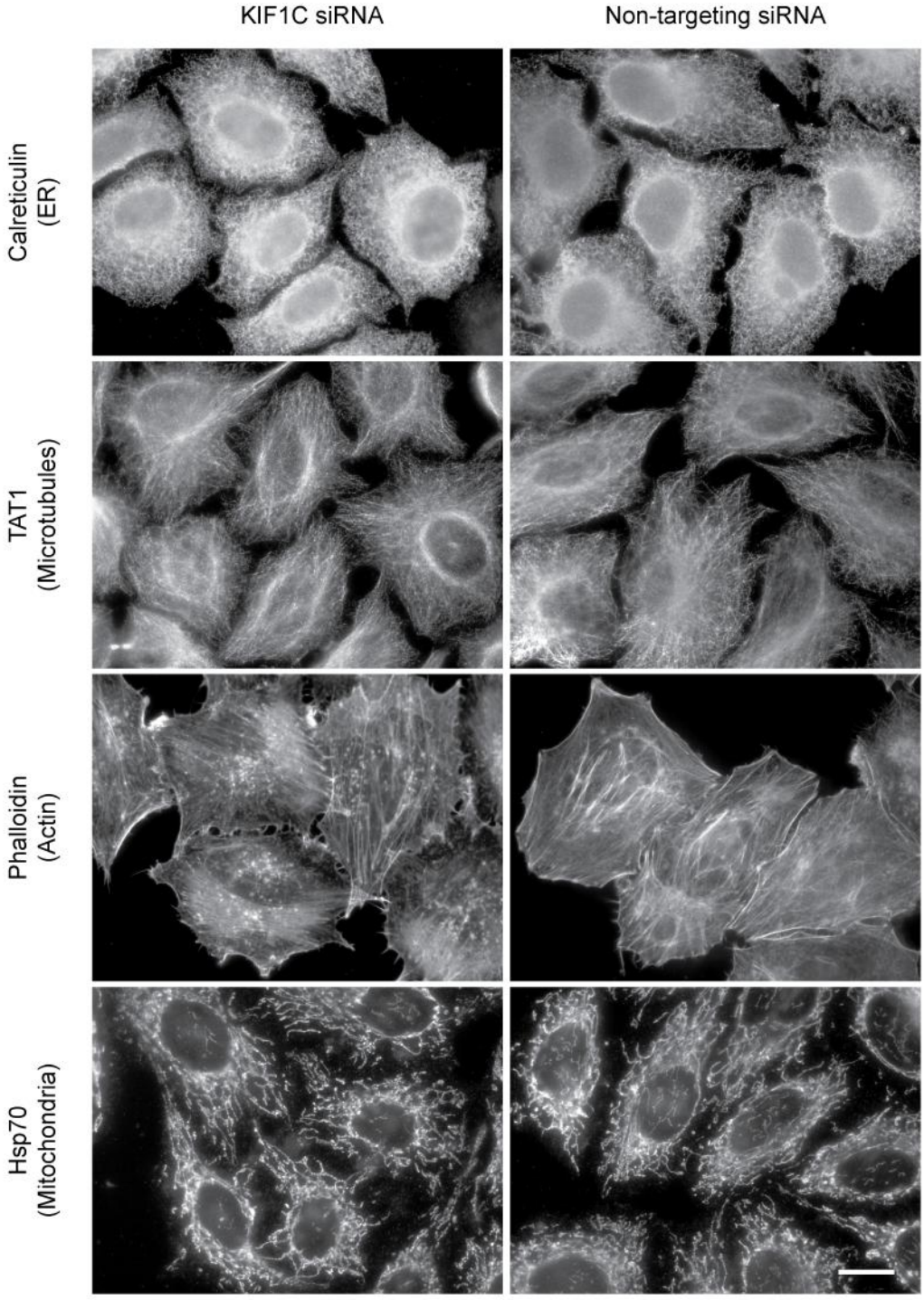

Figure 5.7 - Depletion of KIF1C has no noticeable effects on the position or morphology of a range of cellular structures/organelles in HeLaM cells

HeLaM cells grown on coverslips were transfected with 0.5 nM KIF1C siRNA SMARTpool, or non-targeting siRNA as a negative control, using INTERFERin for 72 hours and then fixed in methanol or 3 % PFA as appropriate. Cells were labelled with the primary antibodies anti-calreticulin, anti-TAT1, or anti-Hsp70 or the Alexa594-phalloidin dye. Alexa594 or Alexa488 were used as secondary antibodies as appropriate. Scale bar is 20 μm.

In an identical experiment transferrin receptor (a marker for the recycling endosome), early endosomes, the ERGIC compartment and lysosomes were visualised in control and KIF1C-depleted HeLaM cells using the anti-transferrin receptor, anti-EEA1, anti-ERGIC53 and anti-LAMP1 antibodies respectively. Again, no obvious differences between non-targeting siRNA treated and KIF1C-depleted cells in the localisation or morphology of these structures were observed in fixed cells (Figure 5.8).

Initial experiments revealed that depletion of KIF1C using KIF1C-specific siRNA did not have any noticeable effect by eye upon the ability of mApple-Golgi BFA-induced tubules to form in comparison to non-targeting siRNA treatment (data not shown), and consequently data was not quantified. It was therefore decided to combine the KIF1C siRNA and expression of dominant negative kinesins in an attempt to more efficiently perturb KIF1C function. Moreover, it was thought if multiple motors contribute to the motility of BFA-induced tubules *in vivo*, this may be exposed by inhibiting combinations of motors simultaneously.

5.2.3 Combining dominant negative kinesin expression with KIF1C depletion

5.2.3.1 cis-Golgi tubulation

HeLaM cells were treated with KIF1C-specific siRNA for 48 hours, or non-targeting siRNA as a negative control, and then transfected with GFP, GFP-KHCct, KAP3B-Myc, KIF1CΔ305-9 or GFP-KBPΔ250-81, along with mApple-Golgi to assess cis-Golgi tubulation, and left for a further 24 hours. The cells were treated with BFA for 10 minutes, which was the length of time determined to give the highest percentage of cells displaying cis-Golgi tubules in untreated HeLaM cells. Coverslips were fixed and immunolabelled as necessary, and the percentage of transfected cells displaying mApple-Golgi-positive BFA tubules was determined. To analyse the data, the non-targeting siRNA treated cells combined with GFP transfection was used as the control, where a mean of 77.7 % of cells displayed mApple-Golgi-positive tubules following BFA treatment. No significant change in the percentage of cells displaying mApple-Golgi-positive tubules was detected following transient transfection of any dominant negative kinesin constructs, irrespective of whether KIF1C levels were also depleted using siRNA (Figure 5.9).

It was next determined whether microtubule dynamics are playing a role in moving tubules away from the cis-Golgi in response to BFA. In this scenario tubules could perhaps attach to the plus tips of growing microtubules, to form a so-called tip attachment complex, and thereby move outwards, even under conditions in which motors are inhibited [300, 301]. This possibility could explain the failure to observe any inhibition of cis-Golgi BFA tubule motility even when multiple motors are inhibited. Perhaps under conditions in which microtubule dynamics are inhibited a dependence of cis-Golgi BFA-induced tubule motility upon a particular motor(s) would be revealed.

It was decided to use low doses of the microtubule-depolymerising agent nocodazole to inhibit microtubule dynamics. Live cell imaging of the plus-end microtubule tracking protein EB3 was used to determine the optimal concentration at which to use nocodazole. HeLaM cells were transiently transfected with tomato-EB3 and GFP-tubulin for 24 hours and live cell imaging of

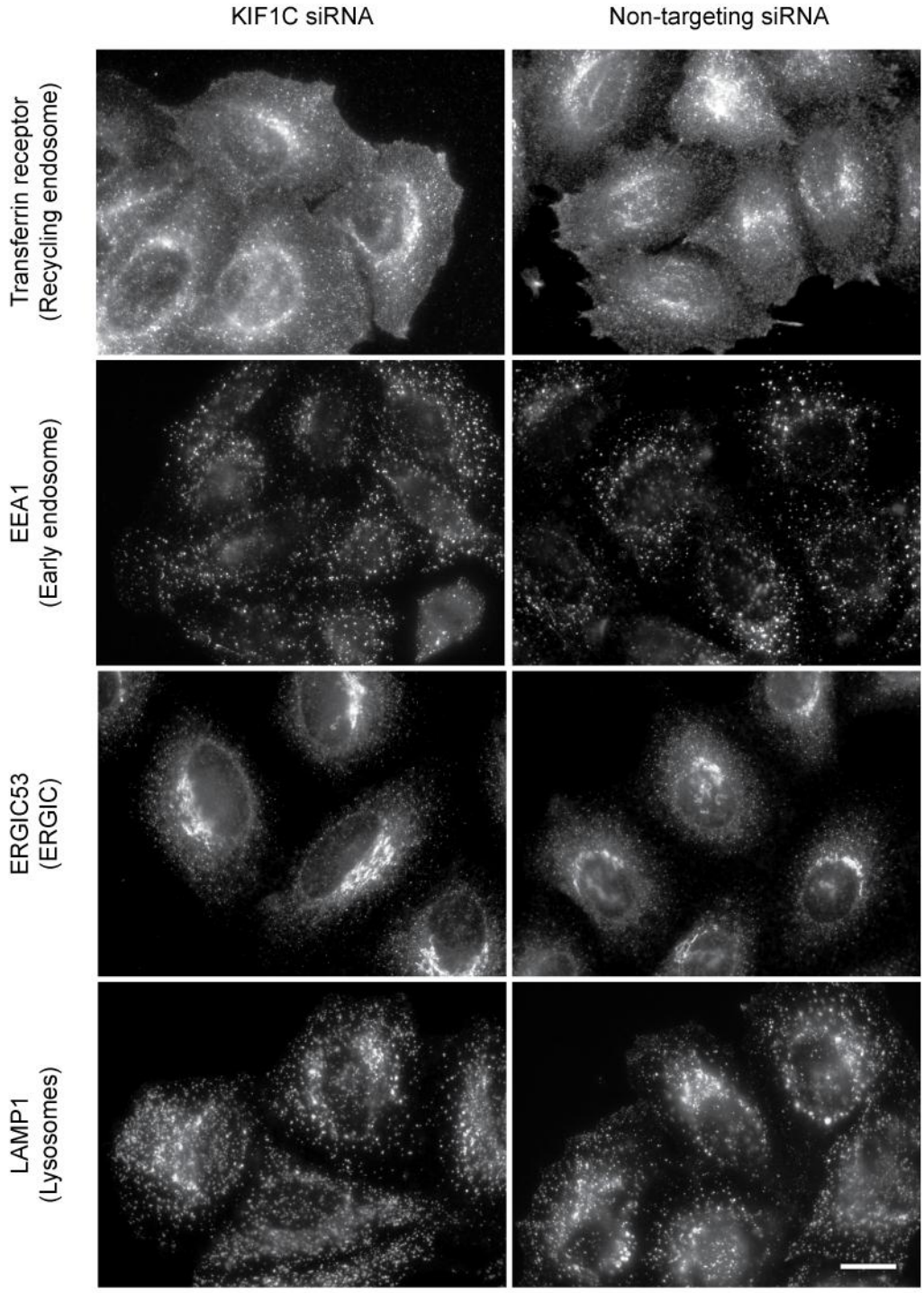

Figure 5.8 - Depletion of KIF1C has no noticeable effects on the position or morphology of a range of endocytic/secretory pathway markers in HeLaM cells

HeLaM cells grown on coverslips were transfected with 0.5 nM KIF1C siRNA SMARTpool, or non-targeting siRNA as a negative control, using INTERFERin for 72 hours and then fixed in methanol or 3 % PFA as appropriate. Cells were labelled with the primary antibodies anti-transferrin receptor, anti-EEA1, anti-ERGIC53, or anti-LAMP1. Alexa594 or Alexa488 were used as secondary antibodies as appropriate. Scale bar is 20 μm.

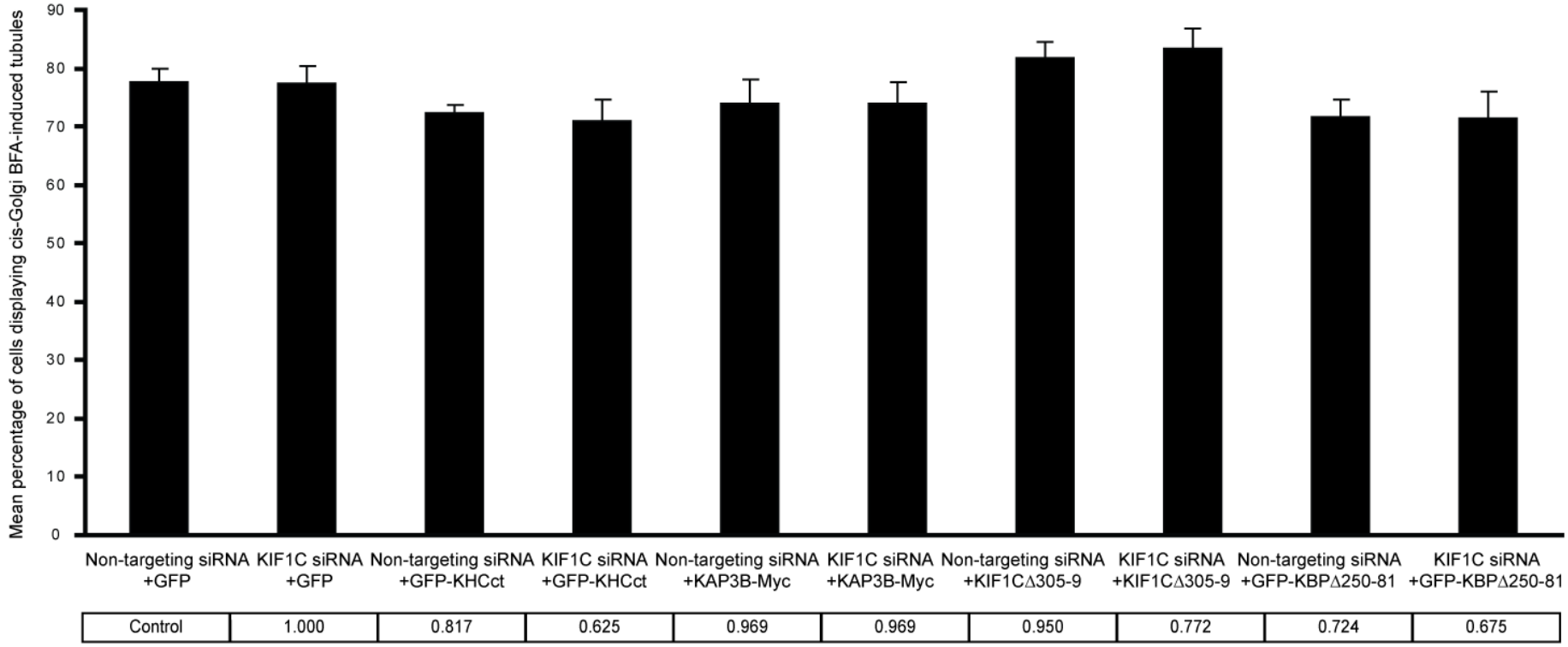

Figure 5.9 - Depletion of KIF1C in conjunction with transfection of various dominant negative kinesin constructs has no effect upon the ability of cis-Golgi BFA-induced tubules to form in HelaM cells

HeLaM cells grown on coverslips were treated with 0.5 nM KIF1C siRNA SMARTpool, or non-targeting siRNA, for 48 hours using INTERFERin and then transfected with various dominant negative kinesin constructs along with the cis-Golgi marker, mApple-Golgi, using JetPEI and left for a further 24 hours. Cells were treated with 2 µg/ml BFA for 10 minutes, fixed in methanol and immunolabelled as necessary. The ability of cis-Golgi BFA tubules to form was measured by counting the percentage of cells displaying mApple-Golgi-positive tubules with 100 cells scored per condition. Each experiment was repeated two additional times to obtain three mean values per condition. A mean of these three separate mean values is shown. Error bars + SEM. P-values (shown in boxes underneath the relevant result) were calculated using a two-sided Dunnett's post-hoc test following a one-way ANOVA using non-targeting siRNA treatment and GFP transfection as the control.

the proteins in cells treated with a variety of concentrations of nocodazole was performed. A concentration of 100 nM of nocodazole was determined to inhibit microtubule dynamics, as adjudged by loss of tomato-EB3 signal, without stimulating microtubule depolymerisation (data not shown).

The ability of cis-Golgi tubules to form was then assessed under conditions in which dynamic microtubules were inhibited and motor function was perturbed. HeLaM cells were treated with KIF1C-specific siRNA for 48 hours, or non-targeting siRNA as a negative control, and then transfected with GFP, GFP-KHCct, KAP3B-Myc, KIF1CΔ305-9 or GFP-KBPΔ250-81 along with mApple-Golgi to assess cis-Golgi tubulation, and left for a further 24 hours. Cells were treated with 100 nM nocodazole for 5 minutes to prevent microtubule dynamics, or an equal volume of the solvent DMSO. Cells were then treated with BFA for 10 minutes (with or without 100 nM nocodazole), and then fixed and immunolabelled as necessary. The ability of mApple-Golgi tubules to form in response to BFA under all of the conditions tested was analysed as previously described. Non-targeting siRNA treatment combined with GFP transfection and DMSO treatment was designated the control for statistical analysis, where 80.0 % of cells displayed mApple-Golgi tubules following BFA treatment (Figure 5.10). No significant change in the percentage of cells displaying mApple-Golgi-positive tubules was detected following transient transfection of any of the dominant negative kinesin constructs, irrespective of whether KIF1C levels are depleted using siRNA or microtubule dynamics have been inhibited using nocodazole. This data indicates microtubule dynamics are not necessary for the motility of cis-Golgi BFA-induced tubules in HeLaM cells.

Due the failure to observe any effects upon the tubulation of the cis-Golgi in response to BFA, it was decided to investigate tubulation of other components of the secretory and endocytic pathways.

5.2.3.2 TGN and endosomal tubulation

TGN, endosomal and lysosomal markers have been reported to exhibit tubules in response to BFA [136, 302, 303]. Furthermore, tubules formed in response to BFA *in vitro* have been shown to be positive for cis-Golgi, recycling endosome and TGN markers [144]. It was therefore hypothesised that the effects of GST-KBPΔ250-81 upon BFA-induced tubule formation *in vitro* previously observed (Figure 5.2), may reflect a role of KIF1C in the tubulation of these compartments, rather than the cis-Golgi. To investigate this possibility the effects of combining KIF1C depletion with transient transfection of dominant negative kinesins upon the tubulation of early endosomes, recycling endosomes and TGN in HeLaM cells were studied. Experiments were performed as previously described except cells were not transfected with mApple-Golgi but were immunolabelled with a range of antibodies raised against markers of these different compartments, including an anti-EEA1 antibody to label tubules derived from early endosomes. The effects of combining KIF1C depletion together with expression of dominant negative kinesins upon BFA-induced tubules were studied rather than investigating each treatment separately since, as previously mentioned, it was thought KIF1C function would be more robustly inhibited if simultaneously targeted by two different approaches.

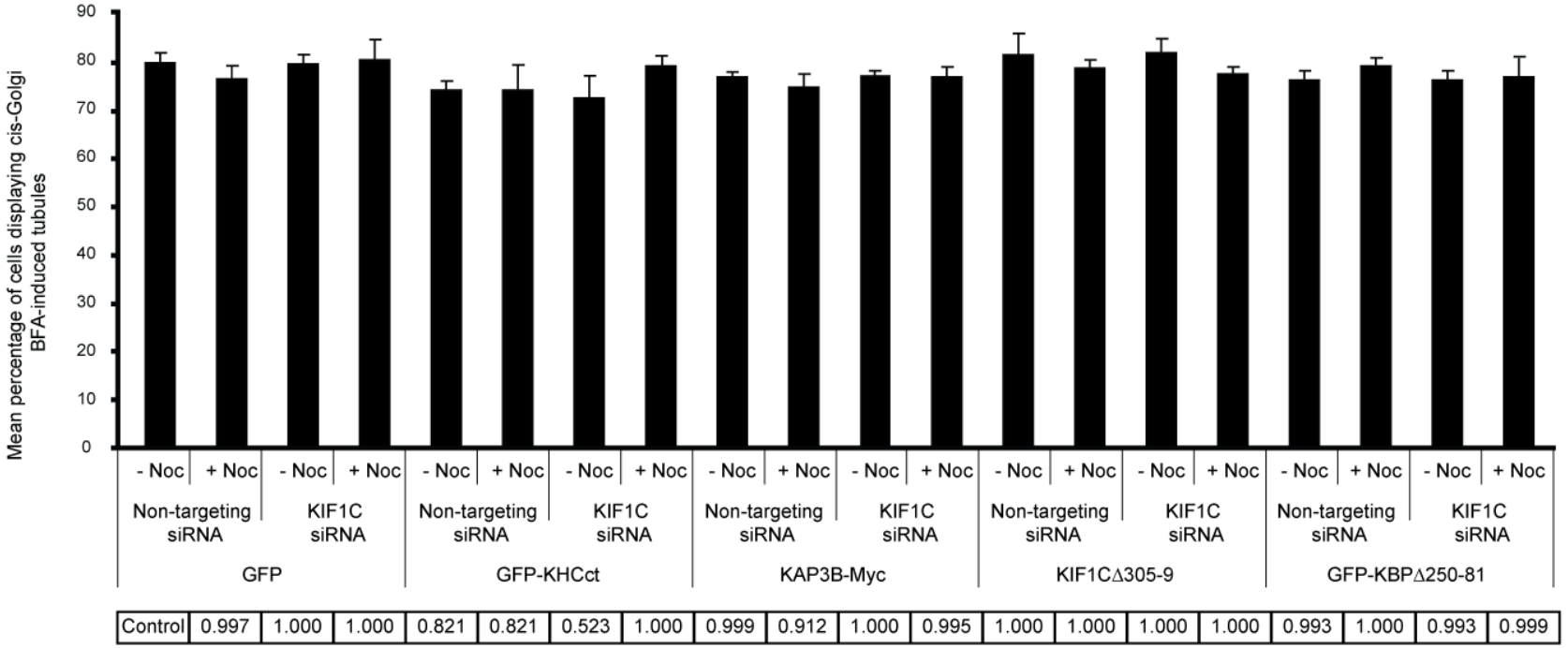

Control	0.997	1.000	1.000	0.821	0.821	0.523	1.000	0.999	0.912	1.000	0.995	1.000	1.000	1.000	1.000	0.993	1.000	0.993	0.999

Figure 5.10 - Inhibition of microtubule dynamics does not affect the ability of cis-Golgi BFA tubules to form in non-targeting siRNA treated or KIF1C-depleted HelaM cells transfected with various dominant negative kinesin constructs

HeLaM cells grown on coverslips were transfected with 0.5 nM KIF1C siRNA SMARTpool or non-targeting siRNA for 48 hours using INTERFERin and then transfected with various dominant negative kinesin constructs along with the cis-Golgi marker, mApple-Golgi, using JetPEI and left for a further 24 hours. Cells were treated with 100 nM nocodazole for 5 minutes to prevent microtubule dynamics (+ Noc), or an equal volume of DMSO as a negative control (- Noc) and then with 2 µg/ml BFA for 10 minutes (with or without 100 nM nocodazole). Cells were fixed in methanol and immunolabelled as necessary. The ability of cis-Golgi tubules to form in response to BFA was measured by counting the percentage of cells which display mApple-Golgi-positive tubules with 100 cells scored per condition. Each experiment was repeated two additional times to obtain three mean values per condition. A mean of these three separate mean values is shown. Error bars + SEM. P-values (shown in boxes underneath the relevant result) were calculated using a two-sided Dunnett's post-hoc test following a one-way ANOVA using non-targeting siRNA treatment and GFP transfection as the control.

It was first determined whether tubulation of these various compartments could be observed in HeLaM cells following BFA treatment. HeLaM cells were treated with BFA for 8 minutes, 10 minutes or 12 minutes, or the same volume of methanol as a negative control, and immunolabelled using the anti-EEA1, anti-transferrin receptor or anti-TGN46 antibodies, respectively. Treatment with BFA for these lengths of time was adjudged to give the highest percentage of untransfected cells displaying tubules positive for each marker (data not shown), and were used in all subsequent experiments. Anti-EEA1 is an antibody raised against the human early endosomal antigen-1 protein and is a widely used marker for early endosomes in a range of cell lines, including HeLa cells (e.g. [176]). Anti-transferrin receptor is an antibody raised against the recycling endosome marker, transferrin receptor [304, 305]. Anti-TGN46 is an antibody raised against the human TGN localised protein TGN46, and is a widely used marker of the TGN in human cell lines (e.g. [306]). Tubules positive for each of these markers were apparent following treatment with BFA (Figure 5.11). Since lysosomal tubulation in response to BFA has also been reported [136, 302, 303], preliminary experiments in which HeLaM cells were treated with BFA and stained with the lysosomal antibody anti-LAMP1 were also performed. However, no tubules were observed using this antibody despite cells being incubated with BFA for up to 6 hours (data not shown). Consequently the effects of kinesin inhibition upon BFA-induced lysosomal tubulation were not investigated further.

The effects of motor inhibition upon BFA-induced tubulation of early endosomes were first investigated. HeLaM cells were treated with KIF1C-specific siRNA for 48 hours, or non-targeting siRNA as a negative control, and then transfected with GFP, GFP-KHCct, KAP3B-Myc, KIF1CΔ305-9 or GFP-KBPΔ250-81 and left for a further 24 hours. Cells were treated with BFA for 8 minutes or an equal volume of methanol. Coverslips were fixed and immunolabelled with the early endosomal antibody anti-EEA1. When initially observing coverslips stained with the anti-EEA1 antibody following BFA treatment, it was apparent that a lower percentage of cells displayed tubules compared to when the cis-Golgi marker mApple-Golgi was used (Figure 5.9). Therefore it was thought any subtle effects of kinesin inhibition upon the number of cells displaying BFA-induced EEA1-positive tubules would be harder to detect. For this reason a higher number of cells per condition were scored compared to experiments using mApple-Golgi as a marker. A total of 300 transfected cells per treatment were scored according to whether EEA1-positive tubules could be seen. The percentage of transfected cells displaying EEA1-positive tubules was then calculated. To statistically analyse the data, the non-targeting siRNA treated cells combined with GFP transfection was designated as the control, where a mean of 23.8 % of cells displayed EEA1-positive tubules in the absence of BFA, compared to 30.7 % of cells in the presence of BFA (Figure 5.12). The mean percentage of cells displaying EEA1-positive tubules in the absence of BFA treatment did not change significantly following transient transfection of any dominant negative kinesin constructs, irrespective of whether KIF1C levels are also depleted using siRNA.

However, the expression of GFP-KHCct significantly reduced the mean percentage of cells displaying EEA1-positive tubules following BFA treatment from 30.7 % to 20.2 % in non-

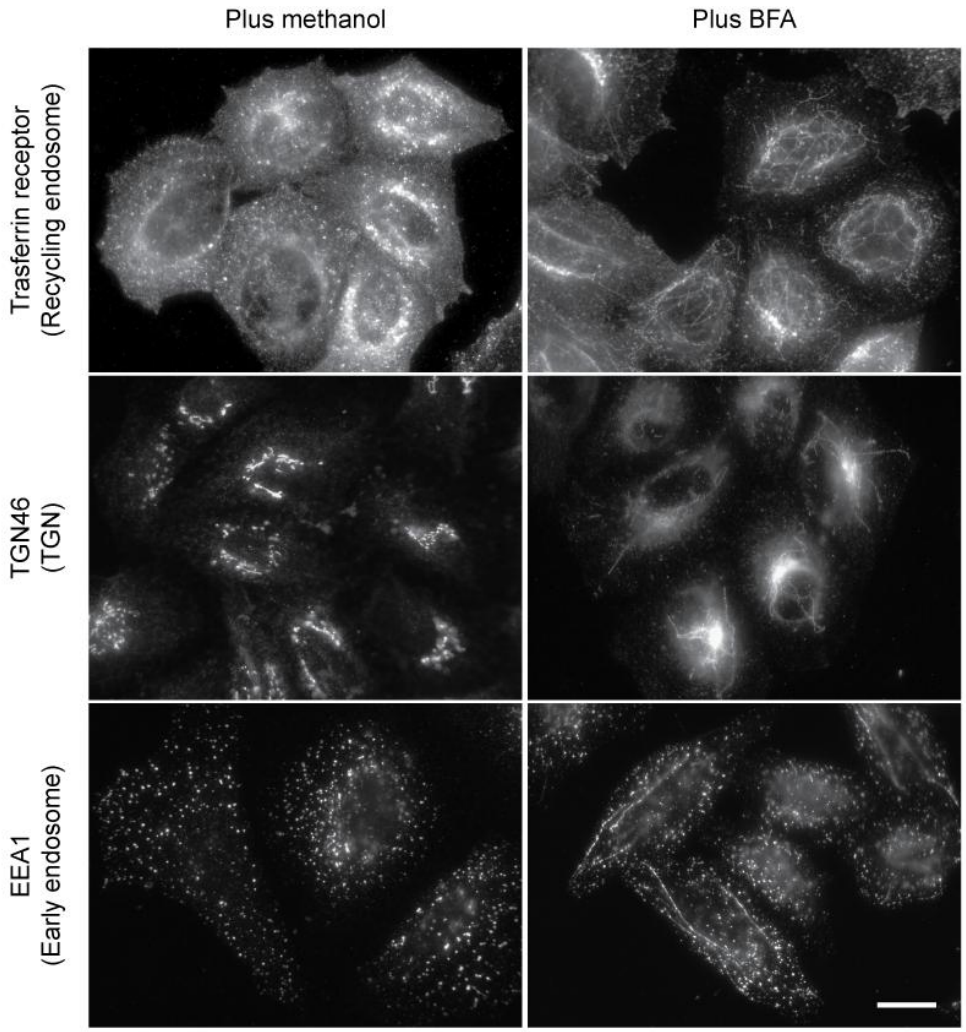

Figure 5.11 - Treatment with BFA induces tubulation of recycling endosomes, the TGN and early endosomes in HeLaM cells

HeLaM cells grown on coverslips were treated with 2 µg/ml BFA (or an equal volume of methanol as a negative control) for 10 minutes, 12 minutes or 8 minutes, fixed as appropriate, and immunolabelled with anti-transferrin receptor, anti-TGN46 or anti-EEA1 antibodies, respectively. Alexa594 or Alexa488 were used as secondary antibodies as appropriate. Scale bar is 20 µm.

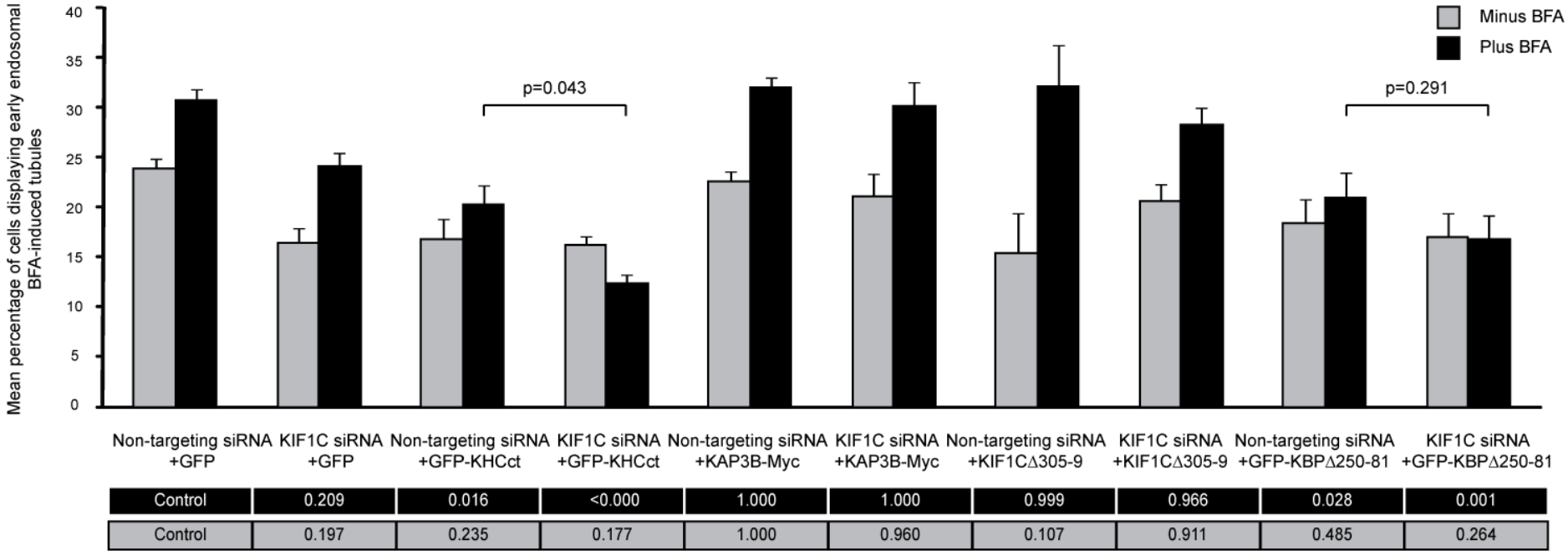

Control	0.209	0.016	<0.000	1.000	1.000	0.999	0.966	0.028	0.001
Control	0.197	0.235	0.177	1.000	0.960	0.107	0.911	0.485	0.264

Figure 5.12 - Transfection of GFP-KHCct or GFP-KBPΔ250-81 inhibits the formation of BFA-induced early endosomal tubules in HeLaM cells irrespective of whether KIF1C protein levels have been depleted using siRNA

HeLaM cells grown on coverslips were treated with 0.5 nM KIF1C siRNA SMARTpool or non-targeting siRNA for 48 hours using INTERFERin and then transfected with various dominant negative kinesin constructs, using JetPEI and left for a further 24 hours. Cells were treated with 2 µg/ml BFA for 8 minutes, or an equal volume of methanol as a negative control, fixed in PFA and immunolabelled with the anti-EEA1 antibody and marker antibodies as necessary. The ability of early endosomal BFA-induced tubules to form was measured by counting the percentage of cells displaying EEA1-positive tubules with 300 cells scored per condition. Each experiment was repeated two additional times to obtain three mean values per condition. A mean of these three separate mean values is shown. Error bars + SEM. P-values (shown in boxes underneath the relevant result) were calculated using a two-sided Dunnett's post-hoc test following a one-way ANOVA, using non-targeting siRNA treatment and GFP transfection as the control. To compare transfection of GFP-KHCct or GFP-KBPΔ250-81 in KIF1C-specific siRNA or non-targeting siRNA treated cells, independent two-sample student t-tests were used and the p-values are shown below the relevant bars.

targeting siRNA treated cells with a p-value of 0.016 (Figure 5.12). This value was further reduced to 12.4 % when GFP-KHCct expression was performed in conjunction with KIF1C-specific siRNA treatment, which corresponds to a p-value of less than 0.001 from the non-targeting siRNA treatment combined with GFP transfection control. It was determined that depletion of KIF1C in combination with GFP-KHCct transfection significantly reduced the mean percentage of cells displaying EEA1-positive tubules in comparison to non-targeting siRNA treatment with the same transfection, correlating to a p-value of 0.043. This data suggests kinesin-1 and KIF1C motors function, perhaps in combination, in moving BFA-induced early endosomal tubules.

The expression of GFP-KBPΔ250-81 also significantly reduced the mean percentage of cells displaying EEA1-positive tubules following BFA treatment from 30.7 % to 20.9 % in non-targeting siRNA treated cells (Figure 5.12). This value was not significantly reduced when GFP-KBPΔ250-81 expression was performed in conjunction with KIF1C-specific siRNA treatment. This data supports a role for KIF1C in the movement of early endosomal BFA-induced tubules.

The expression of KAP3B-Myc or KIF1CΔ305-9 had no significant effect upon the mean percentage of cells displaying EEA1-positive tubules compared to the GFP control, irrespective of whether KIF1C levels had also been depleted using siRNA. This suggests kinesin-2 does not play a role in moving early endosomal tubules in response to BFA. The lack of any effect of KIF1C305-9 expression is surprising given the previously described data suggests KIF1C plays a role in the movement of BFA-induced early endosomal tubules [146]. Perhaps KIF1CΔ305-9 is not a potent inhibitor of KIF1C function *in vivo*, or its dominant negative effects are very dependent upon the level or duration of expression.

When identical experiments were performed using anti-transferrin receptor and anti-TGN46 antibodies to investigate tubulation of recycling endosomes and TGN respectively in response to BFA, a higher percentage of cells exhibited tubules in the order of 75-85 % (data not shown). This made it easier to judge whether there were obvious changes to the number of cells displaying tubules when function or expression of the various kinesins was perturbed. No obvious differences in the number of cells displaying tubules could be observed by eye and data was not quantified.

The effects of dominant negative kinesin expression along with KIF1C-specific siRNA treatment, upon tubulation of the cis-Golgi, TGN, early endosomes and recycling endosomes as adjudged using the mApple-Golgi marker and anti-TGN46, anti-EEA1 and anti-transferrin receptor antibodies respectively, are summarised in Figure 5.13. The only statistically significant changes were observed upon EEA1-positive tubules following GFP-KHCct or GFP-KBPΔ250-81 expression as already discussed (Figure 5.12).

The difficulty in identifying an effect of GFP-KBPΔ250-81 expression upon the ability of BFA-induced tubules to form *in vivo* was surprising given such apparently potent inhibition with GST-

COMPARTMENT / TREATMENT		cis-Golgi (mApple-Golgi positive)	TGN (TGN46 positive)	Early endosome (EEA1 positive)	Recycling endosome (Transferrin receptor positive)
KIF1C siRNA		ND (x1)	?	?	?
Transient transfection of dominant negative kinesin constructs	GFP-KHCct	NSD (x3)	ND (x2)	ND (x1)	ND (x1)
	KAP3B-Myc	NSD (x3)	ND (x2)	ND (x1)	ND (x1)
	KIF1CΔ305-9	NSD (x3)	ND (x2)	ND (x1)	ND (x1)
	GFP-KBPΔ250-81	NSD (x3)	ND (x2)	ND (x1)	ND (x1)
Non-targeting siRNA + transient transfection of dominant negative kinesin constructs	GFP-KHCct	NSD (x3)	ND (x2)	Significantly reduced (x3)	ND (x2)
	KAP3B-Myc	NSD (x3)	ND (x2)	NSD (x3)	ND (x2)
	KIF1CΔ305-9	NSD (x3)	ND (x2)	NSD (x3)	ND (x2)
	GFP-KBPΔ250-81	NSD (x3)	ND (x2)	Significantly reduced (x3)	ND (x2)
KIF1C siRNA SMARTpool + transient transfection of dominant negative kinesin constructs	GFP	NSD (x3)	ND (x2)	NSD (x3)	ND (x2)
	GFP-KHCct	NSD (x3)	ND (x2)	Significantly reduced (x3)	ND (x2)
	KAP3B-Myc	NSD (x3)	ND (x2)	NSD (x3)	ND (x2)
	KIF1CΔ305-9	NSD (x3)	ND (x2)	NSD (x3)	ND (x2)
	GFP-KBPΔ250-81	NSD (x3)	ND (x2)	Significantly reduced (x3)	ND (x2)
In vitro motility assay following pre-treatment of rat liver Golgi membranes with antibody	H1	Significantly reduced network length (x3)			
	SUK4	NSD (x3)			
	k2.4	NSD (x3)			
In vitro motility assay following pre-treatment of rat liver Golgi membranes with protein	GST-KHCct	NSD (x3)			
	GST-KAP3B	NSD (x3)			
	GST-KHCct+GST-KAP3B	NSD (x3)			
	GST-KBPΔ250-81	Significantly reduced network length (x3)			

Figure 5.13 - Summary of the effects of motor disruption upon BFA-induced tubule formation *in vitro* and *in vivo*

The effects of KIF1C siRNA SMARTpool treatment and 24 hour transient transfection of dominant negative kinesin constructs, either separately or in combination with each other, upon the BFA-induced tubulation of various compartments in HeLaM cells are summarised. Also included are the effects upon BFA-induced tubules following pre-incubation of rat liver Golgi membranes with antibodies or proteins which have an inhibitory effect upon various motors. For conditions which have been quantified in three separate experiments a two-sided Dunnett's post-hoc test was used following a one-way ANOVA to determine whether any changes are significantly different. If no significant difference was observed this is recorded as NSD (no significant difference). If experiments have not been repeated three times this is because no obvious difference in the data was apparent by eye. In such cases no statistical analysis was performed and this is recorded as ND (no difference). The figure in brackets indicates the number of times the experiment has been repeated. A question mark indicates the experiment has not been performed.

KBPΔ250-81 was observed *in vitro* (Figure 5.3). It has been reported that KBP binds to another member of the KIF1 family, KIF1Bα, *in vivo*. It was therefore hypothesised that the effects observed in the *in vitro* assay upon BFA-induced tubule formation in the presence of GST-KBPΔ250-81 could perhaps be due to inhibition of KIF1Bα, rather than KIF1C. Since KIF1Bα has been reported to localise to mitochondria in NIH-3T3 cells [51], it was felt the level of KIF1Bα in the rat liver Golgi fraction would be low, but this could not be tested due to the lack of an anti-KIF1B antibody which works for immunoblotting. Attempts were made to deplete KIF1B and the other member of the KIF1 family, KIF1A, using specific siRNA SMARTpools in HeLaM cells. No obvious effects upon the ability of BFA-induced tubules to form were observed by eye. Treatments with combinations of siRNA SMARTpools targeted against KIF1A, KIF1B or KIF1C were also tested, but again no obvious effects upon BFA-induced tubule formation was observed by eye (data not shown). However, due to a lack of KIF1A and KIF1B antibodies which work for immunoblotting, it was not possible to check whether the protein level of each of these motors had been effectively depleted following siRNA treatment.

6. Discussion – Motility of BFA-induced tubules

Tubules emanating from several compartments located with the endocytic and secretory pathways are generated in a microtubule-dependent fashion in response to the fungal metabolite BFA [135-139]. Despite attempts by several previous studies to decipher the motor(s) responsible for this motility, its identity remains unknown. The aim of this work was to assess the contributions of kinesin-1, kinesin-2 and KIF1C to these processes.

6.1 Reconstitution of BFA-induced tubule formation *in vitro*

The process of BFA-induced tubule formation has previously been reconstituted *in vitro* by combining a rat liver Golgi fraction with interphase *Xenopus laevis* egg extract cytosol in the presence of BFA [144]. A slightly modified version of this assay was used initially in this study, where Golgi membranes were treated with kinesin function-blocking antibodies or dominant negative proteins prior to mixing with cytosol. This approach was chosen for several reasons. The behaviour of microtubule motors has often proved easier to study initially *in vitro* [30], and previously this assay has been used successfully to show that the motor(s) responsible for BFA-induced tubule motility is regulated in a cell cycle-dependent manner [144]. Additionally, the perturbation of kinesin motors is more complex *in vivo,* where the level or duration of an inhibitory treatment is more of a concern and there is the inherent problem of cooperation between motor proteins potentially masking phenotypes. Moreover, this assay allows BFA-induced tubules positive for cis-Golgi, early endosomal and TGN markers to be observed simultaneously. If an effect upon tubule motility was observed *in vitro*, it was planned *in vivo* studies would then be incorporated to determine whether the findings could be replicated.

Initially the function-blocking antibodies SUK4 and k2.4 were used to perturb kinesin-1 and kinesin-2 function respectively *in vitro* and found to have no significant effect upon the generation of BFA tubules. The lack of a role for kinesin-1 in moving BFA-induced tubules *in vitro* is in agreement with previously published work [144]. These antibodies have been successfully used in similar assays to reveal a role for kinesin-1 in *Xenopus laevis* ER motility during development [218], and for kinesin-2 in rat liver Golgi vesicle motility (personal communication, Dr. Marcin Woźniak). These observations indicate that SUK4 and k2.4 are able to effectively inhibit motor function *in vitro* and allay fears that the negative result obtained could simply be due to the antibody having a weak inhibitory effect. This supports the work of Feiguin and co-workers in which suppression of KHC levels in cultured rat hippocampal neurons is observed to have no effect upon the BFA-induced redistribution of cis/medial/trans-Golgi contents back to the ER [145]. In agreement with previous studies, the H1 antibody was found to strongly inhibit tubule formation, although the target of the antibody remains to be determined [143, 144]. Immunoprecipitations could be performed from the rat liver Golgi fraction using the H1 antibody to attempt to identify which protein(s) the antibody recognises. Immunoprecipitates could be run on SDS-PAGE gels and stained with colloidal Coomassie, and any interesting bands could be analysed using mass spectrometry.

All the data reported here looks at the extent of tubule formation after 1 hour of incubation in the flow cell. It is possible that perturbation of kinesin-1 or kinesin-2 function delays tubule formation

or reduces the speed at which tubules move, which may not be apparent at the 1 hour time point. Although no defect in tubule motility was apparent by eye, quantification of the network length at earlier time points, together with analysis of tubule speed, could be performed to comprehensively characterise the contribution of these motors to this process. Similar speed calculations have been made from VE-DIC movies in previous studies using the RETRAC object tracking system [144, 218]. The effects of KIF1C inhibition in this experiment could not be investigated since no antibody which is known to specifically perturb KIF1C function has been identified. The addition of the available anti-KIF1C antibody, which was raised against amino acids 850-900 of the human protein, had no effect upon BFA-induced tubule formation *in vitro* (data not shown).

Incubations with dominant negative kinesin proteins were next used to complement the function-blocking antibody data. GST-KHCct and GST-KAP3Bct were used to perturb kinesin-1 and kinesin-2 function, respectively. These proteins have been used successfully in previous assays to reveal a role for kinesin-1 in rat liver ER motility [30], and for kinesin-2 in rat liver Golgi vesicle motility (personal communication, Dr. Marcin Woźniak). Again, despite no effect of kinesin-1 or kinesin-2 inhibition upon network formation being observed after 1 hour, a delay in network formation or alteration in tubule speed cannot be excluded.

The GST-KBPΔ250-81 protein, which has been previously shown to perturb KIF1Bα function *in vivo* and *in vitro*, was found to significantly inhibit BFA-induced tubule formation [51]. Since KIF1Bα is reported to be primarily localised to mitochondria, it was felt that perturbation of the Golgi localised KIF1C, which also binds KBP, was more likely to be responsible for this inhibition. However, it was not possible to verify the levels of KIF1Bα or KIF1C on rat liver Golgi membranes since no antibody which recognised the rat forms of the proteins was available. No effects of GST-KBPΔ250-81 upon Golgi vesicle motility were observed revealing that this protein has no off-target effects upon kinesin-1 or kinesin-2. However, it cannot be verified that the inhibition of BFA-induced tubule formation observed in the presence of GST-KBPΔ250-81 is due exclusively to perturbation of KIF1C function. Since no additional inhibitory effect was detected when combinations of motors were inhibited simultaneously it was concluded that the motor perturbed by GST-KBPΔ250-81, likely KIF1C, was solely responsible for the motility of BFA-induced tubules *in vitro*.

Another drawback of using GST-KBPΔ250-81 is that it is not fully understood how the protein exerts its dominant negative effects. Although it has been demonstrated that KBPΔ250-81 is unable to bind KIF1B (and presumably KIF1C) [51], it is uncertain how this would disrupt binding of endogenous KBP to the motor. Furthermore, if KBP binds KIF1C *in vivo* it may be expected that KBP would localise to the Golgi, since the motor has been reported to be enriched here [146, 147]. However, only mitochondrial staining was observed in immunofluorescence studies using an anti-KBP antibody in NIH-3T3 cells [51]. Ideally another KIF1C dominant negative protein would have been incorporated into the assay, to verify that the phenotype observed with GST-KBPΔ250-81 is a direct consequence of KIF1C inhibition.

The binding of cargoes to KIF1C is expected to occur via the more C-terminal portion of the motor [50, 51] and therefore addition of this fragment of the protein to the assay may potentially compete with and displace the endogenous motor from rat liver Golgi membranes. Another approach may be to overexpress the region of the Golgi receptor responsible for binding KIF1C. However, since this protein is yet to be identified this was not possible. The only documented KIF1C dominant negative protein is the ATPase-deficient mutant KIF1CΔ305-9 [146] and there is no precedence for recombinantly expressing this protein. Indeed, at over 1,100 amino acids it is likely that bacterial expression of the protein would prove problematic. It is probable that if recruitment of KIF1C from *Xenopus laevis* egg extract cytosol to the rat liver Golgi membrane is responsible for BFA tubule motility, this would be unmasked by immunodepletion of the motor using an anti-KIF1C antibody. However, since an antibody which recognises the *Xenopus laevis* form of the protein by immunoblotting was not available, it was not possible to determine whether any such recruitment is occurring and furthermore any depletion of KIF1C from the cytosol could not be verified.

6.2 Motility of BFA-induced tubules *in vivo*

The motility of BFA-induced tubules in HeLaM cells was next investigated to determine whether the phenotypes observed *in vitro* were replicated *in vivo*. Initially, tubulation of the cis-Golgi was probed using the mApple-Golgi construct since the effects of BFA upon this compartment have been well characterised previously. Similar to the *in vitro* assay, a variety of dominant negative proteins were used to disrupt kinesin motor function. Additionally KIF1CΔ305-9, an ATPase deficient mutant previously shown to perturb BFA-induced redistribution of the cis-Golgi to the ER in NIH-3T3 cells [146], was included as another means of interfering with KIF1C activity. The thinking behind this was that the effects of KIF1CΔ305-9 expression could be compared to those of GFP-KBPΔ250-81 and thereby hopefully provide confirmation that both proteins target KIF1C.

One disadvantage of using these dominant negative proteins to perturb kinesin function was that no positive controls could be identified, despite the morphology of several organelles and cytoskeletal filaments being screened (data not shown). This meant there was no verification that the appropriate motor was being specifically and robustly inhibited by each reagent. Furthermore, it was unsure whether the duration or length of expression of the dominant negative kinesin was also linked to its inhibitory effects. Indeed it has been previously shown that perturbation of ER tubule motility by GFP-KHCct only occurs when the DNA is microinjected into the nucleus leading to high levels of the protein being rapidly expressed, whereas following transiently transfection no phenotype is observed [197]. Attempts were made to microinject both the GFP-KBPΔ250-81 construct and GST-KBPΔ250-81 protein into HeLaM cells transfected with mApple-Golgi, to identify whether the rapid expression of high levels of the dominant negative reagent perturb BFA-induced tubules forming from the cis-Golgi. However, mApple-Golgi tubules were found to form normally in microinjected cells (data not shown). This lack of positive controls is surprising given the wide range of cargoes kinesin-1, kinesin-2 and

KIF1C are documented to move. Furthermore, previously reported changes in organelle positioning, such as mitochondrial clustering induced by expression of an untagged version of KBP∆250-81 in NIH-3T3 cells [51], were not observed. The inability to recapitulate such phenotypes in this study is not understood. It is possible that the effects are cell type-specific, or as previously mentioned are sensitive to the duration and length of expression. Alternatively, perhaps a higher level of motor cooperation or redundancy occurs in HeLaM cells meaning phenotypes are masked when motors are inhibited individually.

Early on in this study it was decided to combine transient transfection of dominant negative proteins with siRNA-mediated depletion of KIF1C. This decision was taken for several reasons. During initial experiments looking at the effects of dominant negative protein expression upon cis-Golgi tubulation it became apparent that none of these reagents had a striking phenotype upon tubule formation. Since the *in vitro* assay data presented here and work from a previous study [146] suggested a role for KIF1C in tubule formation, perturbation of this motor rather than kinesin-1 or kinesin-2 was focussed upon. Due to the lack of positive controls it was felt that KIF1C function should be disrupted by several approaches, in an attempt to ensure any negative results were not simply due to the failure of the dominant negative proteins to have a complete inhibitory effect *in vivo*. It was thought that KIF1C function would be more robustly perturbed when targeted simultaneously by two separate methods. Moreover, if several motors contribute to BFA-induced tubule motility this may only be exposed if multiple motors are inhibited simultaneously. No changes in the morphology or positioning of a wide range of organelles and cytoskeletal filaments were detected in fixed HeLaM cells depleted of KIF1C, compared to those treated with a scrambled siRNA control. However, it remains possible that perturbation in the motility of these structures may be identified if observed in living cells. It should also be noted that it cannot be verified that all cells were completely depleted of KIF1C. Ideally, the level of KIF1C present in each of the cells observed would have been assessed. Attempts were made to use the anti-KIF1C antibody in immunofluorescence studies to determine the relative levels of KIF1C protein in each of the cells scored in every experiment. However, the KIF1C antibody was found to give a weak signal even in control cells which localised to no particular cellular compartment, despite attempts to optimise fixation conditions. Furthermore, this staining did not disappear upon depletion of KIF1C and it was therefore concluded that the antibody does not work by immunofluorescence. To more accurately determine the level of KIF1C remaining after siRNA treatment, attempts are being made in the laboratory to perform quantitative PCR. If it can be shown that the amount of KIF1C DNA is reproducibly reduced to a similarly low level following siRNA treatment, this would more conclusively show that each of the cells observed is depleted of KIF1C to a similar level.

Despite investigating the effects of overexpression of the dominant negative proteins in the background of KIF1C depletion, no effects upon the percentage of cells displaying tubules positive for mApple-Golgi (cis-Golgi marker), TGN46 (TGN marker) or transferrin receptor (recycling endosome marker) were detected. The inhibition of microtubule dynamics using low doses of nocodazole also had no significant effects upon cis-Golgi tubulation, indicating that

microtubule polymerisation does not contribute to tubule extension. It should be noted that in each of these experiments cells were scored in a binary fashion according to whether tubules were present or absent. It is possible that the frequency of tubules per cell, the length of tubules, or the speed of tubule translocation varies between conditions. This data presented here is in agreement with the study of Nakajima and co-workers, in which BFA-induced trans-Golgi tubules were observed to form normally in lung fibroblasts isolated from a KIF1C knockout mouse [147]. However, the data is at odds with that reported by Dorner and co-workers in which transient transfection of KIF1CΔ305-9 was found to inhibit redistribution of the cis-Golgi marker p58 to the ER in response to BFA in NIH-3T3 cells [146]. The reason for this discrepancy is not known although it is possible that KIF1CΔ305-9 is not a potent inhibitor of KIF1C function in HeLaM cells, or that perturbation is sensitive to the level or duration of expression. It should also be noted that this paper provides no quantification or statistical analysis of the inhibitory effect.

The percentage of HeLaM cells displaying BFA-induced tubules positive for the early endosomal marker EEA1 was significantly influenced by kinesin motor inhibition. Expression of GFP-KHCct reduced the percentage of cells in which EEA1-positive tubules were observed, and this value was further lowered when combined with KIF1C depletion. This data indicates kinesin-1 and KIF1C both contribute to the movement of early endosomal tubules formed in response to BFA. The fact that a partial effect upon tubule formation is not observed when KIF1C depletion is combined with the control GFP transfection suggests the function of KIF1C in this process may only be exposed when kinesin-1 is also inhibited.

If KIF1C does contribute to tubule motility it may be expected that expression of KIF1CΔ305-9 would also generate a phenotype. Such an effect was not observed and the reason for this is not fully understood. As previously mentioned the effects of KIF1C inhibition upon early endosomal tubulation may only be exposed when performed in conjunction with inhibition of another motor. Alternatively, KIF1CΔ305-9 may not be a potent inhibitor of KIF1C function in HeLaM cells. Contrastingly, expression of GFP-KBPΔ250-81 significantly reduces the percentage of cells displaying EEA1-positive tubules irrespective of whether KIF1C levels have also been depleted. This suggests GFP-KBPΔ250-81 is a more potent inhibitor of KIF1C function than KIF1CΔ305-9 or that it disrupts the function of another motor(s) *in vivo* aside from KIF1C.

The observation that perturbation of kinesin-1 function has no significant effect upon the percentage of cells displaying BFA-induced transferrin receptor-positive tubules is seemingly at odds with data presented by Lin and co-workers. In this study, disruption of kinesin-1 activity in Chinese hamster ovary cells by microinjection of a function-blocking antibody was found to slow the recycling of transferrin to the cell surface, suggesting this motor is involved in the movement of transferrin, and perhaps other cargoes, away from the recycling endosome to the plasma membrane [169]. However, the reagent used was a pan-kinesin antibody meaning the inhibitory effects observed cannot be attributed solely to disruption of kinesin-1 function.

It remains to be determined whether the tubulation induced by BFA *in vivo* represents an accentuated version of a transport pathway which operates routinely in untreated cells. Tubule motility is apparent *in vitro* when rat liver Golgi membranes are combined with *Xenopus laevis* egg extract cytosol, even when BFA is excluded [232], although both tubule morphology and the rate of tubule extension differ between the two conditions [144, 232]. Several studies have observed tubules emanating from the Golgi and early endosomes in the absence of the drug. Induced and uninduced tubules appear to be morphologically distinct with the latter being shorter, more branched and less abundant [135, 151, 307]. The rate at which cis-Golgi tubules move in control and BFA-treated HeLa cells is identical, perhaps indicating the same machinery operates in each setting [151]. It is interesting to speculate upon the purpose of these tubules in untreated cells. Tubulation appears to be an inherent and prominent property of Golgi membranes. Indeed, tubules are known to connect adjacent Golgi stacks allowing extensive remodelling of organelle structure, and tubules arising from the Golgi are frequently observed to detach and move towards the cell periphery [151]. Interestingly, live cell imaging of GFP-KDEL receptor-positive tubules has revealed that following translocation towards the cell periphery the fluorescence signal abruptly and rapidly disappears [151]. This suggests that cargo has been delivered and deposited at a specific cellular destination, likely the ER, and indicates Golgi-derived tubules in untreated cells may have a carrier function within a membrane trafficking pathway.

6.3 Discrepancies between *in vivo* and *in vitro* results

The *in vitro* data presented here supports a role for KIF1C in moving BFA-induced tubules in agreement with previously published data [146], although doubts remain over the specificity of the KBPΔ250-81 dominant negative protein. This is at odds with the work of Nakajima and co-workers in which the retrograde movement of cis- and trans-Golgi markers back to the ER in response to BFA is unaffected in the KIF1C knockout mouse. The mechanism of motor perturbation may provide one explanation for this inconsistency. The use of dominant negative proteins should prevent compensation by other motors, and furthermore, cargo motility was studied shortly after motor inhibition. The absence of KIF1C in the knockout mouse can be potentially compensated for by other motors and the time between motor perturbation and experimentation is longer meaning cells can possibly adjust to the loss of the motor.

The interpretation of the *in vivo* data presented here is a little more complex. The only significant effect observed was a contribution of both KIF1C and kinesin-1 towards the movement of early endosomal tubules. One difficulty in ascertaining the effects of motor inhibition upon EEA1-positive tubules is that even in control samples a portion of cells display tubules and this was not dramatically increased following incubation with BFA, despite attempts to optimise the length of drug treatment to maximise the percentage of cells displaying tubules. This meant large amounts of cells had to be scored to ensure accurate results were obtained. There is no precedence for labelling BFA-induced tubules emanating from early endosomes with an anti-EEA1 antibody, and the analysis of tubule formation may have proved easier if a

different marker had been used. For example, cells could have been pulsed with fluorescently-conjugated transferrin protein and providing BFA treatment and fixation were performed promptly, early endosomes would be labelled. One concern of using the anti-EEA1 antibody is that recruitment of the protein to endosomes is dependent upon the phospholipid phosphatidylinositol 3-phosphate [308]. Therefore it is feasible that changes in the phosphoinositide balance across the endosomal network may also influence the number of EEA1-positive tubules. Labelling early endosomal BFA-induced tubules using other markers would provide a means of overcoming this problem.

Although a role for KIF1C is in agreement with the *in vitro* data, perturbation of kinesin-1 function had no significant effect upon rat liver Golgi BFA tubule formation. The reason for this discrepancy is not known although it is possible that the reconstitution of microtubule-driven membrane motility *in vitro* provides a simplified representation of the *in vivo* system. Indeed rat liver ER tubule motility is driven exclusively by kinesin-1 *in vitro* [30], but cytoplasmic dynein-1 also contributes to ER movement in VERO cells [197]. Perhaps a role for kinesin-1 is only exposed when looking at early endosomal tubules in isolation which is not possible in the *in vitro* assay where networks positive for cis-Golgi, TGN and early endosomal markers are generated. Another key difference between the two assays is that the presence of the actin depolymerising agent cytochalasin D *in vitro* prevents any actin-based movement of BFA-induced tubules, whereas this remains viable *in vivo*. A function for myosin II in the BFA response has been previously reported since the perturbation of myosin II function results in a delay in retrograde trafficking from the Golgi to the ER following BFA treatment in HeLa cells [150]. Interestingly, tubules positive for the cis/medial Golgi marker mannosidase II are still observed when myosin II is inhibited, and it remains undetermined which stage of Golgi-to-ER trafficking myosin II contributes to. Alternatively, it is possible that the *in vitro* assay is not faithfully mimicking the *in vivo* process. It should be noted, however, that it is a common observation of this laboratory that motor perturbation *in vitro* generates very obvious defects in cargo movement, whereas the situation proves considerably more complex and difficult to replicate *in vivo*.

6.4 Future work

As previously mentioned the *in vitro* assay used in this study is devoid of actin-based motility due to the inclusion of cytochalasin D. It is feasible that the contribution of myosin motors is masking the effects of kinesin inhibition upon BFA-induced tubule motility *in vivo,* which are exposed in the *in vitro* assay. To investigate this possibility the *in vitro* assays could be repeated in the absence of cytochalasin D, to determine whether the addition of GST-KBPΔ250-81 still reduces network formation to the background baseline level. If this was found to be the case it would indicate that myosin motors do not contribute to tubule movement *in vitro* and the motor(s) inhibited by GST-KBPΔ250-81 is solely responsible for moving BFA-induced tubules in this assay. In a complementary approach *in vivo* studies could be performed in the presence of cytochalasin D, where perhaps more severe effects of microtubule motor inhibition upon BFA-

induced tubule formation may be revealed, although this may prove problematic due to the rounding up of cells.

If an anti-KIF1C antibody which works by immunofluorescence could be identified it would be interesting to determine whether colocalisation with a particular subset of BFA-induced tubules is observed. If KIF1C staining was present on EEA1-positive tubules, but absent from cis-Golgi and TGN tubules, this would support the hypothesis that the motor is specifically involved in moving early endosomal BFA-induced tubules. Similar experiments could be performed using anti-kinesin-1 antibodies to determine whether the motor is localised to a specific subset of BFA-induced tubules.

Doubts remain over the specificity of the GST-KBPΔ250-81 protein *in vitro*. It has been showed that human KBP binds to KIF1Bα between amino acids 270 and 350 located at the C-terminus of the motor domain [51]. Since the KIF1 proteins are extremely homologous within this region it is likely that the interaction with KBP is not limited to KIF1Bα and KIF1C, but extends to all KIF1 isoforms. It is therefore feasible that the inhibitory effect exerted by GST-KBPΔ250-81 *in vitro* is due to perturbation of any of the KIF1 isoforms and not specifically KIF1C. Furthermore, expression at the mRNA level of each of the KIF1 family members has been reported in the human lung epithelial cell lines A549 and NHBE [24], despite the assumption that KIF1A is specifically expressed in neurons [55], indicating they may be ubiquitously expressed. It would be interesting to determine whether other KIF1 isoforms function in moving BFA-induced tubules in HeLaM cells, a scenario which could explain the inconsistencies between the *in vivo* and *in vitro* data. Although preliminary experiments indicate siRNA-mediated depletion of KIF1A or KIF1B either in isolation or in combination has no effect upon the ability of BFA-induced tubules to form, the efficiencies of the knockdowns needs to verified using quantitative PCR or immunoblotting.

Previous studies indicate the speed at which BFA-induced tubules move *in vivo* is much faster to that observed *in vitro*. An average rate of BFA-induced cis-Golgi tubule movement of 0.6 µm per second has been measured in HeLa cells [151], which is considerably faster than the average rate of 0.25 µm per second measured *in vitro* [144]. The reason for this discrepancy is unknown, although it may be linked to the lower temperature at which the *in vitro* assay is performed. Alternatively, this inconsistency may suggest that factors normally act to assist motor activity *in vivo,* which are absent in the *in vitro* situation. It would therefore be interesting to determine whether binding partners of the KIF1 motors differ between the assays which could explain this disparity.

As previously mentioned the tubulation of the Golgi induced by BFA may represent an enhanced version of a constitutive recycling pathway which operates from the Golgi back to the ER. If this is the case it is probable that the motor(s) responsible for moving BFA-induced tubules also functions within this transport pathway. It may therefore prove insightful to investigate whether Golgi tubulation in untreated cells is perturbed when the function of various

kinesin motors, either in isolation or in combination with each other, is disrupted with a particular emphasis on KIF1C. If conditions can be identified under which tubule formation is blocked or reduced, the effects upon cargo movement could be probed further in an attempt to ascertain those cargoes whose retrograde trafficking to the ER is dependent upon Golgi tubulation.

7. Unifying Discussion

Kinesin motors constitute a diverse superfamily of microtubule motors and perform essential functions within the cell, being implicated in the transport of a wide range of cargoes as described in section 1. The concept of regulation of microtubule motor activity is becoming increasingly prevalent as a means of controlling cargo movement and preventing the mislocalisation of motors. The aim of this work was to analyse the function of kinesin motors in two particular settings. Firstly, the regulation of kinesin-1 in a cell cycle-dependent manner was investigated and secondly, the contributions of kinesin-1, kinesin-2 and KIF1C to BFA-induced tubule motility were probed. The reconstitution of microtubule motor-driven cargo motility *in vitro*, by combining fractions enriched in ER or Golgi isolated from rat liver with *Xenopus laevis* egg extract cytosol, formed the basis of this work.

Rat liver ER tubule motility, which has been previously shown to be driven exclusively by kinesin-1 *in vitro* [30], was significantly reduced in mitotic and meiotic *Xenopus laevis* egg extract cytosol. A number of potential scenarios which could potentially underlie this inhibition of cargo movement were investigated and discounted, and the exact mechanism responsible remains elusive. Interestingly, the level of kinesin-1 associated with ER membranes was unchanged between interphase and metaphase, indicating the activity of the motor is modulated whilst membrane-bound. It is hypothesised that the differential interaction of kinesin-1 with a binding partner which has an activating or inhibitory effect upon motor activity occurs specifically in one situation, although this could not be fully investigated due to technical difficulties. This data provides the first evidence that kinesin-1 activity changes during the cell cycle, at least *in vitro*. If such behaviour is replicated *in vivo* it may have far-reaching consequences, and could potentially contribute to changes in organelle positioning and reduction in the flux of cargoes through trafficking pathways which occur during cell division.

BFA is a fungal metabolite which disrupts COPI coat formation leading to perturbation of ER-to-Golgi transport and microtubule-dependent tubulation of several organelles located within the secretory and endocytic pathways. Both kinesin-1 and KIF1C, a member of the kinesin-3 family, have previously been implicated in the movement of BFA-induced tubules [143, 146], although this data has since been contested [144, 147]. Due to the uncertainty regarding the identity of the motor(s) responsible for BFA tubule motility it seemed pertinent to reassess the contributions of kinesin-1, kinesin-2 and KIF1C to this process. KIF1C was found to exclusively drive BFA-induced tubule motility *in vitro*. However, this result was not fully replicated in HeLaM cells, where inhibition of kinesin-1, kinesin-2 or KIF1C through various means was found to have no effect upon BFA-induced tubules derived from the cis-Golgi, TGN, or recycling endosome. The reason for this discrepancy is uncertain, although it is possible that the *in vitro* assay provides a simplified version of the *in vivo* situation. However, the ability of early endosomal tubules to form in response to BFA was found to be affected by inhibition of kinesin-1 and KIF1C. These observations raise the possibility that BFA-induced tubules emanating from particular compartments are moved by specific subsets of motors which perhaps operate in combination with each other, meaning a single motor is not wholly responsible for all tubule

motility. This thinking could explain, at least in part, the conflicting data previously published regarding the involvement of KIF1C in this process.

The discrepancies observed between the *in vivo* and *in vitro* data highlight the concept of cooperation and coordination between motor proteins. In this scenario a cargo is not moved exclusively by a single motor, but multiple motors operate in synergy with each other to drive movement (reviewed in [230]). For example, the activities of kinesin-2 and cytoplasmic dynein-1 are reported to be coordinated on *Xenopus* melanosomes, dependent upon an extracellular signal regulated-kinase pathway [309, 310]. If crosstalk between motors occurs, it is possible that a level of redundancy is in operation meaning the loss or perturbation of a particular motor can be compensated for. This may explain in part the difficulties encountered in replicating the *in vitro* data *in vivo*, and the lack of positive controls for motor inhibition in HeLaM cells. When movement is reconstituted *in vitro,* motor compensation is perhaps not such an issue since a single motor is often exclusively responsible for the motility of a specific cargo. The efficiencies of the dominant negative reagents *in vivo* remain unclear, and the expression of these constructs over 24 hours in cells is in contrast to the *in vitro* assay, where cargo motility was assessed soon after motor inhibition. It is possible that the length of time between motor perturbation and the observation of cargo motility is critical to detect any cargo transport defects. Indeed, a portion of outward ER tubule movement has been shown to be inhibited when observed 4 hours after microinjection of constructs encoding KHCct, whereas 24 hours after transient transfection, the protein had been degraded and no perturbation of ER motility was observed [197]. Similarly, knockdown of KIF1C expression in this study was performed over 72 hours, meaning cells may have the opportunity to compensate and adjust to the loss of the motor. These difficulties make the analysis of cargo transport defects *in vivo* inherently more problematic, and may contribute to the more subtle changes in BFA tubule formation observed in HeLaM cells following inhibition of kinesin motors.

Future studies similar to those undertaken in this work may benefit from various technological improvements. For example, the *in vitro* assay could be developed by attempting to combine rat liver fractions with interphase and metaphase cytosols prepared from rat cells. This would remove the heterogeneity that exists within the current system where rat and *Xenopus laevis* samples are combined. Nevertheless, the *in vitro* assays cannot completely mimic the *in vivo* situation. Studies in which combinations of kinesin motors are depleted simultaneously in cultured cells may provide further insight into how motors cooperate and coordinate with each other, and may reveal further, perhaps unexpected, phenotypes which warrant investigation. Ideally, the effects of kinesin perturbation upon cargo transport in whole animals would also be probed. This approach may involve the manipulation of gene expression in mice or rats, perhaps using gene knockout technology. Whilst it is likely that the perturbation of various kinesin motors simultaneously will prove embryonically lethal, it may still be possible to isolate particular tissues and culture cells derived from these animals. These samples could then be used to provide further insight the contribution of these motors to various processes, including BFA-induced tubule formation and cargo transport during cell division.

References

1. Alberts, B., A. Johnson, J. Lewis, M. Raff, K. Roberts, and P. Walter, *Molecular Biology of the Cell, Fourth Edition*. 2002: Garland Science.

2. Krendel, M. and M.S. Mooseker, *Myosins: tails (and heads) of functional diversity.* Physiology (Bethesda), 2005. **20**: p. 239-51.

3. Helfand, B.T., A. Mikami, R.B. Vallee, and R.D. Goldman, *A requirement for cytoplasmic dynein and dynactin in intermediate filament network assembly and organization.* J Cell Biol, 2002. **157**(5): p. 795-806.

4. Prahlad, V., M. Yoon, R.D. Moir, R.D. Vale, and R.D. Goldman, *Rapid movements of vimentin on microtubule tracks: kinesin-dependent assembly of intermediate filament networks.* J Cell Biol, 1998. **143**(1): p. 159-70.

5. Gyoeva, F.K. and V.I. Gelfand, *Coalignment of vimentin intermediate filaments with microtubules depends on kinesin.* Nature, 1991. **353**(6343): p. 445-8.

6. Howard, J. and A.A. Hyman, *Dynamics and mechanics of the microtubule plus end.* Nature, 2003. **422**(6933): p. 753-8.

7. Zilberman, Y., C. Ballestrem, L. Carramusa, R. Mazitschek, S. Khochbin, and A. Bershadsky, *Regulation of microtubule dynamics by inhibition of the tubulin deacetylase HDAC6.* J Cell Sci, 2009. **122**(Pt 19): p. 3531-41.

8. Joshi, H.C., *Microtubule dynamics in living cells.* Curr Opin Cell Biol, 1998. **10**(1): p. 35-44.

9. Musch, A., *Microtubule organization and function in epithelial cells.* Traffic, 2004. **5**(1): p. 1-9.

10. Stearns, T., L. Evans, and M. Kirschner, *Gamma-tubulin is a highly conserved component of the centrosome.* Cell, 1991. **65**(5): p. 825-36.

11. Rivero, S., J. Cardenas, M. Bornens, and R.M. Rios, *Microtubule nucleation at the cis-side of the Golgi apparatus requires AKAP450 and GM130.* Embo J, 2009. **28**(8): p. 1016-28.

12. Akhmanova, A. and C.C. Hoogenraad, *Microtubule plus-end-tracking proteins: mechanisms and functions.* Curr Opin Cell Biol, 2005. **17**(1): p. 47-54.

13. Miki, H., M. Setou, K. Kaneshiro, and N. Hirokawa, *All kinesin superfamily protein, KIF, genes in mouse and human.* Proc Natl Acad Sci U S A, 2001. **98**(13): p. 7004-11.

14. Hirokawa, N., *Kinesin and dynein superfamily proteins and the mechanism of organelle transport.* Science, 1998. **279**(5350): p. 519-26.

15. Hirokawa, N., Y. Noda, Y. Tanaka, and S. Niwa, *Kinesin superfamily motor proteins and intracellular transport.* Nat Rev Mol Cell Biol, 2009. **10**(10): p. 682-96.

16. Vale, R.D., T.S. Reese, and M.P. Sheetz, *Identification of a novel force-generating protein, kinesin, involved in microtubule-based motility.* Cell, 1985. **42**(1): p. 39-50.

17. Brendza, R.P., L.R. Serbus, J.B. Duffy, and W.M. Saxton, *A function for kinesin I in the posterior transport of oskar mRNA and Staufen protein.* Science, 2000. **289**(5487): p. 2120-2.

18. Tanaka, Y., Y. Kanai, Y. Okada, S. Nonaka, S. Takeda, A. Harada, and N. Hirokawa, *Targeted disruption of mouse conventional kinesin heavy chain, kif5B, results in abnormal perinuclear clustering of mitochondria.* Cell, 1998. **93**(7): p. 1147-58.

19. Asbury, C.L., A.N. Fehr, and S.M. Block, *Kinesin moves by an asymmetric hand-over-hand mechanism.* Science, 2003. **302**(5653): p. 2130-4.

20. Gauger, A.K. and L.S. Goldstein, *The Drosophila kinesin light chain. Primary structure and interaction with kinesin heavy chain.* J Biol Chem, 1993. **268**(18): p. 13657-66.

21. Steinberg, G. and M. Schliwa, *The Neurospora organelle motor: a distant relative of conventional kinesin with unconventional properties.* Mol Biol Cell, 1995. **6**(11): p. 1605-18.

22. Kanai, Y., Y. Okada, Y. Tanaka, A. Harada, S. Terada, and N. Hirokawa, *KIF5C, a novel neuronal kinesin enriched in motor neurons.* J Neurosci, 2000. **20**(17): p. 6374-84.

23. Aizawa, H., Y. Sekine, R. Takemura, Z. Zhang, M. Nangaku, and N. Hirokawa, *Kinesin family in murine central nervous system.* J Cell Biol, 1992. **119**(5): p. 1287-96.

24. Jaulin, F., X. Xue, E. Rodriguez-Boulan, and G. Kreitzer, *Polarization-dependent selective transport to the apical membrane by KIF5B in MDCK cells.* Dev Cell, 2007. **13**(4): p. 511-22.

25. Strausberg, R.L., E.A. Feingold, L.H. Grouse, J.G. Derge, R.D. Klausner, F.S. Collins, L. Wagner, C.M. Shenmen, G.D. Schuler, S.F. Altschul, B. Zeeberg, K.H. Buetow, C.F. Schaefer, N.K. Bhat, R.F. Hopkins, H. Jordan, T. Moore, S.I. Max, J. Wang, F. Hsieh, L. Diatchenko, K. Marusina, A.A. Farmer, G.M. Rubin, L. Hong, M. Stapleton, M.B. Soares, M.F. Bonaldo, T.L. Casavant, T.E. Scheetz, M.J. Brownstein, T.B. Usdin, S. Toshiyuki, P. Carninci, C. Prange, S.S. Raha, N.A. Loquellano, G.J. Peters, R.D. Abramson, S.J. Mullahy, S.A. Bosak, P.J. McEwan, K.J. McKernan, J.A. Malek, P.H. Gunaratne, S. Richards, K.C. Worley, S. Hale, A.M. Garcia, L.J. Gay, S.W. Hulyk, D.K. Villalon, D.M. Muzny, E.J. Sodergren, X. Lu, R.A. Gibbs, J. Fahey, E. Helton, M. Ketteman, A. Madan, S. Rodrigues, A. Sanchez, M. Whiting, A. Madan, A.C. Young, Y. Shevchenko, G.G. Bouffard, R.W. Blakesley, J.W. Touchman, E.D. Green, M.C. Dickson, A.C. Rodriguez, J. Grimwood, J. Schmutz, R.M. Myers, Y.S. Butterfield, M.I. Krzywinski, U. Skalska, D.E. Smailus, A. Schnerch, J.E. Schein, S.J. Jones, and M.A. Marra, *Generation and initial analysis of more than 15,000 full-length human and mouse cDNA sequences.* Proc Natl Acad Sci U S A, 2002. **99**(26): p. 16899-903.

26. Junco, A., B. Bhullar, H.A. Tarnasky, and F.A. van der Hoorn, *Kinesin light-chain KLC3 expression in testis is restricted to spermatids.* Biol Reprod, 2001. **64**(5): p. 1320-30.

27. Rahman, A., D.S. Friedman, and L.S. Goldstein, *Two kinesin light chain genes in mice. Identification and characterization of the encoded proteins.* J Biol Chem, 1998. **273**(25): p. 15395-403.

28. McCart, A.E., D. Mahony, and J.A. Rothnagel, *Alternatively spliced products of the human kinesin light chain 1 (KNS2) gene.* Traffic, 2003. **4**(8): p. 576-80.

29. Khodjakov, A., E.M. Lizunova, A.A. Minin, M.P. Koonce, and F.K. Gyoeva, *A specific light chain of kinesin associates with mitochondria in cultured cells.* Mol Biol Cell, 1998. **9**(2): p. 333-43.

30. Wozniak, M.J. and V.J. Allan, *Cargo selection by specific kinesin light chain 1 isoforms.* Embo J, 2006. **25**(23): p. 5457-68.

31. Gyoeva, F.K., E.M. Bybikova, and A.A. Minin, *An isoform of kinesin light chain specific for the Golgi complex.* J Cell Sci, 2000. **113 (Pt 11)**: p. 2047-54.

32. Cole, D.G., W.Z. Cande, R.J. Baskin, D.A. Skoufias, C.J. Hogan, and J.M. Scholey, *Isolation of a sea urchin egg kinesin-related protein using peptide antibodies.* J Cell Sci, 1992. **101 (Pt 2)**: p. 291-301.

33. Cole, D.G., S.W. Chinn, K.P. Wedaman, K. Hall, T. Vuong, and J.M. Scholey, *Novel heterotrimeric kinesin-related protein purified from sea urchin eggs.* Nature, 1993. **366**(6452): p. 268-70.

34. Brownhill, K., L. Wood, and V. Allan, *Molecular motors and the Golgi complex: staying put and moving through.* Semin Cell Dev Biol, 2009. **20**(7): p. 784-92.

35. Davidovic, L., X.H. Jaglin, A.M. Lepagnol-Bestel, S. Tremblay, M. Simonneau, B. Bardoni, and E.W. Khandjian, *The fragile X mental retardation protein is a molecular adaptor between the neurospecific KIF3C kinesin and dendritic RNA granules.* Hum Mol Genet, 2007. **16**(24): p. 3047-58.

36. Yang, Z., E.A. Roberts, and L.S. Goldstein, *Functional analysis of mouse kinesin motor Kif3C.* Mol Cell Biol, 2001. **21**(16): p. 5306-11.

37. Takeda, S., H. Yamazaki, D.H. Seog, Y. Kanai, S. Terada, and N. Hirokawa, *Kinesin superfamily protein 3 (KIF3) motor transports fodrin-associating vesicles important for neurite building.* J Cell Biol, 2000. **148**(6): p. 1255-65.

38. Berezuk, M.A. and T.A. Schroer, *Dynactin enhances the processivity of kinesin-2.* Traffic, 2007. **8**(2): p. 124-9.

39. Jimbo, T., Y. Kawasaki, R. Koyama, R. Sato, S. Takada, K. Haraguchi, and T. Akiyama, *Identification of a link between the tumour suppressor APC and the kinesin superfamily.* Nat Cell Biol, 2002. **4**(4): p. 323-7.

40. Yamazaki, H., T. Nakata, Y. Okada, and N. Hirokawa, *Cloning and characterization of KAP3: a novel kinesin superfamily-associated protein of KIF3A/3B.* Proc Natl Acad Sci U S A, 1996. **93**(16): p. 8443-8.

41. Signor, D., K.P. Wedaman, L.S. Rose, and J.M. Scholey, *Two heteromeric kinesin complexes in chemosensory neurons and sensory cilia of Caenorhabditis elegans.* Mol Biol Cell, 1999. **10**(2): p. 345-60.

42. Setou, M., T. Nakagawa, D.H. Seog, and N. Hirokawa, *Kinesin superfamily motor protein KIF17 and mLin-10 in NMDA receptor-containing vesicle transport.* Science, 2000. **288**(5472): p. 1796-802.

43. Wong, R.W., M. Setou, J. Teng, Y. Takei, and N. Hirokawa, *Overexpression of motor protein KIF17 enhances spatial and working memory in transgenic mice.* Proc Natl Acad Sci U S A, 2002. **99**(22): p. 14500-5.

44. Nonaka, S., Y. Tanaka, Y. Okada, S. Takeda, A. Harada, Y. Kanai, M. Kido, and N. Hirokawa, *Randomization of left-right asymmetry due to loss of nodal cilia generating leftward flow of extraembryonic fluid in mice lacking KIF3B motor protein.* Cell, 1998. **95**(6): p. 829-37.

45. Takeda, S., Y. Yonekawa, Y. Tanaka, Y. Okada, S. Nonaka, and N. Hirokawa, *Left-right asymmetry and kinesin superfamily protein KIF3A: new insights in determination of laterality and mesoderm induction by kif3A-/- mice analysis.* J Cell Biol, 1999. **145**(4): p. 825-36.

46. Teng, J., T. Rai, Y. Tanaka, Y. Takei, T. Nakata, M. Hirasawa, A.B. Kulkarni, and N. Hirokawa, *The KIF3 motor transports N-cadherin and organizes the developing neuroepithelium.* Nat Cell Biol, 2005. **7**(5): p. 474-82.

47. Marszalek, J.R., X. Liu, E.A. Roberts, D. Chui, J.D. Marth, D.S. Williams, and L.S. Goldstein, *Genetic evidence for selective transport of opsin and arrestin by kinesin-II in mammalian photoreceptors.* Cell, 2000. **102**(2): p. 175-87.

48. Otsuka, A.J., A. Jeyaprakash, J. Garcia-Anoveros, L.Z. Tang, G. Fisk, T. Hartshorne, R. Franco, and T. Born, *The C. elegans unc-104 gene encodes a putative kinesin heavy chain-like protein.* Neuron, 1991. **6**(1): p. 113-22.

49. Matsushita, M., R. Yamamoto, K. Mitsui, and H. Kanazawa, *Altered motor activity of alternative splice variants of the mammalian kinesin-3 protein KIF1B.* Traffic, 2009. **10**(11): p. 1647-54.

50. Nangaku, M., R. Sato-Yoshitake, Y. Okada, Y. Noda, R. Takemura, H. Yamazaki, and N. Hirokawa, *KIF1B, a novel microtubule plus end-directed monomeric motor protein for transport of mitochondria.* Cell, 1994. **79**(7): p. 1209-20.

51. Wozniak, M.J., M. Melzer, C. Dorner, H.U. Haring, and R. Lammers, *The novel protein KBP regulates mitochondria localization by interaction with a kinesin-like protein.* BMC Cell Biol, 2005. **6**: p. 35.

52. Lyons, D.A., S.G. Naylor, S. Mercurio, C. Dominguez, and W.S. Talbot, *KBP is essential for axonal structure, outgrowth and maintenance in zebrafish, providing insight into the cellular basis of Goldberg-Shprintzen syndrome.* Development, 2008. **135**(3): p. 599-608.

53. Zhao, C., J. Takita, Y. Tanaka, M. Setou, T. Nakagawa, S. Takeda, H.W. Yang, S. Terada, T. Nakata, Y. Takei, M. Saito, S. Tsuji, Y. Hayashi, and N. Hirokawa, *Charcot-Marie-Tooth disease type 2A caused by mutation in a microtubule motor KIF1Bbeta.* Cell, 2001. **105**(5): p. 587-97.

54. Matsushita, M., S. Tanaka, N. Nakamura, H. Inoue, and H. Kanazawa, *A novel kinesin-like protein, KIF1Bbeta3 is involved in the movement of lysosomes to the cell periphery in non-neuronal cells.* Traffic, 2004. **5**(3): p. 140-51.

55. Okada, Y., H. Yamazaki, Y. Sekine-Aizawa, and N. Hirokawa, *The neuron-specific kinesin superfamily protein KIF1A is a unique monomeric motor for anterograde axonal transport of synaptic vesicle precursors.* Cell, 1995. **81**(5): p. 769-80.

56. Yonekawa, Y., A. Harada, Y. Okada, T. Funakoshi, Y. Kanai, Y. Takei, S. Terada, T. Noda, and N. Hirokawa, *Defect in synaptic vesicle precursor transport and neuronal cell death in KIF1A motor protein-deficient mice.* J Cell Biol, 1998. **141**(2): p. 431-41.

57. Klopfenstein, D.R. and R.D. Vale, *The lipid binding pleckstrin homology domain in UNC-104 kinesin is necessary for synaptic vesicle transport in Caenorhabditis elegans.* Mol Biol Cell, 2004. **15**(8): p. 3729-39.

58. Klopfenstein, D.R., M. Tomishige, N. Stuurman, and R.D. Vale, *Role of phosphatidylinositol(4,5)bisphosphate organization in membrane transport by the Unc104 kinesin motor.* Cell, 2002. **109**(3): p. 347-58.

59. Tomishige, M., D.R. Klopfenstein, and R.D. Vale, *Conversion of Unc104/KIF1A kinesin into a processive motor after dimerization.* Science, 2002. **297**(5590): p. 2263-7.

60. Zhou, H.M., I. Brust-Mascher, and J.M. Scholey, *Direct visualization of the movement of the monomeric axonal transport motor UNC-104 along neuronal processes in living Caenorhabditis elegans.* J Neurosci, 2001. **21**(11): p. 3749-55.

61. Hammond, J.W., D. Cai, T.L. Blasius, Z. Li, Y. Jiang, G.T. Jih, E. Meyhofer, and K.J. Verhey, *Mammalian Kinesin-3 motors are dimeric in vivo and move by processive motility upon release of autoinhibition.* PLoS Biol, 2009. **7**(3): p. e72.

62. Okada, Y. and N. Hirokawa, *A processive single-headed motor: kinesin superfamily protein KIF1A.* Science, 1999. **283**(5405): p. 1152-7.

63. Horiguchi, K., T. Hanada, Y. Fukui, and A.H. Chishti, *Transport of PIP3 by GAKIN, a kinesin-3 family protein, regulates neuronal cell polarity.* J Cell Biol, 2006. **174**(3): p. 425-36.

64. Zhu, C., J. Zhao, M. Bibikova, J.D. Leverson, E. Bossy-Wetzel, J.B. Fan, R.T. Abraham, and W. Jiang, *Functional analysis of human microtubule-based motor proteins, the kinesins and dyneins, in mitosis/cytokinesis using RNA interference.* Mol Biol Cell, 2005. **16**(7): p. 3187-99.

65. Gruneberg, U., R. Neef, X. Li, E.H. Chan, R.B. Chalamalasetty, E.A. Nigg, and F.A. Barr, *KIF14 and citron kinase act together to promote efficient cytokinesis.* J Cell Biol, 2006. **172**(3): p. 363-72.

66. Hoepfner, S., F. Severin, A. Cabezas, B. Habermann, A. Runge, D. Gillooly, H. Stenmark, and M. Zerial, *Modulation of receptor recycling and degradation by the endosomal kinesin KIF16B.* Cell, 2005. **121**(3): p. 437-50.

67. Imamula, K., T. Kon, R. Ohkura, and K. Sutoh, *The coordination of cyclic microtubule association/dissociation and tail swing of cytoplasmic dynein.* Proc Natl Acad Sci U S A, 2007. **104**(41): p. 16134-9.

68. Kon, T., T. Mogami, R. Ohkura, M. Nishiura, and K. Sutoh, *ATP hydrolysis cycle-dependent tail motions in cytoplasmic dynein.* Nat Struct Mol Biol, 2005. **12**(6): p. 513-9.

69. Gee, M.A., J.E. Heuser, and R.B. Vallee, *An extended microtubule-binding structure within the dynein motor domain.* Nature, 1997. **390**(6660): p. 636-9.

70. Vale, R.D., *The molecular motor toolbox for intracellular transport.* Cell, 2003. **112**(4): p. 467-80.

71. Wozniak, M.J. and V.J. Allan, *Carrier Motility*, in *Trafficking Inside Cells: Pathways, Mechanisms and Regulation*, N. Segev, Editor. 2009.

72. Kardon, J.R. and R.D. Vale, *Regulators of the cytoplasmic dynein motor.* Nat Rev Mol Cell Biol, 2009. **10**(12): p. 854-65.

73. Gill, S.R., T.A. Schroer, I. Szilak, E.R. Steuer, M.P. Sheetz, and D.W. Cleveland, *Dynactin, a conserved, ubiquitously expressed component of an activator of vesicle motility mediated by cytoplasmic dynein.* J Cell Biol, 1991. **115**(6): p. 1639-50.

74. Burkhardt, J.K., C.J. Echeverri, T. Nilsson, and R.B. Vallee, *Overexpression of the dynamitin (p50) subunit of the dynactin complex disrupts dynein-dependent maintenance of membrane organelle distribution.* J Cell Biol, 1997. **139**(2): p. 469-84.

75. King, S.J., C.L. Brown, K.C. Maier, N.J. Quintyne, and T.A. Schroer, *Analysis of the dynein-dynactin interaction in vitro and in vivo.* Mol Biol Cell, 2003. **14**(12): p. 5089-97.

76. Holleran, E.A., M.K. Tokito, S. Karki, and E.L. Holzbaur, *Centractin (ARP1) associates with spectrin revealing a potential mechanism to link dynactin to intracellular organelles.* J Cell Biol, 1996. **135**(6 Pt 2): p. 1815-29.

77. King, S.J. and T.A. Schroer, *Dynactin increases the processivity of the cytoplasmic dynein motor.* Nat Cell Biol, 2000. **2**(1): p. 20-4.

78. Culver-Hanlon, T.L., S.A. Lex, A.D. Stephens, N.J. Quintyne, and S.J. King, *A microtubule-binding domain in dynactin increases dynein processivity by skating along microtubules.* Nat Cell Biol, 2006. **8**(3): p. 264-70.

79. Haghnia, M., V. Cavalli, S.B. Shah, K. Schimmelpfeng, R. Brusch, G. Yang, C. Herrera, A. Pilling, and L.S. Goldstein, *Dynactin is required for coordinated bidirectional motility, but not for dynein membrane attachment.* Mol Biol Cell, 2007. **18**(6): p. 2081-9.

80. Kim, H., S.C. Ling, G.C. Rogers, C. Kural, P.R. Selvin, S.L. Rogers, and V.I. Gelfand, *Microtubule binding by dynactin is required for microtubule organization but not cargo transport.* J Cell Biol, 2007. **176**(5): p. 641-51.

81. Colin, E., D. Zala, G. Liot, H. Rangone, M. Borrell-Pages, X.J. Li, F. Saudou, and S. Humbert, *Huntingtin phosphorylation acts as a molecular switch for anterograde/retrograde transport in neurons.* Embo J, 2008. **27**(15): p. 2124-34.

82. Uteng, M., C. Hentrich, K. Miura, P. Bieling, and T. Surrey, *Poleward transport of Eg5 by dynein-dynactin in Xenopus laevis egg extract spindles.* J Cell Biol, 2008. **182**(4): p. 715-26.

83. Ligon, L.A., M. Tokito, J.M. Finklestein, F.E. Grossman, and E.L. Holzbaur, *A direct interaction between cytoplasmic dynein and kinesin I may coordinate motor activity.* J Biol Chem, 2004. **279**(18): p. 19201-8.

84. Lee, K.D. and P.J. Hollenbeck, *Phosphorylation of kinesin in vivo correlates with organelle association and neurite outgrowth.* J Biol Chem, 1995. **270**(10): p. 5600-5.

85. Tsai, M.Y., G. Morfini, G. Szebenyi, and S.T. Brady, *Release of kinesin from vesicles by hsc70 and regulation of fast axonal transport.* Mol Biol Cell, 2000. **11**(6): p. 2161-73.

86. Morfini, G., G. Szebenyi, R. Elluru, N. Ratner, and S.T. Brady, *Glycogen synthase kinase 3 phosphorylates kinesin light chains and negatively regulates kinesin-based motility.* Embo J, 2002. **21**(3): p. 281-93.

87. Addinall, S.G., P.S. Mayr, S. Doyle, J.K. Sheehan, P.G. Woodman, and V.J. Allan, *Phosphorylation by cdc2-CyclinB1 kinase releases cytoplasmic dynein from membranes.* J Biol Chem, 2001. **276**(19): p. 15939-44.

88. Dell, K.R., C.W. Turck, and R.D. Vale, *Mitotic phosphorylation of the dynein light intermediate chain is mediated by cdc2 kinase.* Traffic, 2000. **1**(1): p. 38-44.

89. Niclas, J., V.J. Allan, and R.D. Vale, *Cell cycle regulation of dynein association with membranes modulates microtubule-based organelle transport.* J Cell Biol, 1996. **133**(3): p. 585-93.

90. Ichimura, T., A. Wakamiya-Tsuruta, C. Itagaki, M. Taoka, T. Hayano, T. Natsume, and T. Isobe, *Phosphorylation-dependent interaction of kinesin light chain 2 and the 14-3-3 protein.* Biochemistry, 2002. **41**(17): p. 5566-72.

91. Donelan, M.J., G. Morfini, R. Julyan, S. Sommers, L. Hays, H. Kajio, I. Briaud, R.A. Easom, J.D. Molkentin, S.T. Brady, and C.J. Rhodes, *Ca2+-dependent dephosphorylation of kinesin heavy chain on beta-granules in pancreatic beta-cells. Implications for regulated beta-granule transport and insulin exocytosis.* J Biol Chem, 2002. **277**(27): p. 24232-42.

92. De Vos, K., V. Goossens, E. Boone, D. Vercammen, K. Vancompernolle, P. Vandenabeele, G. Haegeman, W. Fiers, and J. Grooten, *The 55-kDa tumor necrosis factor receptor induces clustering of mitochondria through its membrane-proximal region.* J Biol Chem, 1998. **273**(16): p. 9673-80.

93. De Vos, K., F. Severin, F. Van Herreweghe, K. Vancompernolle, V. Goossens, A. Hyman, and J. Grooten, *Tumor necrosis factor induces hyperphosphorylation of kinesin light chain and inhibits kinesin-mediated transport of mitochondria.* J Cell Biol, 2000. **149**(6): p. 1207-14.

94. Cuchillo-Ibanez, I., A. Seereeram, H.L. Byers, K.Y. Leung, M.A. Ward, B.H. Anderton, and D.P. Hanger, *Phosphorylation of tau regulates its axonal transport by controlling its binding to kinesin.* Faseb J, 2008. **22**(9): p. 3186-95.

95. Glater, E.E., L.J. Megeath, R.S. Stowers, and T.L. Schwarz, *Axonal transport of mitochondria requires milton to recruit kinesin heavy chain and is light chain independent.* J Cell Biol, 2006. **173**(4): p. 545-57.

96. Wang, X. and T.L. Schwarz, *The mechanism of Ca2+ -dependent regulation of kinesin-mediated mitochondrial motility.* Cell, 2009. **136**(1): p. 163-74.

97. Macaskill, A.F., J.E. Rinholm, A.E. Twelvetrees, I.L. Arancibia-Carcamo, J. Muir, A. Fransson, P. Aspenstrom, D. Attwell, and J.T. Kittler, *Miro1 is a calcium sensor for glutamate receptor-dependent localization of mitochondria at synapses.* Neuron, 2009. **61**(4): p. 541-55.

98. Brickley, K., M.J. Smith, M. Beck, and F.A. Stephenson, *GRIF-1 and OIP106, members of a novel gene family of coiled-coil domain proteins: association in vivo and in vitro with kinesin.* J Biol Chem, 2005. **280**(15): p. 14723-32.

99. Hisanaga, S., H. Murofushi, K. Okuhara, R. Sato, Y. Masuda, H. Sakai, and N. Hirokawa, *The molecular structure of adrenal medulla kinesin.* Cell Motil Cytoskeleton, 1989. **12**(4): p. 264-72.

100. Hackney, D.D., J.D. Levitt, and J. Suhan, *Kinesin undergoes a 9 S to 6 S conformational transition.* J Biol Chem, 1992. **267**(12): p. 8696-701.

101. Coy, D.L., W.O. Hancock, M. Wagenbach, and J. Howard, *Kinesin's tail domain is an inhibitory regulator of the motor domain.* Nat Cell Biol, 1999. **1**(5): p. 288-92.

102. Cai, D., A.D. Hoppe, J.A. Swanson, and K.J. Verhey, *Kinesin-1 structural organization and conformational changes revealed by FRET stoichiometry in live cells.* J Cell Biol, 2007. **176**(1): p. 51-63.

103. Blasius, T.L., D. Cai, G.T. Jih, C.P. Toret, and K.J. Verhey, *Two binding partners cooperate to activate the molecular motor Kinesin-1.* J Cell Biol, 2007. **176**(1): p. 11-7.

104. Lanza, D.C., J.C. Silva, E.M. Assmann, A.J. Quaresma, G.C. Bressan, I.L. Torriani, and J. Kobarg, *Human FEZ1 has characteristics of a natively unfolded protein and dimerizes in solution.* Proteins, 2009. **74**(1): p. 104-21.

105. Stenmark, H., *Rab GTPases as coordinators of vesicle traffic.* Nat Rev Mol Cell Biol, 2009. **10**(8): p. 513-25.

106. Echard, A., F. Jollivet, O. Martinez, J.J. Lacapere, A. Rousselet, I. Janoueix-Lerosey, and B. Goud, *Interaction of a Golgi-associated kinesin-like protein with Rab6.* Science, 1998. **279**(5350): p. 580-5.

107. Martinez, O., A. Schmidt, J. Salamero, B. Hoflack, M. Roa, and B. Goud, *The small GTP-binding protein rab6 functions in intra-Golgi transport.* J Cell Biol, 1994. **127**(6 Pt 1): p. 1575-88.

108. Fontijn, R.D., B. Goud, A. Echard, F. Jollivet, J. van Marle, H. Pannekoek, and A.J. Horrevoets, *The human kinesin-like protein RB6K is under tight cell cycle control and is essential for cytokinesis.* Mol Cell Biol, 2001. **21**(8): p. 2944-55.

109. Hill, E., M. Clarke, and F.A. Barr, *The Rab6-binding kinesin, Rab6-KIFL, is required for cytokinesis.* Embo J, 2000. **19**(21): p. 5711-9.

110. Johansson, M., N. Rocha, W. Zwart, I. Jordens, L. Janssen, C. Kuijl, V.M. Olkkonen, and J. Neefjes, *Activation of endosomal dynein motors by stepwise assembly of Rab7-RILP-p150Glued, ORP1L, and the receptor betalll spectrin.* J Cell Biol, 2007. **176**(4): p. 459-71.

111. Jordens, I., M. Fernandez-Borja, M. Marsman, S. Dusseljee, L. Janssen, J. Calafat, H. Janssen, R. Wubbolts, and J. Neefjes, *The Rab7 effector protein RILP controls*

lysosomal transport by inducing the recruitment of dynein-dynactin motors. Curr Biol, 2001. **11**(21): p. 1680-5.

112. Matanis, T., A. Akhmanova, P. Wulf, E. Del Nery, T. Weide, T. Stepanova, N. Galjart, F. Grosveld, B. Goud, C.I. De Zeeuw, A. Barnekow, and C.C. Hoogenraad, *Bicaudal-D regulates COPI-independent Golgi-ER transport by recruiting the dynein-dynactin motor complex.* Nat Cell Biol, 2002. **4**(12): p. 986-92.

113. Reed, N.A., D. Cai, T.L. Blasius, G.T. Jih, E. Meyhofer, J. Gaertig, and K.J. Verhey, *Microtubule acetylation promotes kinesin-1 binding and transport.* Curr Biol, 2006. **16**(21): p. 2166-72.

114. Liao, G. and G.G. Gundersen, *Kinesin is a candidate for cross-bridging microtubules and intermediate filaments. Selective binding of kinesin to detyrosinated tubulin and vimentin.* J Biol Chem, 1998. **273**(16): p. 9797-803.

115. Dunn, S., E.E. Morrison, T.B. Liverpool, C. Molina-Paris, R.A. Cross, M.C. Alonso, and M. Peckham, *Differential trafficking of Kif5c on tyrosinated and detyrosinated microtubules in live cells.* J Cell Sci, 2008. **121**(Pt 7): p. 1085-95.

116. Tokuraku, K., T.Q. Noguchi, M. Nishie, K. Matsushima, and S. Kotani, *An isoform of microtubule-associated protein 4 inhibits kinesin-driven microtubule gliding.* J Biochem, 2007. **141**(4): p. 585-91.

117. Dixit, R., J.L. Ross, Y.E. Goldman, and E.L. Holzbaur, *Differential regulation of dynein and kinesin motor proteins by tau.* Science, 2008. **319**(5866): p. 1086-9.

118. Masson, D. and T.E. Kreis, *Binding of E-MAP-115 to microtubules is regulated by cell cycle-dependent phosphorylation.* J Cell Biol, 1995. **131**(4): p. 1015-24.

119. Sung, H.H., I.A. Telley, P. Papadaki, A. Ephrussi, T. Surrey, and P. Rorth, *Drosophila ensconsin promotes productive recruitment of Kinesin-1 to microtubules.* Dev Cell, 2008. **15**(6): p. 866-76.

120. Scales, S.J., R. Pepperkok, and T.E. Kreis, *Visualization of ER-to-Golgi transport in living cells reveals a sequential mode of action for COPII and COPI.* Cell, 1997. **90**(6): p. 1137-48.

121. Stephens, D.J. and R. Pepperkok, *Imaging of procollagen transport reveals COPI-dependent cargo sorting during ER-to-Golgi transport in mammalian cells.* J Cell Sci, 2002. **115**(Pt 6): p. 1149-60.

122. Presley, J.F., N.B. Cole, T.A. Schroer, K. Hirschberg, K.J. Zaal, and J. Lippincott-Schwartz, *ER-to-Golgi transport visualized in living cells.* Nature, 1997. **389**(6646): p. 81-5.

123. Watson, P., R. Forster, K.J. Palmer, R. Pepperkok, and D.J. Stephens, *Coupling of ER exit to microtubules through direct interaction of COPII with dynactin.* Nat Cell Biol, 2005. **7**(1): p. 48-55.

124. Gupta, V., K.J. Palmer, P. Spence, A. Hudson, and D.J. Stephens, *Kinesin-1 (uKHC/KIF5B) is required for bidirectional motility of ER exit sites and efficient ER-to-Golgi transport.* Traffic, 2008. **9**(11): p. 1850-66.

125. Chen, J.L., R.V. Fucini, L. Lacomis, H. Erdjument-Bromage, P. Tempst, and M. Stamnes, *Coatomer-bound Cdc42 regulates dynein recruitment to COPI vesicles.* J Cell Biol, 2005. **169**(3): p. 383-9.

126. Aridor, M., K.N. Fish, S. Bannykh, J. Weissman, T.H. Roberts, J. Lippincott-Schwartz, and W.E. Balch, *The Sar1 GTPase coordinates biosynthetic cargo selection with endoplasmic reticulum export site assembly.* J Cell Biol, 2001. **152**(1): p. 213-29.

127. Stauber, T., J.C. Simpson, R. Pepperkok, and I. Vernos, *A role for kinesin-2 in COPI-dependent recycling between the ER and the Golgi complex.* Curr Biol, 2006. **16**(22): p. 2245-51.

128. Stephens, D.J., N. Lin-Marq, A. Pagano, R. Pepperkok, and J.P. Paccaud, *COPI-coated ER-to-Golgi transport complexes segregate from COPII in close proximity to ER exit sites.* J Cell Sci, 2000. **113 (Pt 12)**: p. 2177-85.

129. Shima, D.T., S.J. Scales, T.E. Kreis, and R. Pepperkok, *Segregation of COPI-rich and anterograde-cargo-rich domains in endoplasmic-reticulum-to-Golgi transport complexes.* Curr Biol, 1999. **9**(15): p. 821-4.

130. Girod, A., B. Storrie, J.C. Simpson, L. Johannes, B. Goud, L.M. Roberts, J.M. Lord, T. Nilsson, and R. Pepperkok, *Evidence for a COP-I-independent transport route from the Golgi complex to the endoplasmic reticulum.* Nat Cell Biol, 1999. **1**(7): p. 423-30.

131. Short, B., C. Preisinger, J. Schaletzky, R. Kopajtich, and F.A. Barr, *The Rab6 GTPase regulates recruitment of the dynactin complex to Golgi membranes.* Curr Biol, 2002. **12**(20): p. 1792-5.

132. Hoogenraad, C.C., A. Akhmanova, S.A. Howell, B.R. Dortland, C.I. De Zeeuw, R. Willemsen, P. Visser, F. Grosveld, and N. Galjart, *Mammalian Golgi-associated Bicaudal-D2 functions in the dynein-dynactin pathway by interacting with these complexes.* Embo J, 2001. **20**(15): p. 4041-54.

133. Grigoriev, I., D. Splinter, N. Keijzer, P.S. Wulf, J. Demmers, T. Ohtsuka, M. Modesti, I.V. Maly, F. Grosveld, C.C. Hoogenraad, and A. Akhmanova, *Rab6 regulates transport and targeting of exocytotic carriers.* Dev Cell, 2007. **13**(2): p. 305-14.

134. Misumi, Y., Y. Misumi, K. Miki, A. Takatsuki, G. Tamura, and Y. Ikehara, *Novel blockade by brefeldin A of intracellular transport of secretory proteins in cultured rat hepatocytes.* J Biol Chem, 1986. **261**(24): p. 11398-403.

135. Tooze, J. and M. Hollinshead, *In AtT20 and HeLa cells brefeldin A induces the fusion of tubular endosomes and changes their distribution and some of their endocytic properties.* J Cell Biol, 1992. **118**(4): p. 813-30.

136. Lippincott-Schwartz, J., L. Yuan, C. Tipper, M. Amherdt, L. Orci, and R.D. Klausner, *Brefeldin A's effects on endosomes, lysosomes, and the TGN suggest a general mechanism for regulating organelle structure and membrane traffic.* Cell, 1991. **67**(3): p. 601-16.

137. Ladinsky, M.S. and K.E. Howell, *The trans-Golgi network can be dissected structurally and functionally from the cisternae of the Golgi complex by brefeldin A.* Eur J Cell Biol, 1992. **59**(1): p. 92-105.

138. Lippincott-Schwartz, J., J.G. Donaldson, A. Schweizer, E.G. Berger, H.P. Hauri, L.C. Yuan, and R.D. Klausner, *Microtubule-dependent retrograde transport of proteins into the ER in the presence of brefeldin A suggests an ER recycling pathway.* Cell, 1990. **60**(5): p. 821-36.

139. Wood, S.A. and W.J. Brown, *The morphology but not the function of endosomes and lysosomes is altered by brefeldin A.* J Cell Biol, 1992. **119**(2): p. 273-85.

140. Lippincott-Schwartz, J., L.C. Yuan, J.S. Bonifacino, and R.D. Klausner, *Rapid redistribution of Golgi proteins into the ER in cells treated with brefeldin A: evidence for membrane cycling from Golgi to ER.* Cell, 1989. **56**(5): p. 801-13.

141. Wood, S.A., J.E. Park, and W.J. Brown, *Brefeldin A causes a microtubule-mediated fusion of the trans-Golgi network and early endosomes.* Cell, 1991. **67**(3): p. 591-600.

142. Niu, T.K., A.C. Pfeifer, J. Lippincott-Schwartz, and C.L. Jackson, *Dynamics of GBF1, a Brefeldin A-sensitive Arf1 exchange factor at the Golgi.* Mol Biol Cell, 2005. **16**(3): p. 1213-22.

143. Lippincott-Schwartz, J., N.B. Cole, A. Marotta, P.A. Conrad, and G.S. Bloom, *Kinesin is the motor for microtubule-mediated Golgi-to-ER membrane traffic.* J Cell Biol, 1995. **128**(3): p. 293-306.

144. Robertson, A.M. and V.J. Allan, *Brefeldin A-dependent membrane tubule formation reconstituted in vitro is driven by a cell cycle-regulated microtubule motor.* Mol Biol Cell, 2000. **11**(3): p. 941-55.

145. Feiguin, F., A. Ferreira, K.S. Kosik, and A. Caceres, *Kinesin-mediated organelle translocation revealed by specific cellular manipulations.* J Cell Biol, 1994. **127**(4): p. 1021-39.

146. Dorner, C., T. Ciossek, S. Muller, P.H. Moller, A. Ullrich, and R. Lammers, *Characterization of KIF1C, a new kinesin-like protein involved in vesicle transport from the Golgi apparatus to the endoplasmic reticulum.* J Biol Chem, 1998. **273**(32): p. 20267-75.

147. Nakajima, K., Y. Takei, Y. Tanaka, T. Nakagawa, T. Nakata, Y. Noda, M. Setou, and N. Hirokawa, *Molecular motor KIF1C is not essential for mouse survival and motor-dependent retrograde Golgi apparatus-to-endoplasmic reticulum transport.* Mol Cell Biol, 2002. **22**(3): p. 866-73.

148. Shen, X., V. Meza-Carmen, E. Puxeddu, G. Wang, J. Moss, and M. Vaughan, *Interaction of brefeldin A-inhibited guanine nucleotide-exchange protein (BIG) 1 and kinesin motor protein KIF21A.* Proc Natl Acad Sci U S A, 2008. **105**(48): p. 18788-93.

149. Marszalek, J.R., J.A. Weiner, S.J. Farlow, J. Chun, and L.S. Goldstein, *Novel dendritic kinesin sorting identified by different process targeting of two related kinesins: KIF21A and KIF21B.* J Cell Biol, 1999. **145**(3): p. 469-79.

150. Duran, J.M., F. Valderrama, S. Castel, J. Magdalena, M. Tomas, H. Hosoya, J. Renau-Piqueras, V. Malhotra, and G. Egea, *Myosin motors and not actin comets are mediators of the actin-based Golgi-to-endoplasmic reticulum protein transport.* Mol Biol Cell, 2003. **14**(2): p. 445-59.

151. Sciaky, N., J. Presley, C. Smith, K.J. Zaal, N. Cole, J.E. Moreira, M. Terasaki, E. Siggia, and J. Lippincott-Schwartz, *Golgi tubule traffic and the effects of brefeldin A visualized in living cells.* J Cell Biol, 1997. **139**(5): p. 1137-55.

152. Nakagawa, T., M. Setou, D. Seog, K. Ogasawara, N. Dohmae, K. Takio, and N. Hirokawa, *A novel motor, KIF13A, transports mannose-6-phosphate receptor to plasma membrane through direct interaction with AP-1 complex.* Cell, 2000. **103**(4): p. 569-81.

153. Schmidt, M.R., T. Maritzen, V. Kukhtina, V.A. Higman, L. Doglio, N.N. Barak, H. Strauss, H. Oschkinat, C.G. Dotti, and V. Haucke, *Regulation of endosomal membrane traffic by a Gadkin/AP-1/kinesin KIF5 complex.* Proc Natl Acad Sci U S A, 2009. **106**(36): p. 15344-9.

154. Ikonen, E., R.G. Parton, F. Lafont, and K. Simons, *Analysis of the role of p200-containing vesicles in post-Golgi traffic.* Mol Biol Cell, 1996. **7**(6): p. 961-74.

155. Musch, A., D. Cohen, and E. Rodriguez-Boulan, *Myosin II is involved in the production of constitutive transport vesicles from the TGN.* J Cell Biol, 1997. **138**(2): p. 291-306.

156. Sahlender, D.A., R.C. Roberts, S.D. Arden, G. Spudich, M.J. Taylor, J.P. Luzio, J. Kendrick-Jones, and F. Buss, *Optineurin links myosin VI to the Golgi complex and is involved in Golgi organization and exocytosis.* J Cell Biol, 2005. **169**(2): p. 285-95.

157. Warner, C.L., A. Stewart, J.P. Luzio, K.P. Steel, R.T. Libby, J. Kendrick-Jones, and F. Buss, *Loss of myosin VI reduces secretion and the size of the Golgi in fibroblasts from Snell's waltzer mice.* Embo J, 2003. **22**(3): p. 569-79.

158. Varadi, A., E.K. Ainscow, V.J. Allan, and G.A. Rutter, *Involvement of conventional kinesin in glucose-stimulated secretory granule movements and exocytosis in clonal pancreatic beta-cells.* J Cell Sci, 2002. **115**(Pt 21): p. 4177-89.

159. Desnos, C., S. Huet, I. Fanget, C. Chapuis, C. Bottiger, V. Racine, J.B. Sibarita, J.P. Henry, and F. Darchen, *Myosin va mediates docking of secretory granules at the plasma membrane.* J Neurosci, 2007. **27**(39): p. 10636-45.

160. Wozniak, M.J., R. Milner, and V. Allan, *N-terminal kinesins: many and various.* Traffic, 2004. **5**(6): p. 400-10.

161. Verhey, K.J., D. Meyer, R. Deehan, J. Blenis, B.J. Schnapp, T.A. Rapoport, and B. Margolis, *Cargo of kinesin identified as JIP scaffolding proteins and associated signaling molecules.* J Cell Biol, 2001. **152**(5): p. 959-70.

162. Setou, M., D.H. Seog, Y. Tanaka, Y. Kanai, Y. Takei, M. Kawagishi, and N. Hirokawa, *Glutamate-receptor-interacting protein GRIP1 directly steers kinesin to dendrites.* Nature, 2002. **417**(6884): p. 83-7.

163. Lafont, F., J.K. Burkhardt, and K. Simons, *Involvement of microtubule motors in basolateral and apical transport in kidney cells.* Nature, 1994. **372**(6508): p. 801-3.

164. Noda, Y., Y. Okada, N. Saito, M. Setou, Y. Xu, Z. Zhang, and N. Hirokawa, *KIFC3, a microtubule minus end-directed motor for the apical transport of annexin XIIIb-associated Triton-insoluble membranes.* J Cell Biol, 2001. **155**(1): p. 77-88.

165. Merrifield, C.J., M.E. Feldman, L. Wan, and W. Almers, *Imaging actin and dynamin recruitment during invagination of single clathrin-coated pits.* Nat Cell Biol, 2002. **4**(9): p. 691-8.

166. Morris, S.M., S.D. Arden, R.C. Roberts, J. Kendrick-Jones, J.A. Cooper, J.P. Luzio, and F. Buss, *Myosin VI binds to and localises with Dab2, potentially linking receptor-mediated endocytosis and the actin cytoskeleton.* Traffic, 2002. **3**(5): p. 331-41.

167. Driskell, O.J., A. Mironov, V.J. Allan, and P.G. Woodman, *Dynein is required for receptor sorting and the morphogenesis of early endosomes.* Nat Cell Biol, 2007. **9**(1): p. 113-20.

168. Lapierre, L.A., R. Kumar, C.M. Hales, J. Navarre, S.G. Bhartur, J.O. Burnette, D.W. Provance, Jr., J.A. Mercer, M. Bahler, and J.R. Goldenring, *Myosin vb is associated with plasma membrane recycling systems.* Mol Biol Cell, 2001. **12**(6): p. 1843-57.

169. Lin, S.X., G.G. Gundersen, and F.R. Maxfield, *Export from pericentriolar endocytic recycling compartment to cell surface depends on stable, detyrosinated (glu) microtubules and kinesin.* Mol Biol Cell, 2002. **13**(1): p. 96-109.

170. Hehnly, H., D. Sheff, and M. Stamnes, *Shiga toxin facilitates its retrograde transport by modifying microtubule dynamics.* Mol Biol Cell, 2006. **17**(10): p. 4379-89.

171. Hehnly, H., K.M. Longhini, J.L. Chen, and M. Stamnes, *Retrograde Shiga toxin trafficking is regulated by ARHGAP21 and Cdc42.* Mol Biol Cell, 2009. **20**(20): p. 4303-12.

172. Mallet, W.G. and F.R. Maxfield, *Chimeric forms of furin and TGN38 are transported with the plasma membrane in the trans-Golgi network via distinct endosomal pathways.* J Cell Biol, 1999. **146**(2): p. 345-59.

173. Carlton, J.G. and P.J. Cullen, *Sorting nexins.* Curr Biol, 2005. **15**(20): p. R819-20.

174. van Weering, J.R., P. Verkade, and P.J. Cullen, *SNX-BAR proteins in phosphoinositide-mediated, tubular-based endosomal sorting.* Semin Cell Dev Biol, 2010. **21**(4): p. 371-80.

175. Wassmer, T., N. Attar, M. Harterink, J.R. van Weering, C.J. Traer, J. Oakley, B. Goud, D.J. Stephens, P. Verkade, H.C. Korswagen, and P.J. Cullen, *The retromer coat complex coordinates endosomal sorting and dynein-mediated transport, with carrier recognition by the trans-Golgi network.* Dev Cell, 2009. **17**(1): p. 110-22.

176. Traer, C.J., A.C. Rutherford, K.J. Palmer, T. Wassmer, J. Oakley, N. Attar, J.G. Carlton, J. Kremerskothen, D.J. Stephens, and P.J. Cullen, *SNX4 coordinates endosomal sorting of TfnR with dynein-mediated transport into the endocytic recycling compartment.* Nat Cell Biol, 2007. **9**(12): p. 1370-80.

177. Skanland, S.S., S. Walchli, A. Brech, and K. Sandvig, *SNX4 in complex with clathrin and dynein: implications for endosome movement.* PLoS One, 2009. **4**(6): p. e5935.

178. Matteoni, R. and T.E. Kreis, *Translocation and clustering of endosomes and lysosomes depends on microtubules.* J Cell Biol, 1987. **105**(3): p. 1253-65.

179. Valetti, C., D.M. Wetzel, M. Schrader, M.J. Hasbani, S.R. Gill, T.E. Kreis, and T.A. Schroer, *Role of dynactin in endocytic traffic: effects of dynamitin overexpression and colocalization with CLIP-170.* Mol Biol Cell, 1999. **10**(12): p. 4107-20.

180. Brown, C.L., K.C. Maier, T. Stauber, L.M. Ginkel, L. Wordeman, I. Vernos, and T.A. Schroer, *Kinesin-2 is a motor for late endosomes and lysosomes.* Traffic, 2005. **6**(12): p. 1114-24.

181. Bananis, E., S. Nath, K. Gordon, P. Satir, R.J. Stockert, J.W. Murray, and A.W. Wolkoff, *Microtubule-dependent movement of late endocytic vesicles in vitro: requirements for Dynein and Kinesin.* Mol Biol Cell, 2004. **15**(8): p. 3688-97.

182. Soni, L.E., C.M. Warren, C. Bucci, D.J. Orten, and T. Hasson, *The unconventional myosin-VIIa associates with lysosomes.* Cell Motil Cytoskeleton, 2005. **62**(1): p. 13-26.

183. Pines, J., *Four-dimensional control of the cell cycle.* Nat Cell Biol, 1999. **1**(3): p. E73-9.

184. Nurse, P., *Universal control mechanism regulating onset of M-phase.* Nature, 1990. **344**(6266): p. 503-8.

185. Glotzer, M., A.W. Murray, and M.W. Kirschner, *Cyclin is degraded by the ubiquitin pathway.* Nature, 1991. **349**(6305): p. 132-8.

186. Jackman, M., M. Firth, and J. Pines, *Human cyclins B1 and B2 are localized to strikingly different structures: B1 to microtubules, B2 primarily to the Golgi apparatus.* Embo J, 1995. **14**(8): p. 1646-54.

187. Brandeis, M., I. Rosewell, M. Carrington, T. Crompton, M.A. Jacobs, J. Kirk, J. Gannon, and T. Hunt, *Cyclin B2-null mice develop normally and are fertile whereas cyclin B1-null mice die in utero.* Proc Natl Acad Sci U S A, 1998. **95**(8): p. 4344-9.

188. Robertson, A.M. and V.J. Allan, *Cell cycle regulation of organelle transport.* Prog Cell Cycle Res, 1997. **3**: p. 59-75.

189. Boevink, P., K. Oparka, S. Santa Cruz, B. Martin, A. Betteridge, and C. Hawes, *Stacks on tracks: the plant Golgi apparatus traffics on an actin/ER network.* Plant J, 1998. **15**(3): p. 441-7.

190. Lee, C., M. Ferguson, and L.B. Chen, *Construction of the endoplasmic reticulum.* J Cell Biol, 1989. **109**(5): p. 2045-55.

191. Terasaki, M., L.B. Chen, and K. Fujiwara, *Microtubules and the endoplasmic reticulum are highly interdependent structures.* J Cell Biol, 1986. **103**(4): p. 1557-68.

192. Terasaki, M. and T.S. Reese, *Interactions among endoplasmic reticulum, microtubules, and retrograde movements of the cell surface.* Cell Motil Cytoskeleton, 1994. **29**(4): p. 291-300.

193. Waterman-Storer, C.M. and E.D. Salmon, *Endoplasmic reticulum membrane tubules are distributed by microtubules in living cells using three distinct mechanisms.* Curr Biol, 1998. **8**(14): p. 798-806.

194. Lee, C. and L.B. Chen, *Dynamic behavior of endoplasmic reticulum in living cells.* Cell, 1988. **54**(1): p. 37-46.

195. Dabora, S.L. and M.P. Sheetz, *The microtubule-dependent formation of a tubulovesicular network with characteristics of the ER from cultured cell extracts.* Cell, 1988. **54**(1): p. 27-35.

196. Bannai, H., T. Inoue, T. Nakayama, M. Hattori, and K. Mikoshiba, *Kinesin dependent, rapid, bi-directional transport of ER sub-compartment in dendrites of hippocampal neurons.* J Cell Sci, 2004. **117**(Pt 2): p. 163-75.

197. Wozniak, M.J., B. Bola, K. Brownhill, Y.C. Yang, V. Levakova, and V.J. Allan, *Role of kinesin-1 and cytoplasmic dynein in endoplasmic reticulum movement in VERO cells.* J Cell Sci, 2009. **122**(Pt 12): p. 1979-89.

198. Toyoshima, I., H. Yu, E.R. Steuer, and M.P. Sheetz, *Kinectin, a major kinesin-binding protein on ER.* J Cell Biol, 1992. **118**(5): p. 1121-31.

199. Santama, N., C.P. Er, L.L. Ong, and H. Yu, *Distribution and functions of kinectin isoforms.* J Cell Sci, 2004. **117**(Pt 19): p. 4537-49.

200. Ong, L.L., A.P. Lim, C.P. Er, S.A. Kuznetsov, and H. Yu, *Kinectin-kinesin binding domains and their effects on organelle motility.* J Biol Chem, 2000. **275**(42): p. 32854-60.

201. Diefenbach, R.J., E. Diefenbach, M.W. Douglas, and A.L. Cunningham, *The ribosome receptor, p180, interacts with kinesin heavy chain, KIF5B.* Biochem Biophys Res Commun, 2004. **319**(3): p. 987-92.

202. Plitz, T. and K. Pfeffer, *Intact lysosome transport and phagosome function despite kinectin deficiency.* Mol Cell Biol, 2001. **21**(17): p. 6044-55.

203. Tabb, J.S., B.J. Molyneaux, D.L. Cohen, S.A. Kuznetsov, and G.M. Langford, *Transport of ER vesicles on actin filaments in neurons by myosin V.* J Cell Sci, 1998. **111 (Pt 21)**: p. 3221-34.

204. Grigoriev, I., S.M. Gouveia, B. van der Vaart, J. Demmers, J.T. Smyth, S. Honnappa, D. Splinter, M.O. Steinmetz, J.W. Putney, Jr., C.C. Hoogenraad, and A. Akhmanova, *STIM1 is a MT-plus-end-tracking protein involved in remodeling of the ER.* Curr Biol, 2008. **18**(3): p. 177-82.

205. Klopfenstein, D.R., F. Kappeler, and H.P. Hauri, *A novel direct interaction of endoplasmic reticulum with microtubules.* Embo J, 1998. **17**(21): p. 6168-77.

206. Andrade, J., H. Zhao, B. Titus, S. Timm Pearce, and M. Barroso, *The EF-hand Ca2+-binding protein p22 plays a role in microtubule and endoplasmic reticulum organization and dynamics with distinct Ca2+-binding requirements.* Mol Biol Cell, 2004. **15**(2): p. 481-96.

207. Vedrenne, C., D.R. Klopfenstein, and H.P. Hauri, *Phosphorylation controls CLIMP-63-mediated anchoring of the endoplasmic reticulum to microtubules.* Mol Biol Cell, 2005. **16**(4): p. 1928-37.

208. Yang, L., T. Guan, and L. Gerace, *Integral membrane proteins of the nuclear envelope are dispersed throughout the endoplasmic reticulum during mitosis.* J Cell Biol, 1997. **137**(6): p. 1199-210.

209. Waterman-Storer, C.M., J.W. Sanger, and J.M. Sanger, *Dynamics of organelles in the mitotic spindles of living cells: membrane and microtubule interactions.* Cell Motil Cytoskeleton, 1993. **26**(1): p. 19-39.

210. McCullough, S. and J. Lucocq, *Endoplasmic reticulum positioning and partitioning in mitotic HeLa cells.* J Anat, 2005. **206**(5): p. 415-25.

211. Kano, F., H. Kondo, A. Yamamoto, A.R. Tanaka, N. Hosokawa, K. Nagata, and M. Murata, *The maintenance of the endoplasmic reticulum network is regulated by p47, a cofactor of p97, through phosphorylation by cdc2 kinase.* Genes Cells, 2005. **10**(4): p. 333-44.

212. Hetzer, M., H.H. Meyer, T.C. Walther, D. Bilbao-Cortes, G. Warren, and I.W. Mattaj, *Distinct AAA-ATPase p97 complexes function in discrete steps of nuclear assembly.* Nat Cell Biol, 2001. **3**(12): p. 1086-91.

213. Lu, L., M.S. Ladinsky, and T. Kirchhausen, *Cisternal organization of the endoplasmic reticulum during mitosis.* Mol Biol Cell, 2009. **20**(15): p. 3471-80.

214. Poteryaev, D., J.M. Squirrell, J.M. Campbell, J.G. White, and A. Spang, *Involvement of the actin cytoskeleton and homotypic membrane fusion in ER dynamics in Caenorhabditis elegans.* Mol Biol Cell, 2005. **16**(5): p. 2139-53.

215. Lowe, M. and F.A. Barr, *Inheritance and biogenesis of organelles in the secretory pathway.* Nat Rev Mol Cell Biol, 2007. **8**(6): p. 429-39.

216. Estrada, P., J. Kim, J. Coleman, L. Walker, B. Dunn, P. Takizawa, P. Novick, and S. Ferro-Novick, *Myo4p and She3p are required for cortical ER inheritance in Saccharomyces cerevisiae.* J Cell Biol, 2003. **163**(6): p. 1255-66.

217. Allan, V.J. and R.D. Vale, *Cell cycle control of microtubule-based membrane transport and tubule formation in vitro.* J Cell Biol, 1991. **113**(2): p. 347-59.

218. Lane, J.D. and V.J. Allan, *Microtubule-based endoplasmic reticulum motility in Xenopus laevis: activation of membrane-associated kinesin during development.* Mol Biol Cell, 1999. **10**(6): p. 1909-22.

219. Lucocq, J.M. and G. Warren, *Fragmentation and partitioning of the Golgi apparatus during mitosis in HeLa cells.* Embo J, 1987. **6**(11): p. 3239-46.

220. Axelsson, M.A. and G. Warren, *Rapid, endoplasmic reticulum-independent diffusion of the mitotic Golgi haze.* Mol Biol Cell, 2004. **15**(4): p. 1843-52.

221. Zaal, K.J., C.L. Smith, R.S. Polishchuk, N. Altan, N.B. Cole, J. Ellenberg, K. Hirschberg, J.F. Presley, T.H. Roberts, E. Siggia, R.D. Phair, and J. Lippincott-Schwartz, *Golgi membranes are absorbed into and reemerge from the ER during mitosis.* Cell, 1999. **99**(6): p. 589-601.

222. Warren, G., C. Featherstone, G. Griffiths, and B. Burke, *Newly synthesized G protein of vesicular stomatitis virus is not transported to the cell surface during mitosis.* J Cell Biol, 1983. **97**(5 Pt 1): p. 1623-8.

223. Featherstone, C., G. Griffiths, and G. Warren, *Newly synthesized G protein of vesicular stomatitis virus is not transported to the Golgi complex in mitotic cells.* J Cell Biol, 1985. **101**(6): p. 2036-46.

224. Farmaki, T., S. Ponnambalam, A.R. Prescott, H. Clausen, B.L. Tang, W. Hong, and J.M. Lucocq, *Forward and retrograde trafficking in mitotic animal cells. ER-Golgi transport arrest restricts protein export from the ER into COPII-coated structures.* J Cell Sci, 1999. **112 (Pt 5)**: p. 589-600.

225. Berlin, R.D., J.M. Oliver, and R.J. Walter, *Surface functions during Mitosis I: phagocytosis, pinocytosis and mobility of surface-bound Con A.* Cell, 1978. **15**(2): p. 327-41.

226. Warren, G., J. Davoust, and A. Cockcroft, *Recycling of transferrin receptors in A431 cells is inhibited during mitosis.* Embo J, 1984. **3**(10): p. 2217-25.

227. Yang, H.Y., P.E. Mains, and F.J. McNally, *Kinesin-1 mediates translocation of the meiotic spindle to the oocyte cortex through KCA-1, a novel cargo adapter.* J Cell Biol, 2005. **169**(3): p. 447-57.

228. Verlhac, M.H., C. Lefebvre, P. Guillaud, P. Rassinier, and B. Maro, *Asymmetric division in mouse oocytes: with or without Mos.* Curr Biol, 2000. **10**(20): p. 1303-6.

229. Allan, V.J., *Organelle motility and membrane network formation in metaphase and interphase cell-free extracts.* Methods Enzymol, 1998. **298**: p. 339-53.

230. Gross, S.P., M. Vershinin, and G.T. Shubeita, *Cargo transport: two motors are sometimes better than one.* Curr Biol, 2007. **17**(12): p. R478-86.

231. Gross, S.P., M.A. Welte, S.M. Block, and E.F. Wieschaus, *Coordination of opposite-polarity microtubule motors.* J Cell Biol, 2002. **156**(4): p. 715-24.

232. Allan, V. and R. Vale, *Movement of membrane tubules along microtubules in vitro: evidence for specialised sites of motor attachment.* J Cell Sci, 1994. **107 (Pt 7)**: p. 1885-97.

233. Murray, A.W. and M.W. Kirschner, *Cyclin synthesis drives the early embryonic cell cycle.* Nature, 1989. **339**(6222): p. 275-80.

234. Gautier, J., J. Minshull, M. Lohka, M. Glotzer, T. Hunt, and J.L. Maller, *Cyclin is a component of maturation-promoting factor from Xenopus.* Cell, 1990. **60**(3): p. 487-94.

235. Lohka, M.J., M.K. Hayes, and J.L. Maller, *Purification of maturation-promoting factor, an intracellular regulator of early mitotic events.* Proc Natl Acad Sci U S A, 1988. **85**(9): p. 3009-13.

236. Murray, A.W., M.J. Solomon, and M.W. Kirschner, *The role of cyclin synthesis and degradation in the control of maturation promoting factor activity.* Nature, 1989. **339**(6222): p. 280-6.

237. Murray, A.W., *Cell cycle extracts.* Methods Cell Biol, 1991. **36**: p. 581-605.

238. Newmeyer, D.D. and K.L. Wilson, *Egg extracts for nuclear import and nuclear assembly reactions.* Methods Cell Biol, 1991. **36**: p. 607-34.

239. Weaver, C., G.H. Farr, 3rd, W. Pan, B.A. Rowning, J. Wang, J. Mao, D. Wu, L. Li, C.A. Larabell, and D. Kimelman, *GBP binds kinesin light chain and translocates during cortical rotation in Xenopus eggs.* Development, 2003. **130**(22): p. 5425-36.

240. Haraguchi, K., T. Hayashi, T. Jimbo, T. Yamamoto, and T. Akiyama, *Role of the kinesin-2 family protein, KIF3, during mitosis.* J Biol Chem, 2006. **281**(7): p. 4094-9.

241. Yang, Z. and L.S. Goldstein, *Characterization of the KIF3C neural kinesin-like motor from mouse.* Mol Biol Cell, 1998. **9**(2): p. 249-61.

242. Conforti, L., C. Dell'Agnello, N. Calvaresi, M. Tortarolo, A. Giorgini, M.P. Coleman, and C. Bendotti, *Kif1Bbeta isoform is enriched in motor neurons but does not change in a mouse model of amyotrophic lateral sclerosis.* J Neurosci Res, 2003. **71**(5): p. 732-9.

243. Nakagawa, T., Y. Tanaka, E. Matsuoka, S. Kondo, Y. Okada, Y. Noda, Y. Kanai, and N. Hirokawa, *Identification and classification of 16 new kinesin superfamily (KIF) proteins in mouse genome.* Proc Natl Acad Sci U S A, 1997. **94**(18): p. 9654-9.

244. Taya, S., T. Shinoda, D. Tsuboi, J. Asaki, K. Nagai, T. Hikita, S. Kuroda, K. Kuroda, M. Shimizu, S. Hirotsune, A. Iwamatsu, and K. Kaibuchi, *DISC1 regulates the transport of the NUDEL/LIS1/14-3-3epsilon complex through kinesin-1.* J Neurosci, 2007. **27**(1): p. 15-26.

245. Martin, M., S.M. Ahern-Djamali, F.M. Hoffmann, and W.M. Saxton, *Abl tyrosine kinase and its substrate Ena/VASP have functional interactions with kinesin-1.* Mol Biol Cell, 2005. **16**(9): p. 4225-30.

246. Stowers, R.S., L.J. Megeath, J. Gorska-Andrzejak, I.A. Meinertzhagen, and T.L. Schwarz, *Axonal transport of mitochondria to synapses depends on milton, a novel Drosophila protein.* Neuron, 2002. **36**(6): p. 1063-77.

247. Huang, J.D., S.T. Brady, B.W. Richards, D. Stenolen, J.H. Resau, N.G. Copeland, and N.A. Jenkins, *Direct interaction of microtubule- and actin-based transport motors.* Nature, 1999. **397**(6716): p. 267-70.

248. Chen, X., S. Kojima, G.G. Borisy, and K.J. Green, *p120 catenin associates with kinesin and facilitates the transport of cadherin-catenin complexes to intercellular junctions.* J Cell Biol, 2003. **163**(3): p. 547-57.

249. Yanagisawa, M., I.N. Kaverina, A. Wang, Y. Fujita, A.B. Reynolds, and P.Z. Anastasiadis, *A novel interaction between kinesin and p120 modulates p120 localization and function.* J Biol Chem, 2004. **279**(10): p. 9512-21.

250. Cai, Y., B.B. Singh, A. Aslanukov, H. Zhao, and P.A. Ferreira, *The docking of kinesins, KIF5B and KIF5C, to Ran-binding protein 2 (RanBP2) is mediated via a novel RanBP2 domain.* J Biol Chem, 2001. **276**(45): p. 41594-602.

251. Diefenbach, R.J., E. Diefenbach, M.W. Douglas, and A.L. Cunningham, *The heavy chain of conventional kinesin interacts with the SNARE proteins SNAP25 and SNAP23.* Biochemistry, 2002. **41**(50): p. 14906-15.

252. Su, Q., Q. Cai, C. Gerwin, C.L. Smith, and Z.H. Sheng, *Syntabulin is a microtubule-associated protein implicated in syntaxin transport in neurons.* Nat Cell Biol, 2004. **6**(10): p. 941-53.

253. Gindhart, J.G., J. Chen, M. Faulkner, R. Gandhi, K. Doerner, T. Wisniewski, and A. Nandlestadt, *The kinesin-associated protein UNC-76 is required for axonal transport in the Drosophila nervous system.* Mol Biol Cell, 2003. **14**(8): p. 3356-65.

254. Macioce, P., G. Gambara, M. Bernassola, L. Gaddini, P. Torreri, G. Macchia, C. Ramoni, M. Ceccarini, and T.C. Petrucci, *Beta-dystrobrevin interacts directly with kinesin heavy chain in brain.* J Cell Sci, 2003. **116**(Pt 23): p. 4847-56.

255. Kamal, A., G.B. Stokin, Z. Yang, C.H. Xia, and L.S. Goldstein, *Axonal transport of amyloid precursor protein is mediated by direct binding to the kinesin light chain subunit of kinesin-I.* Neuron, 2000. **28**(2): p. 449-59.

256. Konecna, A., R. Frischknecht, J. Kinter, A. Ludwig, M. Steuble, V. Meskenaite, M. Indermuhle, M. Engel, C. Cen, J.M. Mateos, P. Streit, and P. Sonderegger, *Calsyntenin-1 docks vesicular cargo to kinesin-1.* Mol Biol Cell, 2006. **17**(8): p. 3651-63.

257. Kimura, T., H. Watanabe, A. Iwamatsu, and K. Kaibuchi, *Tubulin and CRMP-2 complex is transported via Kinesin-1.* J Neurochem, 2005. **93**(6): p. 1371-82.

258. Semiz, S., J.G. Park, S.M. Nicoloro, P. Furcinitti, C. Zhang, A. Chawla, J. Leszyk, and M.P. Czech, *Conventional kinesin KIF5B mediates insulin-stimulated GLUT4 movements on microtubules.* Embo J, 2003. **22**(10): p. 2387-99.

259. Kelkar, N., C.L. Standen, and R.J. Davis, *Role of the JIP4 scaffold protein in the regulation of mitogen-activated protein kinase signaling pathways.* Mol Cell Biol, 2005. **25**(7): p. 2733-43.

260. Bracale, A., F. Cesca, V.E. Neubrand, T.P. Newsome, M. Way, and G. Schiavo, *Kidins220/ARMS is transported by a kinesin-1-based mechanism likely to be involved in neuronal differentiation.* Mol Biol Cell, 2007. **18**(1): p. 142-52.

261. Bhullar, B., Y. Zhang, A. Junco, R. Oko, and F.A. van der Hoorn, *Association of kinesin light chain with outer dense fibers in a microtubule-independent fashion.* J Biol Chem, 2003. **278**(18): p. 16159-68.

262. Bowman, A.B., A. Kamal, B.W. Ritchings, A.V. Philp, M. McGrail, J.G. Gindhart, and L.S. Goldstein, *Kinesin-dependent axonal transport is mediated by the sunday driver (SYD) protein.* Cell, 2000. **103**(4): p. 583-94.

263. Utton, M.A., W.J. Noble, J.E. Hill, B.H. Anderton, and D.P. Hanger, *Molecular motors implicated in the axonal transport of tau and alpha-synuclein.* J Cell Sci, 2005. **118**(Pt 20): p. 4645-54.

264. Kamm, C., H. Boston, J. Hewett, J. Wilbur, D.P. Corey, P.I. Hanson, V. Ramesh, and X.O. Breakefield, *The early onset dystonia protein torsinA interacts with kinesin light chain 1.* J Biol Chem, 2004. **279**(19): p. 19882-92.

265. Sakamoto, R., D.T. Byrd, H.M. Brown, N. Hisamoto, K. Matsumoto, and Y. Jin, *The Caenorhabditis elegans UNC-14 RUN domain protein binds to the kinesin-1 and UNC-16 complex and regulates synaptic vesicle localization.* Mol Biol Cell, 2005. **16**(2): p. 483-96.

266. Shaner, N.C., M.Z. Lin, M.R. McKeown, P.A. Steinbach, K.L. Hazelwood, M.W. Davidson, and R.Y. Tsien, *Improving the photostability of bright monomeric orange and red fluorescent proteins.* Nat Methods, 2008. **5**(6): p. 545-51.

267. Russo, R.N., N.L. Shaper, D.J. Taatjes, and J.H. Shaper, *Beta 1,4-galactosyltransferase: a short NH2-terminal fragment that includes the cytoplasmic and transmembrane domain is sufficient for Golgi retention.* J Biol Chem, 1992. **267**(13): p. 9241-7.

268. Guan, K.L. and J.E. Dixon, *Eukaryotic proteins expressed in Escherichia coli: an improved thrombin cleavage and purification procedure of fusion proteins with glutathione S-transferase.* Anal Biochem, 1991. **192**(2): p. 262-7.

269. Masson, D. and T.E. Kreis, *Identification and molecular characterization of E-MAP-115, a novel microtubule-associated protein predominantly expressed in epithelial cells.* J Cell Biol, 1993. **123**(2): p. 357-71.

270. Cronan, J.E., Jr., *Biotination of proteins in vivo. A post-translational modification to label, purify, and study proteins.* J Biol Chem, 1990. **265**(18): p. 10327-33.

271. Weisenberg, R.C. and C. Cianci, *ATP-induced gelation--contraction of microtubules assembled in vitro.* J Cell Biol, 1984. **99**(4 Pt 1): p. 1527-33.

272. Allan, V., *Protein phosphatase 1 regulates the cytoplasmic dynein-driven formation of endoplasmic reticulum networks in vitro.* J Cell Biol, 1995. **128**(5): p. 879-91.

273. Welte, M.A., *Bidirectional transport along microtubules.* Curr Biol, 2004. **14**(13): p. R525-37.

274. Newport, J., *Nuclear reconstitution in vitro: stages of assembly around protein-free DNA.* Cell, 1987. **48**(2): p. 205-17.

275. Langan, T.A., J. Gautier, M. Lohka, R. Hollingsworth, S. Moreno, P. Nurse, J. Maller, and R.A. Sclafani, *Mammalian growth-associated H1 histone kinase: a homolog of cdc2+/CDC28 protein kinases controlling mitotic entry in yeast and frog cells.* Mol Cell Biol, 1989. **9**(9): p. 3860-8.

276. Waterman-Storer, C.M., *Microtubule/organelle motility assays.* Curr Protoc Cell Biol, 2001. **Chapter 13**: p. Unit 13 1.

277. Morfini, G., G. Szebenyi, H. Brown, H.C. Pant, G. Pigino, S. DeBoer, U. Beffert, and S.T. Brady, *A novel CDK5-dependent pathway for regulating GSK3 activity and kinesin-driven motility in neurons.* Embo J, 2004. **23**(11): p. 2235-45.

278. Ingold, A.L., S.A. Cohn, and J.M. Scholey, *Inhibition of kinesin-driven microtubule motility by monoclonal antibodies to kinesin heavy chains.* J Cell Biol, 1988. **107**(6 Pt 2): p. 2657-67.

279. Coy, D.L., M. Wagenbach, and J. Howard, *Kinesin takes one 8-nm step for each ATP that it hydrolyzes.* J Biol Chem, 1999. **274**(6): p. 3667-71.

280. Inoue, Y., Y.Y. Toyoshima, A.H. Iwane, S. Morimoto, H. Higuchi, and T. Yanagida, *Movements of truncated kinesin fragments with a short or an artificial flexible neck.* Proc Natl Acad Sci U S A, 1997. **94**(14): p. 7275-80.

281. Kalchishkova, N. and K.J. Bohm, *The role of Kinesin neck linker and neck in velocity regulation.* J Mol Biol, 2008. **382**(1): p. 127-35.

282. Kozielski, F., S. Sack, A. Marx, M. Thormahlen, E. Schonbrunn, V. Biou, A. Thompson, E.M. Mandelkow, and E. Mandelkow, *The crystal structure of dimeric kinesin and implications for microtubule-dependent motility.* Cell, 1997. **91**(7): p. 985-94.

283. Kull, F.J., E.P. Sablin, R. Lau, R.J. Fletterick, and R.D. Vale, *Crystal structure of the kinesin motor domain reveals a structural similarity to myosin.* Nature, 1996. **380**(6574): p. 550-5.

284. Jiang, W., M.F. Stock, X. Li, and D.D. Hackney, *Influence of the kinesin neck domain on dimerization and ATPase kinetics.* J Biol Chem, 1997. **272**(12): p. 7626-32.

285. Yang, J.T., W.M. Saxton, R.J. Stewart, E.C. Raff, and L.S. Goldstein, *Evidence that the head of kinesin is sufficient for force generation and motility in vitro.* Science, 1990. **249**(4964): p. 42-7.

286. Huang, C.Y., C.P. Chang, C.L. Huang, and J.E. Ferrell, Jr., *M phase phosphorylation of cytoplasmic dynein intermediate chain and p150(Glued).* J Biol Chem, 1999. **274**(20): p. 14262-9.

287. Faire, K., C.M. Waterman-Storer, D. Gruber, D. Masson, E.D. Salmon, and J.C. Bulinski, *E-MAP-115 (ensconsin) associates dynamically with microtubules in vivo and is not a physiological modulator of microtubule dynamics.* J Cell Sci, 1999. **112 (Pt 23)**: p. 4243-55.

288. Saffin, J.M., M. Venoux, C. Prigent, J. Espeut, F. Poulat, D. Giorgi, A. Abrieu, and S. Rouquier, *ASAP, a human microtubule-associated protein required for bipolar spindle assembly and cytokinesis.* Proc Natl Acad Sci U S A, 2005. **102**(32): p. 11302-7.

289. Andersen, S.S. and E. Karsenti, *XMAP310: a Xenopus rescue-promoting factor localized to the mitotic spindle.* J Cell Biol, 1997. **139**(4): p. 975-83.

290. Wollert, T., D.G. Weiss, H.H. Gerdes, and S.A. Kuznetsov, *Activation of myosin V-based motility and F-actin-dependent network formation of endoplasmic reticulum during mitosis.* J Cell Biol, 2002. **159**(4): p. 571-7.

291. Marks, D.L., J.M. Larkin, and M.A. McNiven, *Association of kinesin with the Golgi apparatus in rat hepatocytes.* J Cell Sci, 1994. **107 (Pt 9)**: p. 2417-26.

292. Vaughan, P.S., P. Miura, M. Henderson, B. Byrne, and K.T. Vaughan, *A role for regulated binding of p150(Glued) to microtubule plus ends in organelle transport.* J Cell Biol, 2002. **158**(2): p. 305-19.

293. Reaves, B. and G. Banting, *Perturbation of the morphology of the trans-Golgi network following Brefeldin A treatment: redistribution of a TGN-specific integral membrane protein, TGN38.* J Cell Biol, 1992. **116**(1): p. 85-94.

294. Pfister, K.K., M.C. Wagner, D.L. Stenoien, S.T. Brady, and G.S. Bloom, *Monoclonal antibodies to kinesin heavy and light chains stain vesicle-like structures, but not microtubules, in cultured cells.* J Cell Biol, 1989. **108**(4): p. 1453-63.

295. Scholey, J.M., J. Heuser, J.T. Yang, and L.S. Goldstein, *Identification of globular mechanochemical heads of kinesin.* Nature, 1989. **338**(6213): p. 355-7.

296. Tuma, M.C., A. Zill, N. Le Bot, I. Vernos, and V. Gelfand, *Heterotrimeric kinesin II is the microtubule motor protein responsible for pigment dispersion in Xenopus melanophores.* J Cell Biol, 1998. **143**(6): p. 1547-58.

297. Wright, B.D., M. Terasaki, and J.M. Scholey, *Roles of kinesin and kinesin-like proteins in sea urchin embryonic cell division: evaluation using antibody microinjection.* J Cell Biol, 1993. **123**(3): p. 681-9.

298. Betley, J.N., B. Heinrich, I. Vernos, C. Sardet, F. Prodon, and J.O. Deshler, *Kinesin II mediates Vg1 mRNA transport in Xenopus oocytes.* Curr Biol, 2004. **14**(3): p. 219-24.

299. Morris, R.L. and J.M. Scholey, *Heterotrimeric kinesin-II is required for the assembly of motile 9+2 ciliary axonemes on sea urchin embryos.* J Cell Biol, 1997. **138**(5): p. 1009-22.

300. Dailey, M.E. and P.C. Bridgman, *Dynamics of the endoplasmic reticulum and other membranous organelles in growth cones of cultured neurons.* J Neurosci, 1989. **9**(6): p. 1897-909.

301. Waterman-Storer, C.M., J. Gregory, S.F. Parsons, and E.D. Salmon, *Membrane/microtubule tip attachment complexes (TACs) allow the assembly dynamics of plus ends to push and pull membranes into tubulovesicular networks in interphase Xenopus egg extracts.* J Cell Biol, 1995. **130**(5): p. 1161-9.

302. Heuser, J., *Changes in lysosome shape and distribution correlated with changes in cytoplasmic pH.* J Cell Biol, 1989. **108**(3): p. 855-64.

303. Lewis, V., S.A. Green, M. Marsh, P. Vihko, A. Helenius, and I. Mellman, *Glycoproteins of the lysosomal membrane.* J Cell Biol, 1985. **100**(6): p. 1839-47.

304. Hopkins, C.R., *Intracellular routing of transferrin and transferrin receptors in epidermoid carcinoma A431 cells.* Cell, 1983. **35**(1): p. 321-30.

305. Hopkins, C.R. and I.S. Trowbridge, *Internalization and processing of transferrin and the transferrin receptor in human carcinoma A431 cells.* J Cell Biol, 1983. **97**(2): p. 508-21.

306. Yoshino, A., S.R. Setty, C. Poynton, E.L. Whiteman, A. Saint-Pol, C.G. Burd, L. Johannes, E.L. Holzbaur, M. Koval, J.M. McCaffery, and M.S. Marks, *tGolgin-1 (p230, golgin-245) modulates Shiga-toxin transport to the Golgi and Golgi motility towards the microtubule-organizing centre.* J Cell Sci, 2005. **118**(Pt 10): p. 2279-93.

307. Tooze, J. and M. Hollinshead, *Tubular early endosomal networks in AtT20 and other cells.* J Cell Biol, 1991. **115**(3): p. 635-53.

308. Siddhanta, U., J. McIlroy, A. Shah, Y. Zhang, and J.M. Backer, *Distinct roles for the p110alpha and hVPS34 phosphatidylinositol 3'-kinases in vesicular trafficking, regulation of the actin cytoskeleton, and mitogenesis.* J Cell Biol, 1998. **143**(6): p. 1647-59.

309. Gross, S.P., M.C. Tuma, S.W. Deacon, A.S. Serpinskaya, A.R. Reilein, and V.I. Gelfand, *Interactions and regulation of molecular motors in Xenopus melanophores.* J Cell Biol, 2002. **156**(5): p. 855-65.

310. Deacon, S.W., A. Nascimento, A.S. Serpinskaya, and V.I. Gelfand, *Regulation of bidirectional melanosome transport by organelle bound MAP kinase.* Curr Biol, 2005. **15**(5): p. 459-63.